THE MECHANICAL PROPERTIES OF NATURAL FIBER COMPOSITES

by

Ekhlas Aboud Osman Al-Bahadly

A thesis submitted for the degree of Doctor of Philosophy

Faculty of Engineering

Swinburne University of Technology

in January , 2013

Abstract of thesis entitled

The Mechanical Properties of Natural Fiber Composites

Submitted by
Ekhlas Aboud Osman Al-Bahadly

for the degree of Doctor of Philosophy
at Swinburne University of Technology

in January , 2013

The abundant availability and accessibility of natural fibers are the major reasons for an emerging new interest in sustainable technology. Natural fibers, as reinforcement, have recently attracted the attention of researchers because of their advantages over other established materials. They are environmentally-friendly, fully biodegradable, abundantly available, non-toxic, non-abrasive, renewable, and cheap, and have low density.

In this research, the work was divided into four stages. In the first stage, the curing behaviour and mechanical properties of unsaturated polyester was investigated. This investigation was carried out at different concentrations of styrene monomer, with Methyl Ethyl Ketone Peroxide MEKP as initiator and Dimethyl Aniline NNDMA as accelerator. Further, the effects of varying the level of water content on the exothermal behaviour and mechanical properties were investigated. The results show that styrene concentration is an important parameter that affects the curing behaviour and mechanical properties of unsaturated polyester resin. Moreover, the results show that water affects the action of the initiator and accelerator systems and decreases the mechanical properties of matrix.

In the second stage, the physical and mechanical properties of kenaf fiber were observed experimentally, namely, length, diameter, density, fiber surface modification, water absorption, tensile strength and Young's modulus. The percentage ratios of holocellulose content, of bast and core kenaf fiber were investigated. Alkali treatment enhanced the fiber surface by removing wax, oil and other surface impurities. The

treatment also roughened the surface of the fiber bundles and did not have any significant effect on the holocellulose kenaf bast fiber.

The third stage evaluated the various physical and chemical attributes, such as strength, Young's modulus, interfacial adhesion and thermal stability of the kenaf unsaturated polyester composite at different fiber lengths. A general trend was observed whereby alkalized fiber composites possessed superior flexural strength and modulus. The length and weight fraction of fiber effected the mechanical properties of the kenaf unsaturated polyester composites. A comparison was made between experimental data and different theoretical models. The experimental data was cross-matched against composite models, such as Hirsch, Einstein-Guth, modified Bowyer-Bader, Kelly-Tyson, Parallel, modified Guth, Cox-Krenchel, and Halpin-Tsai. The results show a good correlation with Hirsch's model while the results obtained from Cox-Krenchel underestimated the experimental data. In addition, the mechanical properties of the hybrid composites were investigated. The hybrid composites were made via adding different fractions of recycled jute fiber at different lengths to kenaf fiber. The results indicated that; the mechanical properties of kenaf composites were improved for a certain value of weight fraction and length of recycled jute.

Water absorption, thickness swelling behavior of kenaf composites and kenaf/recycle jute composites were investigated. Further study was carried out on the effects, of water uptake on the mechanical properties at two different temperatures. The results show that the percentage of water absorption increases with increasing of fiber weight fractions and environmental temperature. The process of absorption of water was found to approach the Fickian diffusion behavior for both temperatures, the same trend for hybrid composites at room temperature. The values obtained for diffusion coefficients were in the range of 10-12 m^2/sec. SEM analysis showed that the interaction between the hybrid fibers and unsaturated polyester matrix was poor such that fiber debonding, fiber pull-out, matrix fracture and fibers fracture occurred in short kenaf/recycled jute unsaturated polyester composites.

The fourth stage investigated the effects of the fiber content on the dynamic properties and degradation temperature of the kenaf/unsaturated polyester composites (KFUPC), using DMA test and, Thermo Gravimetric Analysis TGA, respectively. The T_g temperature shifted positively with the addition of fiber. Furthermore, the thermal behaviour of the neat resins for various styrene concentrations was comparable indicated on the two-stage weight loss mechanism, while three-stage weight loss
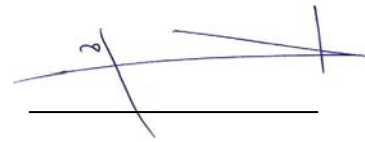
mechanism for composites. Dynamic mechanical analysis was performed to obtain strain and creep compliance for kenaf composites at various styrene concentrations and fiber content. The time-temperature superposition principle was applied to the viscoelastic properties of a kenaf fiber unsaturated polyester composite, and its validity was tested. The primary creep strain model was fitted to 60 min creep data. The resulting equation was then extrapolated to 5.5 days; the creep strain model of power-law was successfully used to predict the long-term creep behavior of natural fiber/thermoset composites.

DECLARATION

I declare that this thesis:

Represent my own work and has not been previously included in a thesis, exposition or report submitted to this university or to any other institution for a degree, diploma or other requirement, excluding where due acknowledgement and reference is made; to the best of my knowledge, contains no material formerly published or written by another person, except where due reference is made; and where the work is based on joint research or publication, discloses the comparative contributions of the respective authors.

Signature: _____

Ekhlas Aboud Osman

ACKNOWLEDGEMENTS

TABLE OF CONTENTS

LIST OF TABLES

LIST OF FIGURES

coefficient at 50°C

LIST OF SYMBOLS

Chapter 1

DMA – Dynamic mechanical analysis

MEKP – Methyl Ethyl Ketone Peroxide

NaOH – Sodium hydroxide

NNDMA - Dimethyl Aniline

PLA – Poly (lactic acid)

PMCs – Polymer matrix composites

PVC – Polypropylene and polyvinyl chloride

RNCF –Recycled newspaper cellulose fibers

SEM – Scanning electron microscopy

SLS – Sodium Lauryl Sulfate

TGA – Thermo gravimetric analysis

UP – Unsaturated polyester

Chapter 2

AAP – Acetyl acetone peroxide

BPO – Benzoyl peroxide

TBPB – T-butyl perbenzoate

PVAc – Polyvinyl acetate

T_g – Glass transition temperature

V_f –Fiber volume fraction

V_{min} – Minimum value of fiber volume fraction

V_{crit} – Critical volume fraction of fiber

NaOH –Sodium hydroxide

Na_2SO_3 – Combinations of sodium hydroxide and sodium sulphite

SMC – Sheet molding composites

BMC –Bulk molding composites

E_L – Modulus composites in the fiber direction

σ_c – Strength of composites in the fiber direction

E_m – modulus of matrix

E_f – Modulus of fiber

V_m – Volume fraction of matrix

σ_f – Fiber strength

σ_m – Matrix strength

L – Fiber length

L_c – Critical length fiber

τ_y – Shear stress

d – Fiber diameter

σ_{fu} – The maximum permissible fiber stress

ε_f – Fiber strain

ε_m – Matrix strain

K_2 – Fiber length factor

K_1 – Orientation factor

X – Empirical parameter

η_{LS} – length efficiency factor

η_o – Orientation factor of fiber

S – Ratio of the length-to-width of fiber

G_m – Shear modulus of matrix

v_m – Poisson's ratio of matrix

A – Measure of fiber geometry

TS – Tensile strength

EM – Modulus of elasticity

α – Empirical constants

β – Empirical constants

K_{Fs} – Kenaf fibers

WF – Wood flour

PP – Polypropylene

CTE – Coefficient of Thermal Expansion

TMA – Thermo-Mechanical Analysis

DSC – Differential Scanning Calorimetry

E' – Storage modulus (real part)

E'' – Loss modulus (imaginary part)

ω – Frequency

Td – Thermal Decomposition Temperature

Tc – Crystallization temperature

$\Delta_{trs} H$ – Enthalpy change of the transition

$\Delta(q/t)$ – Changing in the heat flow

Chapter 3

$\rho(fl)$ – Density of the composites

W – Mass

V – Volume

$W_{(a)}$ – Composites weight dry

G – Buoyancy of the composites

KFUPC – Kenaf fiber unsaturated polyester composites

PVC – Glue

ST – Styrene

J_o – Initial energy

J_1 – resultant energy

W_o – Denoted oven dry weight

$W_{(t)}$ – Dry weight after time

t – Time

S_o – Denoted oven-dry dimension

$S_{(t)}$ – Dimension after time t, respectively

Chapter 4

$tan\delta$ – Loss factor

Chapter 6

W_f – Weight fraction of fiber

W_m – Weight fraction of matrix

ρ_f – Density of fiber

ρ_c – Density of matrix

V – Void fraction

M_t – Water absorption at time t

M_∞ – Water absorption at the saturation point

K – Coefficient

n – Coefficient

D – Diffusion coefficient

m – Initial slope

h – Thickness of the composite specimens

T_∞ – Equilibrium specimen thickness

T_o – Initial specimen thickness

K_{SR} – Intrinsic relative swelling rate constant

$TS_{(t)}$ – Thickness swelling at time t

SS – Sum squares

y_i – Observed value

$\hat{y}$ – Predicted value

PLA – Polylactic acid

PLA-KF – Kenaf fiber/polylactic acid bicomposites

UD – Unidirectional

CP – Cross-ply

TTS – Time-temperature superposition

TTSP – Time-temperature superposition principle

WLF – William-Landel-Ferry equation

a_T – Horizontal shift factor

c_1 and c_2 – Empirical constants

c_{1g} and c_{2g} – Empirical constants

a, n, and b – Constants depend on the temperature

CHAPTER ONE

INTRODUCTION

1.1   Overview of Composite Materials

Natural fibers like sisal, banana, jute, oil palm, kenaf, recycled jute and coir have been used as a reinforced composite for advanced applications such as aircraft and aerospace structures and for ordinary applications like consumer goods, furniture, low-cost housing and civil structures. The incorporation of stiff fibers in soft matrices can lead to new materials with outstanding mechanical properties encompassing the advantages of both the fiber and matrix (Termonia 1990). Fiber-reinforced composites are strong stiff and lightweight materials that consist of strong, stiff, but commonly, brittle fibers encapsulated in a softer, more ductile matrix material. The matrix transmits applied loads to the reinforcing fibers within the composite, resulting in a material with improved mechanical properties compared to the un-reinforced matrix material (Beckermann 2007). Since the early 1960s, there has been an increase in the demand for stronger, stiffer and more lightweight materials for use in the aerospace, transportation and construction industries. In recent years, natural fibers appear to be the outstanding material which has emerged as a viable and abundant substitute for the expensive and nonrenewable synthetic fiber.

High performance demands on engineering materials have led to extensive research and development of new and improved materials, such as composite materials used for structural purposes. They are often have low densities, resulting in high stiffness to weight and high strength to weight ratios when compared to traditional engineering materials. In addition, the high fatigue strength to weight ratio and fatigue damage tolerance of many composite also makes them an attractive option (Noorunnisa Khanam 2007).

Composite materials can be grouped into five major categories, which are ceramic matrix composites, metal matrix composites, intermetallic matrix composites, carbon-carbon composites and Polymer Matrix Composites (PMCs). The focus of this research is on the development of PMCs. Polymer matrix composites can consist of either a

thermoplastic or thermoset matrix, which is used to bind the reinforcing fibers together, as well as to transfer applied stresses from the composite to the fibers. Thermosets are plastics that cannot be melted once cured, and include resins such as epoxies, polyesters and phenolics. Thermoplastics, on the other hand, are plastics that can be repeatedly melted, thus enabling them to be recycled. Commonly used thermoplastics include polyethylene, polypropylene and polyvinyl chloride (PVC).

The reinforcing fibers in (PMCs) can be either short or continuous, with continuous fiber reinforcement providing the greatest mechanical properties in the direction of fiber alignment. Continuous fiber composites are primarily reinforced with high performance carbon or aramid (e.g. Kevlar^{TM}) fibers. These composites are often utilized in applications such as aircraft composites, where the exceptional fiber properties can be fully exploited. Some commonly used continuous fiber composite processing methods include compression moulding, hand lay-up, filament winding and pultrusion. Short fiber composites, on the other hand, are primarily reinforced with chopped fibers such as glass, graphite and cellulose fibers. These types of composites are cheaper and easier to fabricate, and are well established in many applications where medium to low strengths and stiffness are required. Compared to continuous fiber composites, short fiber composites can easily be processed in a similar manner to the matrix. Short fiber composites with a thermoset matrix can be mass produced by means of compression moulding (Aziz et al. 2004). Composite mechanical properties are strongly influenced by the mechanical properties and distribution of the fibers and matrix, as well as the efficiency of stress transfer between the two components. Mechanical properties such as strength and stiffness are of great importance when designing composite products and can be predicted for short fiber composites with varying degrees of accuracy by means of mathematical prediction models. The mechanical properties of short fiber composites are far more difficult to predict than continuous fiber composites. This is due to the complexities of determining parameters such as fiber dispersion, orientation and geometry (aspect ratio) of the fibers within the composites, fiber and matrix volume fractions and the interfacial shear strength between the fibers and matrix (George et al. 1996).

1.2 Natural Fiber Reinforced Thermoset Composites

The charm of using synthetic fibers in polymer composites is fading because they are expensive, non-biodegradable and pollute the environment. Availability of inexpensive lignocellulosic fibers in tropical countries provides a unique opportunity of exploring the possibility of their utilization for the synthesis of inexpensive biodegradable composites for various applications.

High performance carbon and aramid (e.g. Kevlar^{TM}) fibers are the most commonly used reinforcements for composites where exceptional strength, high stiffness and low density are required. They are prohibitively expensive for use in more general applications; therefore, cheaper alternatives such as glass fiber are more commonly used in industry. Glass fibers have many benefits, including low cost and relative ease of manufacture, as well as possessing moderate strength and stiffness to weight ratios. However, they also have many disadvantages (Wambua et al. 2003).

They tend to be abrasive, thus making them dangerous to work with, as well as increasing the wear on processing machinery. More importantly, glass fibers could present a health risk to those working with them. The biggest problem with glass and other synthetic fibers is that they are difficult to dispose of at the end of their lifetime. Glass fiber reinforced composites cannot be incinerated as the residues tend to cause furnace damage, and there are problems associated with the recycling of glass fiber reinforced thermoplastics due to fiber breakages that occur during reprocessing operations. The only method of disposal is to discard the waste in landfills, which is becoming more costly in many countries with the introduction of landfill taxes (Bos et al. 2002). The properties of natural fiber in relation to those of E-glass can be seen in Table 1.1

Table 1.1 Properties of natural fibers in relation to those of E-glass

Fiber	Density (g/cm^3)	Strength (MPa)	Modulus (GPa)
Indian grass	1.25	264	28
Hemp	1.29	695	42-70
Kenaf	1.4	284-800	21-60
Henequen	1.57	372	10
Pineapple leaf fiber (PALF)	1.44	413-1627	35-83
Jute	1.3-1.45	393-773	13-27
Flax	1.5	345-1100	28-80
E-Glass	2.5	2000-3500	70

Sources: (Mohanty et al. 2000) (Mohanty et al. 2002), (Mohanty et al. 2005), (Cazaurang-Martinez et al.1991), (Aguilar-Vega et al. 1995), (Lee 1991), (Chen et al. 1994).

Natural fibers require very little energy to produce, and because they possess high calorific values, can be incinerated at the end of their lifetime for energy recovery. All plant-derived fibers utilize carbon dioxide when they are grown and can be considered CO_2 natural, meaning that they can be burned at the end of their lifetime without additional CO_2 being released into the atmosphere (Mohanty et al. 2002) . On the other hand, glass fibers are not CO_2 natural and require the burning of fossil fuels to provide the energy needed for production. The burning of fossil fuel-based products releases enormous amounts of CO_2 into the atmosphere and this phenomenon is believed to be the main cause of the greenhouse effect and the climatic changes that are being observed in the world today (Wambua et al. 2003). The geometry and properties of natural fibers depend, for example, on the species, growing conditions, cambium age, harvesting, defibration and processing conditions. Since cellulose fibers have the possibility to show a wide range with both poor and strong bonding to polymer matrix materials, depending on fiber-matrix modification and compatibility, the optimal interface is typically somewhere between the two extreme cases. For instance, if the interface is too strong, the composite material can become too brittle, resulting in a notch-sensitive material with low strength, since stress concentrating defects are inevitable (Gamstedt et al. 2007).

Natural fiber-reinforced thermoset composites are now finding extensive uses in various fields from household articles to automobiles. The primary advantages of natural fibers over synthetic fibers have been their low cost, light weight, high specific strength, renewability, and biodegradability (Mohanty et al. 2002). The physical and mechanical properties of the natural fibers are determined by their chemical and physical composition, such as the structure of the fibers, cellulose content, microfibrillar angle,

cross section, and the degree of polymerization. Absorption of moisture causing swelling of the fibers has been a major drawback for natural fibers, which leads to a weak bond at the fiber resin interface in the composites. Natural fibers, however, display large variations in fiber properties from plant to plant, such as strength, stiffness, fiber length and cross sectional area. These variations can ultimately lead to difficulties in composite design and performance predictions. Natural fibers are also thermally unstable compared to most synthetic fibers, and are limited to processing and working temperatures of 200°C. Another major drawback when using natural fibers is the fact that they are hydrophilic (absorb water) and polar in nature (Plackett 2002), whereas common thermoset matrices such as polyester resin are hydrophobic (do not absorb water) and non-polar.

Polyesters, vinylesters, and epoxies probably account for some 90% of all thermosetting resin systems used in structural composites. The properties are given in Table 1.2. There are two principal types of polyester resins used as a standard laminating system in the composite industry. Orthophthalic polyester resin is the standard economic resin commonly used, and it yields highly rigid products with low heat resistance. Isophthalic polyester resin is now becoming the preferred material in the marine industry, with its superior water resistance (Mohanty et al. 2002).

Table 1.2 A comparative study of polyester, epoxy, and vinylester resin

Properties	Polyester Resin	Epoxy Resin	Vinylester Resin
Density (g/cm^3)	1.2-1.5	1.1-1.4	1.2-1.4
Young's modulus (GPa)	2-4.5	3-6	3.1-3.8
Tensile strength (MPa)	40-90	35-100	69-83
Compressive strength (MPa)	90-250	100-200	----
Tensile elongation to break (%)	2	1-6	4-7
Cure shrinkage (%)	4-8	1-2	----
Water absorption 24 h at 20 °C	0.1-0.3	0.1-0.4	----
Fracture energy (KPa)	----	----	2.5

Sources: (Sarkar et al. 1997), (Iijima et al. 1991)

1.3 Application of Natural Fiber Composites

It is becoming increasingly difficult to ignore the important role of natural fiber composites in advanced technology. Due to the environmental issues, many natural fiber composites are used today at the leading edge of materials technology, enabling

their use in advanced applications such as internal parts of automotive and building structures. The use of natural fibers, such as flax, sisal, or kenaf to reinforce plastic body panels for automotive applications is being introduced for car interior trim parts such as door and window panels, hat shelves, and roofing, as shown in Figure 1.1. Not only do panels made of natural fibers have good mechanical properties but they also are lighter than glass fiber reinforced panels, which means lower fuel consumption and therefore cost saving. Moreover, as a renewable product, natural fibers have a greater environmental interest than oil-based plastics. Recently, plant fibers have also been used in exterior composite components: the engine and transmission covers of a Mercedes-Benz Travego. In 2002, the total consumption of plant fibers was about 17,000 tones, and the average amount of fibers per vehicle was 10-15 kg. The industrial use of plant fibers is not only driven by reductions in cost, but also by issues related to environmental awareness. In Europe, the EU "end of life vehicle" directive imposes that 85 % of the weight of all vehicle components should be recyclable by 2005 which should be increased to 95 % by 2015 (Madson et al. 2003). In relation to plant fiber composites, the term "recyclable" is somewhat unresolved (Peijs 2002). Plant fibers are fully recyclable by combustion, as well as being fully biodegradable, but the same cannot be implied for the remaining synthetic polymeric matrix and chemical additives.
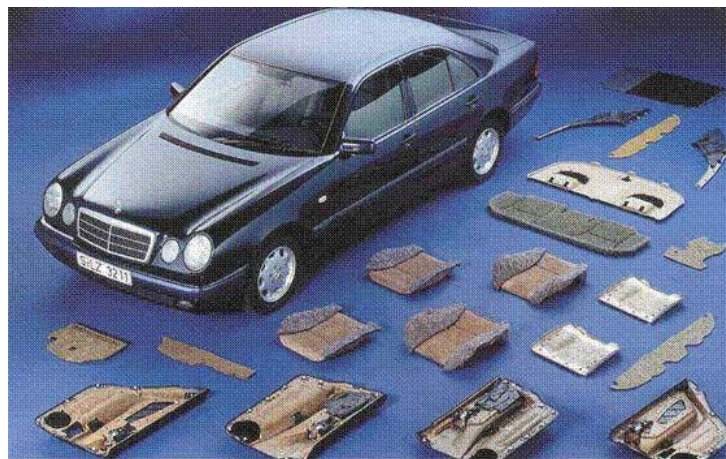
Figure 1.1 Mercedes-Benz 20% weight saving achieved with flax/sisal thermoset door panels (Evans et al. 2002)

Finally, natural fibers can be recycled and reused in a better way than glass fibers. In recent years, there has been an increasing interest in proving the plant's suitability for use in building materials particle boards of various densities, thicknesses, with fire and insect resistance), adsorbents, textiles, livestock feed, and fibers in new and recycled

plastics (injected molded and extruded) (Gharles et al. 2002). The use of natural fiber composites is not limited only to the automotive industry. At least 20 manufacturers are producing wood fiber reinforced thermoplastic decking for the American markets (Clemons 2002). Window and door profile manufacturers from another large industrial segment uses wood fiber reinforced polymers (Plackett 2002). Other natural fiber composites applications that have been reported include walls, flooring, louvers, and indoor and outdoor furniture (Nickel et al. 2003). It is necessary to improve the strength and stiffness of these composites, as well as confront issues such as water absorption and thermal instability before they can be used to their full extent in industry.

1.4 Methodology and Workflow

The aim of this research is to accomplish a greater understanding of the various parameters that contribute to composite strength and stiffness, and to influence these parameters in order to produce an improved hybrid kenaf stem fiber and recycled jute fiber reinforced unsaturated polyester resins. The methodologies included experimental investigations and theoretical modelling. The project was divided into three phases.

In the first phase, the rheological properties of the unsaturated polyester (UP) containing different concentrations of styrene (ST) via measuring viscosity, gel time, maximum exotherm temperature were investigated by adding different ratios of the catalyst Methyl Ethyl Ketone Peroxide (MEKP) and the Dimethyl Aniline (NNDMA), the curing accelerator. Besides, this study looked at the curing reaction process of unsaturated polyester by adding different weight fractions of kenaf fiber. This is a very important stage in processing of unsaturated polyester resin for producing a composite product of high quality. In addition, the study looked at the mechanical properties such as tensile, flexural and impact for UP resin at different ST, MEKP and NNDAM concentrations. Furthermore, the study effects of water absorption on flexural and tensile properties of unsaturated polyester. The dynamic mechanical analysis test was used to study the behaviour of UP resin properties and degradation temperature, using thermo gravimetric analysis TGA.

In the second phase, the physical and mechanical properties of kenaf fiber were observed experimentally. This covered: length, diameter, density, water absorption, tensile strength and Young's modulus, and comparison with the findings reported in literature. The percentage ratio of holocellulose content, of bast and core kenaf fiber was investigated. The effects of chemical treated on kenaf fiber were studied.

The third and final phase saw the study of the most important parts in this research, the physical and mechanical properties of kenaf/unsaturated polyester composites, via adding different styrene concentration. Parametric studies were conducted to identify the influences of several key parameters on the structural of composites fiber loading, fiber length and fiber treatment. The fibers matrix interaction by Scanning Electron Microscopy (SEM) was investigated. Moreover, the study effects of water absorption on the suitability of kenaf composites and kenaf/recycled jute unsaturated polyester composites in outdoor applications. Therefore, the water absorption behavior of kenaf fiber unsaturated polyester composites for different temperatures and various weight fractions of fiber as well as the effects of water absorption on flexural properties, on kenaf fiber composites were investigated. A comparison was made between experimental data and different theoretical models. A comparison was made between experimental data and different theoretical models. The experimental data was cross – matched against composite models, such as Hirsch, Einstein-Guth, modified Bowyer-Bader, Kelly-Tyson, Parallel, modified Guth, Cox-Krenchel, and Halpin-Tsai. In addition, fiber zero-stress aging, have model was used to fit the experimental immersion time data. Finally, the parameters set by the DMA machine; to study in close detail, the changes in loss and storage modulus including the maximum peak reading of tan delta which is known as the term called glass transition temperature. Dynamic mechanical analysis was performed to obtain strain and creep compliance for kenaf composites of various styrene concentrations. It is possible to obtain creep curves at different temperature levels which can be shifted along the time axis to generate a single curve know as a master curve. This technique is known as the time temperature superposition principle. Shift factors conformed to a William-Landel-Ferry (WLF) equation. In addition, this study investigated the effects of the fiber content on the dynamic properties, using DMA test and degradation temperature, and thermo gravimetric analysis TGA.

1.5 Thesis Outline

The following chapters are arranged in the same manner as the workflow and are summarised as follows:

Chapter Two presents a literature review on the research status of the three phases including the methodology and workflow for the purpose of physical and mechanical properties of composites. The chapter covers most of the available methodologies and corresponding outputs at the beginning of this project, and some of the most related current results at the end of the respective projects. The literature review also includes a comparison between the natural fiber properties and thermoset resin.

Chapter Three describes the materials and methods use in this research project. This investigation consists of two major parts: the experimental test and analytical analysis. The experimental work is divided into four stages. The first stage is the preparation of short kenaf and recycled jute fibers. The second stage is to determine the properties of unsaturated polyester, such as viscosity and tensile strength and Young's Modulus. The third stage is about characterization of all the parameters of fibers, such as tensile strength and Young's Modulus. The last stage evaluates the various physical and chemical attributes, such as strength, Young's modulus, interfacial adhesion, and thermal stability for composites.

Chapter Four studies the curing behaviour of unsaturated polyester containing different concentrations of styrene monomer via measuring viscosity, gel time, and maximum exotherm temperature. In addition, the effects of styrene concentrations on the tensile and modulus properties of UP resin are studied. The MEKP with different concentrations was used as initiator for curing the UP resin and NNDMA curing accelerator at different ratios. The effects of varying the level of water content on the exotherm behaviour were investigated. A dynamic mechanical analysis test was used to study the behaviour of UP resin such as glass transition temperature Tg at different ST, MEKP and NNDMA.

The physical and mechanical properties of kenaf fiber were observed experimentally: length, diameter, density, water absorption, tensile strength and Young's modulus. The percentage ratios of holocellulose content, of bast and core kenaf fiber were investigated and water absorption, all these properties are reported in Chapter Five.

The mechanical and dynamics of kenaf composites are the main concern of Chapter Six. These cover the tensile, the flexural and the impact properties. Water absorption, thickness swelling behavior of kenaf composites and kenaf/recycle jute composites were also investigated. Thickness swelling rate model that describes the hygroscopic process of natural fiber based composites was used to obtain the diffusion coefficients and swelling rate parameters by fitting the model predictions with the experimental data. Further, the effects of alkali treatment and post curing on the mechanical properties of composite were investigated. The parameters set by the DMA machine; to study in close detail, the changes in loss and storage modulus including the maximum peak reading of tan delta which is known as the term called glass transition temperature. Short-term creep tests were performed with a DMA machine. The creep tests were run in tensile mode. This procedure was followed for two different temperatures and for various weight fractions of kenaf fiber composites. In addition, the effects of the fiber content on the dynamic properties, using DMA test and degradation temperature, using thermo gravimetric analysis TGA were studied.

The findings and conclusions of this research, as well as suggestions for future work, are summarized in Chapter Seven.

CHAPTER TWO

LITERATURE REVIEW

2.1 Overview

Composite is composed of two main components: the fiber as reinforcement and the matrix. The reinforcing element is able to support high tensile loads although the matrix imparts rigidity to the composite. The application of stress on the composite is results transfer of the loads from one fiber to another, via the matrix. The stiffness of the matrix is often accompanied by brittleness. Nevertheless, the combination of fiber and matrix makes for a tough material. The composites may fail by one or two mechanisms plastic flow or brittle cracking. Based on existing experience and knowledge of synthetic fiber composites, the mechanical behavior of plant fiber composites has been extensively characterized and analyzed. The work has mainly addressed measurements of pure tensile properties, as well as bending and impact properties. A considerable amount of literature has been published on composites containing lignocellulosic fibers produced by the forest and paper industry such as cellulose, wood fiber and wood dust. Other studies have looked at agricultural fibers such as kenaf, pineapple, sisal, hemp, coir and rice husks.

2.2   Natural Fibers

Natural fibers are subdivided based on their origins, whether they are derived from plants, animals, or minerals, Figure 2.1 shows a classification of natural fibers. Plant fibers include bast (or stem or soft or sclerenchyma) fibers, leaf or hard fibers, seed, fruit, wood, cereal straw, and other grass fibers (Ichhaporia 2008). Natural fibers are generally lignocelluloses in nature, consisting of helically wound cellulose micro fibrils in a matrix of lignin and hemicellulose (Taj et al. 2007). The use of natural fibers composites matrices is highly beneficial because the strength and toughness of the resulting composites are greater than those of the un-reinforced matrix. Moreover, cellulose-based natural fibers are strong, light in weight, very cheap, abundant and

renewable. Lignocellulosic natural fibers like the pineapple leaf fiber come as a viable and abundant substitute for the expensive and nonrenewable synthetic fiber (Mokhtar et al. 2005). These fibers with high specific strength improve the mechanical properties of the polymer matrix. In tropical countries, like Malaysia, fibrous plants are available in abundance and at least some of them are agricultural crops. The properties of the single fibers depend on the crystallite content, size, shape, orientation, thickness of cell walls. This different structure is reflected in the stress-strain diagrams of the fibers. The mechanical properties of natural fibers are presented in Table 2.1.
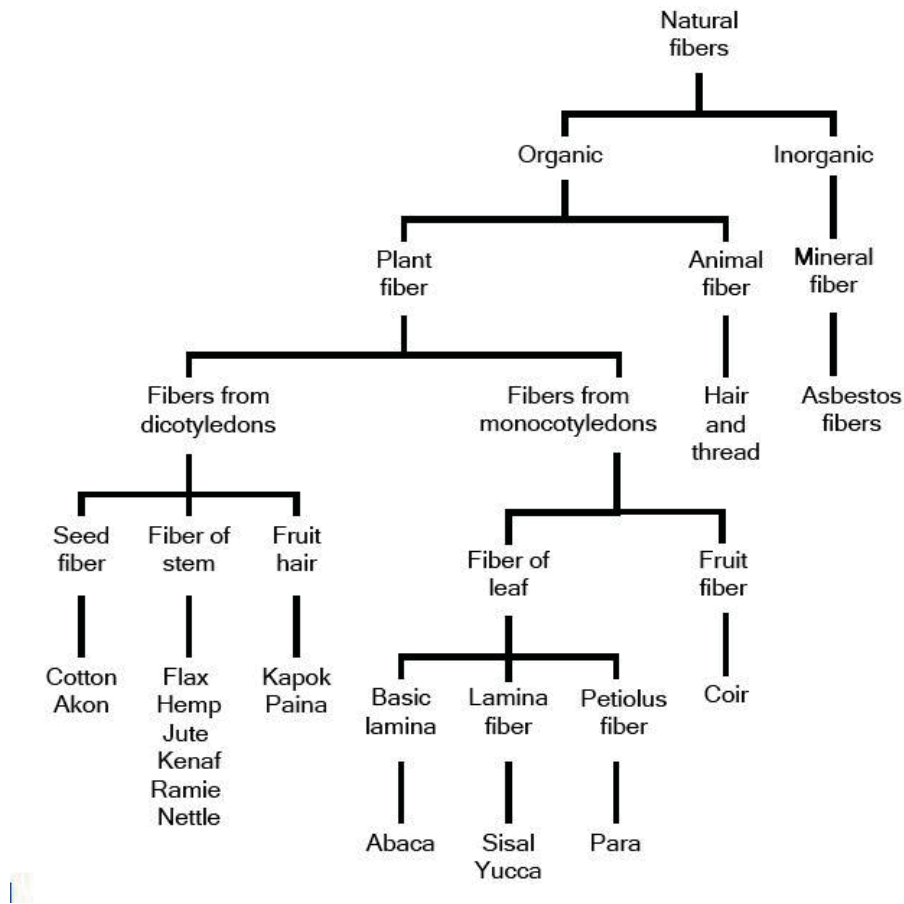
Figure 2.1 Classification of natural fibers (Ichhaporia 2008)

Table 2.1 Properties of natural fibers and synthetic fibers (Ichhaporia 2008)

Type of fiber	Density g/cm3	Tensile Strength MPa	Young's Modulus GPs	Elongation at beark %
Cotton	1.5-1.6	287-800	5.5-12.6	7.0-8.0
Jute	1.3-1.45	393-773	13-26.5	1.16-1.5
Flax	1.50	345-1100	27.6	2.7-3.2
Hemp	-	690	-	1.6
Sisal	1.45	468-640	9.4-22.0	3-7
Kenaf	1.4	930	53	1.6
Pineapple	-	413-1627	34.5-82.51	1.6
Coir	1.15	131-175	4-6	15-40
E-glass	2.5	2000-3500	70	2.5
Carbon	1.7	4000	230-240	1.4-1.8

2.3 Comparisons of Natural Cellulose Fibers

Cellulose fibers have been used for long long time in the manufacture of various products such as rope, string, clothing, carpets and other decorative products. Today, one of the major uses of kenaf fiber is to make a range of paper and cardboard products as a substitute for wood fibers which are the most abundantly used cellulose fibers. The most efficient cellulose fibers are those with high cellulose content coupled with a low micro-fibril angle in the range of 7-12° to the fiber axis (Bos et al. 2002). It was determined that pulping kenaf requires less energy and chemical inputs for processing than standard wood sources. Because of environmental problems (artificial fiber produce long-term pollution), this application of kenaf fiber has drawn tremendous attention in the world (Bert 2002), although the use of other fiber types is increasing.

There are several physical properties that are significant to selecting suitable cellulose fibers for use in composites: fiber dimensions, structure, defects, crystallinity, variability, cost (Rowell 2000). Mechanical properties are even more important when selecting a suitable fiber for composites reinforcement. To produce a strong composites material, it is important to utilize strong reinforcing fibers. Nevertheless, fiber strength

is not the only promoting factor to composites strength, as excellent bonding between the fibers and matrix, good fiber orientation and good fiber dispersion are also demanded. Table 2.2 shows the composites of the kenaf fiber whole stalk.

Table 2.2 Details of the composites of the whole stalk kenaf fiber (Chen et al. 1995)

Kenaf fiber	Ash (%)	A-Cellulose (%)	Semi-cellulose %	Lignin (%)
Bark	5.5-8.3	53.0-57.4	NA	5.9-9.3
Core	2.9-4.2	51.2	NA	17
Whole stalk	2.1-6.5	47.3-57.3	31.5-38.4	4.7-16.1

Kenaf was chosen for this research because it is a new fiber crop grown commercially in the world; other fibers isolated from annual growth crops have a potential as reinforcing fillers in plastics. The choice of the fiber for plastics applications depends on the availability of the fiber in the region and also on the ultimate composites properties needed for the specific application.

2.4 Kenaf fiber

2.4.1 Kenaf Fiber Industrial

The Kenaf whole stalk and outer bast fibers have many potential specific uses, including as paper, textile, and composite. The use of kenaf fibers is also of particular significance from the standpoint of environmental friendliness. Historically, kenaf fibers were used to manufacture rope, twine, sackcloth and fish net because of its rot and mildew resistance (Cook 1960). Currently, various new applications for kenaf products are emerging, including those for paper products, building materials, absorbents, feed, and bedding for livestock (Webber 2002). In view of the resultant environmental problems and increased paper consumption, this application of kenaf fiber has drawn tremendous attention in the world (Bert 2002). The new uses of kenaf include the fields of involving medicine, food additives and mushroom cultivation. The use of the kenaf core with wood powder as a plant medium to produce mushrooms is much better than only wood powder (Liu 2005). The kenaf core is strong and absorbent and it can be used to clean up oil spills as well as chemicals. Kenaf can absorb CO_2 and NO_2 3-5 times faster than forests, and its deep roots can improve that soil (Lam 2000). Lastly kenaf bedding has superior absorbency, and is labor our saving, and cheaper than most traditional litter and

bedding products comprising wood shaving, saw dust or shredded paper (Li 2002). Kenaf natural fiber reinforced plastics are light and easy to process. They can be used to replace glass-reinforced plastics in many cases. Kenaf compound panels have the mechanical and strength characteristics of glass –filled plastics. Besides, they are less expensive and completely recyclable in many instances (Kano 1997). They can be used in the automotive industry, construction, housing, and food package industry (Zhang 2003).

The viability of using kenaf fiber and plastic in producing thermoplastic composite was studied by Chow et al.(2000). They demonstrated the viability of using kenaf fiber and plastics in producing thermoplastic composites. This report presents the progress of their research which concentrates on optimizing the manufacturing techniques and testing both air-laid non-woven and melt-blended kenaf/plastic composite panels from kenaf bark fiber. Table 2.3 summarizes the properties of the kenaf bast fiber.

Table 2.3 Physical and mechanical properties of the kenaf stem fiber

Properties	Units	Kenaf Fiber
Density	(g/cm^3)	1.4
Water absorption in 24 h	%	1.05
Tensile Strength	(MPa)	930
Flexural Strength	(MPa)	98000
Specific Strength	(KN.m/Kg)	61
Young's Modulus	(MPa)	53000
Flexural Modulus	(MPa)	7300
Elongation at Break	(%)	1.6
Fiber length average(range)	(mm)	2-6
Diameter	(μm)	17.7-21.9
Cellulose	(Wt %)	45-57 for Bast 37-49 for Core
Hemicelluloses	(Wt %)	21.5
Lignin	(Wt %)	8-13
Moisture Content	(Wt %)	4.1
Pectin	(Wt %)	3-5

Sources: (Beckermann 2007), (Idicula et al. 2006), (Mohanty et al. 2005), (Mokhtar et al. 2007) and (Taj et al. 2007).

2.4.2 Kenaf Plant Morphology

The kenaf (Hibiscus cannabinus) is an annual non-woody plant which has shown great potential as an alternative source of papermaking fiber. It has a high growth rate, reaching heights of 4-6 m in about 4-5 months and it yields 6-10 tonnes of dry mass per acre each year. It has erect, branched or unbranched stalks reaching a height of 1-4 m, and either slender green, red, or purple prickly.
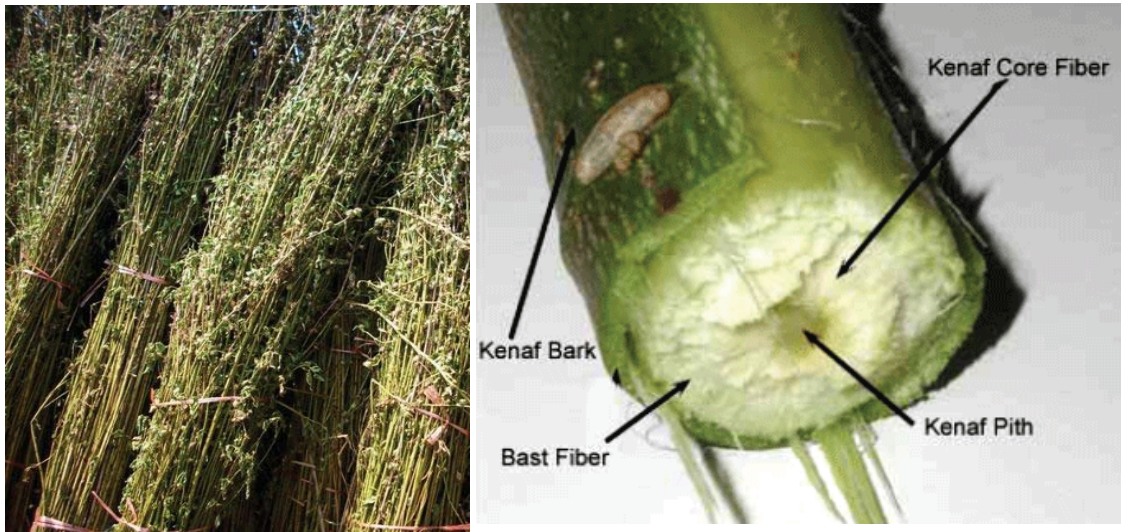
Figure 2.2 Stalk of the kenaf plant (Xue et al. 2007)

The stalks of the kenaf are generally round, and depending on the variety, with tiny thorns on the stalks, as can be seen in Figure 2.2. There are two distinct fiber types of the kenaf: the outer, bast fibers which comprise about 40% of the stalk dry weight and the inner, core fibers that comprise about 60% of the stalk's dry weight (Lin et al. 2004). Figure 2.3 shows the kenaf plant, kenaf long bast fiber and kenaf short fiber. The bast fibers have a lower lignin content, higher cellulose content, and lower hemicellulose content compared to the core fibers. The whole kenaf stem has a lower lignin and cellulose content, and hemicelluloses and ash content comparable to softwood.

Fiber morphology results show that kenaf bast fibers are long and slender, while the core fibers are much shorter and wider (Alireza 2004). The raw kenaf fiber obtained from the outer bark is actually a bundle of lignocellulosic fibers. The fiber bundle size depends on the number of ultimate cells in each bundle. Most lignin is present between the ultimate cells. Kenaf contains approximately 65.7% cellulose, 21.6% lignin and pectin, and other composition. Lignin must be extracted to separate the fibers (Kaldor

1989, Tao et al. 1994, and Tao et al. 1997). The physical dimensions of the fiber are one of the most important factors in the apparel industry. Figure 2.4 shows the photomicrographs of the cross-section of an individual kenaf fiber and fiber bundles (Moreau et al. 1995 and Bel-Berger et al. 1999).

Figure 2.3 The long and short fibers, Kenaf Natural Fiber Industries Sdn. Bhd.
http://www.kenaffiber.com
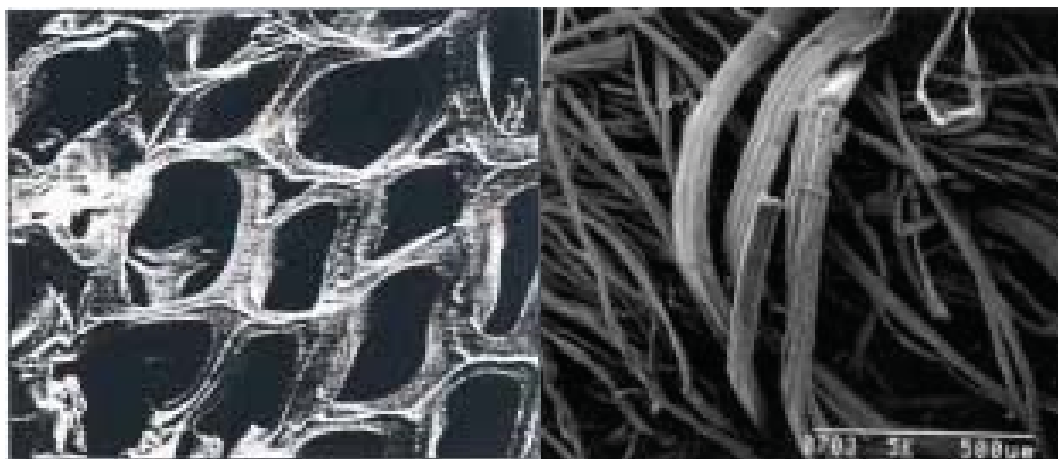
Figure 2.4 The kenaf fiber images (Moreau et al. 1995)

2.4.3 Factors affecting Kenaf Fiber properties

Natural kenaf fiber is like a bundle of lignocellulose fibers. The fiber size depends on the number of ultimate cells in each bundle. Single kenaf fibers are 1-7 mm long and about 10-30 microns wide. The length of kenaf fibers is shorter at the bottom of the

17

stalk and longer at the top (Rowell et al. 1999). The increase in length from the bottom to the top is not gradual, but S-shaped. Fiber length grows in the early part of the plant cycle, and reduces again as the plants mature (Chen et al. 1995). The geometry and properties of natural fibers depend on factors such as species, growing conditions, cambium age, harvesting, defibration and processing conditions. This variation makes it more difficult to analyse the effects of the fibers and their interfaces on the mechanical properties of the composite material. These difficulties call for the development of new strategies to assess the mechanical influence of the interface (Gamstedt et al. 2007). The mechanical properties of single fibers are strongly influenced by many factors, particularly chemical composition and internal fiber structure, which are at variance between different parts of a plant as well as different plants. Other factors that may affect the fiber properties are maturity, separating processes, microscopic and molecular defects such as pits and nodes, soil type and weather conditions under which they are grown. The highly oriented crystalline structure of cellulose makes the fibers stiff and strong in tension, but also sensitive towards kink band formation under compressive loading. The presence of kink bands significantly reduces fiber strength in compression and in tension (Beckermann 2007). Kenaf's production is less costly and less time-consuming than other raw crops, given that it produces a high yield with a minimal use of chemicals (George et al. 1999).

Ochi 2008 investigated the effect of environmental temperature on the growth of the kenaf fiber and on the tensile and elastic properties of the kenaf fiber, an emulsion-type PLA resin composite. He found instituted that the kenaf grown at an average temperature of 22°C was 2000 mm and the kenaf grown at an average temperature of 30°C was 3650 mm after 168 days. In addition, he concluded that the fabrication of high strength kenaf fiber reinforced plastic required fibers obtained from the section of the plants closest to the ground. Figure 2.5 shows the tensile strength and elastic modulus of kenaf fibers grown in different temperatures. It confirms that the tensile strength and elastic modulus of kenaf grown under an average temperature of 30°C were greater than those grown under average temperature of 22°C. Table 2.4 lists the average tensile strength and Young's modulus of kenaf bast fiber based on prior research.
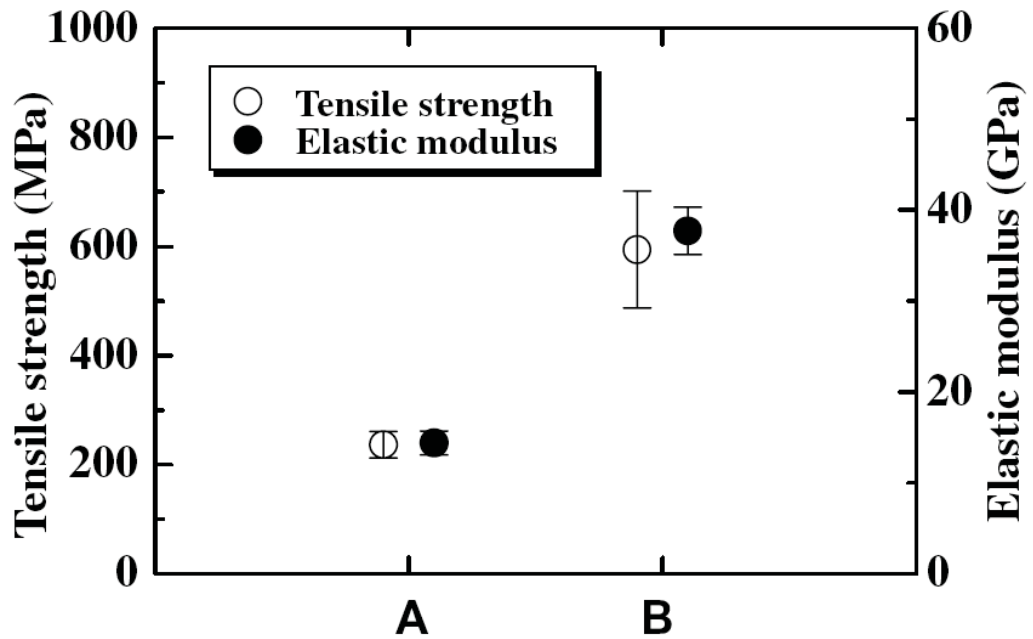
Figure 2.5 Tensile strength and elastic modulus of kenaf fiber, (A=22°C, B=30°C) (Ochi 2008)

Table 2.4 Physical properties of kenaf fiber

Tensile Strength (MPa)	Young Modulus (GPa)	References
930	53	(Mohanty et al. 2005)
400	-	(Kenaf Eco Fiber 2005)
250-600	14-39	(Ochi 2008)
335	22	(Shibata et al. 2006)
350 -600	40	(Kenaf Eco Fiber 2005)
250	4.3	(Lee et al. 2009)
223	15	(Öztrkü 2010)
448	24.6	(Cao et al. 2007)
135-232	15-24	(Harun et al. 2009)

2.5 Matrix Materials

As a whole, matrix materials cover the range from polymers to metals to ceramics. The matrix is a substance that is capable of holding the reinforcing materials together by surface connection. Matrix can also be defined as material that gives body and holds the reinforcement of the composite together, and is generally of lower strength than the

reinforcement. The plastic matrix has a low density but is not very strong or stiff. The fibrous reinforcement can be very strong and stiff, but needs a medium to protect the fibers and transfer loads among them. The combination can offset its constituents' weaknesses and be very light, strong, and durable. Moreover, modifying the choice, proportions, and geometry of the component can give variety to the resulting engineering properties (having different physical properties at different levels of measurement) and over a vast range (Reinhart et al. 1987). The matrix also serves as a binder which holds reinforcing materials in place. Besides that, when a composite is subjected to an applied load, the matrix disintegrates and transfers the external load uniformly to the fibers. The matrix also provides resistance to crack propagation and damage tolerance owing to the plastic flow at cracked tips.

Furthermore, the matrix functions to protect the surface of fibers from adverse environmental effects and abrasion especially during composite processing (Kathiresen 2004). The matrix also keeps the reinforcing fibers in the proper orientation and position so that they carry the intentional loads, distribute the loads more or less evenly among the fibers, provide resistance to crack propagation and damage, and prepare all of the interlaminar shear strength of the composite. Furthermore, the matrix generally determines the overall service temperature limitations of the composite, and also controls its environmental resistance (Reinhart et al. 1987). The matrix is used to embed such strong fibers required to provide a strong and stiff solid base for engineering purposes. The properties of the matrix are usually chosen as complementary to the properties of the fibers; for example, excellent toughness in a matrix complements the tensile strength of the fibers. The resulting combination then achieves high strength and stiffness due to the fibers and resistance to crack propagation, and due to interaction between fibers and the matrix.

Matrices are generally be classified into two major types, which are thermoplastics and thermosets. The selection criteria of the matrices depend only on the composite end use requirements. For example, if chemical resistance together with elevated temperature resistance is needed for a composite material, then thermoset matrices are preferred rather than thermoplastics. In contrast, when a composite material with high damage tolerance and recyclables is needed, then thermoplastics are preferred (Azura 2007).

2.5.1 Thermoset

Thermoset resin is defined as a plastic material which is initially a liquid monomer or a pre-polymer, which is cured by either application of heat or catalyst to become an infusible and insoluble material (Sinha 2000). Thermosets polymers have covalent bonds linking the polymer chains in three dimensions. These links prevent the chains from sliding past one another resulting in a higher modulus and improved creep resistance. This liquid resin is converted to a hard rigid solid by chemical cross-linking through a curing process which involves the application of heat and the addition of curing agents or hardeners. Once cured, a tightly bound three dimensional network structure is formed in the resin and hence the resin cannot be melted, reshaped or reprocessed by heating. Therefore, during composite manufacturing, the impregnation process followed by the shaping and solidification should be done before the resin begins to cure (Kathiresen 2004). Thermosets resins are brittle at room temperature and have low fracture toughness. However, in an environment such as water or moist air, the micro-cracked laminate absorbs considerably more water than an uncracked laminate. This then leads to an increase in weight, moisture attack on the resin and fiber sizing agents, loss of stiffness, and an eventual drop in ultimate properties with time. Increased resin/fiber adhesion is generally derived from both the resin's chemistry and its compatibility with the chemical surface treatments applied to fibers. Here the well-known adhesive properties of epoxy help laminates achieve higher microcracking strains (Penczek 2005). As has been mentioned previously, resin toughness can be hard to measure, but is broadly indicated by its ultimate strain to failure. Figure 2.6 shows comparison for various resin systems. On the other hand, owing to its three dimensional cross-linked structure, thermoset resins have high thermal stability, chemical resistance, high dimensional stability and also high creep properties. Among the most common thermosetting resins used in composite manufacturing are unsaturated polyesters, epoxies, vinyl-esters and phenolics. Usually thermosets are more brittle than thermoplastics (Rahmat et al. 2003).
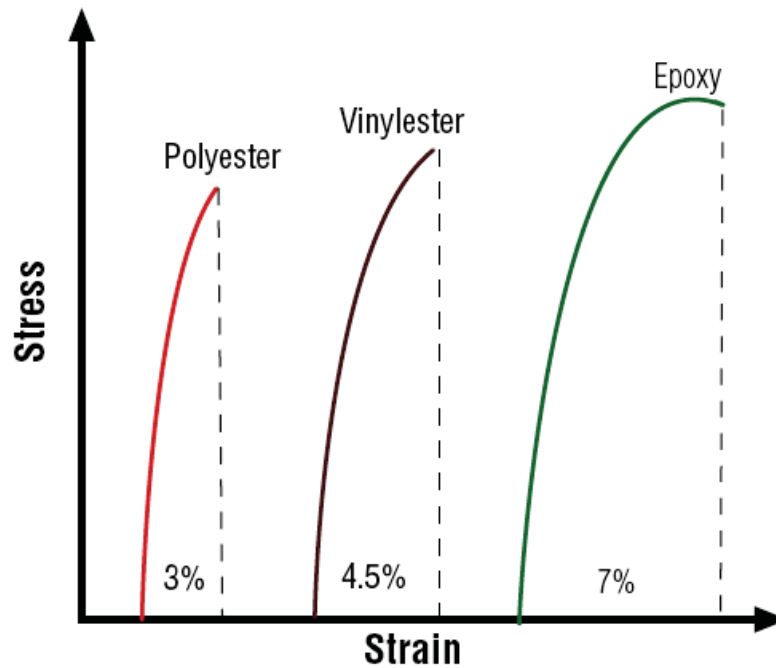
Figure 2.6 Typical resin stress/strain curves (www.spsystems.com**)**

Polyesters, vinylesters, and epoxies probably account for some 90% of all thermosetting resin systems used in structural composites. The main advantages and disadvantages of each of these resins are given in Table 2.5.

Table 2.5 A comparative study of the advantages and disadvantages of thermosetting resins

Resin	Advantages	Disadvantages
Polyester	Easy to use Lowest cost of resins available (£1-2/kg)	Only moderate mechanical properties High styrene emissions in open molds High cure shrinkage Limited range of working times
Vinylester	Very high chemical/environmental resistance Higher mechanical properties than polyesters	Postcure generally required for high properties High styrene content Higher cost than polyesters (£2-4/kg) High cure shinkage
Epoxy	High mechanical and thermal properties High water resistance Long working times available Temperature resistance can be up to 140°C (wet)/220°C (dry) Low cure shrinkage	More expensive than vinylesters (£3-15/kg) Critical mixing Corrosive handling

Sources: (Pritchard 1980), (Sarkar et al. 1997), (Mukherjee et al. 1984), (Iijima et al. 1991)

2.5.2 Crosslinking of Unsaturated Polyesters

Sequentially to get a rigid, structural material the prepolymer-styrene solution can be cross-linked by a user into a rigid thermoset in a free radical copolymerization between the styrene monomer and the polyester double bonds origination from the unsaturated dicarboxylic acid (Skrifvars 2000). The copolymerization is initiated by peroxides activated by a redox reaction with cobalt salts or thermally. Through the crosslinking the resin undergoes gelation, which is a dramatic physical revolution. The viscosity increases rapidly, the resin becomes elastic and begins to behave like rubber (Åström 1997). The extent of the reaction at which an infinite molecular network starts to form is called the gel point, and the time to achieve it is the gel time (Shukla et al. 2006). The chemical reaction continues in the gel state, and more polyester is linked to the network. The polyester will finally be linked to each other at several points in the network, and one gigantic molecule is formed. The crosslinking reaction is an extremely exothermic reaction, and the temperature can increase up to 100-200°C, depending on the resin composition, laminate thickness, and initiator system (Skrifvars 2000). Even when the final solid state is achieved, there will be un-reacted styrene monomers and double bonds left. This residual reactivity can be removed by postcuring simply by heating at a temperature higher than the glass transition temperature of the crosslinked unsaturated polyester. This progression of network formation is often named in the literature as curing, and the degree of cure is taken as the crosslinking density (Shukla et al. 2006).

2.5.3 Curing Agents

The curing system consists of two components, peroxides (catalyst) and cobalt's (accelerator). The most common catalysts used are commercial Methyl Ethyl Ketone Peroxide (MEKP) and Cyclohexanone Peroxide as catalysts and Dimethyle Aniline (NNDAM) as an accelerator. MEKP is in liquid form whilst Cyclohexanone Peroxide is in powder form. MEKP is easily measured using a burette but great care must be taken to ensure the liquid is uniformly spread (Chin 2008). The curing reaction is a very complicated process that is affected by many different factors, such as weather, humidity, resin uniformity, conditions of ingredients as they are stored, suppliers, equipment conditions (Strong 1989).

The curing behaviour of an unsaturated polyester resin was studied by gel time and pseudo-adiabatic exotherm measurements (Beheshty 2005). He concluded that an

increase in the concentrations of initiator (Either Methyl Ethyl Ketone Peroxide or Acetyl Acetone Peroxide) or Cobalt Octoate Accelerator decreased the gel time in a reciprocal fashion and increased the rate of polymerization. Various combinations of low- and high-decomposition temperature initiators and dual promoters were used to cure an unsaturated polyester resin. Methyl Ethyl Ketone Peroxide (MEKP) and Acetyl Acetone Peroxide (AAP) solutions were used as low-temperature initiators Benzoyl peroxide (BPO) and T-Butyl Perbenzoate (TBPB) were used as medium and high-temperature decomposition initiators respectively (Kuang 2006). The dual initiator effect on exotherm reaction has been reported by Atta et al. (2005), and the overall results show that the dual initiator or a dual promoter can avoid short time exothermic reactions. The compressive properties and the curing behaviour of the unsaturated polyester resins in the presence of Vinyl Ester resin were investigated by Cook (1990). His results show that increasing the cure temperature and the vinyl ester content led to a pronounced improvement in compression strength and Young's modulus. There are some additives that slow down the curing reaction such as inhibitors, styrene, filler, oxygen, flame retardants, reinforcements, and mold heat capacity.

Mechanical properties of unsaturated polyester with polyvinyl acetate (PVAc), a curing agent, were studied by Hayaty et al.(2004). They found that the mechanical properties of cured resin decrease with increase of (PVAc). Some researchers recommend levels of MEKP typically between 0.75% and 2.5%. Louis (2007) explains that MEKP is not a single chemical but rather a mixture of monomer, dimer and other components. In addition, he used a percentage of styrene during the fabrication of unsaturated polyester and MEKP to copolymerize material, which helped form a cross-linked network of molecules. Polymerization of the material was formed by the breaking down of the peroxide compound initiator to form free radicals (a compound with a free electron). Interestingly, the heat generated and the chemical changes during the curing process lead to an increase of glass transition temperature T_g, isolating the free radicals to cause a phase change from a liquid to gradually forming a solid piece of material, a process called 'vitrification'. The higher levels of peroxide initiator used during the curing process can lead to the reduction of the cross-linked network in the material, thus lowering the physical properties (density) resulting in a weaker material.

2.6 Issues Related of Using Natural Cellulose Fibers in Composites

Natural fibers present many advantages compared to synthetic or man-made fibers, thus making them attractive reinforcements for composite materials. These advantages are low density, low cost, nonabrasive nature, high tilling levels, low energy consumption, highly acceptable specific strength properties, biodegradability, availability of a fibers throughout the world (Anand el at. 1995), abundance, renewable, ease of separation, and carbon dioxide sequestration. Unlike brittle synthetic fibers, natural fibers are flexible and are less likely to fracture during composite processing. This enables the fibers to maintain the appropriate aspect ratios to provide good composite reinforcement (Mohanty et al. 2005). The role of the reinforcement in a composite material is fundamentally one of increasing the mechanical properties of the neat resin system. All of the different fibers used in composites have different properties and so affect the properties of the composite in different ways. The mechanical properties of most reinforcing fibers are considerably higher than those of corrosion resin systems. The mechanical properties of the fiber/resin composite are therefore dominated by the contribution of the fiber to the composite (Beckermann 2007). The four main factors that govern the fiber's contribution are:

1. The basic mechanical properties of the fiber itself
2. The surface interaction of fiber and resin (the 'interface')
3. The amount of fiber in the composite (fiber weight fraction)
4. The orientation of the fibers in the composite

Other major characteristics of the fibers affecting the properties are their discontinuous length and non-uniform diameter. These have imposed serious problems in characterizing the fiber strength.

2.6.1 Effect of Natural Fiber on Mechanical Properties of Composites

Natural fiber/plastic compounds, on the basis of kenaf, can replace glass-reinforced plastics in many applications such as the automotive industry, packaging, and construction/housing. The compounds have the mechanical and strength characteristics of glass-filled plastics but are less expensive and, in many instances, are completely recyclable (Parikh et al. 2002). There are many studies which have investigated the kenaf fiber properties. One of them focused on improving kenaf sinnability and determined the impact of the retting methods and blending percentage on the properties

of kenaf fiber as well as the yarns and fabrics that contain kenaf in terms of physical properties (Beijing 2003). Many studies have been done around the world to prove that kenaf can be used to produce kenaf-based composites with acceptable physical and mechanical properties. The effect of fiber compression on the composites made from kenaf and bamboo fibres and biodegradable resin were investigated (Shibata et al. 2006). The flexural modulus increased with increase fiber content. Clemons et al (2007) studied the effects of fiber content, coupling agent and temperature on the impact performance of kenaf fiber reinforced polypropylene composite. The tensile properties of kenaf bast fibres bundle and kenaf bast fiber-reinforced epoxy strands were evaluated through extensive experiment and micromechanics-based modelling (Xue et al. 2009).

The incorporation of two or more types of fiber within a single matrix is known as hybridisation and the resulting material is referred to a 'hybrid' or 'hybrid composites'. Several investigations have already been reported in the field of natural fiber hybrid composites. Huda et al.(2007) evaluated the effect of the addition of silane-talc as fillers on the mechanical and physico-mechanical properties of poly(lactic acid) (PLA)/recycled newspaper cellulose fibers (RNCF)/talc hybrid composites the hybrid composites showed improved properties such as flexural strength and modulus. Mechanical properties of banana/kenaf hybrid composites subjected to various chemical treatments such as Sodium Lauryl Sulfate (SLS) and sodium hydroxide (NaOH) were compared (Thiruchitrambalam et al. 2009). Chemical treatment had provided better mechanical properties for both the random mix and woven hybrid composites. After studying the effects of hybrid composites specimen subjected to in-plane tensile and compressive loading, it was found the increase in shear stress was not only dependent on fiber strength but also on the interface between fiber and matrix material (Satish et al. 2010). When mechanical properties of hybrid composites were increased, the volume fraction of matri enhanced the energy-absorbing characteristics of the hybrid composites, where increasing the amount of fiber increased the flexural modulus (Kuan et al. 2009), (Mingchao et al. 2009).

2.6.2 Natural Fiber Bonding and the Effect of Moisture

All plant-derived cellulose fibers are polar and hydrophilic in nature, mainly as a consequence of their chemical structure. Plant fibers contain non-cellulosic components such as hemicelluloses, lignin and pectin, of which the hemicelluloses and pectin are the

most hydrophilic. These components contain many accessible hydroxyl (OH) and carboxylic acid groups, which are active sites for the sorption of water (Lilholt et al. 2000). Generally, a poor and sparse bounding between fibers desired to make the material absorb a lot of moisture. Since cellulose fibers have the possibility to show a wide range of both poor and strong bonding to polymer matrix material, depending on fiber matrix modification and compatibility, the optimal interface is typically somewhere between the two extreme cases (Gamstedt et al. 2007). Hydroxyl groups (---OH) in the main backbone chain of a resin provide sites for hydrogen bonding to the surface of the natural fibers, which contain many hydroxyl groups in their chemical structure. Thus, the polyester resin, having no hydroxyl group in its backbone chain, generally has the weakest bonding. It is necessary to improve the adhesion between the fibers and matrix. This can be achieved by either modifying the surface of the fibers to make them more compatible with the matrix, or by modifying the matrix with the addition of a coupling agent that adheres well to the fibers and matrix (Maldas et al. 1994).

2.6.3 Thermal Stability

Another limiting factor for the extended use of lignocelluloses fibers in composites is their low thermal stability. In order to avoid degradation of the fibers during processing, the temperatures are limited to 200°C with as short a processing time as possible (Wielage et al. 1999), which further restricts the choice of the polymer matrix materials. The temperatures above 150°C can lead to permanent alterations of the physical and chemical properties of lignocellulosic fibers such as wood (Yildiz et al. 2006). Heat treatments at high temperatures can improve the biological durability of wood, but stiffness and strength are reduced.

2.6.4 Moisture Absorption

All natural fibers are hydrophilic in nature and their moisture content can be 3-13 %. This can lead to a very poor interface between the fiber and the matrix, and very poor moisture absorption resistance (Bledzki et al. 1999). Lignocellulosic products have a well-documented problem with water sorption and lack of dimensional stability. A moisture buildup in the fiber cell wall can lead to fiber swelling and dimensional changes in the composite, particularly in the direction of the fiber thickness (Rowell 1997), and the most important problem associated with fiber swelling is a reduction in

the adhesion between the fiber and the matrix (Joseph 2002), ultimately causing debonding. In wet conditions, such composites show very poor mechanical properties. Therefore, drying of fibers before processing is an important factor because water on the fiber surface acts likes a separating agent in the fiber-matrix interface. Moreover, because of evaporation of moisture during the reaction process, voids appear in the matrix. All these lead to a decrease in the mechanical properties of the natural fiber-reinforced composites with time (Bledzki et al. 1999).

2.6.5 Fiber Separation and Dispersion

To obtain a satisfactory performance from the composite, it is necessary to have a good fiber distribution within the matrix. A good distribution implies that the fibers are fully separated from each other, and each fiber is fully surrounded by the matrix. Insufficient fiber dispersion can lead to clumping and agglomeration of the fibers, resulting in an nonhomogeneous mixture of resin-rich and fiber rich areas. This segregation is undesirable, as the resin rich areas are weak, while the fiber rich areas (clumps) are susceptible to micro cracking (Painchaud et al. 2006). Micro cracks contribute to inferior mechanical properties of the composite. Therefore, it is necessary to ensure a homogeneous fiber distribution in order to achieve maximum strength and performance of the composite material.

To achieve a good distribution and dispersion of fibers within a composite matrix, it is necessary to separate the fibers from each other, modify the fibers and/or matrix to improve compatibility, and ensure that the fiber lengths are such that fiber entanglement does not occur (Albuquerque et al. 2000). Pectin and lignin bind the individual fibers together; therefore, to separate the fibers from their fiber bundles, it is necessary to dissolve both the pectin and lignin. To improve the interfacial adhesion between the fiber and matrix, the fibers are chemically modified through various methods like dewaxing, alkali treatment, cyanoethylation, bleaching, and vinyl polymer grafting. As expected, all types of chemical modifications improve the mechanical properties such as tensile strength, flexural strength, and impact strength (Rout 2001). John et al. (2008) carried out the chemical modification of kenaf fibers. They use different concentrations of NaOH and examined the morphological changes through a Scanning Electron Microscope (SEM). It was observed that treated kenaf fibers exhibited better mechanical properties than untreated fibers. Moreover, the optimum concentration of

NaOH was found to be 6%. A decrease in the amount of surface impurities was observed in the case of treated fibers. Fiber bundle tests were also performed and the strength of 6% NaOH-treated fiber bundles was found to be higher by 13%.

2.6.6 Fiber Tensile Strength, Young's Modulus and Weight Fraction

As reinforcing fibers are directly responsible for providing strength and stiffness to a composite, it is necessary to exploit the fiber tensile strength and Young's modulus to produce a composite material with enhanced properties. Fiber volume fraction (V_f) also plays an important part in determining the mechanical properties of the composite. For composites consisting of brittle fibers in a flexible polymer matrix, two possible failure regimes exist depending on whether the fiber volume fraction is above or below a minimum value (V_{min}) as shown in Figure 2.7 If a composite with $V_f < V_{min}$ is stressed, the polymer matrix is able to carry the applied load after fiber fracture. Failure of the fibers does not lead to composite failure but results in a stress increase in the matrix. The failed fibers, which now carry no load, can be related to holes in the polymer matrix. If a composite with $V_f > V_{min}$ is stressed, friable failure of the fibers leads to failure of the whole composite, since the polymer matrix in unable to support the additional load which is transferred into the matrix from the fibers (Bowen et al. 2005). When $V_f > V_{min}$, a point exists where the strength of the composite reaches and then surpasses the strength of the matrix alone, and this is known as the critical fiber volume fraction (Vcrit) (Alger 1996). The effects of fiber volume fraction and fiber length on flexural properties were investigated by Shibata et al. (2006), where the composite was made from kenaf fiber and biodegradable resin and fabricated by a hot-press forming. They found that the flexural modulus increased with the increase of volume fraction of fiber and showed the maximum value of 3991 MPa at 62%. This higher flexural modulus was due to the fiber segregation which was observed in the vicinity of the surface.
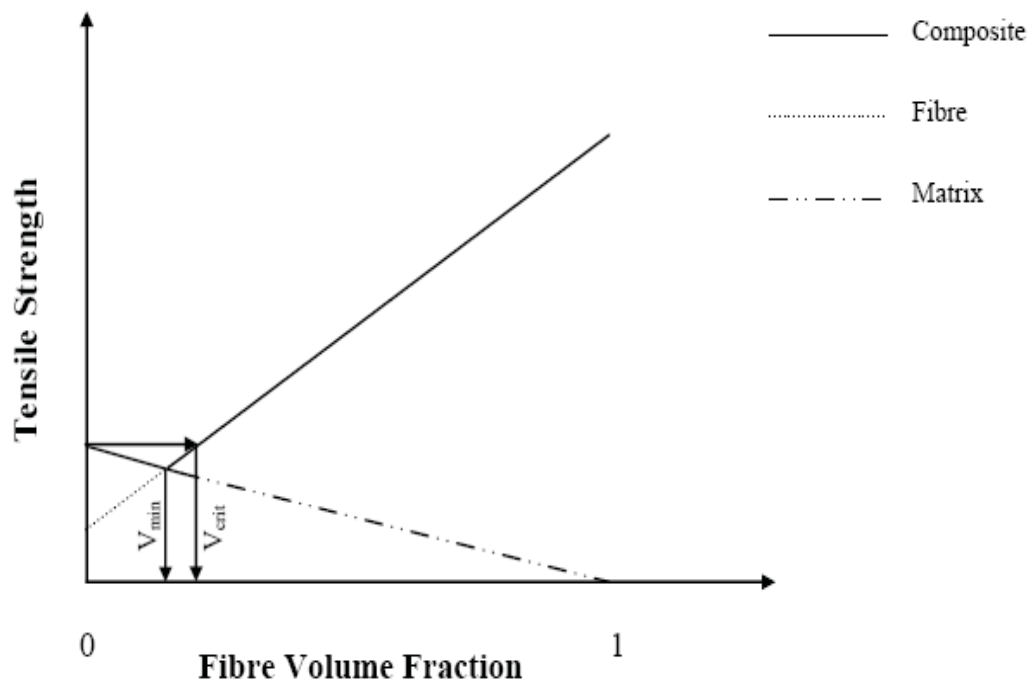
Figure 2.7 Theoretical relationships between tensile strength and fiber volume fraction of short-fiber reinforced composites (Bowen et al. 2005).

2.6.7 The Importance of Hybrid Fiber Composites

Another interesting area is that of hybrid composites. The establishment of a legal corporation of two or more fibers within a single matrix is known as hybridization, and the resulting material is referred to as hybrid composites. One of the aims of this study is to characterize the hybrid composite contenting kenaf and recycled jute fibers. Recycled jute fiber was extracted from grocery sacks. Jute sacks had previously been used to store peanuts.

Several studies have already reported on the field of natural fiber hybrid composites. Huda et al. (2006) evaluated the effect of the addition of silane-talc as fillers on the mechanical and physico-mechanical properties of poly (lactic acid) (PLA)/recycled newspaper cellulose fibers (RNCF)/talc hybrid composites; the hybrid composites showed improved properties such as flexural strength and modulus. Mechanical properties of banana/kenaf hybrid composites subjected to various chemical treatments such as Sodium Lauryl Sulfate (SLS) and sodium hydroxide (NaOH) were compared by Thiruchitrambalam et al. (2009). The conclusion of their investigation was that the SLS chemical treatment had provided better mechanical properties, for both the random mix and woven hybrid composites. Satish et al. (2010) conducted their study on the effects

30

of hybrid composite specimens subjected to in-plane tensile and compressive loading. They concluded that the increase in shear stress was not only dependent on fiber strength but also on the interface between the fiber and matrix material. Besides, the mechanical properties of hybrid composites were investigated by Kuan et al. (2009) and Mingchao et al. (2009). Results showed that increasing the volume fraction of matrix could enhance the energy-absorbing characteristics of the hybrid composites, where increasing the amount of fiber increased the flexural modulus.

2.7 Fiber Treatment and Modification

To enhance interfacial bonding and to reduce moisture absorption, surface modification of the lignocellulosic fibers was performed. Such modifications are achieved through effected by biological, physical and chemical methods.

Alkali Treatment

Alkali treatment is an effective method to improve fiber-matrix adhesion in natural fiber composites. Alkali fiber treatments using sodium hydroxide (NaOH), or combinations of sodium hydroxide and sodium sulphite (Na_2SO_3), have been used extensively in the pulping of wood fiber for paper use (Walker 1993). Some alkali treatments, especially those performed at elevated temperatures can result in the selective degradation of lignin, pectin and hemicelluloses in the fiber wall, whilst having little effect on the cellulose components (Walker 1993). Most of the natural fiber-reinforced thermoset resin composites involve the use of alkali treatment to maximize the efficiency of the fibers as reinforcement. Alkali treatment has been the most simple and economically viable tool to modify natural fibers into a better reinforcement material a part from cyanoethylation, and bleaching (Ray et al. 2001). Onal et al. (2009) studied the effects of alkali treatment on the mechanical properties of carpet waste jute yarn composites. The results showed that composites which received from alkali treatment had better mechanical properties; this may be due to the fact that the treatment improves the adhesive characteristics of fiber surface, and improves the impact strength of the composites. Furthermore, the effects of fiber alignment and alkalization of long and random hemp and kenaf fibers composites on the mechanical and thermal properties were investigated. Researchers observed whether alkalized and long fiber composites

gave higher flexural modulus and flexural strength compared with composites made from as-received fibers (Sharifah et al. 2004). Alkalized long kenaf-polyester composites possess superior mechanical properties compared to alkalized long hemp-polyester composites. In addition, the dynamic mechanical analysis DMA showed that the alkalized fiber composites have higher storage modulus values corresponding to higher flexural modules. Figures 2.8 (a) and (b) show the longitudinal views of the untreated and 6% NaOH treated kenaf fiber bundles, respectively. The presence of surface impurities on the untreated kenaf fiber surface is very obvious. The surface of the 6% NaOH treated kenaf fiber seems uneven and serrated when compared to the untreated fiber. Following 6% NaOH treatment, wax, oil and other surface impurities are removed and the treatment also roughens the surface of the fiber bundles.
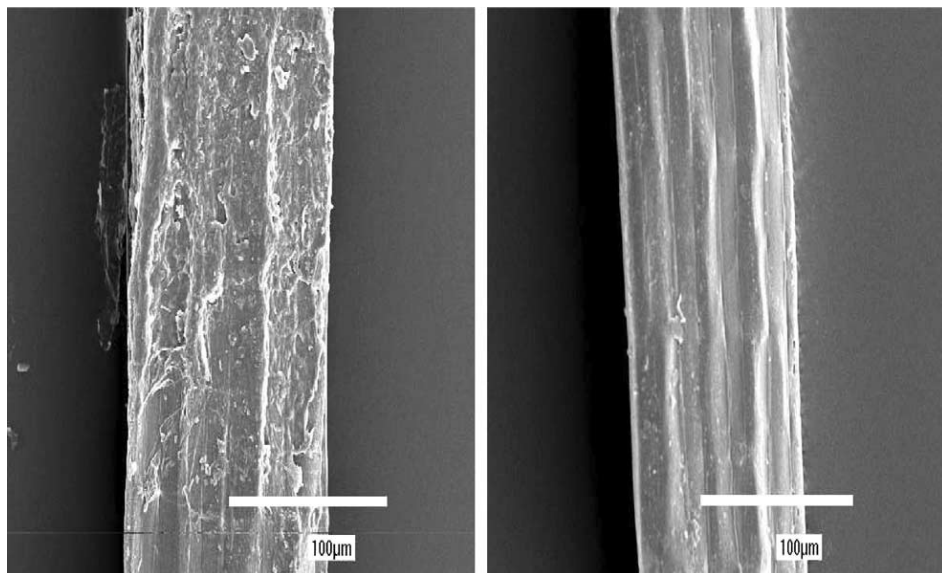
Figure 2.8 The SEM micrographs of longitudinal views of a) untreated kenaf fiber and b) 6% NaOH treated kenaf fiber (Sharifah at el. 2004)

2.8 Processing of Fiber Reinforced Thermoset Composites

Fabrication techniques suitable for manufacturing natural fiber-reinforced thermoset composites include the hand lay-up technique for unidirectional fibers/ mats/ fabric, sheet molding (SMC)/ bulk molding (BMC) for short and chopped fibers, filament winding, and pultrusion for continuous fibers. Anyway, in natural fibers, there are no continuous fibers as in man-made fibers. The length of some natural fibers (single)

reaches up to 4 m, and if it is a bundle of fibers connected to the length direction, then the fiber length can be longer than 4 m (Satyanarayana 1990)

2.8.1 Hand Lay-Up

The hand lay-up is the oldest, (simplest but most widely used) fabrication process for the composite materials. Essentially, it involves manual placement of dry fiber in the mold or mandrel and succeeding application of resin matrix. The wet composite is then rolled using hand rollers to facilitate uniform resin distribution, to ensure better interaction between the reinforcement and the matrix and to achieve the required thickness (Mallick 1993). The layered structure is then cured. In general, the hand lay-up fabrication process is divided into four essential steps: mold preparation, gel coating, lay-up, and curing. Recently, partial automation of the hand lay-up was achieved by spray-up process, in which the application method of the resin matrix was slightly different from hand lay-up. The most expensive piece of equipment typically is a spray gun for resin and gel coat application. Some fabricators pour or brush the resin into the molds so that a spray gun is not required for this step. There is virtually no limit to the size of the part that can be made.

In a particular hand lay-up process (otherwise known as wet lay-up), high solubility resin is sprayed, poured, or brushed into a mold. The reinforcement is then wet out with resin. The reinforcement is placed in the mold. Depending upon the thickness or density of the reinforcement, it may receive additional resin to improve wet out and allow better drapeability into the mold surface (Strong 1989). The reinforcement is then rolled, brushed, or squeezed to distribute the resin uniformly, to remove entrapped air and to compact it against the mold surface. However, not much fiber loading is possible using this technique. The amount of fiber loading depends largely on the processing method. This also depends on the anatomical features of the natural fibers, which have intrafiber voids called lumen. Although, the fiber has large lumens and small cell walls, the fiber loading can be increased by compression of such voids in the fibers. Natural fiber reinforcements should be dried properly in an oven prior to resin impregnation to avoid poor wetting and moisture entrapment in the composites (Satyanarayana 1990). The hand lay-up fabrication process is mainly used in the applications of marine and aerospace structures.

2.8.2 Compression Molding

Compression molding is the most common method of molding thermosetting materials such as SMC (sheet molding compound), BMC (bulk molding compound), and LCM (liquid composite molding). This molding technique involves compressing materials containing a temperature-activated catalyst in a heated matched metal die using a vertical press such as cold press and hot press methods. The procedure is similar to the hand lay-up technique, except that herein a set of matched dies are used, which are closed before a cure takes place with the application of pressure. By this method, nearly 70 wt% of fibers could be incorporated and the thickness of the product can be between 1-10 mm. For cold press and hot press molding, the curing temperature is normally between 40-50°C and 80-100°C for 1-2 hours respectively. Press molding has been successfully used for incorporating up to 40-60 wt% of pineapple fiber (Satyanarayana 1990).

The molding process begins with the delivery of high viscosity uncured composite material such as SMC, BMC, or a mat or performs covered with a medium viscosity resin paste (LCM) to the mold. Mold temperatures typically are in the range of 300-320°F. As the mold closes, composite viscosity is reduced under the heat and pressure approximating 1000 psi. The resin and the isotropically distributed reinforcements flow to fill the mold cavity in the case of SMC and BMC. In LCM, the reinforcements do not move; only the resin paste flows throughout the mold. While the mold remains closed, the thermosetting material undergoes a chemical change (cure) that permanently hardens it into the shape of the mold cavity. Mold closure times vary from 30 seconds up to several minutes depending on the design and material formulation. When the mold opens, parts are ready for finishing operations such as deflashing, painting, bonding, and installation of inserts for fasteners. By varying the formulation of the thermoset material and the reinforcements, parts can be molded to meet applications ranging from automotive class 'A' exterior body panels to structural members such as automobile bumper beams (Strong et al. 1989).

2.9 Theoretical Models for Composite

Discontinuous fibers are commonly used in many composites as a result of the increasing use of fast and efficient moulding techniques adopted from the plastics manufacturing industry. Since understanding of natural fiber composites is at its early stages, the most important parameters, as usual, are stiffness and strength. A number of theoretical models have been put forward to model stiffness of short fiber reinforced composites (Tucker et al. 1999, Fukuda et al. 2000). Although they are very different, they all are based on the same basic assumptions:

- The fibers and the matrix are linearly elastic.
- The matrix is isotropic, and the fibers are either isotropic or transversely isotropic.
- The fibers and matrix are well bonded at their interface, and remain that way throughout deformation.
- The fibers are axi-symmetric and identical in shape.

2.9.1 Rule of mixture

Kelly and Tyson (1965) first proposed the rule of mixtures model for continuous fibers with uniaxial orientation. The rule of mixtures is commonly used to estimate the modulus and strength. In the fiber direction, assuming perfect bonding between fiber and matrix, the properties are:

$$E_L = E_f V_f + E_m V_m \qquad (2.1)$$

$$\sigma_c = \sigma_f V_f + \sigma_m V_m \qquad (2.2)$$

where:

$$V_m = 1 - V_f \qquad (2.3)$$

such that E_L and σ_c are the modulus and strength of composites in the fiber direction. E_m and E_f are the modulus of matrix and fiber. V_m and V_f are the volume fractions of matrix and fiber. σ_f and σ_m are the stresses in fiber and matrix respectively, at fiber failure (Kelly et al. 1965). Compared to the continuous fiber-reinforced thermosetting resins or laminates, the modeling of discontinuous fiber reinforced composite materials is more

complex. The continuous processing, such as extrusion or injection molding, causes complicated fiber orientation and fiber length distribution. To evaluate the properties of these final products, the effects of fiber length distribution and fiber orientation distribution needs to be considered (Xiaolin 2008).

2.9.2 The Critical Aspect Ratio

One of the earliest theories developed by Cox was based on a shear-lag mechanism observed in fibrous composites; shear lag models were the first micromechanical models for short fiber composites. According to Cox et al. (1952) in shear-lag analysis, the main aspects of controlling the properties of composites are the critical length of the fiber and interfacial shear strength between fiber and matrix. For composites containing discontinuous fibers, the applied load is transferred to the fibers by means of shear forces at the fiber-matrix interface, and high shear stresses are experienced at the fiber ends (Kelly et al. 1965). Composite failure mechanisms are administrating by fiber length and sub-critical length fibers $L<L_c$ cannot be fully stressed and will finally debone and be pulled out of the matrix. Critical length fibers $L=L_c$ can only be fully stressed at a very small location in the middle of the fiber, whereas supercritical length fibers ($L>L_c$) can be stressed over a much greater proportion of the fiber. Once the stress in the fiber reaches the fiber tensile strength, fiber fracture occurs. The critical length, L_c is defined as:

$$\frac{L_c}{d} = \frac{\sigma_{fu}}{2\tau_y} \tag{2.4}$$

where τ_y is the shear stress on the cylindrical fiber-matrix interface, d is the fiber diameter, σ_{fu} is the maximum permissible fiber stress. The critical length of the fiber in composites is a parameter which determines the amount of stress transferred to the fiber. In other words, if the length to diameter ratio is higher than the critical aspect ratio L_c/d, composites show superior properties, while for a fiber whose aspect ratio is smaller than the critical aspect ratio L_c/d, composites show weaker properties. The critical fiber length is usually determined by experiments, such as the fiber micro-compression test, the single fiber fragmentation test, the micro-tension (micro-droplet) test and the pull-out test (Kelly et al. 1965). Assuming the interface between the fiber and matrix is

perfect, and the fiber and matrix remain elastic during testing, the Cox model used the classical shear lag theory to get the tensile stress distributions along the fiber length.

$$\sigma_f = E_f \varepsilon_m \left[1 - \frac{\cosh \beta \left(\frac{1}{2} l - x \right)}{\cosh \frac{1}{2} \beta l} \right] \tag{2.5}$$

Thus the fiber strain is given by

$$\varepsilon_f = \varepsilon_m \left[1 - \frac{\cosh \beta \left(\frac{1}{2} l - x \right)}{\cosh \frac{1}{2} \beta l} \right] \tag{2.6}$$

and

$$\beta = \frac{2}{d} \left[\frac{E_m}{E_f \left(1 + V_m \right) \ln \left(\frac{\pi}{4 V_f} \right)^{1/2}} \right]^{1/2} \tag{2.7}$$

Galiotis defined the critical fiber length as the length of fiber required to reach *0.9* times the maximum fiber strain. The ratio of $\varepsilon_f/\varepsilon_m$ reaches the value of *0.9* at somewhere *x* along the fiber. Twice of *x* is the critical fiber length (Xiaolin 2008). Thus, the critical fiber length can be calculated by:

$$L_c = 2.303 \, d \left[\frac{E_f \left(1 + v_m \right)}{E_m} \right]^{1/2} \left[\ln \left(\frac{\pi}{4 V_f} \right)^{1/2} \right]^{1/2} \tag{2.8}$$

where d is the fiber diameter, v_m is the Poisson's ratio of matrix, E_f and E_m the modulus of fiber and matrix, and V_f the volume fraction of fiber. The volume fraction is usually chosen to be *0.1 %* for single fiber composites (Xiaolin 2008). Kelly and Tyson (1965) modified the rule of mixtures model Equation 2.10 by replacing the mean fiber strength σ_f with the average stress along the fiber. The average stress of a sub-critical length fiber is given by the area under the curve in Figure 2.9a divided by the fiber length, and the

37

average stress of a critical length fiber or super-critical length fiber is given by the area under the curve in Figure 2.9b divided by the fiber length.
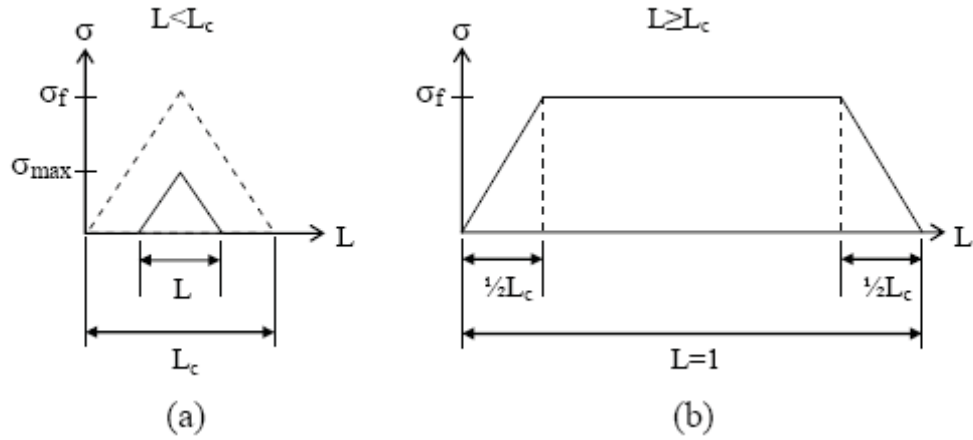
Figure 2.9 Linear build-up of stress inside a fiber: a) L< L_c, (b) L ≥ L_c
(Beckermann 2007)

Thus, the tensile strength σ_c of composites containing fibers shorter than L_c is given by:

$$\sigma_c = V_f \sigma_f \left(\frac{L}{2L_c} \right) + V_m \sigma_m \qquad \text{for L< L}_c \qquad (2.9)$$

and the tensile strength of composites containing fibers longer than L_c is given by:

$$\sigma_c = V_f \sigma_f \left(1 - \frac{L_c}{2L} \right) + V_m \sigma_m \qquad \text{for L≥ L}_c \qquad (2.10)$$

Equations 2.9 and 2.10 can be combined into the following equation to determine the composite tensile strength:

$$\sigma_c = K_2 V_f \sigma_f + V_m \sigma_m \qquad (2.11)$$

where K_2 is a fiber length factor, which can be determined by:

$$K_2 = \frac{L}{2L_c} \qquad \text{for L< L}_c \qquad (2.12)$$

$$K_2 = 1 - \left(\frac{L_c}{2L} \right) \qquad \text{for L ≥ L}_c \qquad (2.13)$$

38

2.9.3 Theoretical Modeling of Tensile Properties

Several research studies have explained about theoretical models of tensile properties of composite materials. These equations are mainly used or the theoretical calculation of the properties. According to this research several models have been used for comparing experimental data with theoretical calculations.

- Hirsch's model

For modulus of elasticity

$$E_c = x\left(E_m V_m + E_f V_f\right) + (1-x)\frac{E_f E_m}{E_m V_f + E_f V_m} \tag{2.14}$$

For tensile strength

$$\sigma_c = x\left(\sigma_m V_m + \sigma_f V_f\right) + (1-x)\frac{\sigma_f \sigma_m}{\sigma_m V_f + \sigma_f V_m} \tag{2.15}$$

where E_f and E_m are modulus, σ_f and σ_m are strengths, V_m and V_m are volume fractions of the fiber and matrix, respectively. An empirical parameter x is introduced in Hirsch's model that characterises the stress transfer between the fiber and matrix, which depends on fiber orientation, fiber length and fiber distribution (Anshid et al. 2008). The value of x can be varied from 0 to 1 to give finest fit.

- Einstein and Guth equations (Anshid et al. 2008)

$$E_c = E_m\left(1 + 2.5V_f + 14.1V_f^2\right) \tag{2.16}$$

$$\sigma_c = \sigma_m\left(1 - V_f^{2/3}\right) \tag{2.17}$$

- Modified Bowyer and Bader's model (Bos 2004)

$$E_c = E_f K_1 K_2 V_f + E_m V_m \tag{2.18}$$

$$\sigma_c = \sigma_f K_1 K_2 V_f + \sigma_m V_m \tag{2.19}$$

where K_1 changes from (0-1), K_2 is the orientation factor and length factor of fiber respectively.

For fibers with L>L$_c$: $K_2 = L - \dfrac{L_c}{2L}$ (2.20)

For fibers with L<L$_c$: $K_2 = \dfrac{L}{2L_c}$ (2.21)

- Kelly and Tyson's model (Kelly et al 1969)

$$\sigma_c = \eta_0\,\eta_{LS}\sigma_f\,V_f + \sigma_m\,V_m$$ (2.22)

where η_{LS} and η_o are length efficiency factor and orientation factor of fiber respectively

- Parallel model (Roger et al 1999)

$$E_c = E_f\,V_f + E_m\,V_m$$ (2.23)

$$\sigma_c = \sigma_f\,V_f + \sigma_m\,V_m$$ (2.24)

- Modified Guth equation (Jeefferie et al. 2011)

$$E_c = E_m\left(1 + 0.675\,S\,V_f + 11.62\,S^2\,V_f^2\right)$$ (2.25)

where S is defined as the ratio of the length-to-width of fiber

- Cox-Krenchel Model

$$E_c = \eta_o\eta_L V_f E_f + \left(1 - V_f\right)E_m$$ (2.26)

$$\eta_L = \left(1 - \frac{\tanh(\beta l_f/2)}{\beta l_f/2}\right)$$ (2.27)

$$\beta = \frac{2}{d_f}\left(\frac{2G_m)}{E_f\,\ln\left(\sqrt{\pi/X_iV_f}\right)}\right)^{\frac{1}{2}}$$ (2.28)

$$G_m = \frac{E_m}{2\left(1 + v_m\right)}$$ (2.29)

where G_m is shear modulus of matrix, v_m Poisson's ratio of matrix. The value of $X_i = 4.0$ for square packing of fibers was adopted in calculation. For random in-plane fiber reinforced composites a fiber orientation factor $\eta_o = 0.375$ can be derived (Roger et al. 1999, Jeefferie et al. 2011)

- Halpin-Tsai model

$$E_c = E_m \left(\frac{1 + A \eta V_f}{1 - \eta V_f} \right) \qquad (2.30)$$

$$\sigma_c = \sigma_m \left(\frac{1 + A \eta V_f}{1 - \eta V_f} \right) \qquad (2.31)$$

$$\eta = \frac{E_{fm}/E_m - 1}{E_f/E_m + A} \qquad (2.32)$$

$$\eta = \frac{\sigma_{fm}/\sigma_m - 1}{\sigma_f/\sigma_m + A} \qquad (2.33)$$

where *A* is the measure of fiber geometry, fiber distribution and fiber loading conditions (Jeefferie et al. 2011)

- Zero-stress aging is defined as the reduction of tensile strength *TS* and modulus of elasticity *EM* when no stress is applied during the time of exposure to a given environment (Barbero et al. 2002, Kalaprasad et al. 1997).

$$E(t) = E_o \left(1 + \alpha t_a \right)^{-\beta} \qquad (2.34)$$

$$\sigma(t) = \sigma_o \left(1 + \alpha t_a \right)^{-\beta} \qquad (2.35)$$

where E_o and σ_o are modulus and strength respectively, at time zero, at the environment of exposure, α and β are the empirical constants adjusted to fit the experimental data.

2.10 Thermal Analysis

Organic materials, including natural fibers and synthetic polymers, experience degradation of their physical and mechanical properties at elevated temperatures in the presence of oxygen. The thermal stability of natural fiber such as kenaf fiber, un-saturated polyester composite can be evaluated by measuring directly, the Heat of Reaction by Differential Scanning Calorimetry DSC; or indirectly, the Glass Transition Temperature (T_g) which is determined from the rate of change of Coefficient of Thermal Expansion (CTE) in the Thermo-Mechanical Analysis (TMA), which measures

dimensional changes in a material as it is heated from room temperature (or below) to a preset final temperature. The change in length (width, or height) with change in temperature is the Coefficient of Thermal Expansion (CTE) (Zgoul et al. 2008). Implement such as the DSC, TMA, and TGA have been used to determine the degree of cure, rates of cure, thermal stability, melting points, heats of reaction, and moisture content among other things. The Glass Transition Temperature (T_g) can be defined in one simple way, "The temperature at which the mechanical properties of a laminate begin to change significantly" (Zgoul et al. 2008). It is that temperature at which a material changes from a hard, brittle "glassy" from to a softer, rubberlike consistency. T_g is the temperature at which polymer segments start to slide relative to each other. Greater long range molecular motion and increased rotational freedom leads to more segmental movement of the polymer chain. There are a number of ways to measure T_g such as, TMA, Quartz Tube Dilatometer, Dynamic Mechanical Analyzer DMA, Differential Scanning Calorimetry DSC. The values obtained with each will be different, because each measures a slightly different property or combination of properties.

2.10.1 Dynamic Mechanical Analysis (DMA)

Dynamic mechanical analysis (DMA) has been a very important tool in interpreting the interphase region in the composites, which reflects the nature of interfacial bonding between the fiber and the matrix and has the most significant contribution to the performance of the composites (Ghosh et al. 1997). DMA yields information about the mechanical properties of a specimen placed in a minor, usually sinusoidal, oscillation as a function of time and temperature by subjecting it to a small, usually sinusoidal, oscillating force. The applied mechanical load, that is, stress, elicits a corresponding strain (deformation) whose amplitude and phase shift can be determined. Figure 2.10 states that the mode of deformation governs whether the complex modulus is E^*, G^*, K^*, or L^*. The other relationships are shown below for the elastic modulus E. The complex modulus E^* is the ratio of the stress amplitude to the strain amplitude and represents the stiffness of the material. The magnitude of the complex modulus is:

$$\left| E^* \right| = \frac{\sigma_A}{\varepsilon_A} \tag{2.36}$$
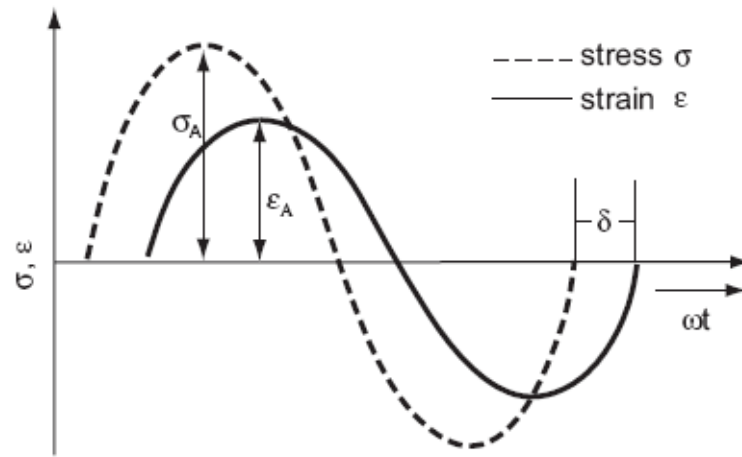
Figure 2.10 Sinusoidal oscillation and response of a linear-viscoelastic material; δ = phase angle, E = tensile modulus, G = shear modulus, K = bulk compression modulus, L = uniaxialstrain modulus (http://files.hanser.de/hanser/docs)

The complex modulus is composed of the storage modulus E' (real part) and the loss modulus E'' (imaginary part).

$$\left|E^*\right| = \frac{\sigma_A}{\varepsilon_A} \tag{2.37}$$

$$\left|E^*\right| = \sqrt{\left[E''(\omega)\right]^2 + \left[E''(\omega)\right]^2} \tag{2.38}$$

$$E'(\omega) = \left|E^*\right| \cdot \cos\delta \tag{2.39}$$

$$E''(\omega) = \left|E^*\right| \cdot \sin\delta \tag{2.40}$$

$$\tan\delta = \frac{E''(\omega)}{E'(\omega)} \tag{2.41}$$

where E' is storage modulus (real part), E'' is loss modulus (imaginary part), ω is frequency and its $\omega = 2\pi f$, δ is the phase angle. *Tan δ* is the loss factor (Saha et al. 1999). These are dynamic elastic characteristics and are material-specific; their magnitude depends critically on the frequency as well as the measuring conditions and history of the specimen. Typical curves of the changes undergone by amorphous thermoplastics are shown in Figure 2.11. At low temperatures, the molecules are so immobile that they are unable to resonate with the oscillatory loads and therefore remain stiff (Ray et al. 2002). Most types of apparatus utilize vertical loading, which allows measurements under bending, tension, compression, and shear. Usually the same apparatus is employed, with interchangeable clamping mechanisms applying the various types of load, as can be seen in Figure 2.12.
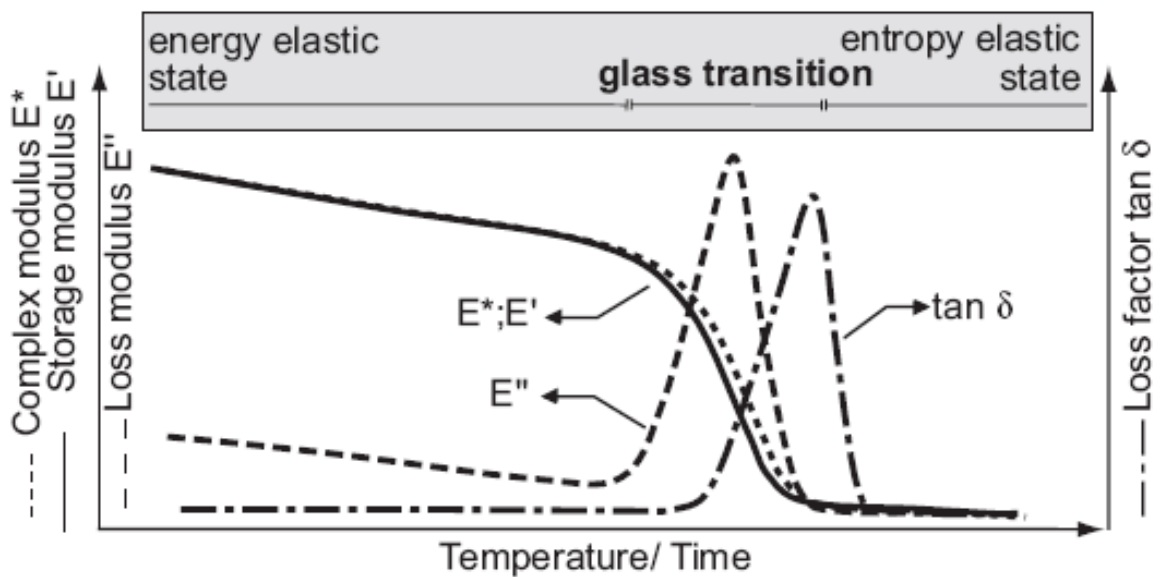
Figure 2.11 Schematic diagram of typical DMA curves for an amorphous polymer
(http://files.hanser.de/hanser/docs)
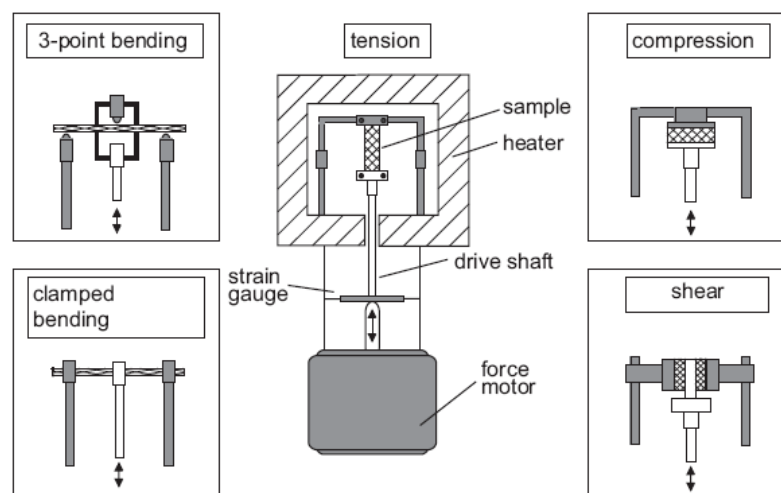
Figure 2.12 Schematic design of a dynamic-mechanical analyzer under vertical load, showing the various possible test arrangements
(http://files.hanser.de/hanser/docs)

Static tensile and flexural tests and dynamic mechanical analysis DMA were carried out by Shibata et al. (2005). They prepared the natural fiber hybrid composite containing equal proportions of kenaf fibers (KFs) and wood flour (WF) as the reinforcements and polypropylene (PP) as the polymer matrix. The hybrid composite exhibited tensile and flexural module and strength values closer to those of the KF composite, which indicated a higher reinforcing efficiency of KFs compared with WF. Sanchez (2000) found that both thermal stability and mechanical properties of a commercial UPE resin

were dependent on the resin's styrene content. Lee et al. (2009) explored the use of carding process for the production of bio-composites of kenaf fibers as reinforcing filler in PLA, and found that the thermal stability towards degradation is slightly decreased relative to the base PLA and ash content is increased. Thermal properties such as glass transition, melting temperature, and percent crystallinity of the PLA matrix are largely unaffected by incorporation into the composites. Biocomposites made of polylactic acid PLA reinforced with natural kenaf bast fiber (KF) using twin screw extruder and injection molding machine were developed by Anuar et al (2011). The effect of kenaf fiber content on crystallization and melting behavior was studied by means of Differential Scanning Calorimetry (DSC). The amourphous state of PLA remaining unchanged with kenaf fiber content. In the same study, the effect of kenaf fiber content on the stiffness of the PLA-KF bicomposites at elevated temperature was investigated using dynamic mechanical analyser (DMA). The storage modulus (E') of the composites was higher as compared to unreinforced PLA, whereas the mechanical loss factor (Tan δ) decreased with increase in kenaf fiber content (Anuar et al. 2011). Tajvidi et al. (2006) studied the effects of natural fibers such as kenaf fibers, wood flour, rice hulls, and newsprint fibers on thermal and mechanical properties of natural fiber polypropylene composites, using dynamic mechanical analysis. The results demonstrate that all composites had storage and loss modulus values higher than those of pure polypropylene, whereas their mechanical loss factor (damping) was lower. Glass transition was slightly shifted to lower temperatures in composites. Finally, because DMA can give an almost instantaneous measurement of modulus, it can be used for a quick one-minute test of a material to determine its modulus and *Tan δ*. However, it can also be used to map the modulus of a specimen to look for surface oxidation or localized embrittlement (Menard 2008).

- **Creep Test**

Short-term creep tests were performed with DMA. The creep tests were run in tensile mode at a small enough stress to be in a linear viscoelastic region. During the test, strain and creep compliance data were collected.

- **Superposition Principle**

Primarily the superposition principle was used to predict the viscoelastic material response at very large time scale. To reduce the time scale, the test temperature was

raised. One can observe that a horizontal shift of a creep curve obtained at one temperature will result in an accurate superposition of a creep curve considered at another temperature, which offers an extension of the curve measured at the second temperature. Mathematically this idea may be expressed as

$$\varepsilon(T_1, t) = \varepsilon\left(T_2 \frac{t}{a_T}\right)$$

(2.42)

where T_1, T_2 are the test temperatures; a_T the temperature shift factor (Hadid et al. 2004).

- **Time-Temperature Superposition Principle (TTSP)**

The effect of time and temperature on a composite material can be determined using the time-temperature superposition principle, the basis of which is the equivalency of time and temperature (Ferry 1980). According to this principle, the effect of a constant temperature change on all time-dependent response functions, such as compliance and modulus, is equivalent to a uniform shift in the logarithmic time scale (Feng 2011). The William-Landel-Ferry WLF equation was employed for the calculation of shift factors, since the reference temperature lies within T_g and $T_g + 100^oC$ (Ferry 1980). If the reference temperature does not lie in this range, then the Arrhenius equation should be used (Ferry 1980). Nielsen et al. (1994) provided a modified WLF equation. By means of Equation 2.43 to determine the shift factors when a temperature other than T_g was selected as the reference temperature.

$$Log(a_T) = \frac{-c_1(T - T_{ref})}{c_2 + (T - T_{ref})}$$

(2.43)

where a_T is the horizontal shift factor for the corresponding elevated temperature, T (°C); T_{ref} is the reference temperature (°C); c_1 and c_2 are the empirical constants determined from Equations 2.44 and 2.45.

$$c_1 = \frac{c_{1g} c_{2g}}{c_{2g} + T_{ref} - T_g}$$

(2.44)

$$c_2 = c_{2g} + T_{ref} - T_g$$

(2.45)

where c_{1g} and c_{2g} are the empirical constants ($c_{1g} = 17.44$ and $c_{2g} = 51.6\ ^oC$), T_g is the glass transition temperature (°C). By substituting the T_g (°C) of kenaf composites, the values of c_1 and c_2 were calculated.

- **Creep Modeling**

According to Betten (2002, 2005), the primary or transient creep characterized by a monotonic decrease in the rate of creep and creep strain can be described by the simple formula

$$\varepsilon_c = a\,\sigma^n\,t^b \qquad\qquad (2.46)$$

where *a*, *n*, and *b* are constants dependent on the temperature. ε is the creep strain and σ is the applied stress. Equation 2.46 was applied to the experimental creep data at room temperature.

2.10.2 Thermo-Gravimetric Analysis (TGA)

Thermo-gravimetric analysis (TGA) measures weight loss as a function of a temperature as a material is heated. It is an analytical technique used for determining the thermal stability and fraction of volatile components in a material by supervising the weight change as the material is heated. The measurements are usually carried out in air or an inert atmosphere, and the weight change is recorded as a function of increasing temperature (Singha et al. 2008). Figure 2.13 shows the TGA curves for four different heating rates. As the heating rate increased, the thermal decomposition temperature T_d increased. The T_d was obtained from the point where the weight loss suddenly increased (Lee et al. 2000).

From TGA some of important parameters can be learned: these parameters are:

- Amount of moisture contained in the sample, which will be driven off at 100°C
- Total volatiles in the sample
- Thermal Decomposition Temperature T_d
- Rate of thermal decomposition
- Ash residue after everything else has been burned off
- Arrhenius plots to predict long-term thermal stability
- Elucidation of structure through the type of gasses given off by looking at weight loss at specific temperatures (Buzarovska et al. 2008).
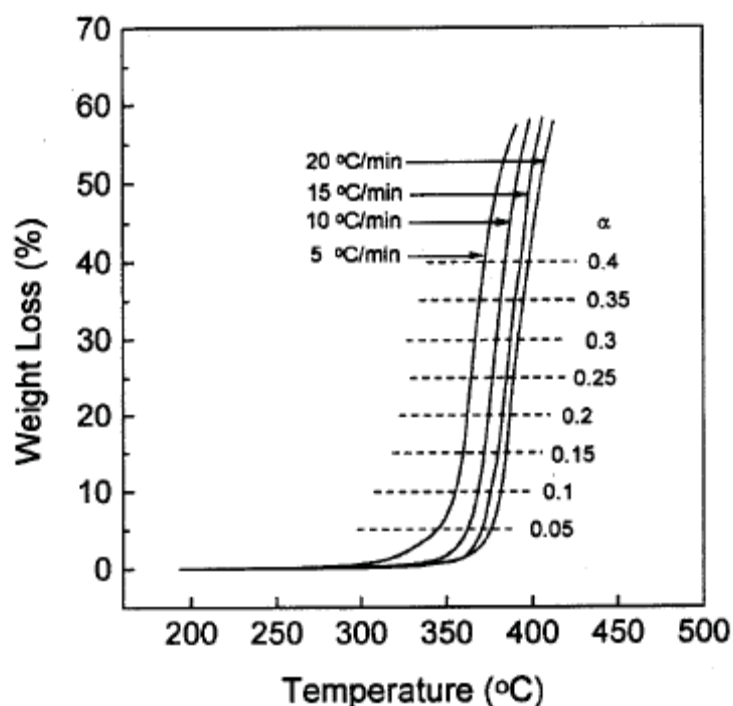
Figure 2.13 TGA for DGEBA/ MDA/ MDA-eendcapped crbn system using Flynn and wall expression (Lee et al. 2000).

2.10.3 Differential Scanning Calorimetry (DSC)

Differential Scanning Calorimetry (DSC) measures changes in heat flow in a material as it is heated from room temperature or below to some predetermined maximum temperature or cooled from that maximum temperature back to a low temperature (below the T_g). It is known as a differential because there is always an aluminum reference measured at the same time as the sample (making the actual measurement the difference between the reference and the sample itself). Chemical reactions and many physical changes, such as melting, result in the absorption or release of heat energy as they occur. Heat given off during a reaction is called an exotherm. The absorption of heat by a material is called an endotherm. By measuring the occurrence of these exotherms and endotherms, it is possible to determine all the chemical and physical state changes that occur in the sample.

There are two different types of DSC-methods, namely, power compensated DSC and heat flux DSC, which although measuring the same properties differ in their instrumentation. In a heat flux DSC machine, the substance which is measured is placed

in an aluminum pan whereas an empty aluminum pan serves as the reference. These two pans are put on an electrically-heated plate in order to make sure that the temperature in the sample is the same as in the reference as can be seen in Figure 2.14. Via those plates and the pans, heat is transferred to the sample and the reference with the use of a defined computer controlled heating program (the rates of the heating can be adapted) (Lukasz et al. 2006). The differential heat flux to the sample and the reference as well as the sample temperature are measured. The output of a DSC measurement, the so-called 'thermogram', is a plot of the difference of heat delivered to the sample and to the reference as a function of the sample temperature. If a physical or a chemical process which is endothermic (consuming energy as heat) is taking place, in order to maintain the same temperature of the two pans, more heat must be delivered to the sample pan than to the reference pan (where of course no transition occurs). The effect is a positive or negative peak in the thermogram (the sign of the peak depends on the definition of the sign for the direction of the heat flow) as can be seen in Figure 2.15. The opposite is true for an endothermic process. Since the enthalpy change of the transition $\Delta_{trs} H$ is linearly related to the area under the curve of the thermogram, it can be easily calculated from the integral (Nishino et al. 2003).

The following values can be determined from the DSC:
- The melt point usually associated with a sharp melt endotherm.
- At what temperature does curing begin to take place, and the period of time that curing continues.
- A difference in cure between various stages for multilayer board by dual T_g values.

The DSC also can give a measure of the T_g of thermoset systems such as epoxy based on identifying energy changes associated with a change in the relationship between crystalline and amorphous segments in the polymer (Zgoul et al. 2008).
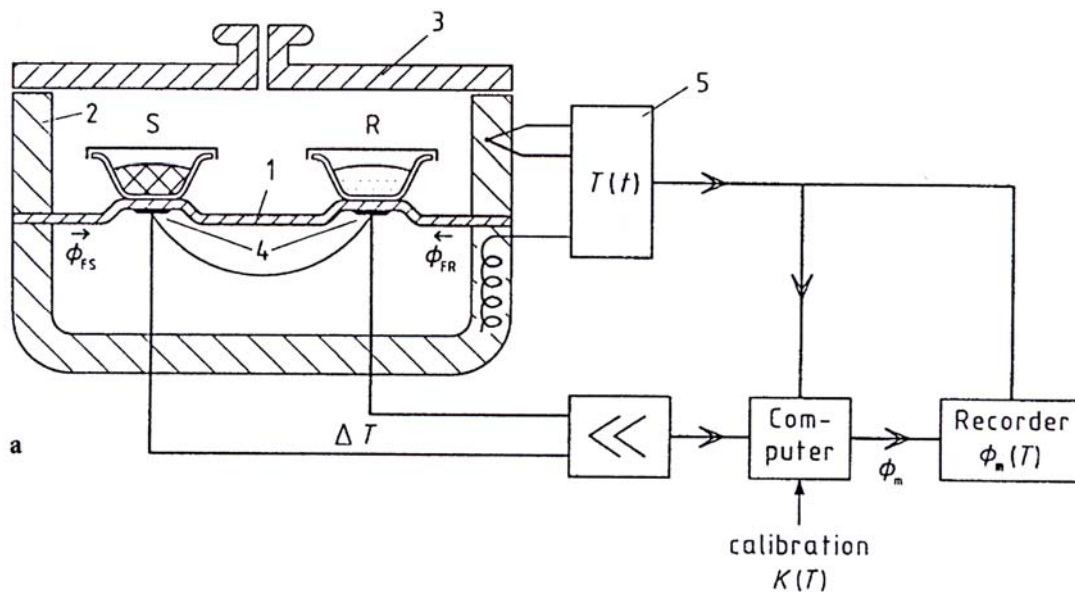
Figure 2.14 Heat flux DSC with disk-type measuring system (Hohane et al. 2003)
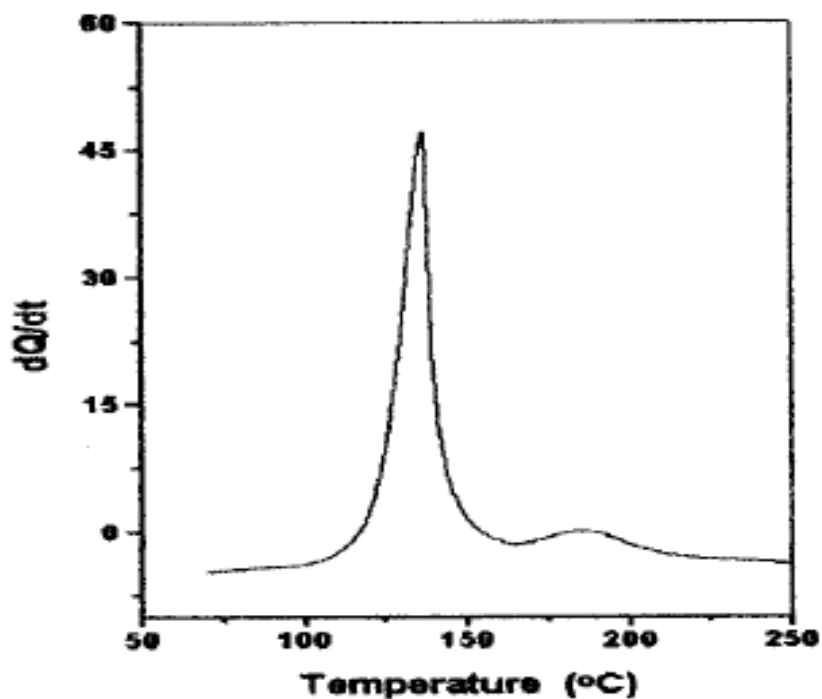
Figure 2.15 A typical DSC thermogram at a heating rate of 10°C/min (Lu et al. 1997)

Heating a polymer after reaching a certain temperature will rise suddenly upward through $\Delta(q/t)$. This change in the heat flow means getting more heat and thus increasing the heat capacity of the polymer. This happens because the polymer has just gone through glass transition. Polymers have higher heat capacities than glass transition.

Because of this change in heat capacity of polymers at glass transition temperature, DSC can be used to measure the polymer's glass transition temperature. Since the change in the heat flow does not occur rapidly but over a temperature range ΔT_g, it makes picking one discrete T_g value complicated. Therefore, the middle of the incline is picked as T_g (Zgoul et al. 2008). Beyond glass transition, a polymer has a lot of mobility. It never stays in one position for a long time. When it reaches the right temperature, it moves into an ordered arrangement (crystal arrangement). In a crystal arrangement, polymers emit heat. A drop in polymer heat can be seen as a full-size dip in the plot of heat flow q/t versus temperature T as shown in Figure 2.16. The temperature at the lowest point of the dip is usually considered to be the polymer's crystallization T_c. Heating a polymer beyond T_c results in a positive jump in the heat flow (melting transition) with melting point T_m. When the polymer reaches the melting temperature T_m, crystals start to fall apart and melt. The chains depart from their ordered arrangement and start to move freely. For melting the polymer crystals, they must absorb energy (heat). Melting is a first order transition, i.e., when a polymer reaches the melting temperature, the polymer's temperature will not rise until all the crystals have melted. Accordingly, the little heater under the sample pan has to supply the polymer with a lot of more heat in order to melt crystals and to keep temperature rising at the same rate as that of the reference pan (Gere 2004). This extra-heat flow during melting appears as a peak on the DSC plot in Figure 2.16.
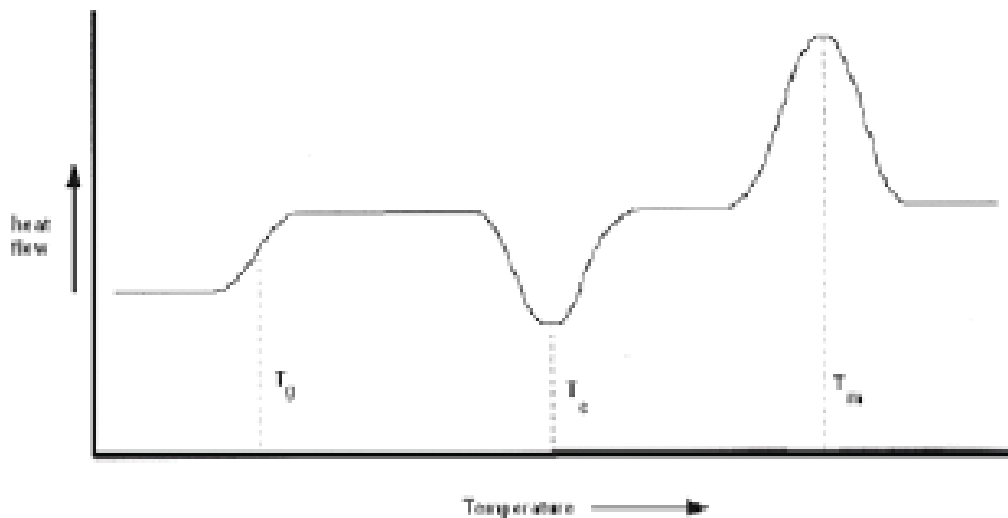
Figure 2.16 The whole DSC test operation

51

2.11 Summary

This chapter presented a literature review of the research status for experimental and analytical investigations on the physical, mechanical and dynamic properties for kenaf fiber unsaturated polyester composites.

Kenaf is an ancient crop and has a long history of being planted and used by human beings. It was considered an alternative crop and the products from it were simple and cheap. Kenaf's strength and resistance to rot and mildew make the kenaf unsaturated polyester composites well suited for selected industrial applications. The crosslinking reaction is a very important stage in the processing of unsaturated polyester into a composites product. A considerable amount of literature has been published on the physical and mechanical properties of unsaturated polyester of various styrene concentrations using traditional and standard tensile, flexural and impact tests. Other studies investigated dynamic and thermal properties using the DMA test. Further studies investigated the effects of the compatibility between the kenaf fiber and other natural fiber on the mechanical properties of hybrid composites. The important parameters affecting the fibers type, fiber weight fraction, type of matrix, chemical treatment, compatibility between the fiber and the matrix, and moisture uptake on the mechanical and thermal properties were studied for of natural fiber composites. More work has to be done to explore fully the properties of natural fiber composites to study the suitability of these materials for industrial applications. The current study is motivated by the need to understand the performance of kenaf fiber unsaturated polyester composites at different parameters. In addition, investigations were done on viscoelastic properties via creep test using DMA. . It is possible to obtain creep curves at different temperature levels which can be shifted along the time axis to generate a single curve know as a master curve. This technique is known as the time temperature superposition principle. Shift factors conformed to a William-Landel-Ferry (WLF) equation.

CHAPTER THREE

MATERIALS AND METHODS

3.1 Experimental Overview

The purpose of this research is to investigate the mechanical and dynamic properties of the kenaf and recycled jute fibers reinforced unsaturated polyester composites. The identification of these properties was attempted by optimizing various composite parameters, such as fiber strength, fiber processing methods, composite processing methods and fiber-matrix interfacial adhesion. In order to achieve this objective, kenaf and recycled jute fibers were chemically treated to improve the fiber strength and fiber separation, and modify the fiber surface. Composites were produced by compounding chopped fibers and unsaturated polyester resin by hand lay-up.

This chapter describes the materials and methods use in this research project. The experimental work was divided into four stages. The first stage involved the preparation of short kenaf and recycled jute fibers. The second stage attempted to determine the properties of unsaturated polyester, such as viscosity and tensile strength and Young's Modulus. The third stage looked into characterization all parameters of fibers, such as tensile strength, Young's Modulus, moisture content and density. The last stage evaluated the mechanical properties, such as strength, Young's modulus, interfacial adhesion and thermal stability for the kenaf and hybrid composites.

3.2 Preparation of Kenaf Fiber

The kenaf natural fiber was received from the Kenaf Natural Fiber Industries Sdn. Bhd. in the form of long and particle fibers. The preparation process of the core and stem fiber of the kenaf plant was carried out using two different processes as follows:

3.2.1 Kenaf Long Fiber

The physical treatment of the kenaf was done by cleaning where the fiber was washed thoroughly in 2% detergent solution at 100°C followed by tap water and then dried in several different weather conditions in order to get the optimum or the most excellent drying results for the fiber. The process of drying under three conditions was as follows:

a) The fibers were dried for 55 hours under laboratory conditions at 24°C near the window and then dried in an electric oven (Ecoocell LSIS-B2V/EC55) at 100°C for 6 hours.

b) The fibers were dried for 17 hours under laboratory conditions at 24°C near the window and then dried in an oven at 100°C for 11 hours.

c) The fibers were dried about17 hours under laboratory conditions at 24°C near the window followed by 5 hours outside at 34°C under the sun and then dried in an oven at 100°C for 5 hours.

these different conditions were expected to indicate number of hours the fiber would need to become fully dry. The kenaf long fiber was chopped using the decorticating machine. In order to maintain the fiber length to be between 3-6 mm, a sample of 122 short kenaf fibers were selected randomly and measured. The fibers were grouped together and stored under laboratory conditions before characterizing and chemical treatment for further processing.

3.2.2 Kenaf Particle Fiber

A sieve was used to separate desired elements from unwanted material using a tool. Sieving is a simple and convenient method of separating particles of different sizes; sieves with different types of holes were used for the classification of the kenaf particle fiber. The separation process of the raw particle fibers was done using round vibratory sieves (Unit Test) for different sizes of sieves, namely 1.18 mm, 600 μm, 400 μm, 300 μm, 200 μm and 150 μm. Figure 3.1 shows the round vibratory sieves and the sieves of different sizes. The separation sieving times in this work was 10 minutes for each operation. The particle fibers went through the same process of physical treatment as the long kenaf fibers.

a   b
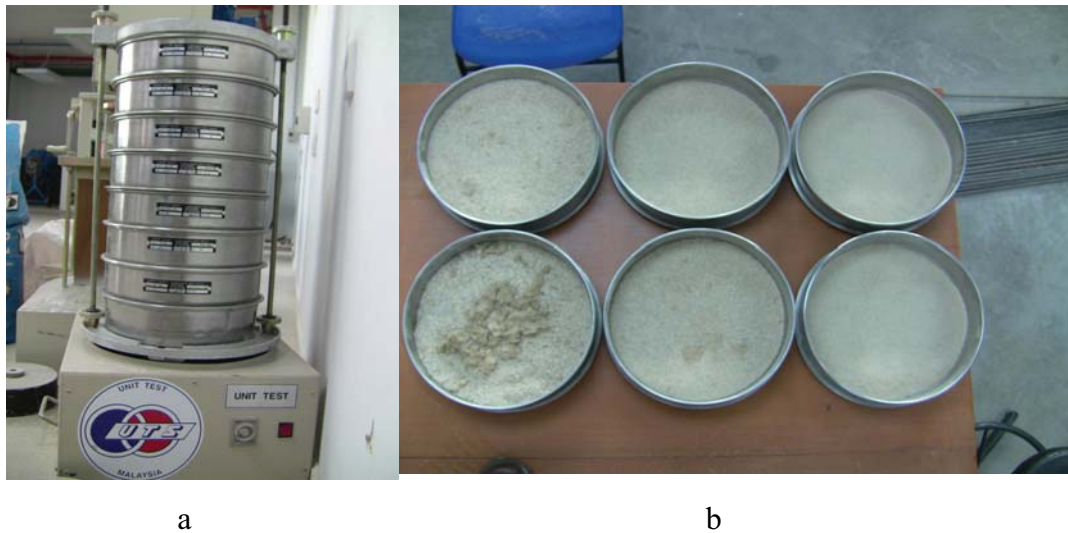
Figure 3.1 (a) The round vibratory sieves (Unit Test) and (b) the sieves with different sizes of kenaf fiber

The conditions for drying the kenaf short fiber was 48 hours outside the laboratory followed by 7 hours in an electrical oven at a temperature of 100ºC. The particle fibers were dried first outside the laboratory for 24 hours followed by 24 hours in an electrical oven at a temperature 100ºC. This was to make sure that the fiber was fully dry. The fibers were grouped together and stored in a cool and dry place before characterization and chemical treatment for further processing.

3.2.3 Recycled Jute Fiber

Recycled jute stacks were purchased from a grocery store as shown in Figure 3.2. The jute sacks had previously been used to store peanuts, dried chilies, or various beans. The quality of the jute sacks varied as there were some contaminants (woodchips, string, dust) embedded in the hemp and the sacks were damaged (holes, broken fibers) in some areas. The jute stacks were dirty and, sometimes, visibly damaged. All the jute sacks were machine washed and sun-dried before use. Physical treatment was done and the fiber was chopped manually to three various lengths (10, 20, and 30mm respectively).

Figure 3.2 Recycled jute sacks

3.2.4 Fiber Modification and Evaluation

Kenaf and recycled jute fibers were soaked separately in 6wt% concentration of NaOH solution in a water bath where the temperature was maintained throughout at room temperature for 48 hours, such that the fiber:liquor ratio was 1:7 (by weight). The fibers were rinsed several times to remove any NaOH solution sticking to the fiber surface and then dried in an oven for 24 hours at 100°C. This treatment consisted in dissolving lignin and hemicelluloses in order to recover celluloses fibers. The presence of surface impurities on the untreated kenaf fiber surface was very obvious. The surface of the treated fiber seemed rough when compared to the untreated fiber. Following 6% NaOH treatment, wax, oil and other surface impurities were removed.

3.2.5 Holocellulose Extracted form Kenaf Fiber

Holocellulose is the main component of natural fibers. Therefore, to extract the holocellulose, two samples from alkali treated kenaf fiber 2g each from bast and particles (core) with different sizes (0.15, 0.2, 0.3, 0.4, 0.6, 1, and 3mm) were used. The first step was to wash the samples by adding 200 ml Ethanol/Toluene 1:2 mixing ratio at 100ºC. The washing process was repeated 6 to 7 times and it took about 8-9 hours as shown in Figure 3.3. After the washing was done, the fibers were fully dried in an oven for 24hours at 100ºC.

The second stage involved adding 100ml distilled water, 1.5g sodium chlorite, and 5ml 10% acetic acid solution to the fiber, and heating the mixture inside a boiling water bath as shown in Figure 3.4. After 30minutes, 5ml of 10% acetic acid solution and 1.5g sodium chlorite were added alternate acetic acid and sodium chlorite additions were continued at 30minutes intervals until 6g of sodium chlorite was added. After last addition of sodium chlorite the mixture was left in the boiling water bath for 30 minutes. The white residue and kenaf structure were retained.

In the third stage the suspension was cooed in an ice bath to avoid the evaporation of sodium chlorite, and then filtered into a weighed fritted glass crucible (porosity 1) and washed with iced distilled water. Finally, was washed with acetone for fast drying. The residue was allowed to stand in the open laboratory until it was cooled and free of acetone. Then the extracted holocellulose was dried in an oven at 100°C for 12 hours to ensure the holocellulose was fully dry.

a   b
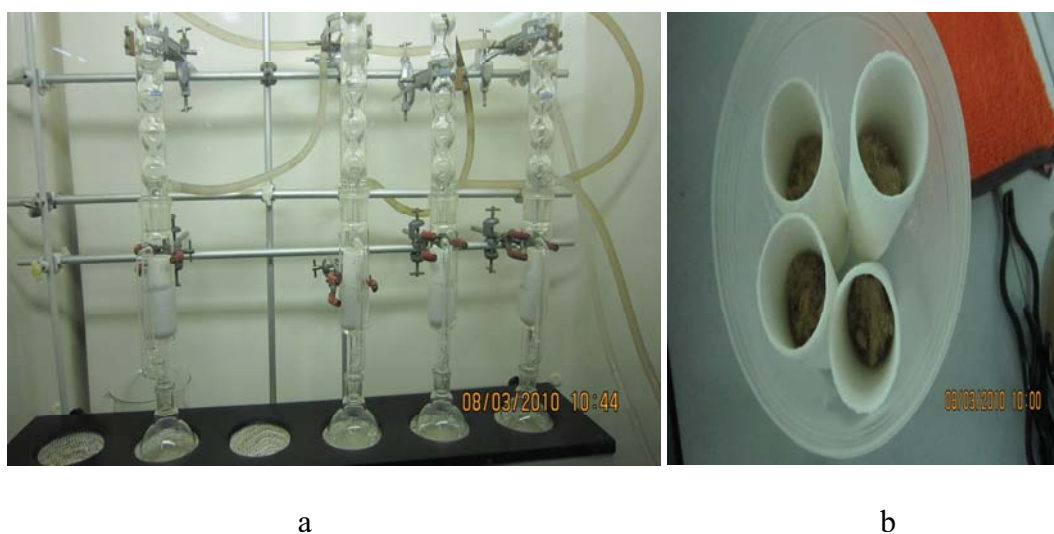
Figure 3.3 (a) Ethanol/Toluene washing device, (b) (2g) of fiber specimen

a   b

Figure 3.4 (a) Boiling water bath, (b) glass crucible wash

3.3 Physical Test of Fibers

3.3.1 Fiber Diameter

The purpose of this test was to determine the average diameter of the kenaf fiber using the single fiber tensile test. Diameters of selected fibers were then measured under a microscope by means of a calibrated eyepiece with 100 times magnification power. Ten fibers with 50 mm length at 17 locations were measured.

3.3.2 Kenaf Bast Fiber Density

The Archimedes Test using canola oil as an immersion fluid is a simple and effective method for general use in measuring kenaf fiber density. The procedure in this study was to:

- use a minimum 0.5g of kenaf fiber per specimen
- soak the samples in canola oil for 1 minute
- place the specimens in vacuum desiccators' for 5 minutes to remove trapped air from between the fiber cells
- completely immerse the specimens in canola oil and take a mass reading
- calculate the fiber density from the canola oil density and ratio of recorded masses.

The density of canola oil was 0.8828 g/cm^3 after taking the average of 10 samples. The density of canola oil was calculated using Equation 3.1.

$$\rho\left(fl\right)=\frac{W}{V} \tag{3.1}$$

where ρ (fl) is the density of the sample, W is the mass, V is the volume.

The density of kenaf bast fiber was calculated using Equation 3.2.

$$\rho=\frac{W\left(a\right).\rho\left(fl\right)}{0.99983\,G}+0.0012 \tag{3.2}$$

where W(a) is the (dry) weight dry for samples, G is the buoyancy of the sample, 0.0012is the density of air under standard conditions, 0.99983 is the correction factor (Sartorius User's Manual, 2008). The same method was used to calculate the densities of the kenaf fiber unsaturated polyester composites (KFUPC).

3.3.3 Moisture Content and Moisture Absorption

The objective of these tests was to determine the moisture content of the fibers before they were dried in an oven and control the low moisture content of the fibers before the composite fabrication. The apparatus and material in this test included an oven, balance weight with a sensitivity of four digits, and weighing containers and desiccant (calcium chloride). The oven was thermostatically controlled at a temperature of 105°C with fan-forced ventilation. To avoid moisture regain when weighing the dried fibers, the balance weight equipped with tight fitting covers and desiccants are placed in the covers. Two samples of 2g each were used to study the water absorption of bast and core kenaf fibers. A ceramic crisple was used as a container for the samples. The samples were dried in an oven at 105°C for 5hours, and then kept in an oven to be cooled down to room temperature. The samples were weighed and left in laboratory surroundings at room temperature. The first reading was taken after 5hours, and then the second reading was after 24hours, and then after 48hours and so on. The weight was recorded as a function of time until it reached the saturation limit. All procedures were repeated for the three specimens of the kenaf fiber.

3.4 Single Fiber Tensile Testing

The elementary kenaf fiber was separated from their fiber bundles by hand, and mounted on 1mm thick cardboard mounting-cards as Figure 3.5 shows. The fibers were glued by PVC glue to the cardboard on either side of the two edges; fibers were carefully put into place using a microscope to ensure that only a single fiber was present on each card. The Tinius Olsen tensile machine with 10 N load cells was used for the tensile test of a single fiber. The mounted fibers were placed in the grips of the tensile testing machine, and the cardboard was cut with a pair of scissors.
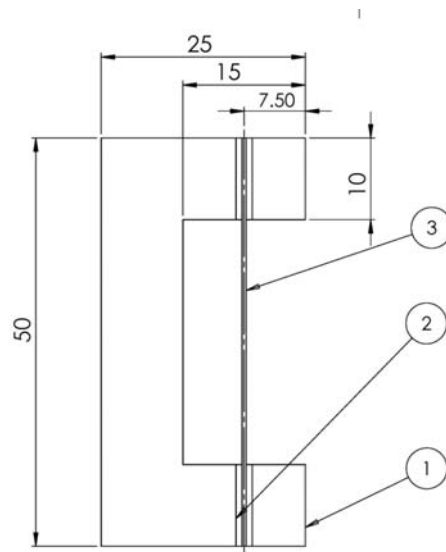
Figure 3.5 Tensile single fiber specimens of the kenaf fiber

3.5 Scanning Electron Microscopy (SEM)

The Scanning Electron Microscopy (SEM) JSM-5300LV technique was used to study the impurities of treated and untreated of single kenaf fibers. In addition, the SEM technique was used to revise the cross section of the fibers. The failed composite specimens were examined to observe the morphology of fracture surface of the composites, such as the interfacial interaction between the kenaf fiber and unsaturated polyester, as well as the interaction between the varying dimensions of hybrid composites including kenaf/recycled jute fibers and unsaturated polyester resin.

3.6 Materials and Experiments

3.6.1 Unsaturated Polyester

Unsaturated polyester (UP) (60%UP + 40%ST), and styrene (ST) with density (0.909) g/cm^3 were obtained from BORNEO INDAH SDN BHD with properties such as appearance (pink), density (1.12 g/cm$^{3)}$, and stability in the dark below 25ºC. The unsaturated polyester containing 50% styrene was prepared by adding 20g of styrene to 100g from unsaturated polyester (60%UP + 40%ST).

3.6.2 Curing Agents

Methyl ethyl ketone Peroxide (MEKP) and Dimethyl Aniline NNDMA were obtained from the same supplier for unsaturated polyester resin and used as a catalyst and accelerator, respectively. The properties of DMA were as follows:

- the density at 20-24ºC temperature - (0.955-0.960) g/cm^3
- molecular weight - 121.18 g/ml
- the chemical symbols - C8H11N.

3.6.3 Setting Time Test

The workability of resin is influenced by the setting time. Therefore, it is very important to design a suitable setting for the resin to avoid early setting. The setting time is influenced by the curing system with either at room temperature or an elevated temperature. The curing system was initiated by adding the catalyst, Methyl Ethyl Ketone Peroxide (MEKP) to the unsaturated polyester resins. As the catalyst mixes with the resin, a chemical reaction occurs, creating heat which cures (hardens) the resin. The manual method to determine the gelation time of the polyester resin is calculating the setting time of the resin as a function of the amount of catalyst. The apparatus includes a container, stirring rod, timing device and thermometer. An amount of 0.5% of catalyst is mixed in the resin. The timing device is started once the catalyst is mixed. The stirring rod is stirred by continuously moving the rod one complete revolution of the diameter container until gelation occurs. The procedures are repeated for 1, 2, 3 and 4 % respectively of catalyst. The graph of gelation time as a function of catalyst amount was drawn. The procedure was completed under the Fume-Hood vacuum system.

3.6.4 Viscosity Test

LVDV-II+Pro Viscometer Brookfield was used to measure the viscosity of the unsaturated polyester at different styrene concentrations for various temperatures. A standard Griffin beaker with 600ml was used in the test. The experiments were started at 26 ºC and repeated until 50ºC. Brookfield viscometers were used to measure the viscosity of unsaturated polyester resin (UP) with different ratio of styrene (ST) as summarized in Table 3.1.

Table 3.1 Different mixing ratios of unsaturated polyester resin (UP) and styrene (ST)

Unsaturated Polyester UP (wt %)	Styrene ST (wt %)
50	50
40	60
30	70

3.6.5 Curing Process of Composites

The polyester resin containing different concentrations of styrene was mixed at different volume fractions of MEKP at 26ºC for 1 minute. Then the mixture was poured into a paper cup (9.5cm diameter and 9cm deep) and weighed using a weighing scale. With a weight of approximately 112.7g, 10 wt% of kenaf fiber size 1-6 mm was added. The temperature data was measured by placing a thermocouple covered by aluminum foil at the center of the isolated paper cup connected to a digital thermometer. A stopwatch was used to measure the gel time.

3.6.6 Matrix Tensile Test

A tensile test was done according to the ASTM D 638 standard using a universal tensile machine. The specimens were prepared for three different styrene concentrations namely (60%UP + 40%ST), (50%UP + 50%ST) and (40%UP + 60%ST). MEKP was added at 1, 2, 3 and 4% respectively at a volume of 100 ml of UP resin, mixing manually for 3 minutes and placed in a mold for 24 hours. The detailed dimensions of the specimen for the unsaturated polyester resin are shown in Figure 3.6. To ensure that the mold was very clean and dry, a release agent (wax) was put in the mold before the powering mixture. The same process was applied to prepare the resin specimens with fixed MEKP concentrations of 1% and varying NNDMA volume fractions from 0.1%, 0.2% and 0.3%. Figure 3.7 shows the mold of the tensile specimens of the matrix. The mold consisted of three parts; the base part and the upper part were made form aluminum while the intermediate gasket was made from Teflon. The specimens were posited vertically in the grips of the testing machine with 50 mm gauge length. The stress strain curve was plotted during the test for the determination of the ultimate

tensile strength and elastic modulus. Young's modulus represents the slope of the stress-strain curve. Four specimens were evaluated for this test.
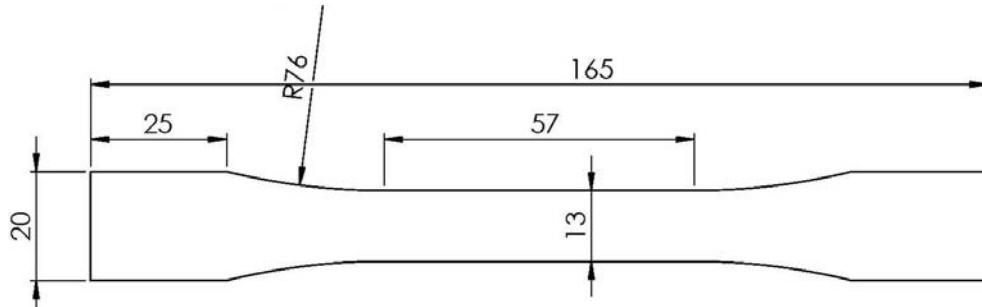
Figure 3.6 The dimensions of the tensile test specimen for matrix (thickness=3mm)

Figure 3.7 Mole of tensile specimens for resin and composites

3.6.7 Charpy Impact Test

The determination of the impact strength of unsaturated polyester as polymer and kenaf unsaturated polyester as composites is a technique of comparing its toughness with other polymers and composites. The Charpy Impact Test was used in this study to measure the impact strength of the resulting composite materials. The testing apparatus used was a pendulum type tester supplied by Lotus Scientific Sdn. called LS-22 006-50J. The Charpy Impact Tester had an initial energy of 50J at the initial height as shown in Figure 3.8. The impact specimens in this apparatus had dimensions of 10 x10 x 60 mm, with a v-notch 2 mm deep at 45º angle on one side at the center. The impact test

was done accordance with the ASTM E-23., Figure 3.9 shows the failed impact specimens for resin and composite. The impact strength was calculated as follows:

$$\text{Impact strength} = \frac{E}{A} \qquad\qquad (3.3)$$

$$E = J_o - J_1 \qquad\qquad (3.4)$$

where
J_o = initial energy at the initial height

J_1= resultant energy (conversion from Table LS-22006-50J in the Charpy Izod Impact manual)

A= Area of the specimen

Figure 3.8 Impact test setup

Figure 3.9 Broken specimens of resin and composites

3.6.8 Matrix Flexural Test

Flexural strength was measured under a three-point bending approach using a universal testing T-machine according to ASTM D790 as shown in Figure 3.10. The dimensions of the samples were 127mm x 12.7mm x 3.2mm. The distance between the spans was 100mm, and the strain rate was 5 mm/min. Four specimens were tested for each case; the averages were reported as results.

Figure 3.10 The flexural test setup

3.6.9 Differential Scanning Calorimetry (DSC) Test

The Differential Scanning Calorimetery Test was carried out in a TA Instrument DSC 2960, which calculated the glass transition temperature (T_g) for unsaturated polyester resin at various styrene (ST) concentrations. The sample weight was between 5-10mg at a heating rate of 10ºC/min.

3.6.10 Thermo Gravimetric Analysis (TGA)

The Thermal Gravimetric Analysis was analyzed for both the resin and composites using Thermo Gravimetric Analysis SDT 2960 simultaneous DSC-TGA, the samples of matrix and composites having masses from 5-10mg. The heating rate was 10ºC/min over the temperature range from 30 to 400°C; a nitrogen atmosphere was employed.

The equipment used to perform the thermo gravimetric analysis is shown in Figure 3.11. It was mainly used to measure the weight loss with temperature and time as a function continuously in a confined space and controlled atmosphere and to characterize polymers. This equipment is used (nowadays) in various research, quality control and fabrication operates.

Figure 3.11 SDT 2960 simultaneous DSC- TGA

3.6.11 Dynamic Mechanical Analysis (DMA)

Dynamic mechanical analysis was conducted on the DMA 2980 analyzers of TA Instruments under the flexural mode of testing. The specimens were fastened in a single cantilever clamp setup; the DMA machine analyzed the rectangular cross section of the sample using the "Stiffness Model Equation". The DMA 2980 shown in Figure 3.12 has 6 possible modes to choose from, each having a different category of experiments; the mode used is shown in Figure 3.13 (Manual 2002). The temperature range of the investigations was set from 30-150°C and the corresponding heating rate to 3K/min. The cycle time for each experiment was approximately 20-25 minutes of temperature ramping to 150°C. Standard air pressure of about 420-425 KPa was maintained in an air pressure filter regulator at room temperature. The investigations were performed under constant excitation amplitude of 10 μm and an oscillating (single) frequency of 1 Hz. The following parameters were measured and stored during the experimental investigations: tan delta, storage and loss moduli. Selected results conducted using the

DMA measurements are presented in Figure 3.14. Short-term creep tests were performed with the DMA. The specimen dimensions were 25mm, 14mm, 4mm as length, width and thickness respectively. The creep tests were run in tensile mode for a total duration of 60 minutes at a stress of 0.25MPa at 30ºC and 50ºC. This was a small enough stress to be in a linear viscoelastic region. During the test, strain and creep compliance data were collected, and they were plotted versus time at different styrene concentrations. This procedure was followed for two different temperatures and for all weight fractions of kenaf fiber composites.
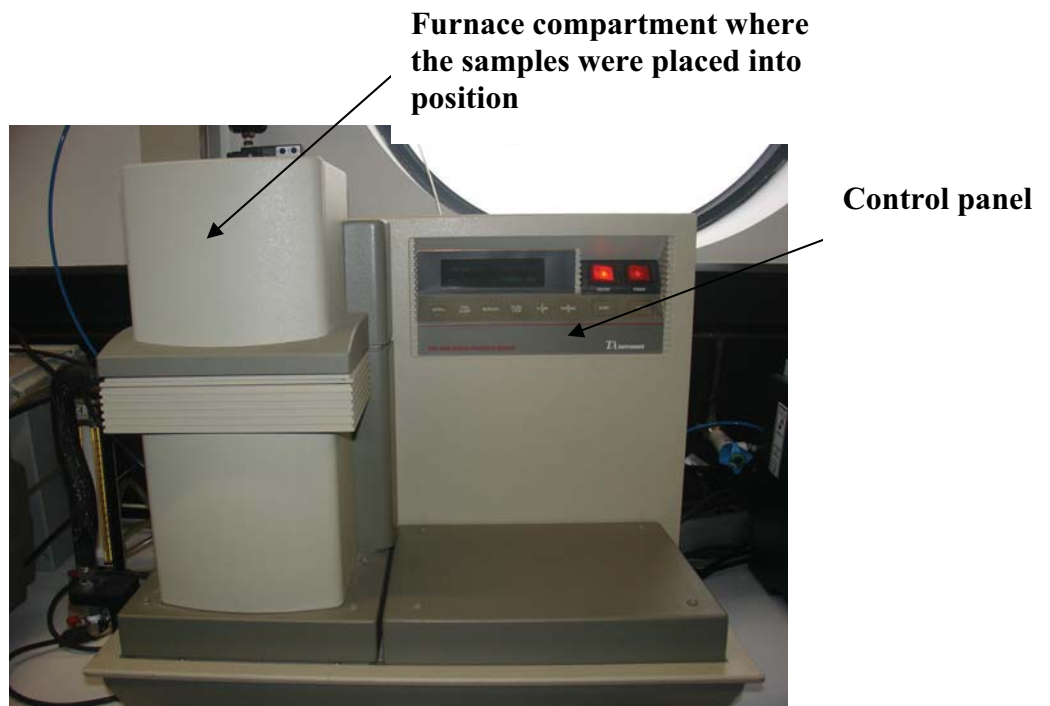
Figure 3.12 The DMA 2980
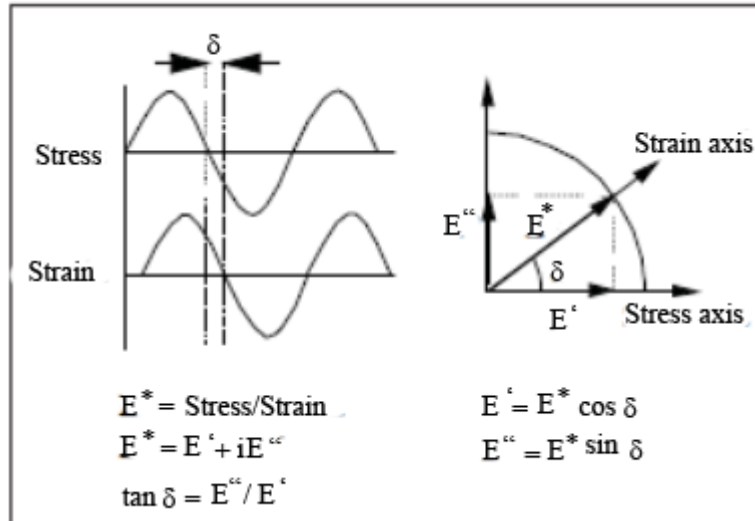
Figure 3.13 The principles of viscoelastic material
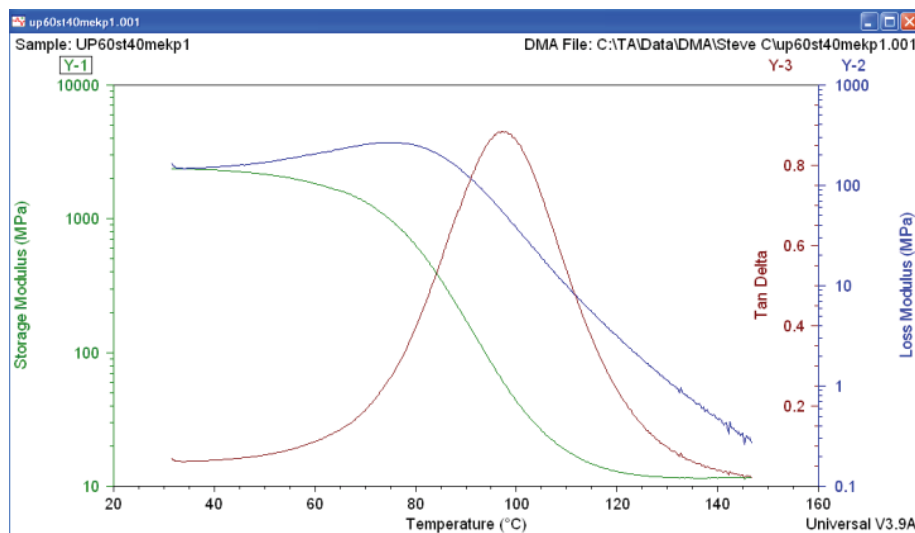
Figure 3.14 *Tanδ*, storage and loss modli captured using the DMA test

3.7 Preparation of Composites

3.7.1 Composite Fabrication

- **Kenaf Composites**

A compression molding process was used for the fabrication process. Specimens from 10% to 40% weight percentage of fibers were fabricated to produce kenaf/unsaturated polyester composites (KFUPC) of various styrene concentrations. The prepared resin (60%UP+ 40%ST) and (50%UP+50%ST) + 1 vol% MEKP was blended to fiber size (1-

6) mm to prepare 60KFUPC and 50KFUPC. In addition, the prepared resin (60%UP+40%ST) + 1% MEKP was blended to a fiber size of 10-30mm. the composite mixture was poured into the mold cavities. The mixture was gently pressed using the fingers to make sure each cavity of mold was properly filled. The composites were left for a few minutes to allow air bubbles to escape from the surface of the resin. The top plate was put in place and the mixture was left to relax for 10 minutes. Then, the top plate was screwed tightly in place. The composite was left to cure for about 24 hours at 25 ± 2ºC. The specimens were ground to trim the flushes of resin during the fabrication process. Certain composite specimens were post cured in an oven for 5 hours at 60ºC.

- **Hybrid Composites**

Four composites formulations were produced as shown in Table 3.2. A compression moulding process was used for the fabrication process. Specimens with 20wt% weight percentage of fibres were fabricated for flexural and impact test, while those with 30wt% weight percentage of fibres were fabricated for tensile test. The prepared resins were blended to a kenaf fiber size of (1-6) mm and for kenaf/recycled jute fibers at three different sizes of recycled jute fiber. Composite codes were used, such as 20W(75K-25J10mm) which means the percentage of fiber was 20 wt%, this percentage including 75% of kenaf fiber and 25% recycled jute fiber at 10mm length. Certain composites specimens were then post cured in an oven for 5 hours at 60ºC.

Table 3.2 Composition of the studied formulations for flexural and impact tests

Composite code	Unsaturated polyester (%)	Treated kenaf content (%)	Treated Recycled Jute content (%)	MEKP (%)
20WK and 30WK		100	0	
20,30W(75K-25J10mm)		75	25	
20,30W(50K-50J10mm)		50	50	
20,30W(25K-75J10mm)		25	75	
20,30WJ10mm		0	100	
20,30W(75K-25J20mm)	60%UP + 40%ST	75	25	1
20,30W(50K-50J20mm)		50	50	
20,30W(25K-75J20mm)		25	75	
20,30WJ20mm		0	100	
20,30W(75K-25J30mm)		75	25	
20,30W(50K-50J30mm)		50	50	
20,30W(25K-75J30mm)		25	75	
20,30WJ30mm		0	100	

3.7.2 Composite Test Setup

The tensile test specimens were prepared in accordance with ASTM D608. A load cell of 50kN was selected for this test. The specimen was loaded in tension at a constant stroke rate of 5 mm/min. An extensometer of 50 mm gage length was mounted on the specimen for the measurement of the strain as Figure. 3.15(a) shows, dumbbell shape (Type I) specimens with dimensions 165 mm of overall length, 13 mm width overall, 3mm for thickness. Flexural strength was measured under a three-point bending approach using a universal testing T-machine according to ASTM D790. The dimensions of the samples were 127mm x 12.7mm x 3.2mm. The distance between the spans was 100mm, and the strain rate was 5mm/min as seen in Figure 3.15(b). The Charpy Impact Test was used to measure the impact strength; the testing apparatus used was a pendulum type tester supplied by Lotus Scientific Sdn. called LS-22 006-50J Charpy Impact Tester with an initial energy of 50J at the initial height. The impact specimens' dimensions were 10 x10 x 60 mm, with a v-notch 2 mm deep and 45º angles on one side at the center. The Impact test was done in accordance with the ASTM E-23. Four specimens were tested for each case; the averages were reported as results. Figure 3.16 represents the specimen mold for impact and DMA composites test. The sample of treated kenaf fiber of different sizes and sample of unsaturated polyester resin are also shown.

a   b
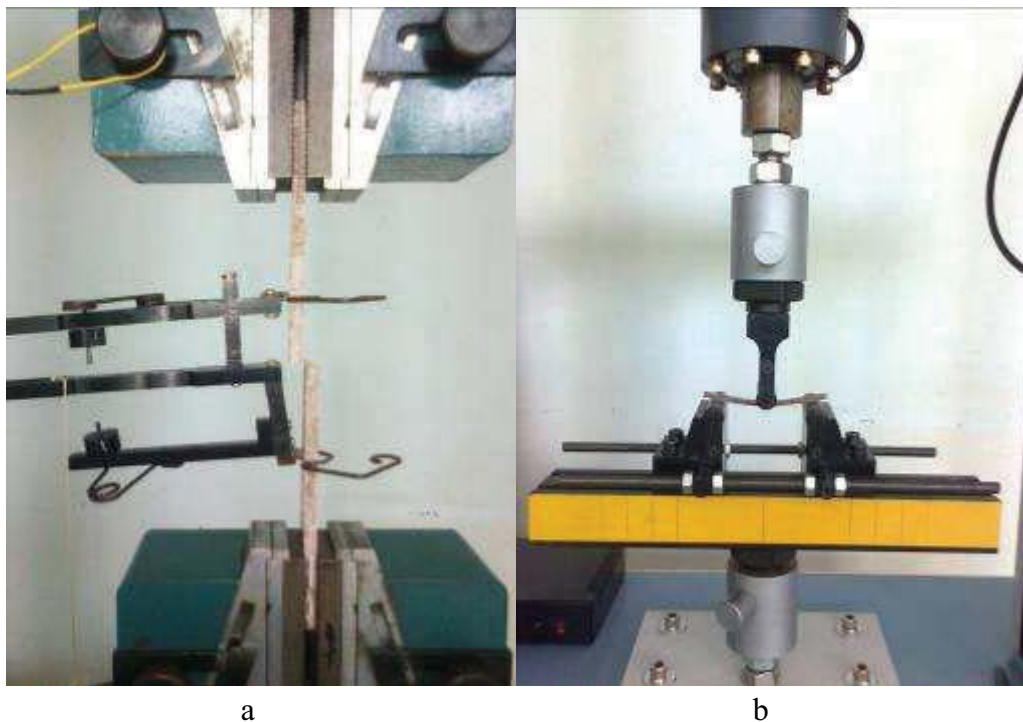
Figure 3.15 Universal testing T-machine: a) tensile test, b) flexural test

Figure 3.16 Kenaf fibers of different sizes, unsaturated polyester and fabrication mold

3.7.3 Water Absorption and Thickness Swelling Test

Water absorption and thickness swelling tests were carried out according to ASTM D570-81. Specimens of each formulation were dried in an oven for 2 hours at 105ºC. The weight was measured to a precision of 0.0001g using four digit balances; thickness and width at three different locations and length were measured to a precision 0.01mm using a digimatic caliper, respectively. Kenaf/recycled jute composites specimens were placed in distilled water at 25±2ºC. In addition, kenaf composites specimens were immersed in distil water at 25 ± 2 ºC. For each measurement, specimens were removed from the water, surface water was wiped off using a soft dry cloth, and they were weighed and measured for thickness, width and length. After these measurements the samples were immersed again in water. The process was continued until the saturation period was reached after 868hours. The values of water absorption and orthotropic swelling in percentage were calculated using the following formulas (Dhakal et al. 2007).

$$W(\%) = \frac{W_{(t)} - W_o}{W_o} \times 100 \qquad\qquad (3.5)$$

$$S(\%) = \frac{S_{(t)} - S_o}{S_o} \times 100 \qquad\qquad (3.6)$$

where W_o and $W_{(t)}$ denote oven-dry weight and weight after time t, respectively, S_o and $S_{(t)}$ denote oven-dry dimension and dimension after time t, respectively.

3.8 Summary

The experimental programmed was carried out according to the relevant standards and recommendations by researchers. A sieve separation was done for the core kenaf fiber using a mechanical method as explained in this chapter. The kenaf physical treatment and chopping process were carried out. Chemical treatment was done using 0.6% NaOH. Physical test and tensile test of kenaf bast fiber were successfully conducted. The test methods and procedures are discussed in detail. Resin casting was carried out for unsaturated polyester at three different mixtures of styrene. MEKP and NNDMA were added at different volume ratios. The kenaf bast fiber reinforced unsaturated polyester composites were fabricated under closed mold hand layup for different styrene concentrations and different kenaf fibers length and weight fractions. The kenaf/recycled jute unsaturated polyester composites were fabricated under closed mold hand layup for various recycled jute fiber lengths and weight fractions. The mechanical test for tensile, flexural and impact tests of resin and composites was carried out according to the standards. Furthermore, dynamic and thermal properties of resin and composites were conducted according to standards. Dynamic mechanical analysis was performed to obtain strain and creep compliance for kenaf composites various styrene concentrations. SEM analysis examined the surfaced and cross section of single treated and untreated kenaf fibers. Finally, SEM analysis was done for composites to investigate the interaction between the fibers and unsaturated polyester resin.

CHAPTER FOUR

CURING BEHAVIOUR AND PROPERTIES OF UNSATURATED POLYESTER RESIN

4.1 Introduction

Unsaturated polyester resins are one of the most important thermoset materials used in the composites industry for the preparation of molding compounds, laminates, coatings, and adhesives as they are of low cost and have good mechanical properties (Andjelkovic et al. 2009 and Shenoy et al. 2007). Thermoset resin is defined as a plastic material which is initially a liquid monomer or oligomer or a pre-polymer, which is cured by either application of heat or a catalyst to become an infusible and insoluble material (Sinha 2000). Unsaturated polyester resins are viscous liquids consisting of oligomeric unsaturated polyester and polymerizable diluents (e.g. styrene or acrylate/methacrylates), as well as polymerization inhibitors.

This chapter presents investigation into the curing behaviour of UP resin containing different concentrations of styrene monomer via measuring viscosity, gel time, and maximum exotherm temperature. In addition, the effect of styrene concentrations on the mechanical properties of unsaturated polyester is studied. The MEKP at different concentrations was used as an initiator for curing the unsaturated polyester and NNDMA curing accelerator at various volume fractions starting with 0.1, 0.2 and 0.3. The effect of varying the level of water content on the exotherm behaviour was investigated. In this research, a detailed investigation was carried out to study the flexural and tensile properties and to optimize the impact strength of unsaturated composites via different concentrations of styrene, MEKP and NNDMA. A dynamic mechanical analysis test was used to study the behaviour of the UP resin. The results revealed varying changes due to the different mixtures of ST, at a fixed MEKP concentration.

4.2 Measurement of Viscosity

Figure 4.1 illustrates the distribution of the viscosity with temperature. As expected with increase temperature the viscosity dropped significantly. It was observed that the viscosity decreased with an increase in styrene concentration ratio. The results show that the viscosity was 219.3cP at 26ºC and 64.5cP at 50ºC and the percentage decreasing was 29.48 % for the first ratio of (60%UP +40%ST), while the percentage decrease for the ratio of (50%UP +50%ST) was 64.93%; for the last styrene ratio of (40%UP +60%ST) it was 61.79%.
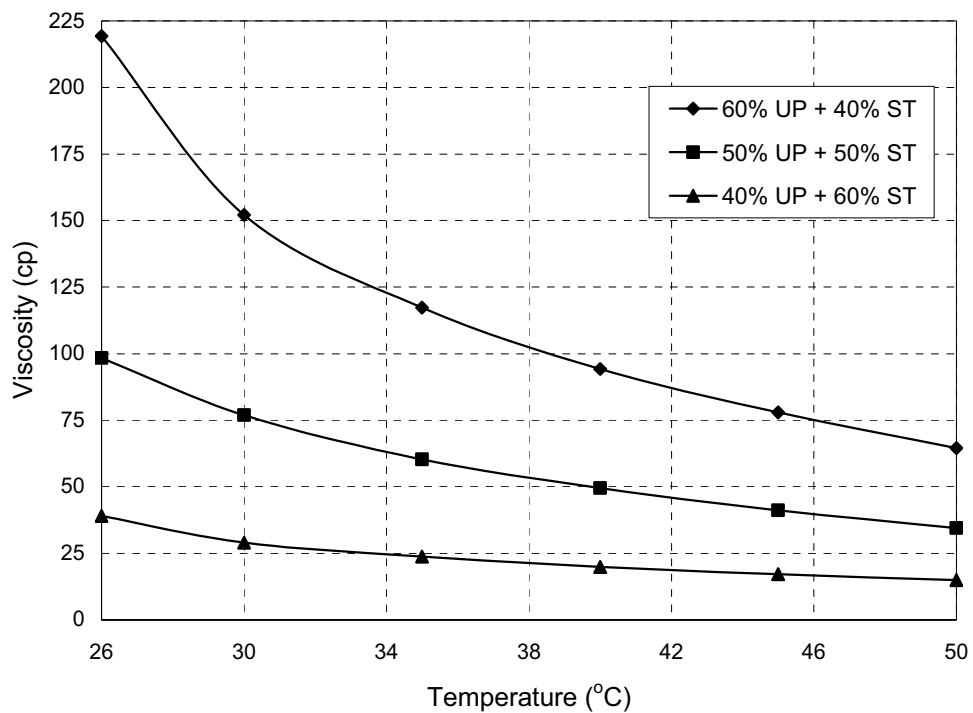
Figure 4.1 Viscosity change with temperature at different concentrations of styrene

Figure 4.2 shows that due to the various proportions of water content namely (1, 2 and 3 vol%), the distribution of the viscosity with time decreased with increase water content. It was observed that the 0 vol% water sample reached the maximum values of viscosity of 1200cp in 17.5 seconds, while it was 23.1, 28.3 and 34.55 seconds for 1, 2 and 3 vol% water content respectively. This could be due to the high amount of water content that led to a decrease in the physical properties of the resin.
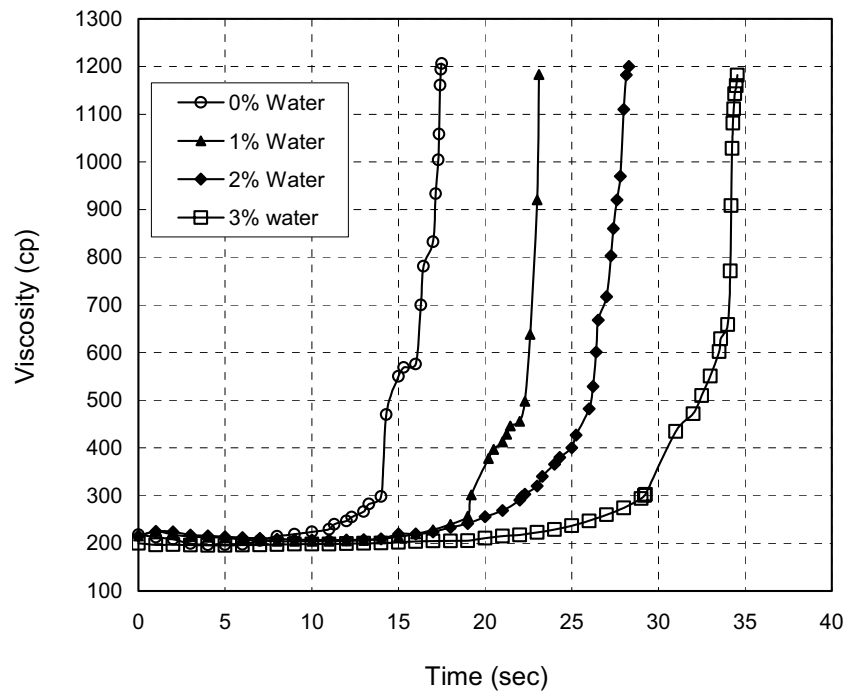
Figure 4.2 Viscosity change with water content for (60%UP+40%ST) resin

4.3 Measurement of Density

The styrene ratio controlled the reactivity of the unsaturated polyester and also the crosslinking density of the final network. Figure 4.3 explains the density variations with the increase in styrene concentration at 26ºC. It is clear that the density of the matrix decreased when the styrene ratio was increased.

4.4 Cure Characteristics

4.4.1 Curing Time and Peak Exotherm Temperature

The cross-linking reaction is a very important stage in the processing of unsaturated polyester into a composite product, as well as the exotherm temperature of cure after the completion of the processing. The crosslinking reaction is a highly exothermic reaction, and the temperature can increase up to 100-200ºC. Figure 4.4 explains clearly the different exotherm temperatures for the three different styrene concentrations of unsaturated polyester. The maximum exotherm temperature was about 156ºC for the ratio 50% of styrene followed 60% at about 132.9ºC and 40% at about 128ºC.

Figure 4.5 presents the gel time for different ratios of unsaturated polyester containing various concentrations of MEKP. The fastest curing took place at 40% ST, compared to both 50%ST and 60%ST. This increase in gel time is a clear indication of increasing styrene concentration. This means that the styrene works as a dilution agent for a certain value of MEKP.
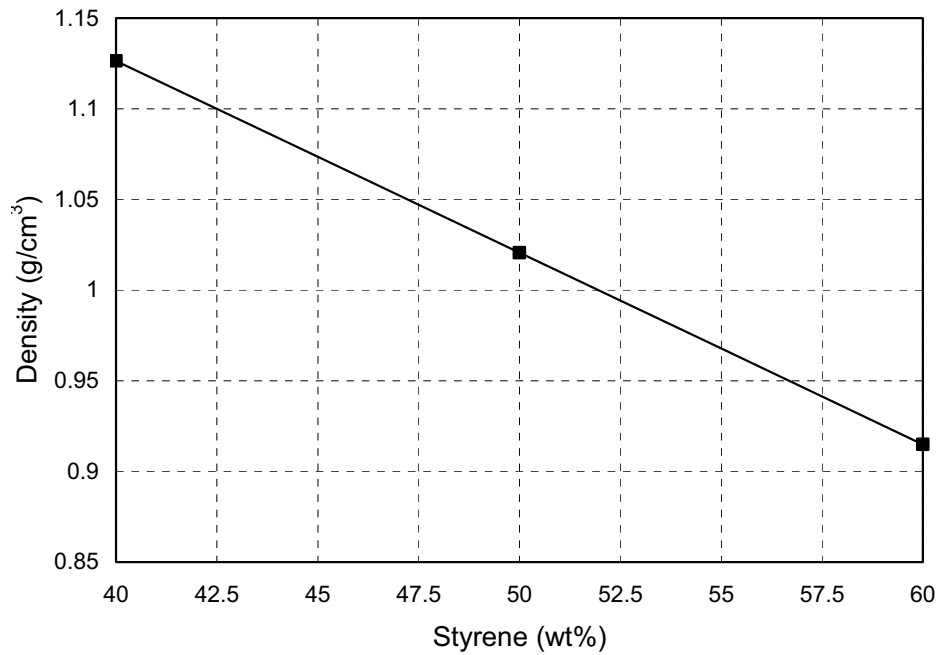
Figure 4.3 Density change with styrene concentration ratio for unsaturated polyester resin
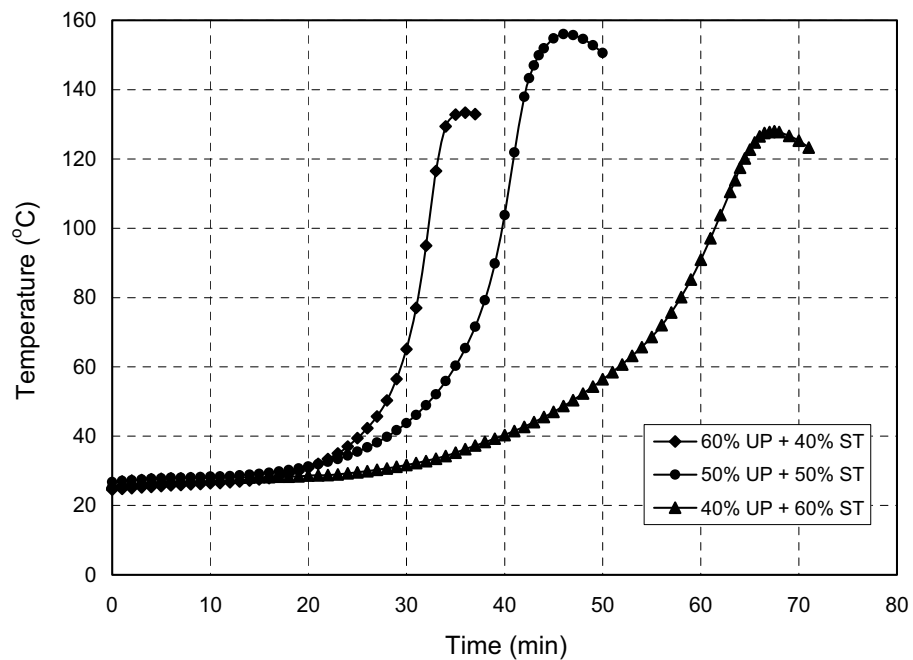
Figure 4.4 Curing time for different volume fractions of unsaturated polyester at 1% MEKP
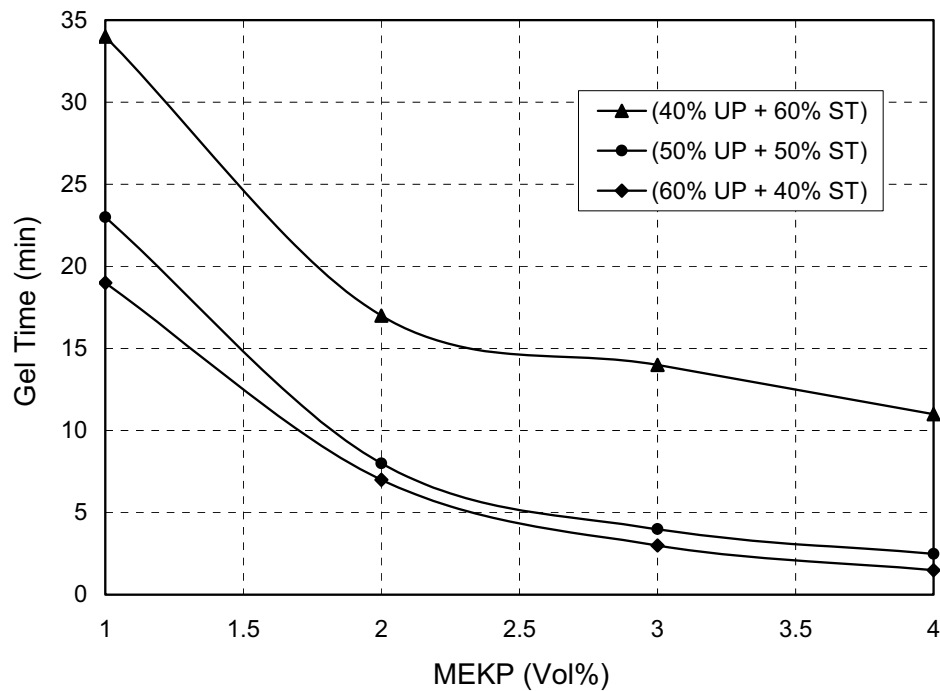
Figure 4.5 Gel time for unsaturated polyester containing different concentrations of styrene and MEKP ratios

Figure 4.6 presents the time-to-peak for different ratios of unsaturated polyester containing different concentrations of MEKP. It is observed that the time-to-peak shows a similar behaviour with respect to the MEKP concentration ratio. One can observe the time-to-peak significantly changed when the styrene concentration increased. The second effect of styrene is its ability to act as a crosslinking agent. Therefore, the styrene made the crosslinking occur more quickly and readily. This means the styrene speeded up the reaction process, although this effect was usually observed later in the overall curing cycle. Consequently, the time-to-peak decreased when the styrene concentration ratio increased. Generally, increasing the MEKP concentration decreased the time to peak.

Styrene worked as a crosslinking agent; the free radical could react with the styrene to form a bridge to another polyester chain. In forming this bridge, a free radical was created on the second polyester molecule. Heat evolved with each bond that was formed. Figure 4.7 explicates that 40%ST produces a lower exotherm temperature than both 50%ST and 60%ST. This lower exotherm could potentially make it easier in handling when making the composites; furthermore, it reduced the shrinkage of the material (Kuang et al. 2007).
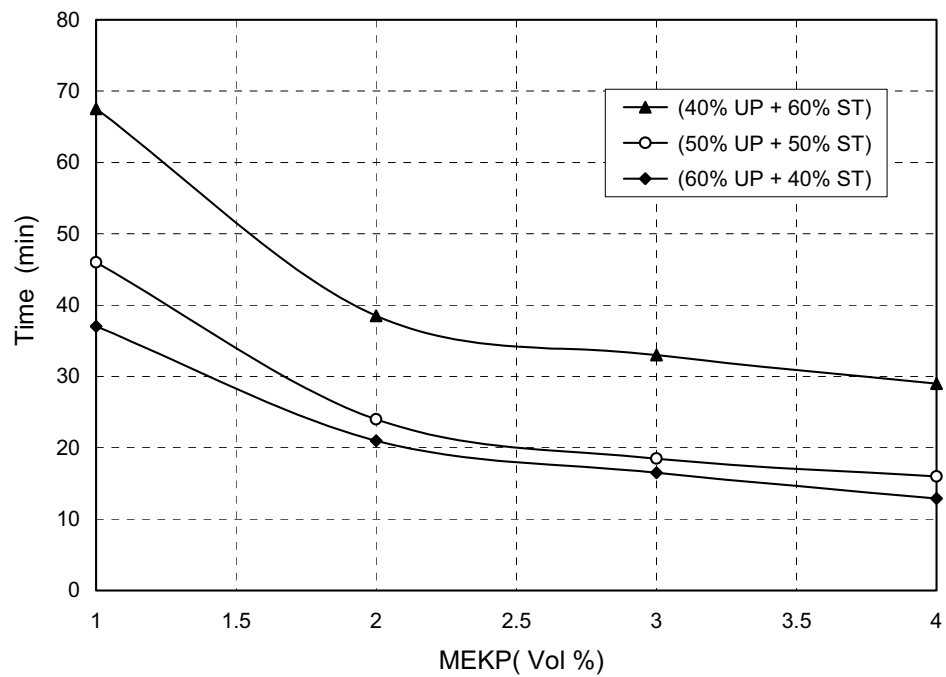
Figure 4.6 Time to peak for unsaturated polyester containing different concentrations of styrene and MEKP
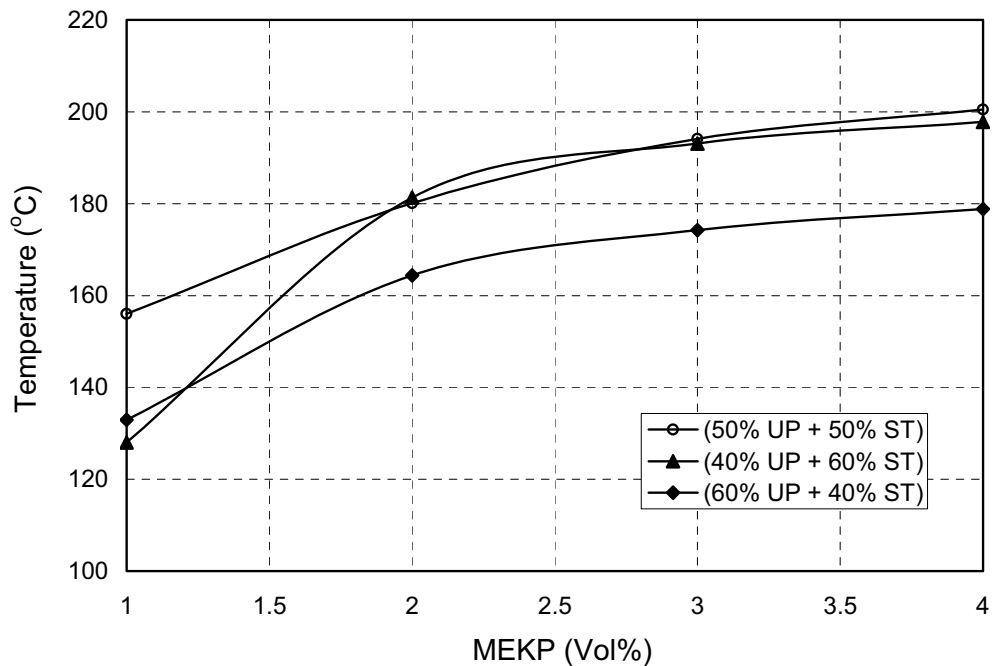
Figure 4.7 Exotherm temperatures for unsaturated polyester containing different concentrations of styrene and MEKP

The accelerator NNDMA affected the gel time, time to peak and the exotherm temperature for the unsaturated polyester at different styrene concentrations as shown in Figure 4.8. The increase in NNDAM volume fraction decreased both the gel time and time to peak. In addition, the increase of NNDMA volume fraction increased the

exotherm temperatures only for the first addition ratio of NNDMA 0.1vol %, while there was insignificant change in the exotherm temperature above 0.2vol% of MEKP for the same styrene concentration ratio. Table 4.1 summarizes the exotherm temperatures, gel time, and time-to-peak for different styrene concentrations. The test results were very important for proving the information about the gel time variation during the preparation of the composites product.
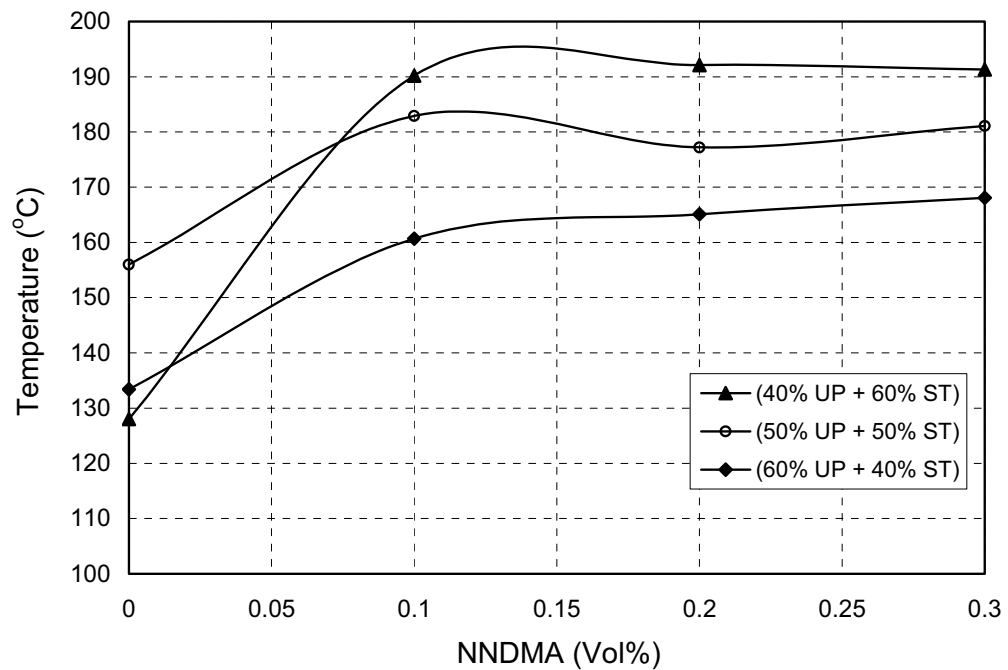
Figure 4.8 Exotherm temperatures for unsaturated polyester containing different concentrations of styrene and NNDMA

Table 4.1 Effects of NNDMA concentration on cure characteristics at different styrene concentrations

	NNDMA (vol %)	0	0.1	0.2	0.3
60% UP + 40% ST	Gel Time (min)	14	2.8	1.5	1
	Time to Peak (min)	36	12.5	10	9.5
	Exotherm Temperature (ºC)	133.4	160.5	165.1	168.1
50% UP +50% ST	Gel Time (min)	35	3	1.5	1
	Time to Peak (min)	67.5	15	11	10
	Exotherm Temperature (ºC)	128	190.2	192.1	191.3
40% UP + 60% ST	Gel Time (min)	23	2	1	0.8
	Time to Peak (min)	46	11	8.5	7.5
	Exotherm Temperature (ºC)	156	182.9	177.2	181.1

4.5 Effects of Reinforcement on the Curing Process

Table 4.2 obviously explains that the fiber inert to the crosslinking reactions for one volume fraction of MEKP as an initiator and for the unsaturated polyester at two different volume fractions of styrene. The gel time increased with the increase in kenaf fiber weight fraction. The delay in gel time due to the presence of kenaf fiber can be attributed to the absorption of heat generated in the exothermic reaction (Waigaonkar et al. 2011). At 10 wt% weight fraction of fiber, the gel time was decreased compared to 0 wt% in the same time it was affected the exotherm temperature and the time to peak. For the 30 wt% the curing was not stared and the exotherm temperature reached about 35ºC at time to peak about 105 minutes, after that it started to decrease without any curing reaction for (60%UP+40%ST). Furthermore, for the resin ratio (50%UP+50%ST) the curing not started at kenaf weight fraction of 20 wt% while the exotherm temperature reached 37ºC at the time to peak about 71 minutes and continued for 10 minutes at the same temperature before starting to decrease due to heat loss to the environment. For the same 30 wt% fiber and resin (60%UP+40%ST), an addition of 1vol% MEKP and 0.1vol% NNDMA caused the curing process to start and complete under the same circumstances as with the curing process; gel time and time to peak were the same for resin with and without fiber. However, the exotherm was affected by decreases in temperature from 160.5ºC to 102.3ºC after adding of kenaf fiber.

Table 4.3 shows the minimum concentration of MEKP to start the curing process for different kenaf fiber weight fraction and styrene concentrations. Therefore, the concentration ratio of MEKP increased with the increase of fiber weight fraction.

Table 4.2 Effects of kenaf fiber weight fraction on curing reaction for1% MEKP

Styrene ratio %	Kenaf Fiber (wt %)	Gel Time (min)	Peak time (min)	Exotherm Temperature (ºC)
60%UP+40%ST	0	19	36	133.4
	10	14	29.5	131.8
	20	33	51	89.8
	30	Curing not start		
50%UP+50%ST	0	23	46	156
	10	19	45	136.3
	20	Curing not started		

Table 4.3 Effects of constant kenaf weight fraction on curing reaction for different MEKP concentrations

Styrene ratio %	MEKP (Vol %)	Gel Time (min)	Peak Time (min)	Exotherm Temperature (^{o}C)
60%UP+40%ST+ (30wt%) fiber	1	Curing not started		
	2	14	30	109.5
	3	9	23	104.6
50%UP+50%ST+ (20wt%) fiber	1	Curing not started		
	2	20	35	109.8
	3	12	26	114.7

4.6 Effects of Moisture Content

The effect of varying the level of water concentration on the exotherm behaviour of unsaturated polyester for 40%ST is shown in Figure 4.9. At the onset of the reaction of water with unsaturated polyester, the rate of temperature increase was almost the same, but gelation time increased. It is because the water slowed the reaction by absorbing the heat from the system. Gel time was 35minutes for the 0vol% of water, 38.5minutes for the 1vol% of water, and 44 minutes for the 2vol% of water. However, when the concentration of water was 3vol%, the gel time decreased and reached 37minutes only 2minutes above the 0vol% of water concentration. That means after the 2vol% of water concentration ratio, there was no action affecting the gel time. Otherwise it could affect the mechanical properties. Furthermore, the water affected the action of the initiator and accelerator system. Bubbles appeared in the resin because water can increase reactivity in some peroxide systems as shown in Figure 4.10, the first specimen from the left side is 0vol% water, the second is with 1vol% water, and the last one is with 2vol% water.
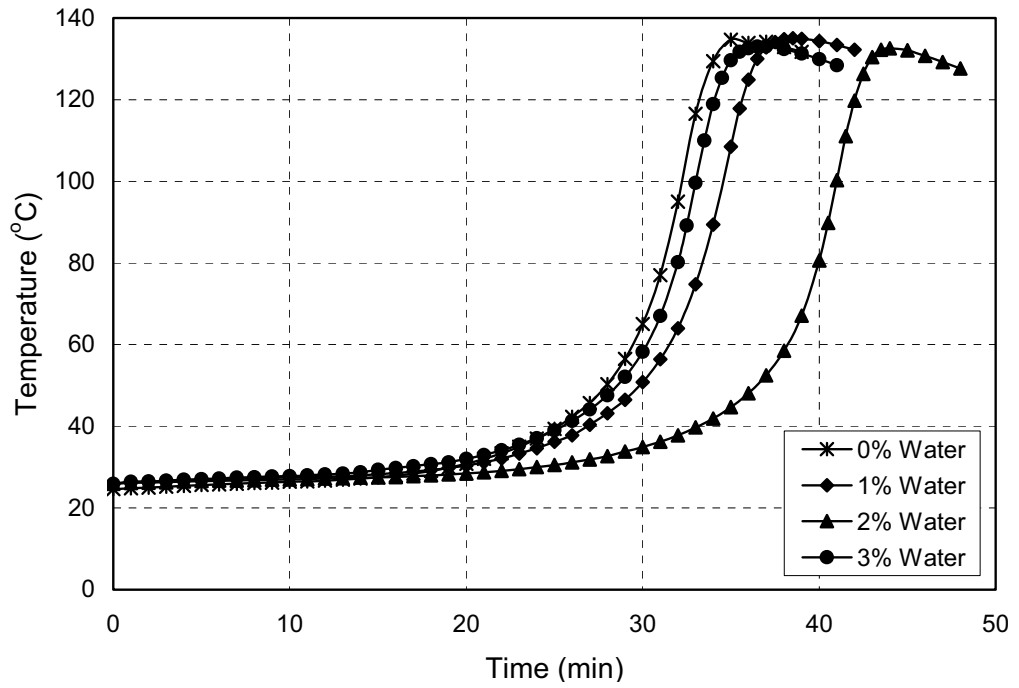
Figure 4.9 Curing time for unsaturated polyester (60%UP+40%ST) at different volume fractions of water for 1vol% MEKP
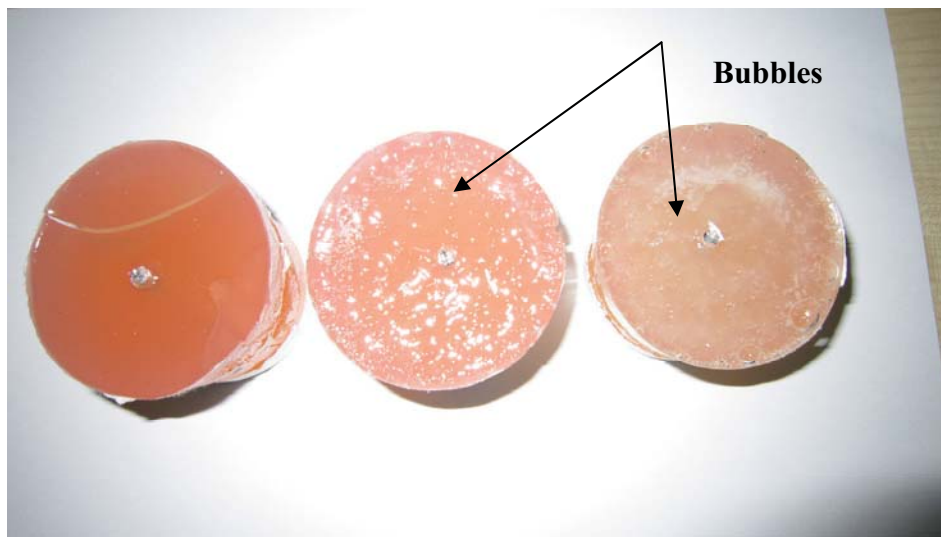
Figure 4.10 Bubbles appear in the unsaturated polyester

4.7 Mechanical Properties

4.7.1 Tensile Properties

- **Effects of MEKP and Styrene Concentrations on Tensile Strength**

The results of mechanical properties for the resin were calculated using Figure 4.11. The effect of MEKP concentration on the tensile strength of cured samples at a fixed (60%UP+40%ST) was observed. It can be seen that the load increased to the maximum value and then suddenly declined as a brittle fracture occurred in the material. The tensile strength did not significantly change with the increase in MEKP ratio. In actual fact, the percentage of increase between the strength for 4vol% MEKP and the other ratio was less than 9%. For the other ratios (1, 2, 3)vol% the percentage was about (2-3)%. The mechanical properties of the cured samples varied from soft to hard, depending on the molar mass of the end grouping. The unsaturated polyester of higher styrene contents gave films of lower rubberlike elasticity compared with those of lower styrene contents, and for this reason the molecular weight between crosslinks increased with increase styrene content (Imai et al. 1967). A high molecular mass gave a higher hardness, tensile and flexural strength of the final cured material. If the molecular mass is too low, the mechanical properties of the cured resin will be poor (Kuang et al. 2007).
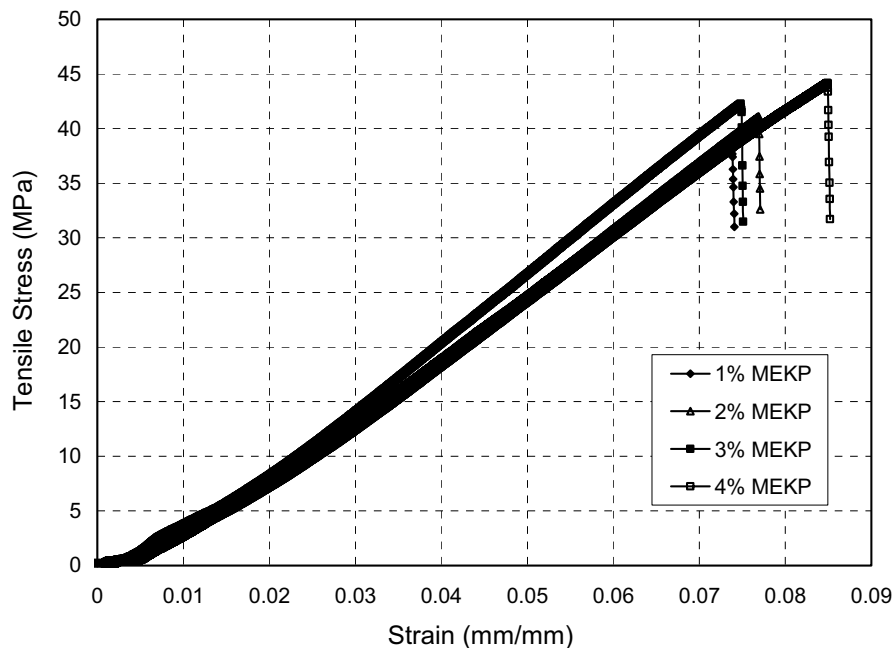
Figure 4.11 Effects of MEKP concentrations for (60%UP+40%ST) on tensile stress and strain

Figure 4.12 summarizes the behavior of the stress strain curves for (60%UP+40%ST) resin with 1vol% MEKP at various NNDMA concentrations. It was observed that stresses increased as the NNDMA increased for a certain value of NNDMA which was 0.2vol% compared to (60%UP+40%ST) resin with 1vol% MEKP. In general, the stresses decreased as the NNDMA increased. Generally the NNDMA dramatically affected the mechanical properties of (60%UP+40%ST) resin.
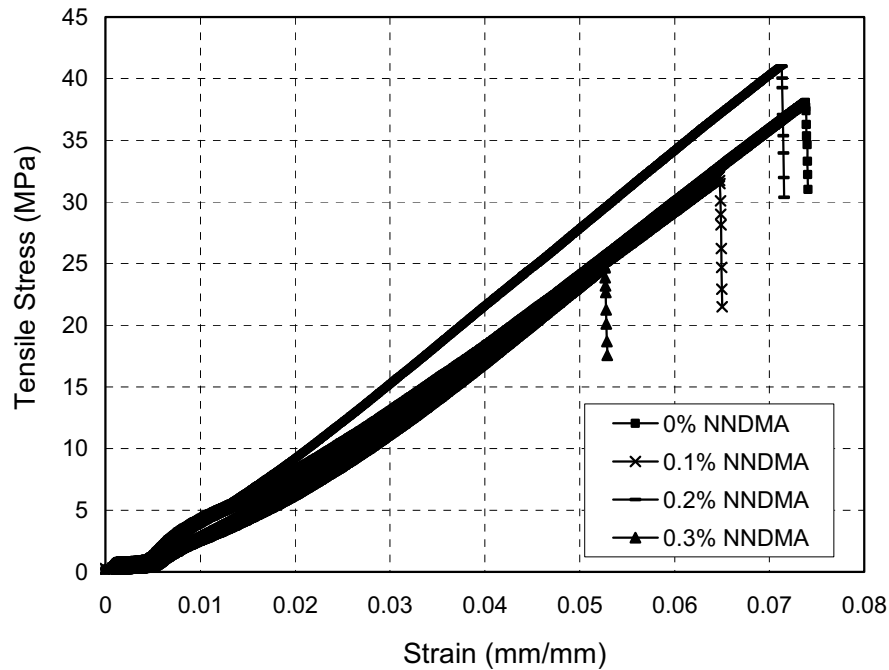
Figure 4.12 Effects of NNDMA concentrations for (60%UP+40%ST) on tensile stress and strain

Figure 4.13 shows the photograph of matrix specimens after failure. It can be seen that the failures of the specimen was in the gauge zone and close to centre, which proves that the specimen fabrication was accurate. Styrene will generally add brittleness to the specimen, therefore the embrittlement decreased the internal stresses in the part because of the increases in part shrinkage that occurred with higher degrees of crosslinking. In another expression the tensile strength increases with decreasing of styrene concentration ratio at a constant volume fraction of MEKP as shown in Figure 4.14.

Figure 4.13 Photograph of the failed tensile test specimens for unsaturated polyester
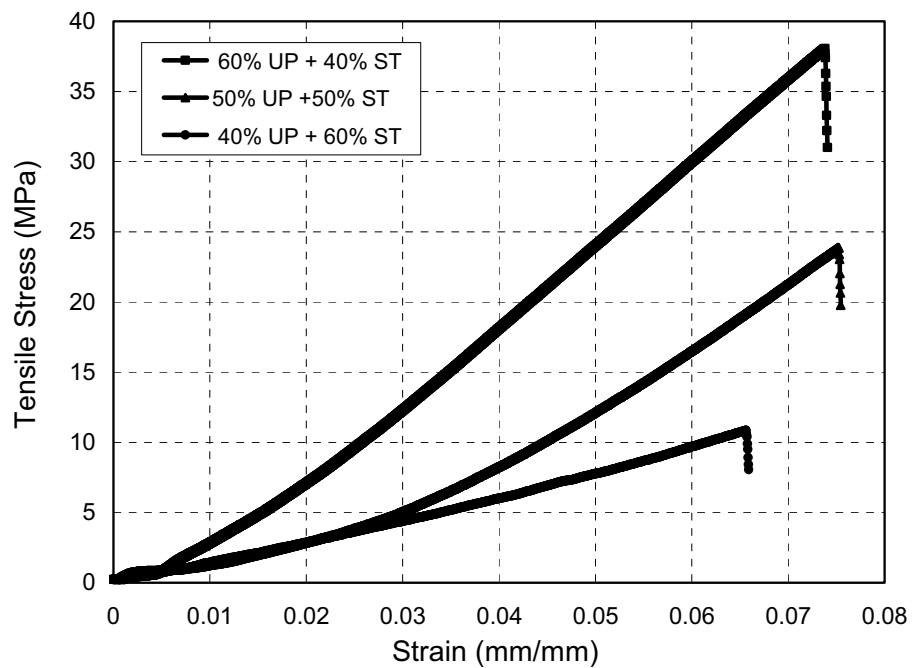
Figure 4.14 Effects of styrene concentration ratios on mechanical properties for unsaturated polyesters, 1vol% MEKP

Figure 4.15 illustrates the effects of styrene ratio on the maximum strength of the unsaturated polyesters at different volume fractions of MEKP. In general, it was observed that the maximum strength increases with decreasing of styrene concentration. For the first mixture of (60%UP+40%ST) resin, the maximum strength was found at 1vol% of MEKP, while the maximum strength for (50%UP+50%ST) started to decrease

with the increase in the initiator volume fraction until 3vol% of MEKP. Then the maximum strength rose with the increase of MEKP volume fraction to the optimum value at 4vol% of MEKP. Furthermore, the maximum strength for (40%UP+60%ST) started to increase with a rise in the initiator ratio until 3vol% of MEKP and the maximum strength decreased with the increase in MEKP volume fraction.
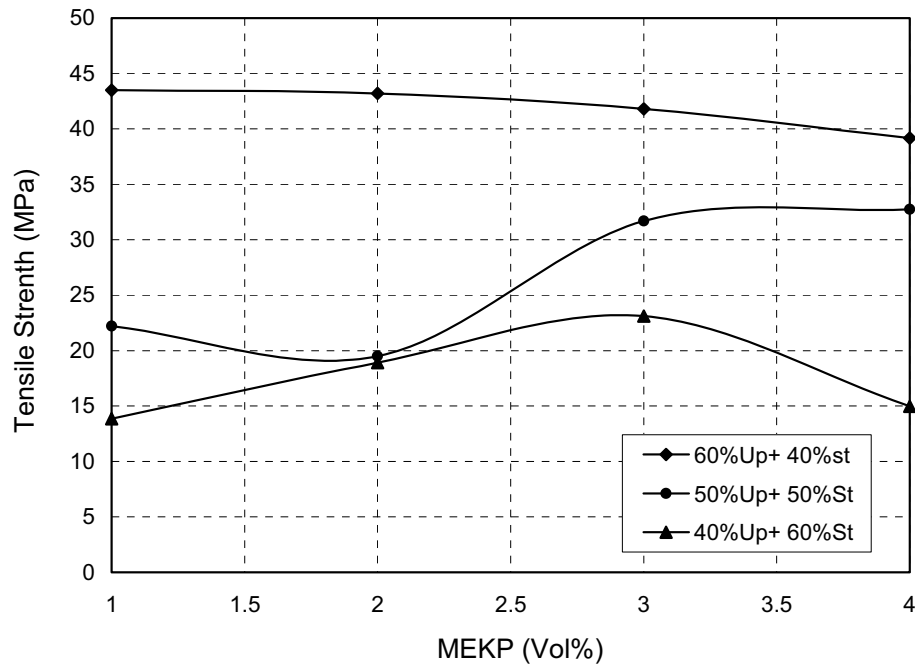
Figure 4.15 Effects of styrene concentration ratios on maximum strength for unsaturated polyester at different MEKP concentrations

- **Effects of MEKP and Styrene Concentrations on Tensile Modulus**

The styrene ratio had an effect on the modulus of the unsaturated polyesters for different volume fractions of curing agent MEKP and this is explained clearly in Figure 4.16. In fact, there was no significant change in the modulus of elasticity. With an increase in the initiator for unsaturated polyester mixture of (60%UP+40%ST) resin, the maximum modulus was found to be at 2vol% of MEKP. For the mixture of (50%UP+50%ST) resin, the maximum modulus was found to be at 3vol% of MEKP, while for (40%UP+60%ST) resin the modulus increased with increase initiator volume fraction until 2vol%., then the modulus started to decrease with an increase in volume fraction of the curing agent MEKP. This obviously proves that the unsaturated polyester with two different styrene concentrations (60%UP+40%ST), (40%UP+60%ST) were found to have the same trend.
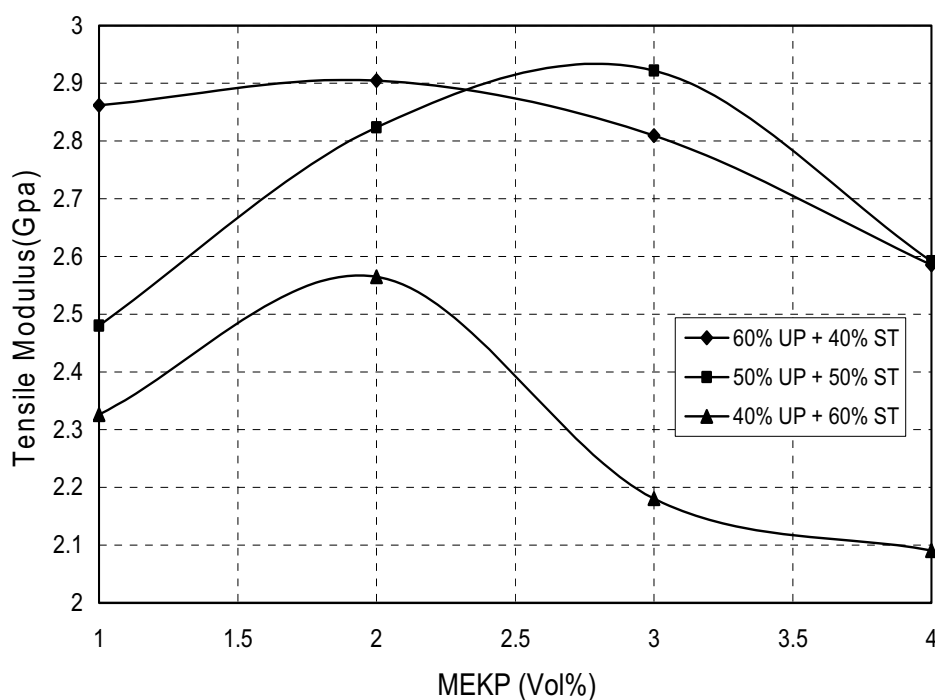
Figure 4.16 Effects of styrene concentration ratios on modulus for unsaturated polyesters

The maximum tensile strength and the tensile modulus had the same trend- both of them decreased with an increase in the styrene volume fraction for the fixed volume fraction of the initiator, as shown in Figure 4.17.

- **Effects of NNDMA Concentrations on Tensile Properties**

The tensile strength and modulus of cured resins for various styrene concentrations at different volume fractions of NNDMA are shown in Figures 4.18 and 4.19 respectively. These results suggest that the strength for 40%ST decreased with increase NNDMA volume fraction; the percentage decreased about 23.5%. The results also absorbed that the strength increased for both 50%ST and 60%ST with increase NNDMA volume fraction; the maximum improvement was about 59.2% for 50%ST while for 60%ST it was more than double. The modulus had different trends for various volume fractions of NNDMA; it is considered that there is insignificant change in modulus as shown in Figure 4.19, with the decreasing or increasing percentage as follows, 5.7% as the decreasing percentage for 40%ST, 6.49% as the increasing percentage for 50%ST and 14.2% as the increasing percentage for 60%ST.
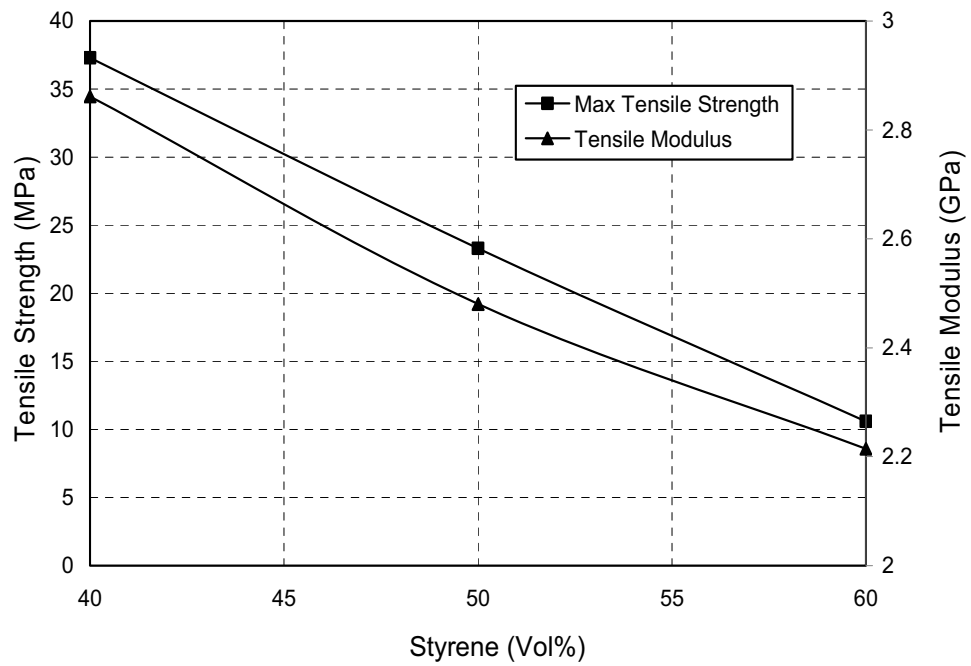
Figure 4.17 Distribution of modulus and maximum tensile strength at different styrene concentrations
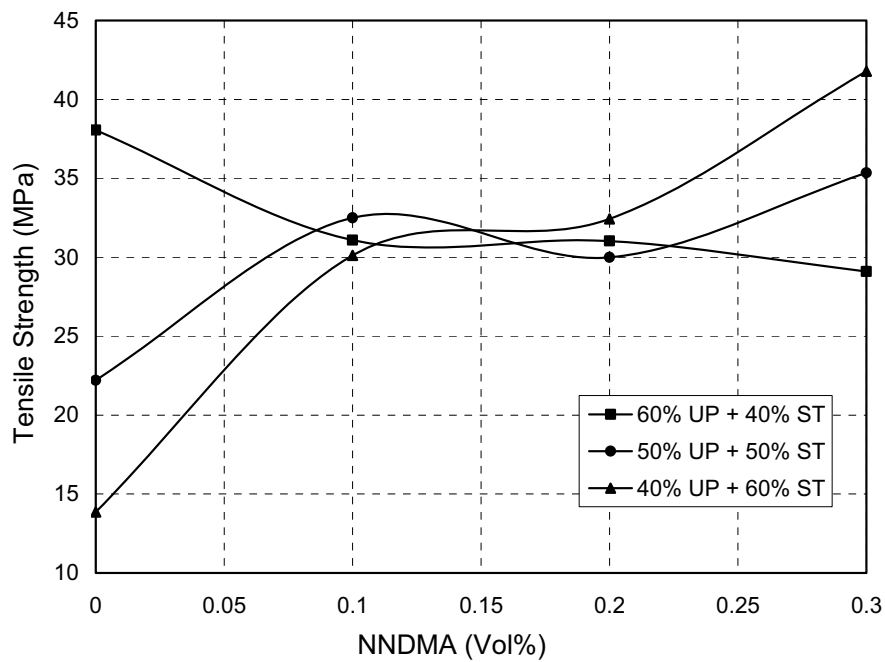
Figure 4.18 Effects of styrene concentration ratios on maximum strength for unsaturated polyester at different NNDMA concentrations
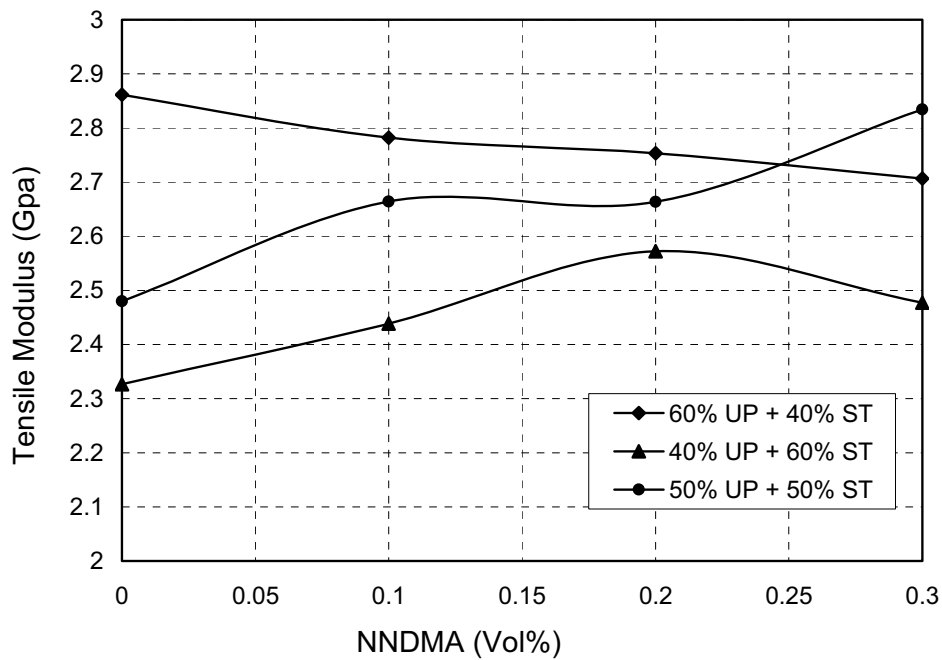
Figure 4.19 Effects of styrene concentration ratios on modulus for unsaturated polyester at different NNDMA concentrations

4.7.2 Flexural Properties

The flexural strength and modulus were not significantly affected by changing the amount of MEKP from 3vol% to 4vol%. The change in MEKP from 1vol% to 2vol% led to a slightly lower flexural strength and flexural modulus for (60%UP+40%ST) resin as Figures 4.20 and 4.21 clarify. In contrast, the flexural properties for (50%UP+50%ST) resin and the change in MEKP from 3vol% to 4vol% led to steady values. The change in MEKP from 1vol% to 2vol% led to increase flexural strength and flexural modulus for (50%UP+50%ST) resin. The explanation for these phenomena was that a high molecular mass will give a higher hardness such as flexural strength of the final cured material. If the molecular mass is too low, the mechanical properties of the cured resin will be poor. An extremely high molecular mass increases the viscosity of the resin solution, which will cause problems with the processing of the resin. Air entrapment in the laminate, poor wetting of the reinforcement, long mold filling times and processing times are typical practical problems due to the resin viscosity (skrifvars 2000).

The flexural properties of the (60%UP+40%ST) resin modified by NNDMA for 1vol% MEKP, firstly exhibited decreasing tendency, and increased after successively reaching

0.2vol% of NNDMA and continued a decreasing trend. The opposite trend for (50%UP+50%ST) resin modified by NNDMA, firstly exhibited an increasing tendency, and decreased after successively reaching their maxima as Figures 4.22 and 4.23 show.
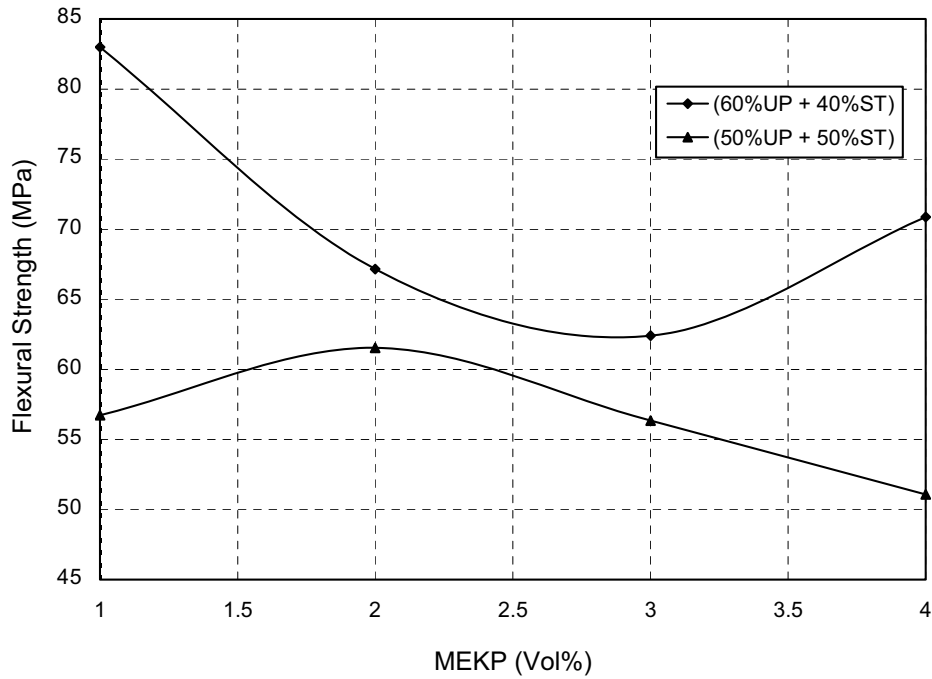
Figure 4.20 Effects of styrene concentration ratios on flexural strength at different MEKP concentrations
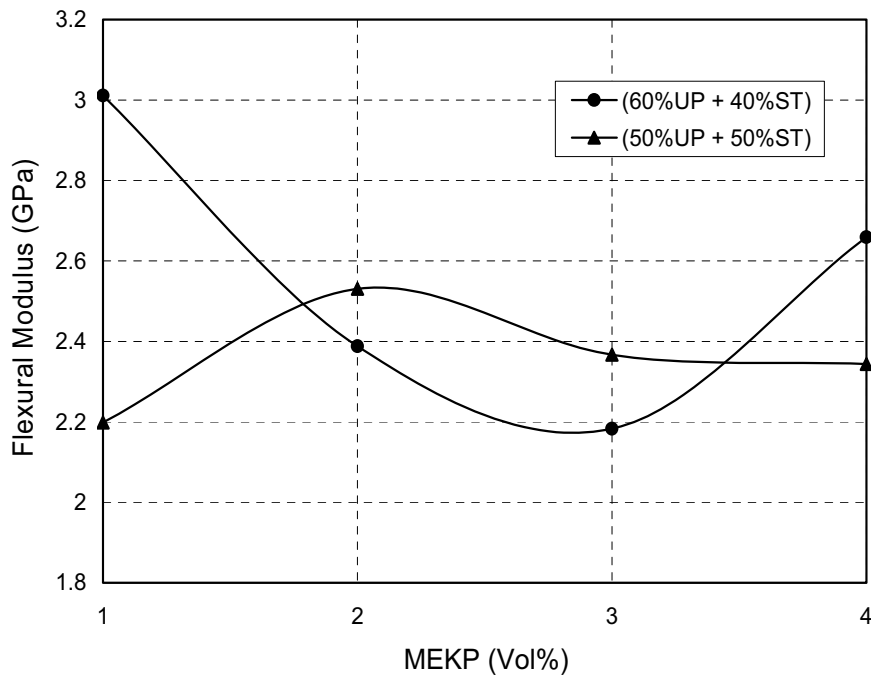
Figure 4.21 Effects of styrene concentration ratios on flexural modulus at different MEKP concentrations
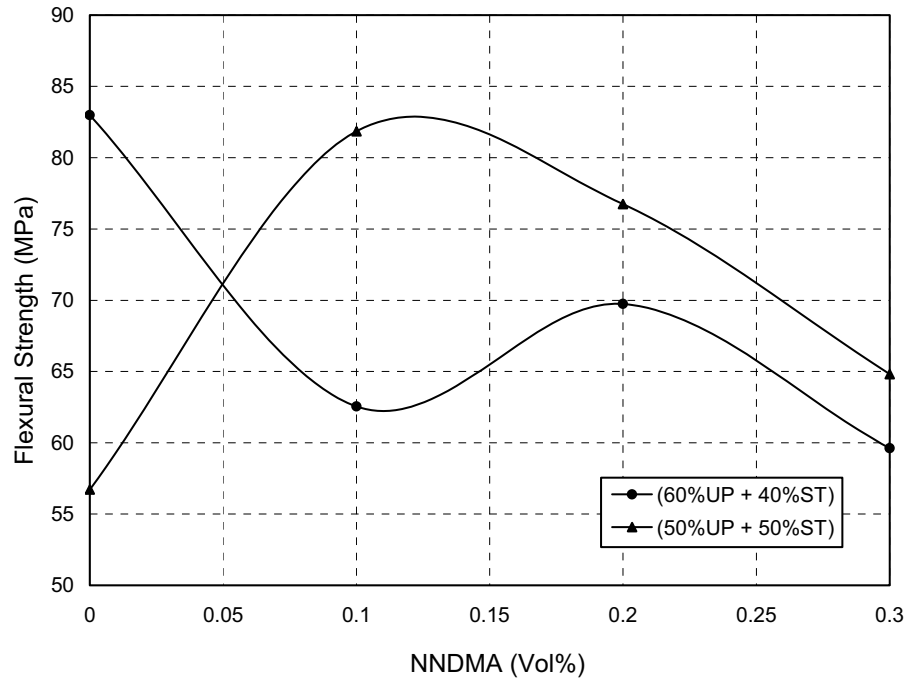
Figure 4.22 Effects of styrene concentration ratios on flexural strength at different NNDMA concentrations
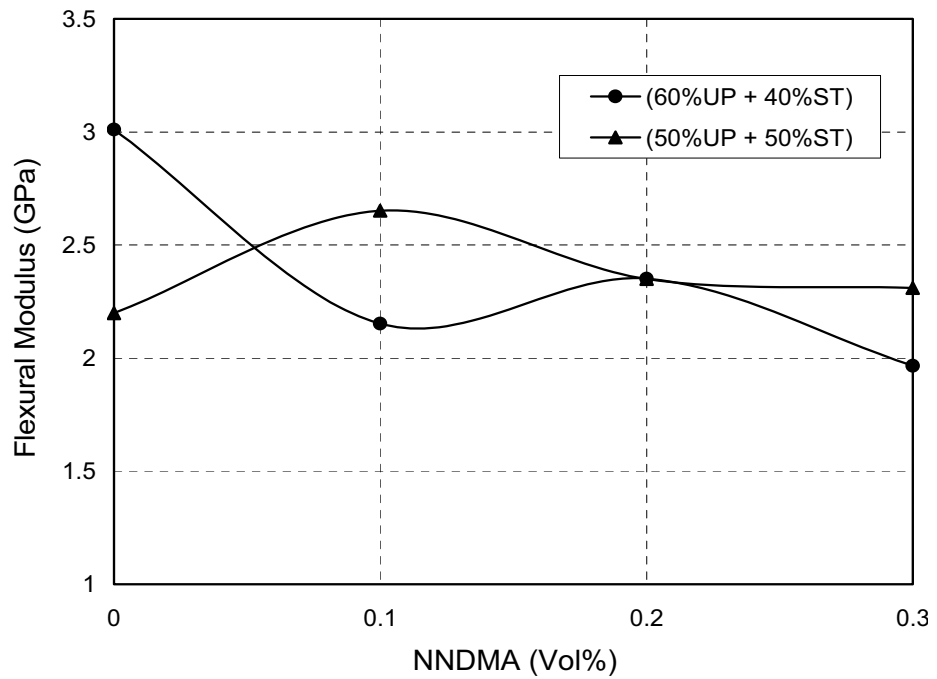
Figure 4.23 Effects of styrene concentration ratios on flexural modulus at different NNDMA concentrations

4.7.3 Impact Properties

- **Effects of Styrene Concentration Ratios**

Impact strength decreased with increase styrene concentration as shown in Figure 4.24. This means increasing the styrene concentration decreases the material toughness and the material becomes more brittle.

- **Effects of MEKP and NNDMA Concentration Ratios**

The impact strength decreased with the increase in NNDMA volume fraction for (60%UP+40%ST) resin, which means that the matrix resistance to crack propagation is decreased. This fact was evident that the resin became more brittle. On the other hand, the energy absorbed by (50%UP+50%ST) resin increased with increase NNDMA volume fraction for a certain value of 0.2vl%. After this value, there was no significant change in impact strength. Unlike the effects of MEKP on impact strength, the unsaturated polyester for different styrene concentrations had the opposite trend with increase NNDMA volume fraction. The impact strength decreased with increaseMEKP volume fraction for different styrene concentrations, as shown in Figures 4.25 and 4.26. The summary of test results of (60%UP+40%ST) matrix resin is given in Table 4.4.
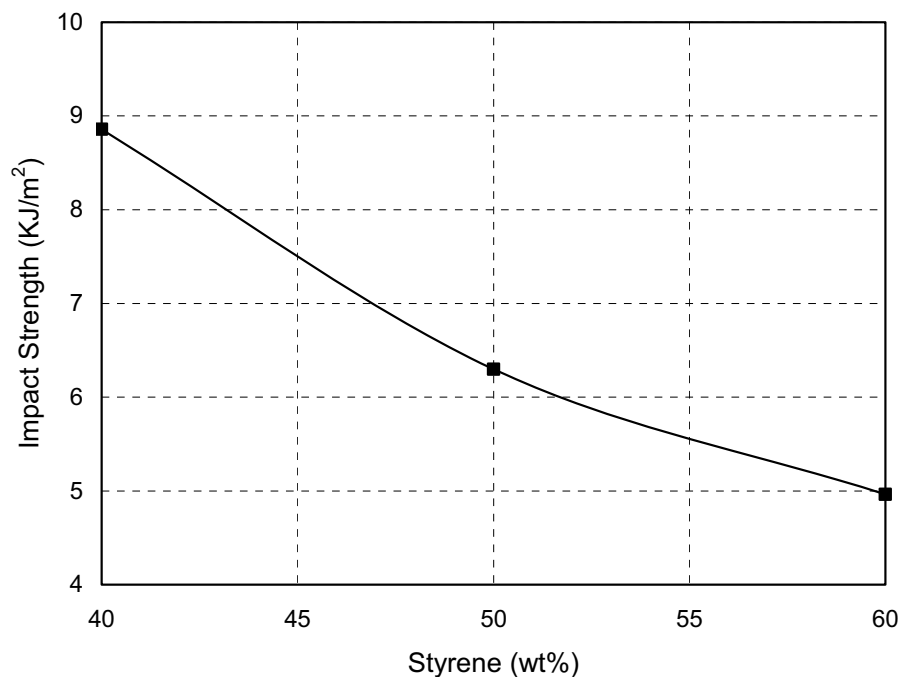
Figure 4.24 Comparison of different styrene concentration ratios
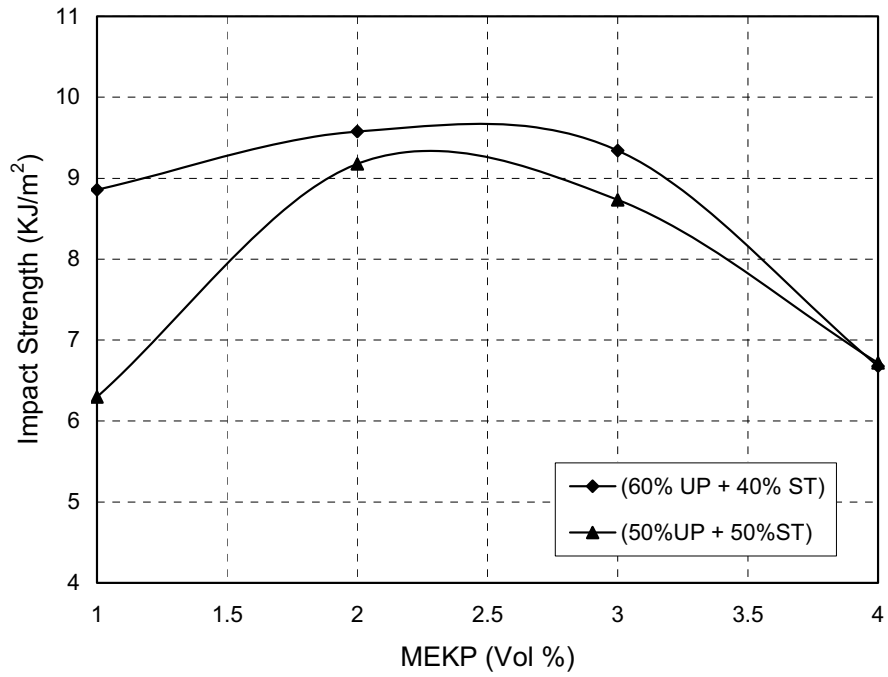
Figure 4.25 Effects of MEKP ratios for different styrene concentrations
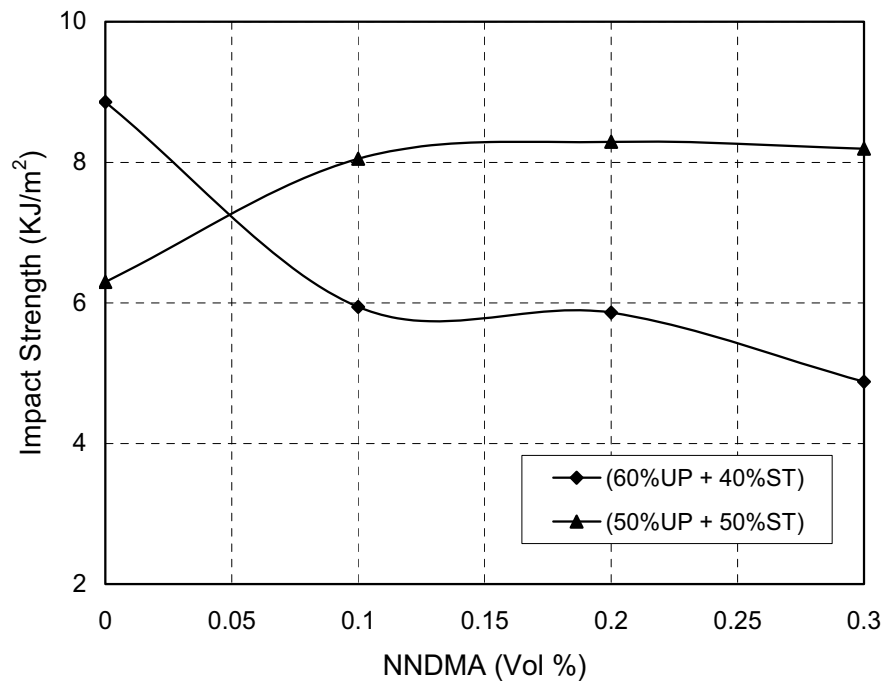
Figure 4.26 Effects of NNDMA ratios for different styrene concentration ratios

Table 4.4 Summary of mechanical and chemical properties of (60%UP+40%ST) unsaturated polyester resin

Viscosity (cp) at 25 ± 2ºC	219.3
Density (cm^3/g) at 25 ± 2ºC	1.12
Gel time (minutes) at 25 ± 2ºC	14
Time to peak (minutes) at 25 ± 2ºC	36
Exotherm temperature (ºC) at 25 ± 2ºC	133.4
Styrene content vol%	40
MEKP (initiator) vol%	1
Modulus of elasticity (GPa)	2.86
Tensile Strength (MPa)	37.3
Flexural Strength (MPa)	82.9
Flexural Modulus (GPa)	3.0
Impact Strength kJ/m^2	3.85

4.8 Effects of Amount of Water on Mechanical Properties

Viscous white layer was visible on the specimen's surfaces as well as small voids as a result of adding about 1.5vol% of water to the UP resin. When the water content was increased, the white layer became thicker and the number and size of voids clearly increased Figure 4.27 shows the effect of water volume fraction on tensile strength and tensile modulus of the UP resin. It can be seen that the tensile properties of the composites decreased with increase water volume fraction where this shows the clear indication of the ability of water to impart smaller stiffness to the UP resin. A ductile behavior was observed- with a large decrease in mean fracture stress, there was an abrupt decrease in elasticity modulus, as well as a significant drop in the flexural strength and flexural modulus as Figures 4.27, 4.28 explicates. The flexural properties of the UP resin decreased drastically on exposure to water volume fraction. This decrease in flexural properties was due to the formation of hydrogen bonding between the water molecules and UP resin. This led to dimensional and color variations of the UP resin product. The average impact test results of UP resin after addition of water at room temperature is presented in Figure 4.29. There was an abrupt increase (approximately 21%) in toughness for water content specimens compared to dry specimens. This increase in energy absorption was indicative of the softening of the wet specimens. The increase in impact resistance properties of UP resin samples after water volume fraction increased could be due to the acceptable level of damage in the

interface region due to water volume fraction. The water volume fraction provided an effect on the plasticization and finally caused increase of toughness. Thus, improvement of impact strength is greatly related to the attack of water, which diffuses into the interface (Rong et al. 2001).
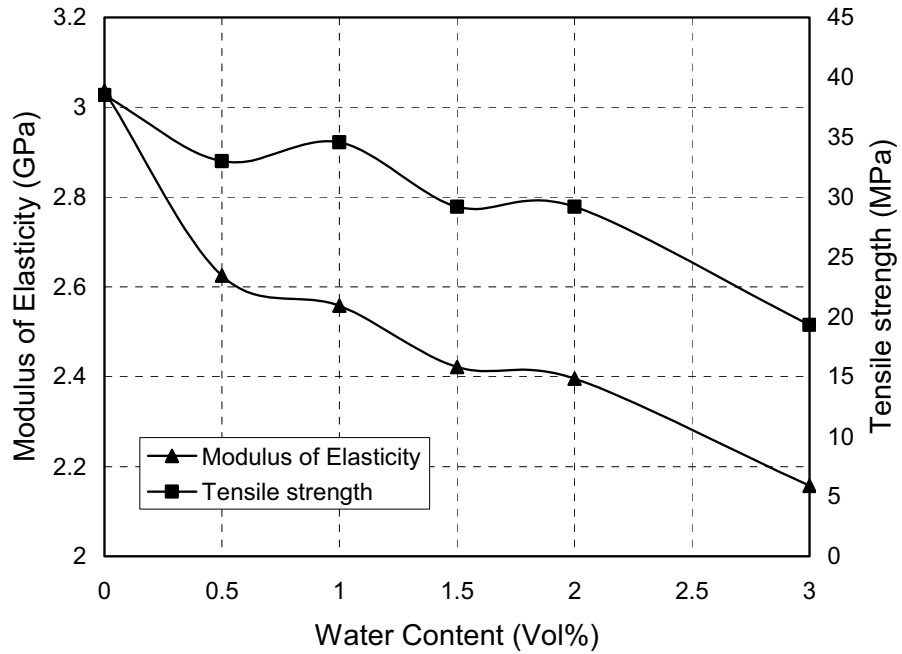
Figure 4.27 Effects of water amount on tensile properties
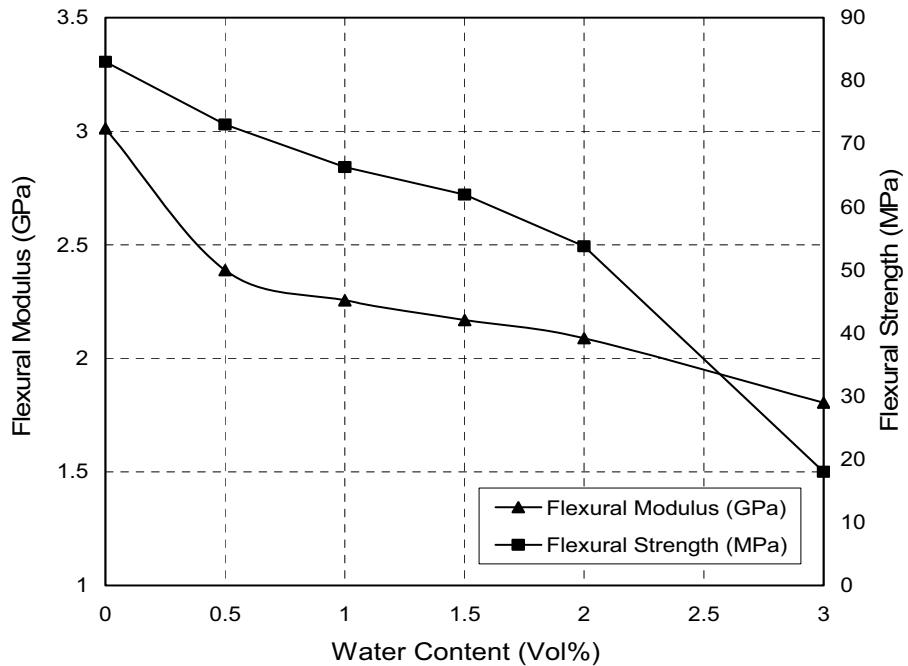
Figure 4.28 Effects of water amount on flexural properties
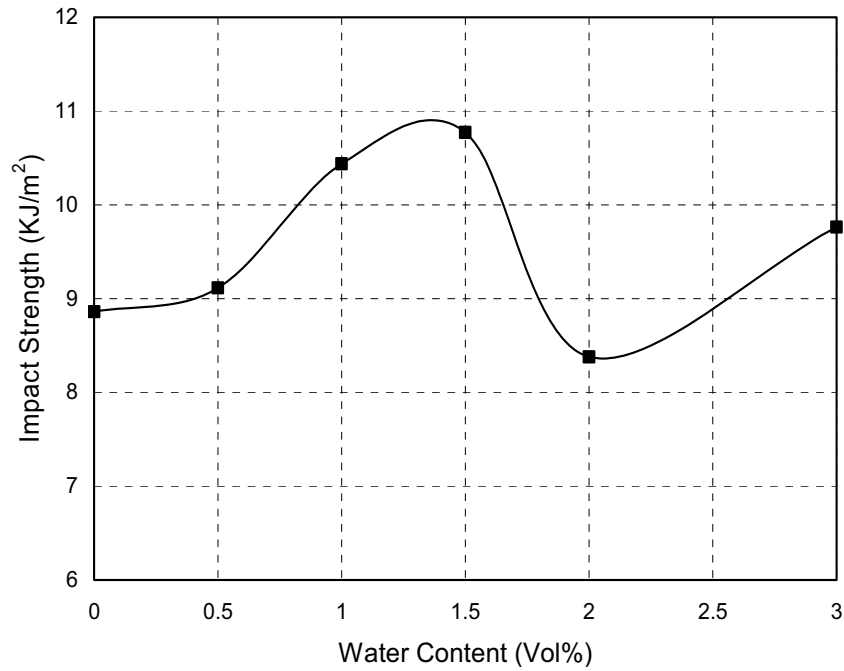
Figure 4.29 Effects of water amount on impact properties

4.9 Thermal and Dynamic Properties

4.9.1 DSC Results for Different Styrene Concentrations

The output of a DSC measurement is a plot of the difference of heat delivered to the sample and to the reference as a function of the sample temperature for (60%UP+40%ST) unsaturated polyester resin with 1vol% MEKP as shown in Figure 4.30. Table 4.5 summarizes the significant changes in T_g of unsaturated polyester for different styrene concentrations at different MEKP and NNDMA volume fractions. In the first ratio of styrene 40% there was an insignificant change with increasing MEKP, while T_g decreased with the addition of 0.1vol% of NNDMA, then started to increase with increasing NNDMA volume fraction. However, for the second ratio of styrene, the maximum transition temperature was at 2vol% of MEKP and after that it started to decrease with increasing MEKP volume fraction. The glass transition temperature had the same trend for NNDMA and the maximum was at 0.2vol%. It is evident that T_g measured by DSC increases as the MEKP level increases for certain levels and then decreases. Similar results have been reported by Waigaonkar et al. (2011).
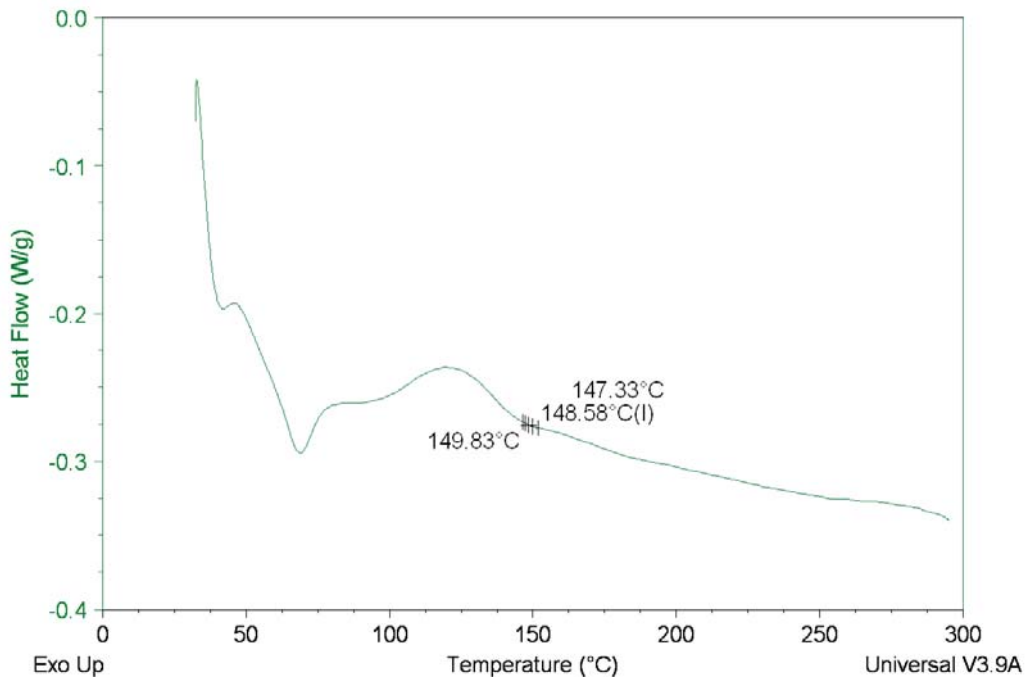
Figure 4.30 Example of thermogram curve for DSC Measurement, (60%UP+40%ST) unsaturated polyester resin at 1%MEKP

Table 4.5 Effects of MEKP and NNDMA concentrations on T_g Temperature for different styrene concentrations

60%UP + 40%ST	**MEKP (Vol %)**	**1**	**2**	**3**	**4**
	Glass transition temperature T_g (ºC)	148.58	149.51	147.54	144.96
	NNDMA (Vol %)	**0**	**0.1**	**0.2**	**0.3**
	Glass transition temperature T_g (ºC)	148.58	143.91	146.37	149.44
50%UP + 50%ST	**MEKP (Vol %)**	**1**	**2**	**3**	**4**
	Glass transition temperature T_g (ºC)	135.35	149.51	149.11	147.39
	NNDMA (Vol %)	**0**	**0.1**	**0.2**	**0.3**
	Glass transition temperature T_g (ºC)	135.35	148.66	149.96	148.47

4.9.2 TGA Results for Different Styrene Concentrations

Instruments such as the TGA have been used to determine the degree of cure, rates of cure, thermal stability, melting points, heats of reaction, and moisture content among other things. The TGA data for the various styrene concentrations for 1%vol MEKP is demonstrated in Figure 4.31. on the whole, the curves endorse that thermal degradation begins to occur only after the materials have absorbed certain amounts of heat energy.

97

In all TGA curves of (60%UP+40%ST) resin, two stages of weight loss were observed. The first was in the range of 40 to 240ºC involving the loss of about 4.5% of the total mass. It can be ascribed to the elimination of water adsorbed by the hydrophilic polymer. The second stage was the fragmentation of the polymer (Cerit et al. 2011). The thermograms show that the second degradation temperature of the (60%UP+40%ST) resin was about 380ºC. A sudden drop in the mass of the sample indicates the thermal degradation of the materials. As illustrated in Figure 4.31 the thermal stability decreased with increase in ST concentration. For (50%UP+50%ST) resin, the first stage of weight loss started at range (40-60)ºC and the second stage started at 90ºC to 340ºC.
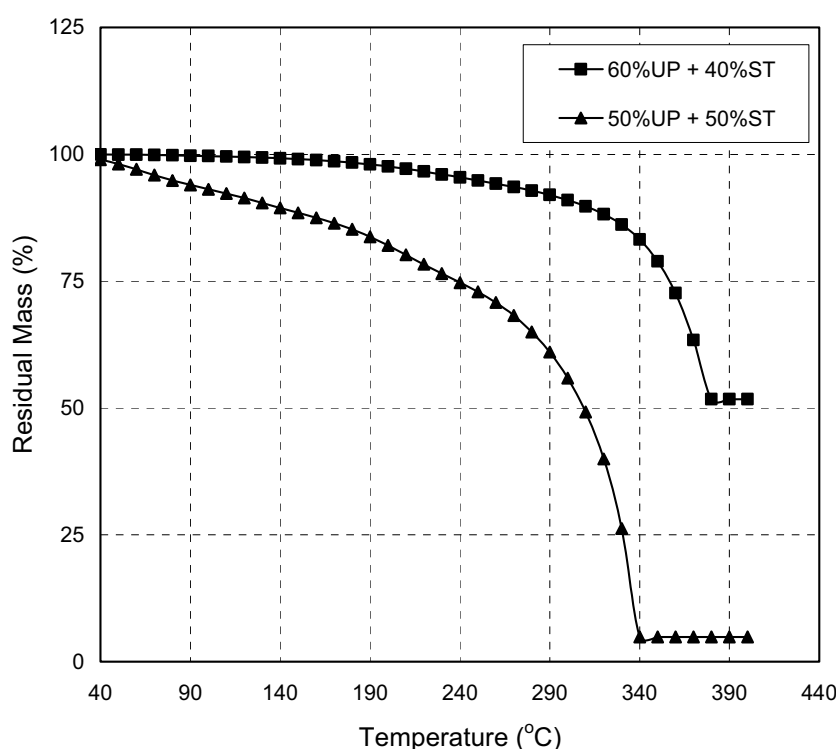
Figure 4.31 TGA curves of UP resin for different ST concentrations

4.9.3 DMA Results for Different Styrene Concentrations

Dynamic mechanical analysis is an effective, way to study the network structure, morphology, and thermo-stable properties of a cured system. The dynamic mechanical results expressed as storage modulus E', loss modulus E'' and loss tangent $tan\delta$ as a function of temperature and resin compositions are revealed in Figure 4.32 a, b and c, respectively. The E' of (60%UP+40%ST) resin was about 2.313 GPa, higher than the E' of (50%UP+50%ST) resin which was about 2.279 GPa. These results indicate that an

increase in styrene concentration affects the stiffness of material. From DMA curves, E' values fell steeply around the glass transition temperature T_g of the resins.

Table 4.6 summarizes the results of the dynamic mechanical properties for UP resin at various styrene concentrations, MEKP and NNDMA volume fractions. Firstly, the E' and E'' for (60%UP+40%ST) resin decreased with increase MEKP volume fraction for a certain value of MEKP which was 0.2vol%, an abrupt increase in E' and E'' with an increase of MEKP volume fraction. In addition, a significant increment and drop in $tan\delta$ and T_g occurred respectively with increasing MEKP. The influence of MEKP concentration was such that the dynamic mechanical results of the (50%UP+50%ST) resin was a completely different trend. There was a sudden increase in the E', E'' and the loss factor $tan\delta$ at 0.2vol% MEKP and a significant drop the dynamic mechanical properties with increasing MEKP.

a

b

c
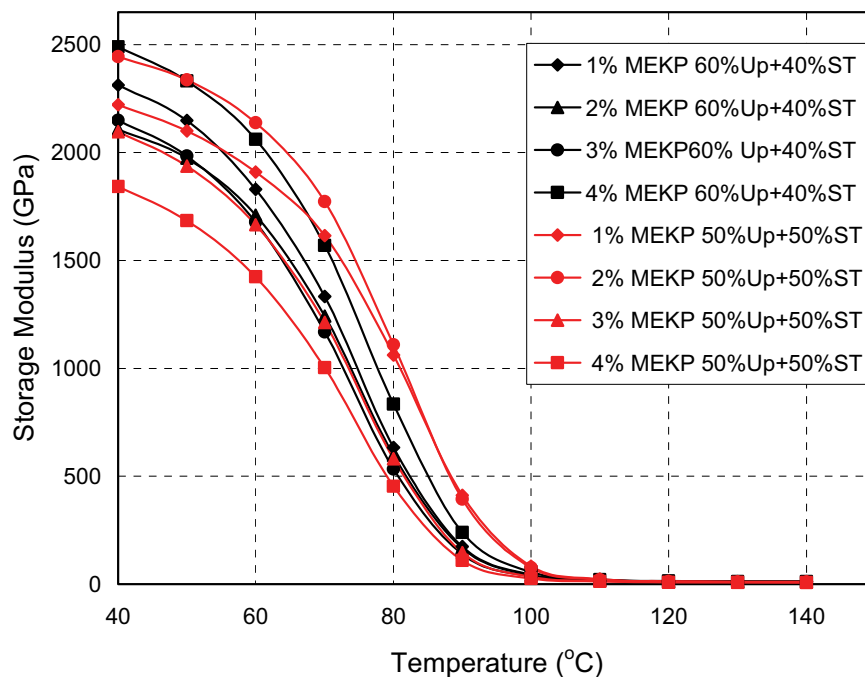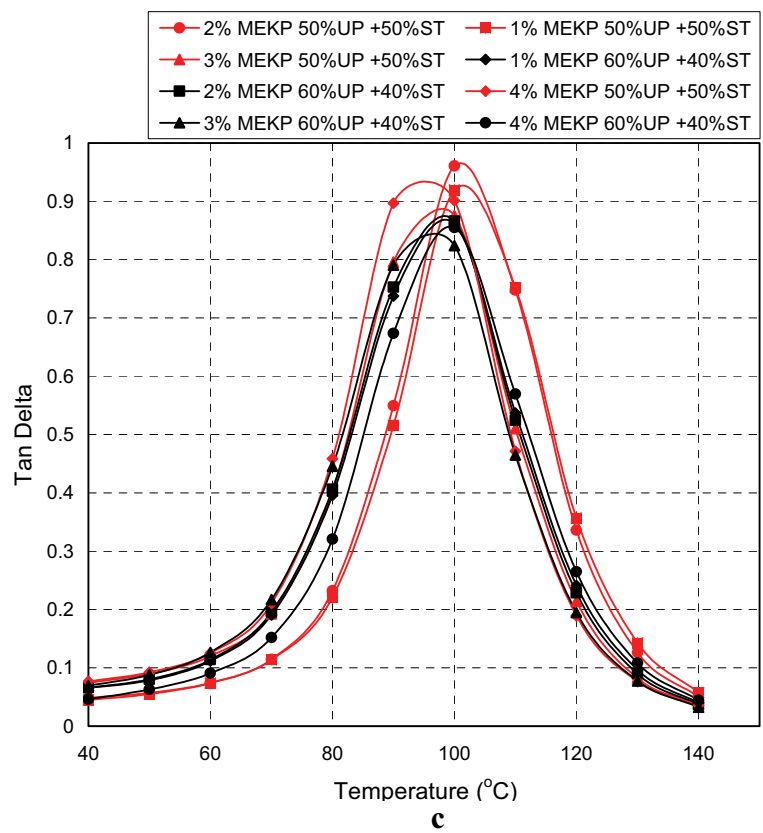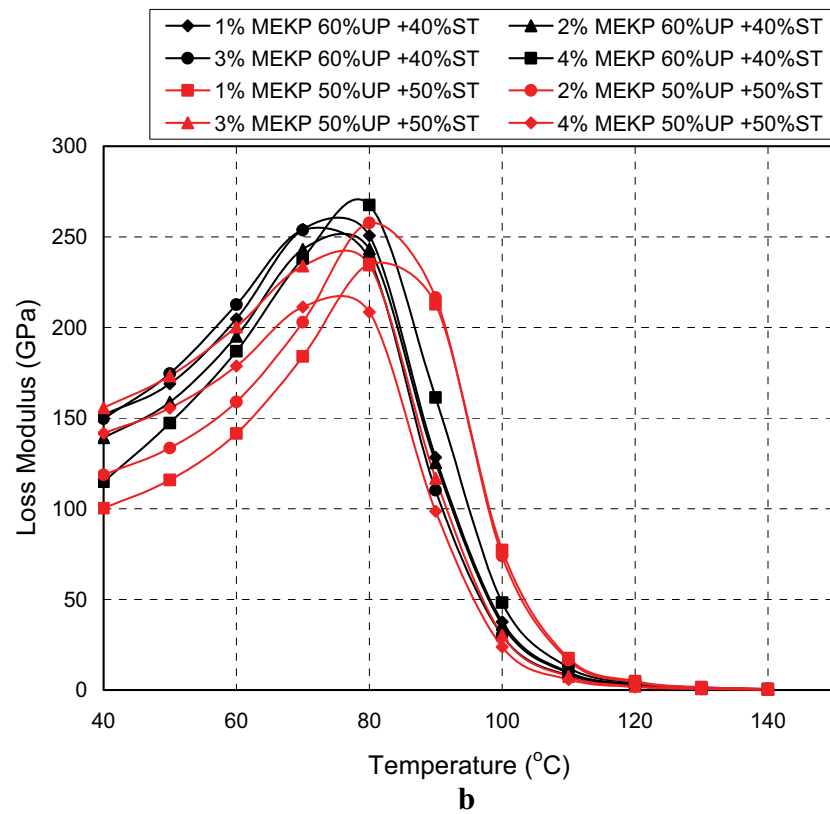
Figure 4.32 Effects of styrene concentrations on (60%UP+40%ST) resin for different MEKP concentrations: (a) storage modulus, (b) loss modulus, (c) *tanδ* via temperature

100

In *tanδ* curves of the (50%UP+50%ST) resin, there was only one peak for each value of MEKP and the peak became broader than that of (60%UP+40%ST) resin for the same MEKP concentration, which suggests that the (60%UP+40%ST) resin and (50%UP+50%ST) resin had excellent compatibility. *Tanδ* peak values of the UP resin of various styrene concentrations are summarized in Table 4.7. The larger *tanδ* peak values mean that the damper properties of the (50%UP+50%ST) resin was enhanced. Furthermore, compared to the (60%UP+40%ST) resin, the T_g of the (50%UP+50%ST) resin shifted to the higher temperature, namely from 70°C to 80°C for 1vol% MEKP, which suggests that the (50%UP+50%ST) resin had an improvement in thermo-stability than that of the (60%UP+40%ST) resin. The increase observed in T_g is concluded to be due to the steric effect of the styrene molecules (Takahashi 1964). In the copolymerization reaction of unsaturated polyester, it seems that increasing the styrene content in feed does not increase the crosslinking density but lengthens the styrene chains which connect the polyester chains (Imai 1967). The same behaviour for (60%UP+40%ST) resin and (50%UP+50%ST) resin for 1vol% MEKP at various NNDMA volume fractions is recapitulated in Table 4.6.

Table 4.6 Dynamic mechanical results for UP resin at various styrene, MEKP and NNDMA concentrations

	MEKP (vol %)	1	2	3	4
(60%UP+40%ST)	Storage modulus (GPa)	2.313	2.108	2.150	2.489
	Loss modulus (GPa	0.2541	0.2432	0.2536	0.2675
	Tan δ	0.8612	0.8662	0.8241	0.8550
	Glass transition temperature T_g (ºC)	70	80	70	80
	NNDMA (vol%)	0.1	0.2	0.3	
	Storage modulus (GPa)	2.459	2.185	2.461	
	Loss modulus (GPa)	0.2707	0.2467	0.279	
	Tan δ	0.8452	0.8516	0.8149	
	Glass transition temperature T_g (ºC)	70	80	60	
	MEKP (vol %)	1	2	3	4
(50%UP+50%ST)	Storage modulus (GPa)	2.279	2.485	2.097	1.843
	Loss modulus (GPa)	0.2349	0.2576	0.2345	0.2113
	Tan δ	0.9193	0.9606	0.8756	0.9012
	Glass transition temperature T_g (ºC)	80	80	80	70
	NNDMA (vol%)	0.1	0.2	0.3	
	Storage modulus (GPa)	1.843	2.201	2.067	
	Loss modulus (GPa)	0.2113	0.2499	0.2485	
	Tan δ	0.9012	0.9757	0.9773	
	Glass transition temperature T_g (ºC)	70	80	80	

4.10 Summary

The conducted studies revealed the following: the physical parameters of unsaturated polyester resin such as viscosity and density decreased with the increase in environmental temperature and styrene concentration. The styrene concentration controlled the reactivity of the unsaturated polyester and as well as the crosslinking density of the final network by increasing the gel time, time to peak, and exotherm temperature. The presence of kenaf fiber usually inanimate the crosslinking reactions, by adding mass which absorbed the heat that occurred and delayed the gel time. The moisture content in the resin affected the curing reaction by increasing the gel time and time to peak, while there was insignificant effect on the exotherm temperature for the same MEKP concentration and same surrounding temperature.

Maximum strength and modulus of elasticity had the same trend for different concentration ratios of styrene and for certain concentrations of styrene; different volume fractions of MEKP and NNDMA had a significant effect on the maximum tensile strength, and at the same time NNDMA had an insignificant effect on the modulus of elasticity. Impact strength decreased with increase styrene concentration. This means increasing the styrene concentration decreases the material toughness and the material becomes more brittle. The impact strength decreased with increase NNDMA volume fraction for (60%UP+40%ST) which means that the matrix resistance to crack propagation decreased. This fact was evident as the resin became more brittle. Alternatively, the energy absorbed by (50%UP+50%ST) increased with increase NNDMA for a certain volume fraction. The flexural strength and modulus for unsaturated polyester various styrene concentrations had different trends with an increase in MEKP volume fraction above 2vol%. The increase in MEKP volume fraction led to a slightly lower flexural strength and flexural modulus for (60%UP+40%ST) resin. On the contrary, an (50%UP+50%ST) resin increase in MEKP volume fraction above 2vol% led to steady values. The increase of MEKP volume fraction from 1vol% to 2vol% led to an increase in flexural properties of (50%UP+50%ST) resin. The reason for these phenomena is that a high molecular mass will give a higher hardness of the final cured material. The flexural properties of the (60%UP+40%ST) resin modified by NNDMA volume fraction, firstly exhibited decreasing tendency, and increased after successively reaching 0.2vol% of NNDMA and continued the decreasing trend. The opposite trend was seen for (50%UP+50%ST) resin modified by NNDMA volume fraction. It initially exhibited an increasing tendency, and decreased after reaching its maxima.

Dynamic mechanical properties and thermal stability of UP resin and short kenaf fiber were considerably dependent on the styrene concentration. The glass transition temperature T_g decreased with increase of styrene concentration for 1vol% MEKP. Beyond that there was an insignificant effect on T_g with an increase in MEKP and NNDMA. The thermal behavior of the neat resins for various styrene concentrations was comparable as indicated on the two-step weight loss mechanism.

CHAPTER FIVE

PHYSICAL AND MECHANICAL PROPERTIES OF THE KENAF BAST FIBER

5.1 Introduction

In this chapter, the physical and mechanical properties of the kenaf fiber observed experimentally are reported. These cover length, diameter, density, water absorption, tensile strength and Young's Modulus. The percentage ratio of holocellulose content, of bast and core kenaf fiber was also investigated. The effect of chemical treatment on the fiber was observed. The change in fiber surface was examined using Scan electrode microscopy SEM.

5.2 Physical Properties of the Kenaf Fiber

5.2.1 Preparing the Fiber

- **Kenaf Bast Fiber**

The properties of the kenaf fiber as it was received from the company are shown in Table5.1. Figure 5.1 shows the kenaf particles and long fibers. In order to check the short fiber length, a sample of 122 short kenaf fibers were selected randomly and measured. The normal distribution was drawn in terms of a histogram to get the length distribution of the kenaf fiber as shown in Figure 5.2. The results show that the length was between 2.5-6.8mm and the average length was 4.525mm.

Table 5.1 Properties of the kenaf fiber

Fiber type	Length (mm)	Price (RM/kg)
Kenaf long fiber	120	2.0
Particle kenaf fiber	3	0.3

(a)   (b)   (c)
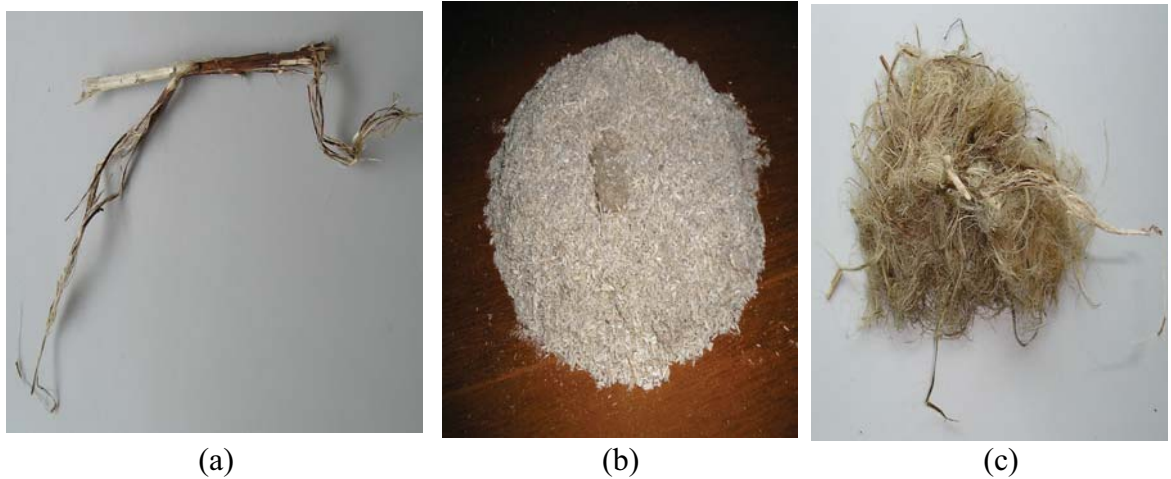
Figure 5.1 Kenaf fibers: a) kenaf plant, b) particle fiber (core), c) long fiber (stem)
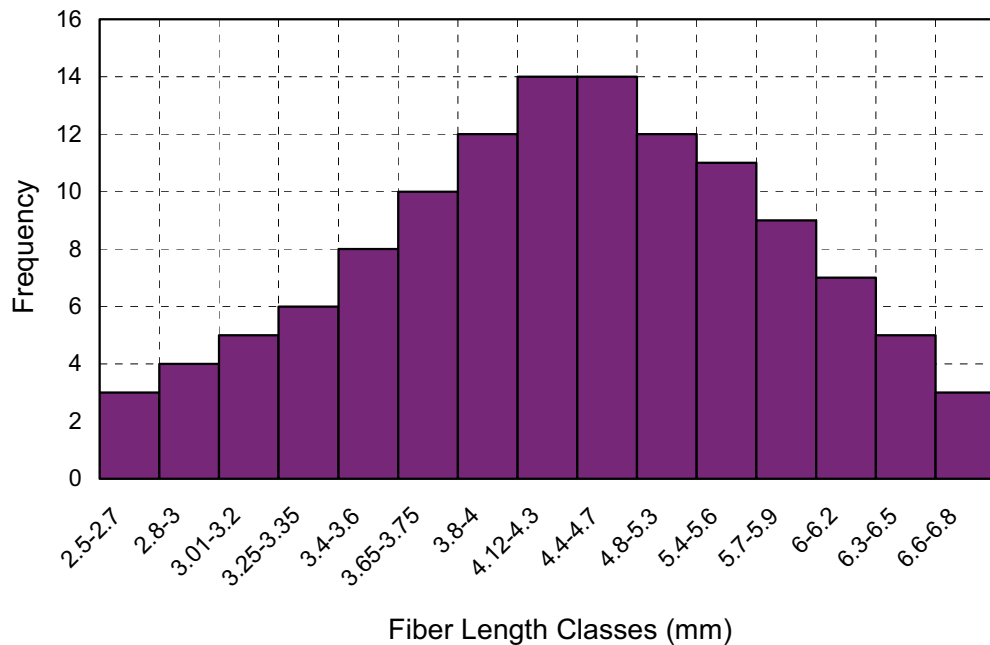
Figure 5.2 Short fiber distributions for manual chopping for the long kenaf fiber

- **Recycled Jute Fiber Chopping**

A random selection of 100 fibers of each length was taken out after the chopping process as a sample to calculate and estimate the average length of overall fibers. From Figures 5.3, 5.4 and 5.5, one can see that the majority of the fiber lengths were within the range of ± 1mm. Thus, it is assumed that the remaining fibers were also of the same length.
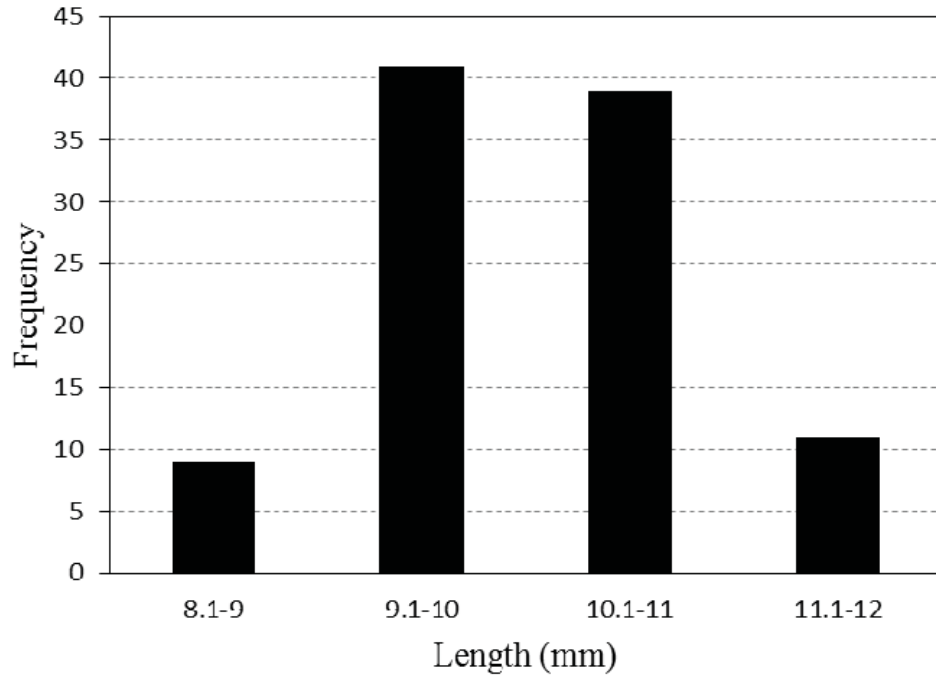
Figure 5.3 Average lengths for 10mm of recycled jute fiber
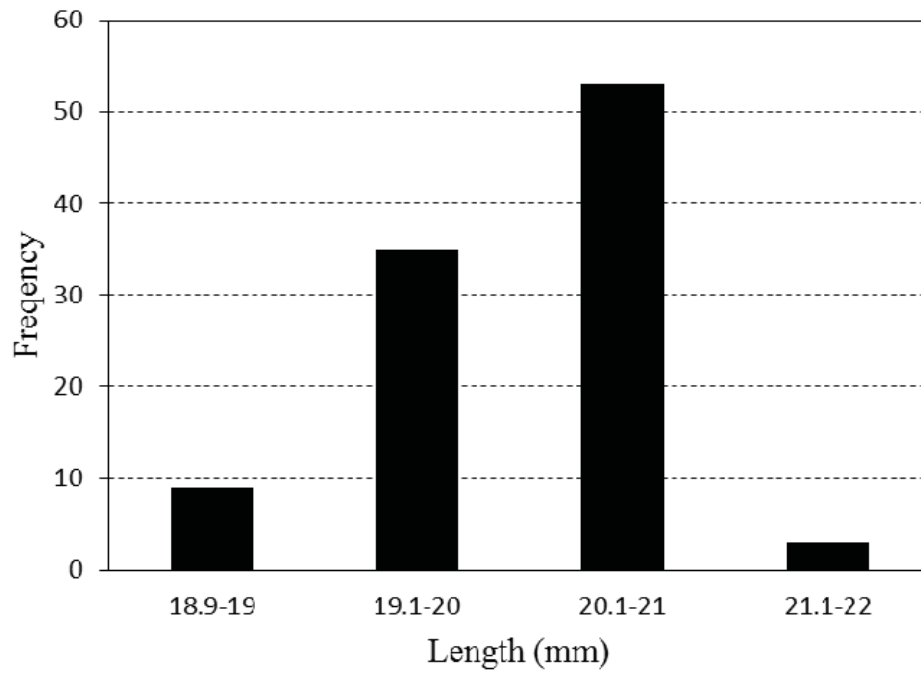
Figure 5.4 Average lengths for 20mm of recycled jute fiber
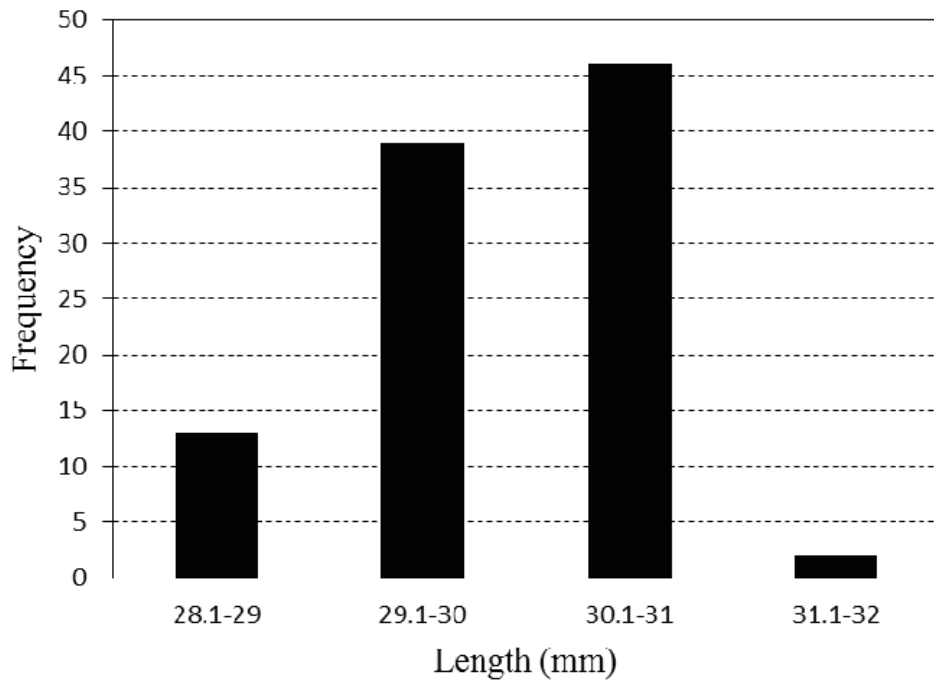
Figure 5.5 Average lengths for 30mm of recycled jute fiber

5.2.2 Fiber Diameter

The SEM micrographs technique was used to study the cross section of the fiber. The kenaf had an ellipse cross section as shown in Figure 5.6. It is interesting to note that the same bundle had different sizes of ellipse cross sections and even a circular section. It is obvious that the internal fiber structure differed between different parts of a plant as well as different plants. This strongly influenced the mechanical properties of single fibres. The average diameter was taken in the calculation in the single fiber tensile test. Figure 5.7 demonstrates the results of measuring the diameters of the kenaf bast fiber. The range of the fiber diameter was between 50-65μm.
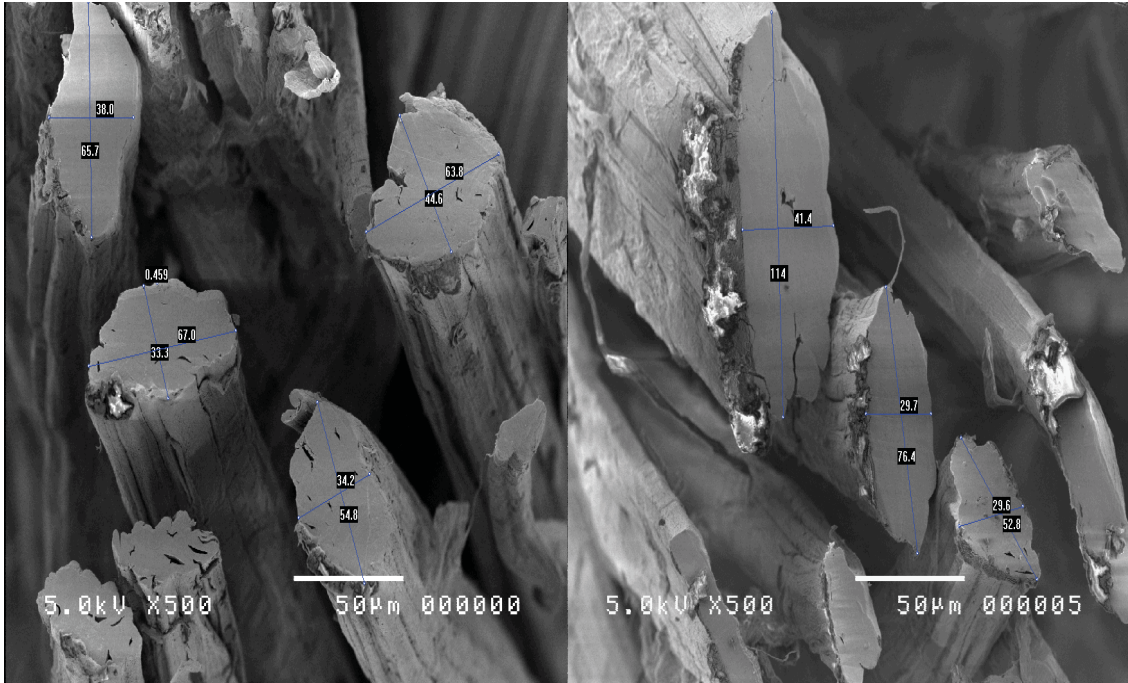
Figure 5.6 Cross section and diameter measurements for the kenaf fibers
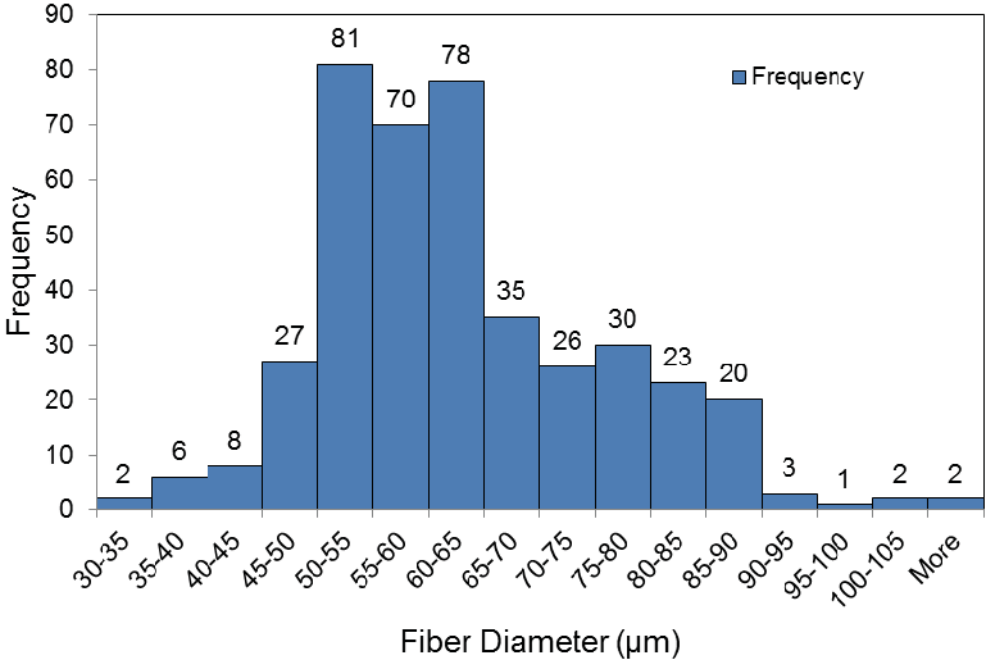
Figure 5.7 Histogram showing the diameter of the kenaf fibers

5.2.3 Holocellulose Extracted from the Kenaf Fiber

Table 5.2 summarizes the holocellulose percentage ratio of the bast and core kenaf fibers. It can be seen that the holocellulose content of the bast fiber was greater than that of the core fiber.

Table 5.2 Kenaf holocellulose content

Type of Fiber	Holocellulose %	References
Bast Fiber	66.2	Current research
Core Fiber	57.2	
Bast Fiber	60.8	(Du et al. 2008)
	53.0-57.4	(Chen et al. 1995)
	45-57	(Mokhtar et al. 2007)
	65.7	(Batra 1983)
	47.6-49	(Ochi 2010)
Core Fiber	50.6	(Du et al. 2008)
	51.2	(Chen et al. 1995)
	37-49	(Mokhtar et al. 2007)

5.2.4 Water Absorption for the Kenaf Fiber

Kenaf bast fiber showed the lowest water consumption from the surrounding, the reason depend on the kenaf morphology which were holocellulose, hemicelluloses working as absorbing water agent, lignin, and pectin. Table 5.2 clearly shows the holocellulose ratio content for bast and core kenaf fibers. In bast fiber had more holocellulose than the kenaf core fiber; therefore, the other fibers had limited ratio and a limited fiber mechanical property. The same impression was investigated for the kenaf core fiber of different sizes from about 0.15-1mm. There was insignificant change for absorbing moisture content. Water consumption for 3mm was very near to the absorbing ratio for bast fiber, as shown in Figure 5.8.
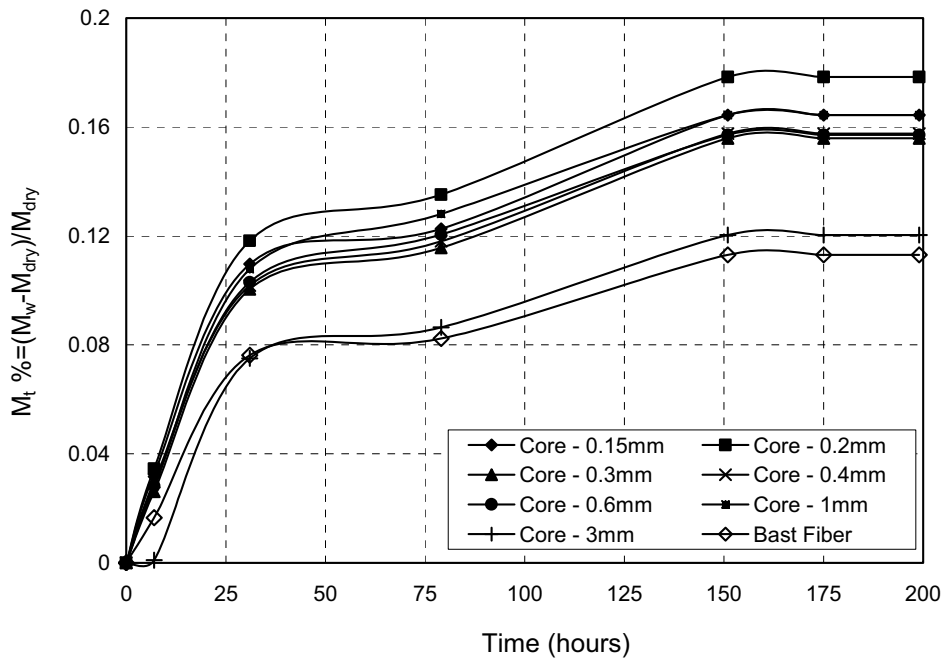
Figure 5.8 Moisture content as a function of time for core and bast kenaf fibers

5.3 Fiber Modification and Evaluation

5.3.1 Physical Treatment of Fiber

The results of the physical treatment of the kenaf are shown in Figure 5.9. It is evident that the weather conditions are an important factor which can decrease or increase the time of oven drying and lead to a decrease or increase of the power consumption of energy for fiber drying. In addition, by doing this, one can know how many hours the fiber will need for full drying at different weather conditions before the fabrication of kenaf fiber composite.
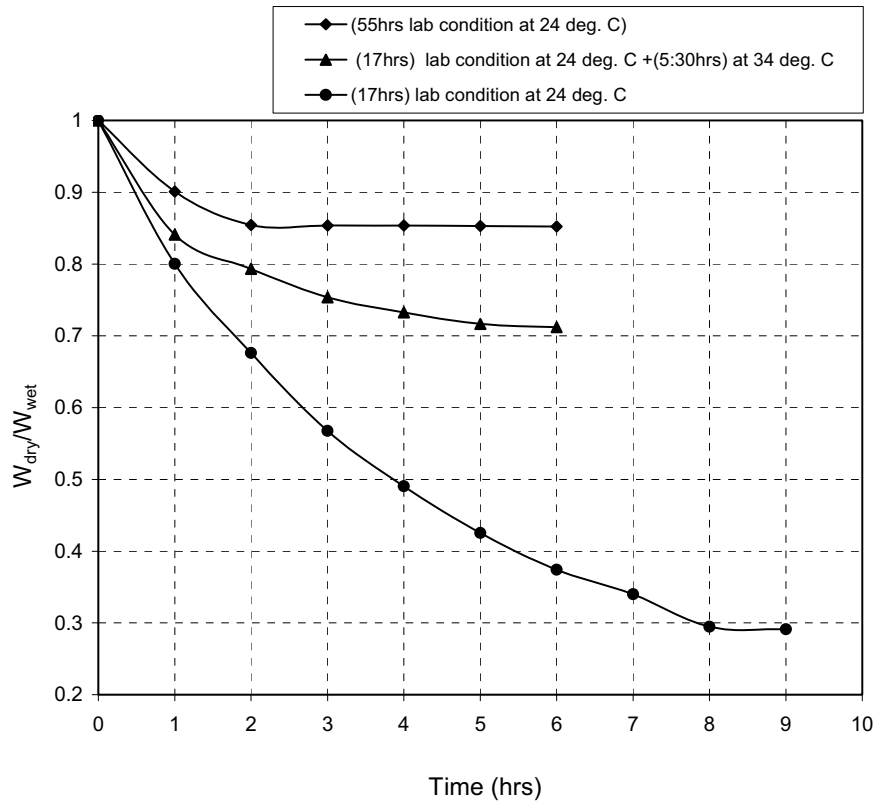
Figure 5.9 Long fibers drying under different conditions

5.3.2 Alkali Treatment

Figure 5.10 shows the SEM micrographs of the fiber surface of the treated and untreated single kenaf fiber. The presence of surface impurities on the untreated kenaf fiber surface is very obvious. The surface of the treated fiber seems rough when compared to the untreated fiber. Following 6% NaOH treatment, wax, oil and other surface impurities were removed and the treatment also roughened the surface of the fiber bundles. Figure 5.11 shows treated and untreated jute fiber.
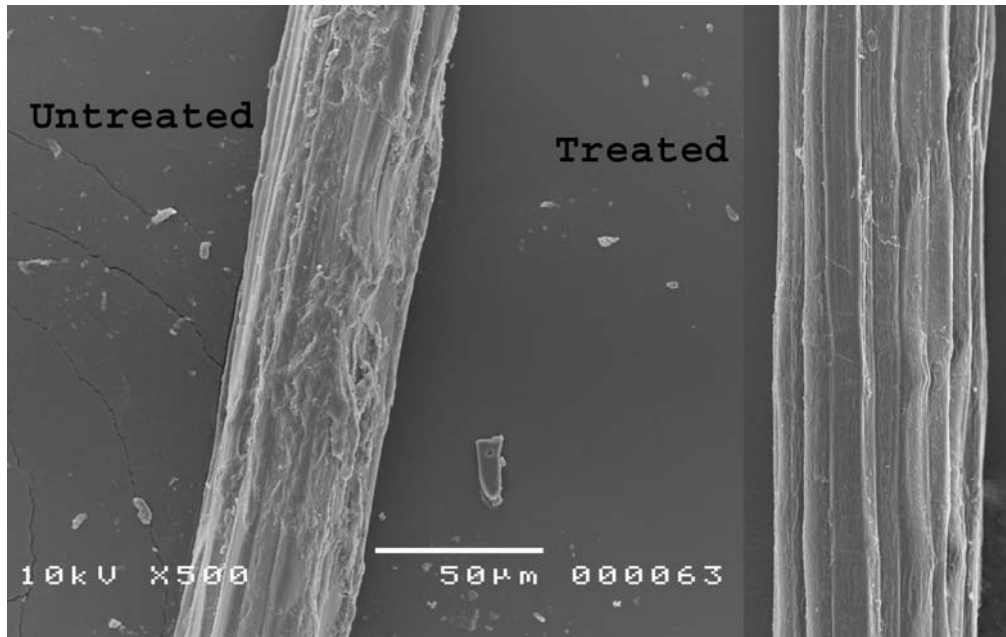
Figure 5.10 Micrographs of untreated and treated single kenaf fiber

Figure 5.11 Jute treated and untreated fiber

5.4 Single Fiber Tensile Testing

Figure 5.12 expresses the stress-strain curves obtained using the results from 40 specimens of treated kenaf fiber. Table 5.3 reveals the average tensile strength and Young's Modulus of the kenaf bast fiber in comparison with the data from the literature.
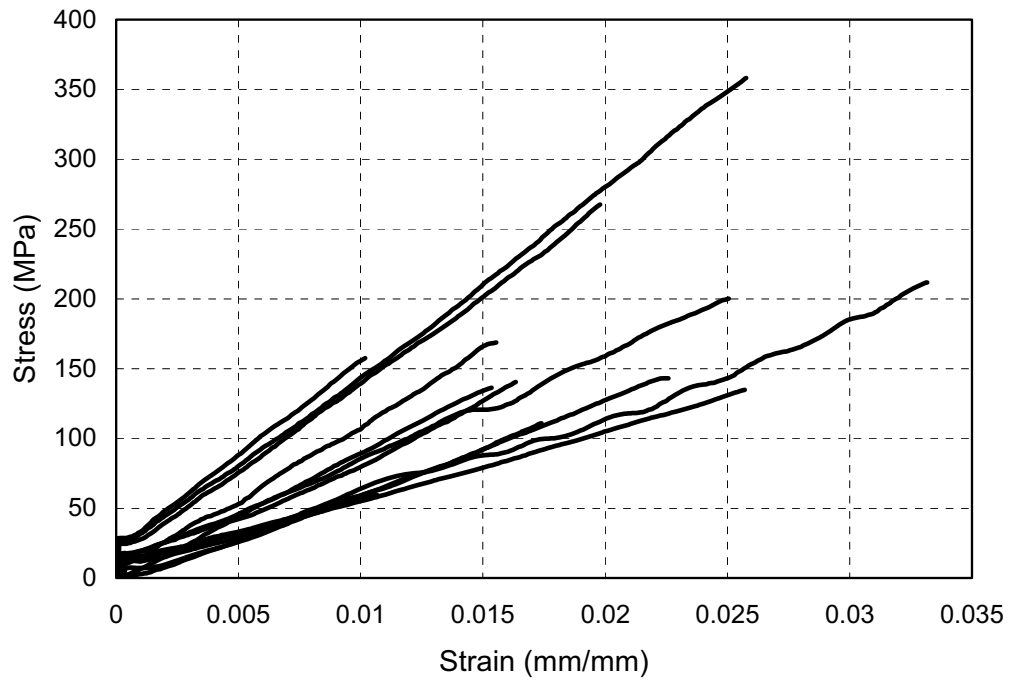
Figure 5.13 Maximum tensile stresses for single bast treated kenaf bast fiber

Table 5.3 A comparison between the experimental results of physical properties of the kenaf fiber and results from the literature

Density (g/cm³)	Tensile Strength (MPa)	Young Modulus (GPa)	Fiber Diameter (mm)	Fiber length (mm)	References
1.386	110-358	17-25	0.061	4.525	Current
1.45	930	53	-	-	(Mohanty et al. 2005)
1.2	400	-	-	-	(Kenaf Eco Fiber 2005)
-	250-600	14-39	-	-	(Ochi 2008)
-	335	22	0.106	-	(Shibata et al. 2006)
1.5	350 -600	40	-	-	(Kenaf Eco Fiber 2005)
1.4	250	4.3	0.081	60	(Lee et al. 2009)
-	223	15	0.14	8-12	(Öztrkü 2010)
1.04	448	24.6	0.078	-	(Cao et al. 2007)
-	135-232	15-24	0.02424	2.48	(Harun et al. 2009)

5.5 Summary

The holocellulose content of bast fiber was greater than the core fiber which means the mechanical properties of the bast fiber are better than the core fiber. The holocellulose percentage ratios are 66.2% and 57.2% for bast and core kenaf fiber, respectively. There was a good correlation of the results obtained compared to the literature. Therefore, the kenaf bast fiber was chosen for fabrication of composite specimens. The range of the kenaf bast fiber diameter was between 50-65mm. Alkali treatment improved the impurities of the fiber surface and removed the interface between the fiber and matrix. In term of water absorption from surrounding, the kenaf bast fiber had lower percentage compared to the core kenaf fiber at different sizes of 0.15-1mm; the reason insignificant change in water absorbing compared to the kenaf bast fiber. The tensile test for the single kenaf fiber reveals the average tensile strength and Young's Modulus of the kenaf bast fiber in comparison with the literature.

CHAPTER SIX

MECHANICAL AND DYNAMIC PROPERTIES OF NATURAL FIBER UNSATURATED POLYESTER COMPOSITES

6.1 Introduction

A detailed investigation was carried out to study the mechanical properties of kenaf/unsaturated polyester composites (KFUPC) via increasing the weight fraction of the kenaf fiber. Further investigation considered the effect of alkali treatment, post curing and fiber length on the mechanical properties of composites. In addition, the mechanical properties of the kenaf/recycled jute of various lengths reinforced unsaturated polyester composites were investigated. The SEM test was carried out to investigate the possibility of combining a kenaf fiber reinforced unsaturated polyester with a recycled jute composite.

The effects of water absorption behavior on the kenaf fiber unsaturated polyester composites at two different temperatures and various weight fractions of fiber were investigated. Furthermore, the effects of water absorption on flexural and tensile properties of kenaf fiber composites and kenaf/recycled jute composites are reported. Water absorption, thickness swelling behavior of kenaf composites and kenaf/recycle jute composites were studied. Thickness swelling rate model that developed a swelling model describing the hygroscopic process of natural fiber based composites was clarified in this part of this research by fitting the model predictions with experimental data using nonlinear curve fitting.

Finally, the present study dealt with the effects of weight fraction of treated fiber on thermal and dynamic properties of unsaturated polyester resin. Beside, dynamic mechanical analysis was performed to obtain strain and creep compliance for the kenaf composite of various styrene concentrations. It is possible to obtain creep curves at different temperature levels which can be shifted along the time axis to generate a single curve know as a master curve.

6.2 Kenaf Fiber Composites

6.2.1 Densities and Void Content

Theoretical density of composites materials in terms of weight fraction can be obtained from Equation 6.1 (Roger et al. 1997).

$$\rho_{theor} = \frac{1}{\dfrac{w_f}{\rho_f} + \dfrac{w_m}{\rho_m}}$$

(6.1)

where w and ρ represent the weight fraction and density respectively. The suffix f and m stand for (fiber) and (matrix) respectively.

Void content of the KFUPC was determined using Equation 6.2 (ASTM D2734 – 94)

$$V = 1 - \rho_c \left(\frac{w_f}{\rho_f} + \frac{w_m}{\rho_m} \right)$$

(6.2)

where V represents void fraction (volume %), ρ_c, ρ_f and ρ_m are the densities (g/cm3) of the composites, fiber and matrix respectively.
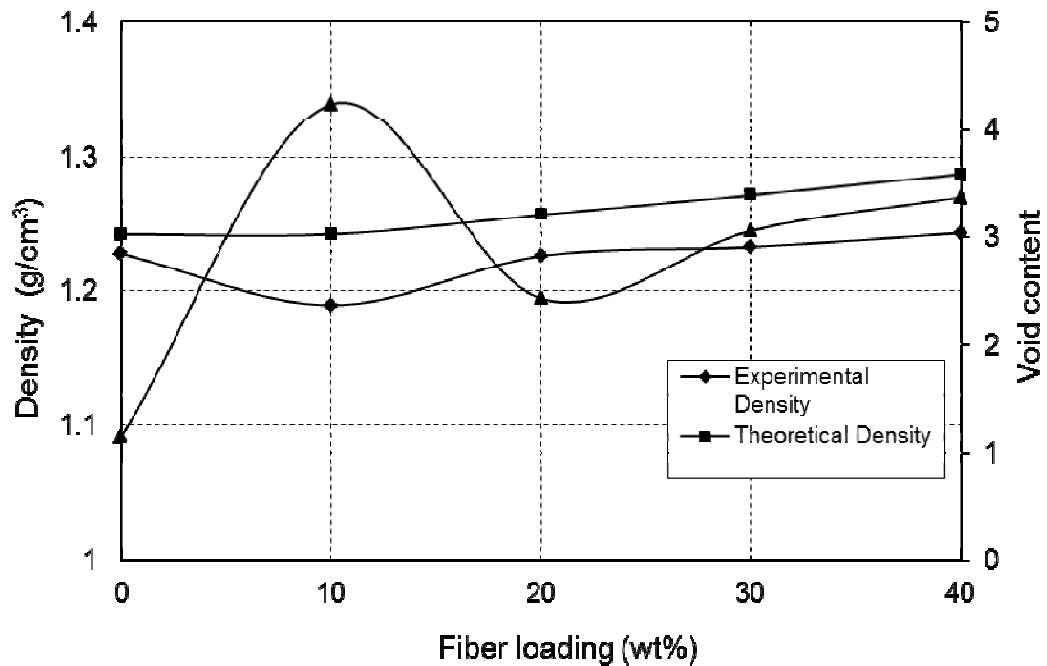
Figure 6.1 Theoretical and experimental densities of the KFUPC

Figure 6.1 displays the densities of the KFUPC. It can be seen that the experimental density is lower than the theoretical; two curves have the same trend. Both densities

were found to increase as the percentage of kenaf weight fraction was increased. The results revealed the void content to be between 1.14-4.24%; the void content increased as the nominal fiber weight fraction increase for a certain value of fiber. However, the void content in the later weight fraction of fiber composites reduced slightly and then increased after 30wt% of kenaf weight fraction. Generally, the voids were closely related to the processing conditions.

6.2.2 Tensile Properties

- **Stress-Strain Behaviour**

Figure 6.2 clarifies the stress-strain curves of the KFUPC. These curves consist of various weight fractions of treated-post curing fiber. The tensile properties increased with increase in fiber content for certain weight fractions; after this maximum value, the properties declined dramatically. This is due to fiber-to-fiber contact and poor adhesion between the fiber and matrix. The maximum value of the tensile strength was 24.5MPa at 20wt%.
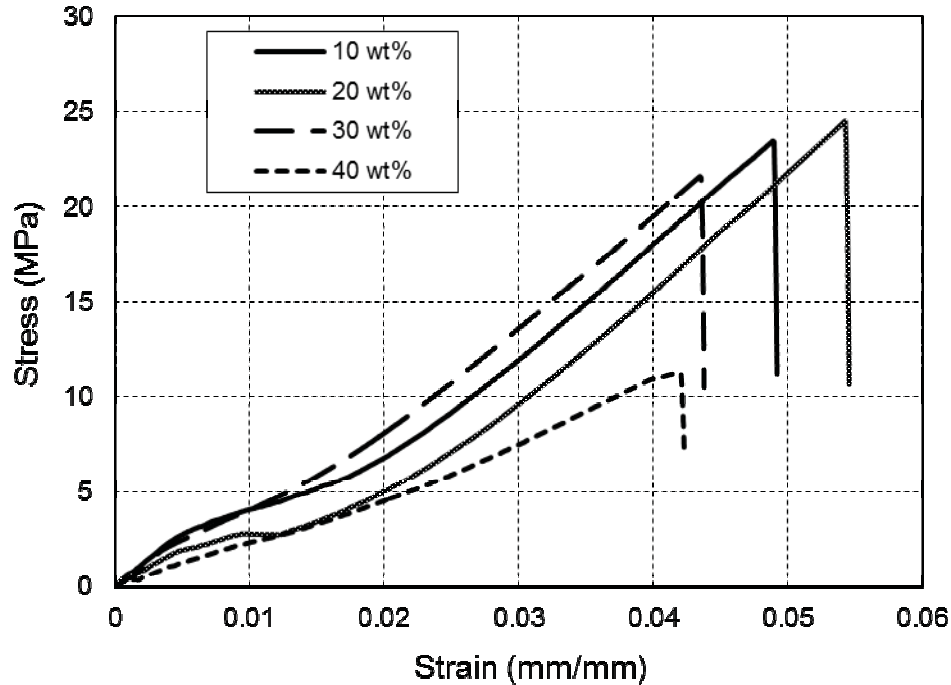
Figure 6.2 Stress-strain of polyester-kenaf composites consisting of various weight fractions of treated fiber

- **Effects of Fiber Modification**

The tensile strength of composites is more sensitive to the matrix's interfacial properties; to improve the tensile strength, a strong interface, low stress concentration, and fiber orientation are required (Acha et al. 2005). In short fibers, it is very difficult to control the fiber orientations. It is observed that the strength decreases with increase fiber content for various treatment and post curing methods as shown in Figure 6.3. The effects of modification and post curing on the modulus of elasticity for KFUPC are illustrated in Figure 6.4. The modulus is dependent on the fiber properties; to improve the tensile properties, alkali treatment was done on the fiber to influence adhesion at the interface between the fiber and matrix. It was observed that the treated-post curing composites exhibited better modulus of elasticity and the maximum values were 3.98GPa at 30wt% and 3.56GPa for treated-post curing and untreated fiber composites respectively, with the increasing percentage about 12%.
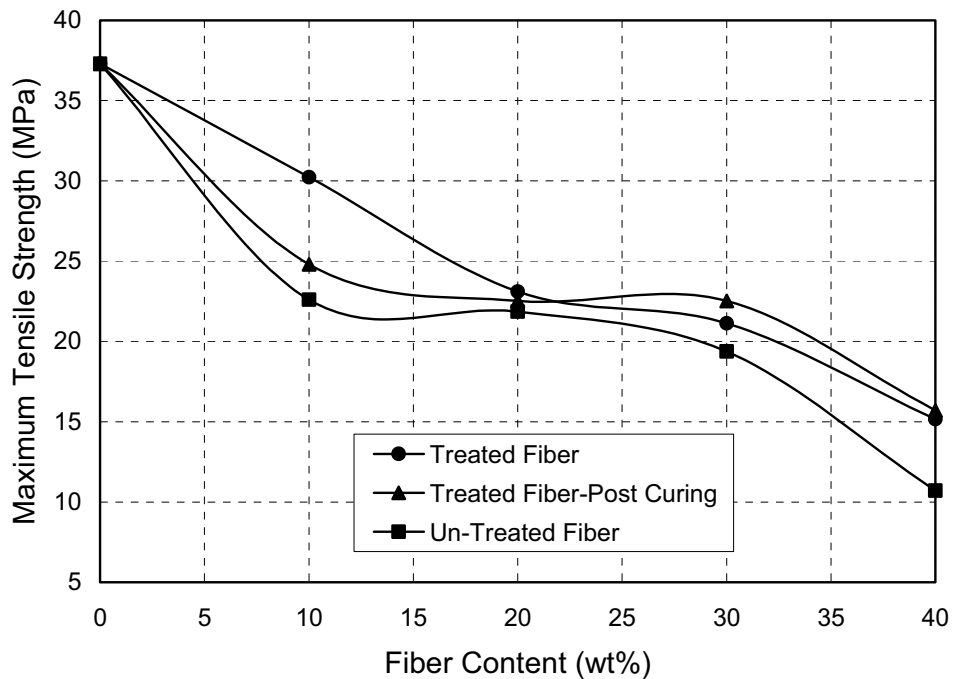
Figure 6.3 Tensile strength of kenaf/unsaturated polyester composites
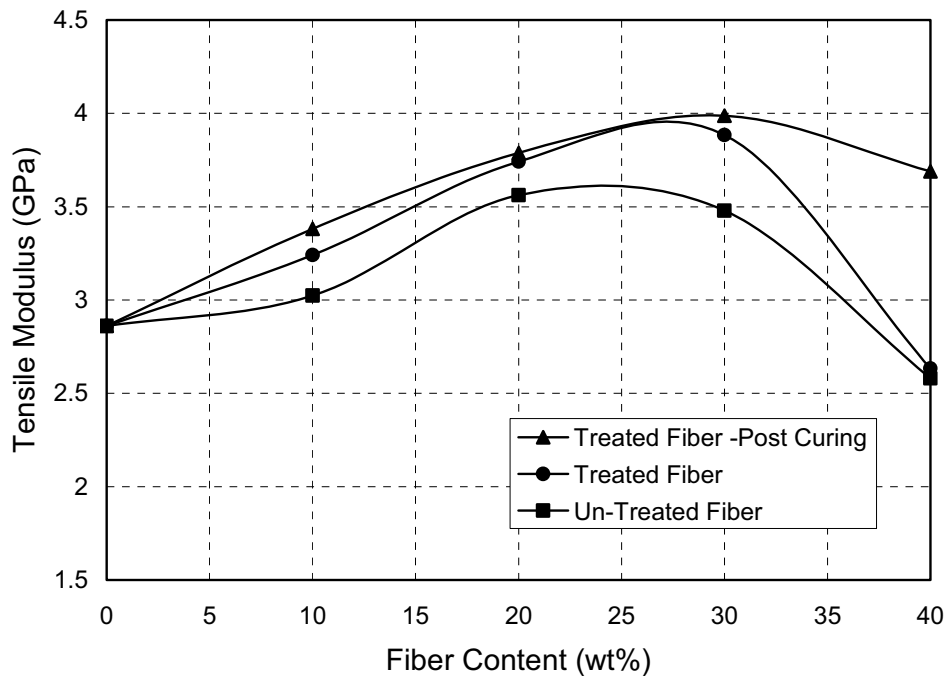
Figure 6.4 Modulus of elasticity of kenaf/unsaturated polyester composites

- **Effects of Fiber Length**

Figures 6.5 and 6.6 show the modulus of elasticity and tensile strength at various lengths of treated-post curing fiber composites. Modulus of elasticity increased with increase in fiber length as shown in Figure 6.5. The maximum values of modulus of elasticity were at 30wt% for both lengths of fiber and then decreased considerably. The maximum modulus of elasticity for fiber lengths of 10-30mm and 1-6mm were 4.97GPa and 3.98GPa at 30wt% respectively, which means fiber length, is one of the important parameters that affect the modulus of elasticity. This is obvious that there is a critical fiber length for each fiber to control the stress transfer from fiber to matrix. At a fiber length of 10-30mm, tensile strength increases with increasing fiber weight fraction. The tensile strength of 40wt% is 33.2MPa while it is 24.8MPa at 10wt% as shown clearly in Figure 6.6.
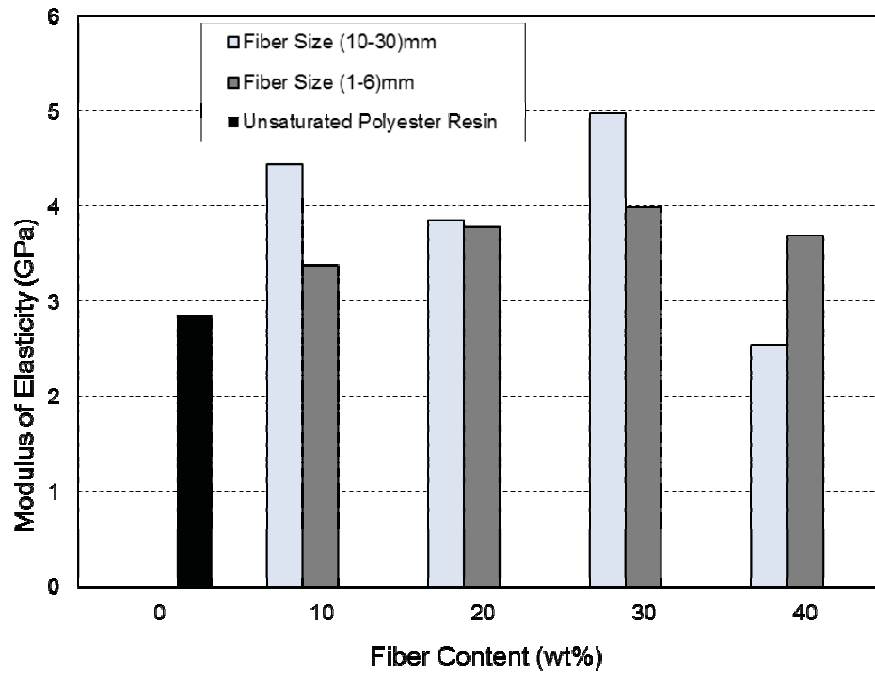
Figure 6.5 Modulus of elasticity of kenaf/unsaturated polyester composites consisting of various lengths of treated fiber with post curing
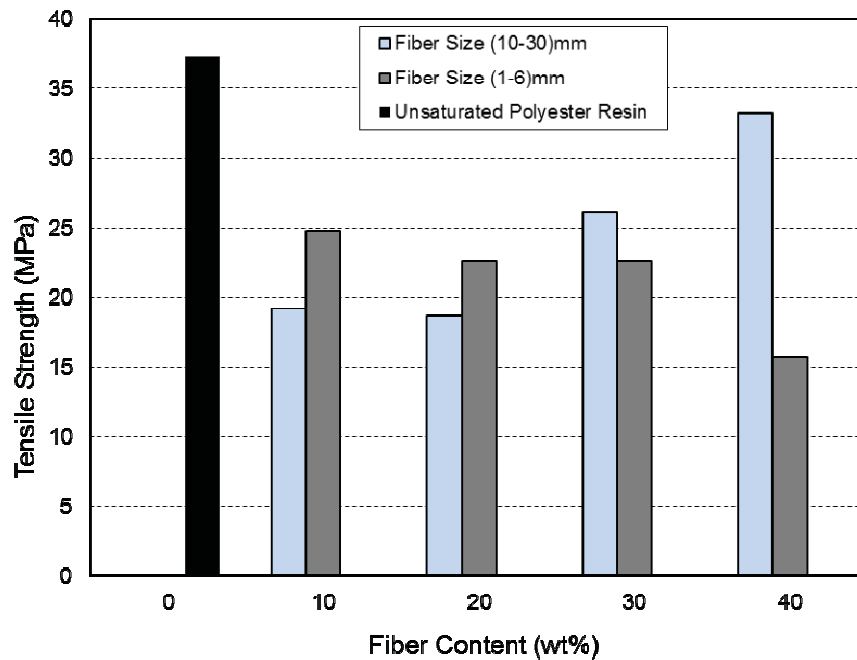
Figure 6.6Tensile strength of kenaf/unsaturated polyester consisting of various lengths of treated fiber with post curing

6.2.3 Theoretical Modelling of Tensile Properties

A number of theoretical models for the prediction of the elastic properties of short-fiber reinforced composites have been elaborated differing in accuracy and complexity

120

(Andersons et al. 2006 and Kalaprasad et al. 1997). In this research several models were used for comparison of experimental data with theoretical calculations.

- Hirsch's model

For modulus of elasticity

$$E_c = x\left(E_m V_m + E_f V_f\right) + (1-x)\frac{E_f E_m}{E_m V_f + E_f V_m} \tag{6.3}$$

For tensile strength

$$\sigma_c = x\left(\sigma_m V_m + \sigma_f V_f\right) + (1-x)\frac{\sigma_f \sigma_m}{\sigma_m V_f + \sigma_f V_m} \tag{6.4}$$

where E_f and E_m are modulus, σ_f and σ_m are strengths, V_m and V_m are volume fractions of the (fiber) and (matrix) respectively. An empirical parameter x is introduced in Hirsch's model that characterises the stress transfer between fiber and matrix, which depends on fiber orientation, fiber length and fiber distribution. The value of x can be varied from 0 to 1 to give best fit.

- Einstein and Guth equations (Anshid et al. 2008)

$$E_c = E_m\left(1 + 2.5V_f + 14.1V_f^2\right) \tag{6.5}$$

$$\sigma_c = \sigma_m\left(1 - V_f^{2/3}\right) \tag{6.6}$$

- Modified Bowyer and Bader's model (Bos 2004)

$$E_c = E_f K_1 K_2 V_f + E_m V_m \tag{6.7}$$

$$\sigma_c = \sigma_f K_1 K_2 V_f + \sigma_m V_m \tag{6.8}$$

Where values of K_1 change from (0-1)

K_2 are the orientation factor and length factor of fiber respectively.

For fibers with L>Lc   : $K_2 = L - \dfrac{L_c}{2L}$ $\tag{6.9}$

For fibers with L<Lc   : $K_2 = \dfrac{L}{2L_c}$ (6.10)

- Kelly and Tyson's model (Anshid et al. 2008)

$$\sigma_c = \eta_0 \, \eta_{LS} \sigma_f \, V_f + \sigma_m \, V_m$$ (6.11)

where η_{LS} and η_o are length efficiency factor and orientation factor of fiber respectively

- Parallel model (Roger et al. 1999)

$$E_c = E_f V_f + E_m V_m$$ (6.12)

$$\sigma_c = \sigma_f V_f + \sigma_m V_m$$ (6.13)

- Modified Guth equation (Jeefferie et al. 2011)

$$E_c = E_m \left(1 + 0.675\, S\, V_f + 11.62\, S^2\, V_f^2\right)$$ (6.14)

where S is defined as the ratio of the length-to-width of fiber

- Cox-Krenchel Model

$$E_c = \eta_o \eta_L V_f E_f + \left(1 - V_f\right) E_m$$ (6.15)

$$\eta_L = \left(1 - \dfrac{\tanh(\beta l_f / 2)}{\beta l_f / 2}\right)$$ (6.16)

$$\beta = \dfrac{2}{d_f}\left(\dfrac{2G_m)}{E_f \ln\left(\sqrt{\pi / X_i V_f}\right)}\right)^{\frac{1}{2}}$$ (6.17)

$$G_m = \dfrac{E_m}{2\left(1 + v_m\right)}$$ (6.18)

where G_m is the shear modulus of the matrix and v_m Poisson's ratio of the matrix. The value of $X_i = 4.0$ for square packing of fibers was adopted in calculation. For random in-

plane fiber reinforced composites a fiber orientation factor $\eta_o = 0.375$ can be derived (Roger et al. 1999 and Jeefferie et al. 2011).

- Halpin-Tsai model

$$E_c = E_m \left(\frac{1 + A\eta V_f}{1 - \eta V_f} \right) \tag{6.19}$$

$$\sigma_c = \sigma_m \left(\frac{1 + A\eta V_f}{1 - \eta V_f} \right) \tag{6.20}$$

$$\eta = \frac{E_{fm}/E_m - 1}{E_f/E_m + A} \tag{6.21}$$

$$\eta = \frac{\sigma_{fm}/\sigma_m - 1}{\sigma_f/\sigma_m + A} \tag{6.22}$$

where A is the measure of fiber geometry, fiber distribution and fiber loading conditions (Jeefferie et al. 2011).

Figure 6.7 explains the comparison of the variation in theoretical and experimental tensile strength (*TS*) values of random oriented composites with weight fraction of fibers. Theoretical values were calculated using various models. It can be seen that in all cases, *TS* increases regularly with increase in the weight fraction of fibers. A near correlation between theoretical and experimentally observed *TS* was seen in those models predicted using modified Bowyer-Bader for $L<L_c$ and Einstein-Guth equations. The curves showing modified Bowyer-Bader for $L>L_c$, Kelly-Tyson, Hirsch and Halpin-Tsai models agree the least with the experimental values. Usually, the Hirsch model is a combination of parallel and series models; these models are used to describe the strength of continuous fiber reinforced ploymeric composites. The stress transfer mechanism of continuous fiber composites is different from that of short fiber composites. In the case of short fiber composites, the stress transfer depends largely on

fiber orientation, stress concentration at fiber ends, critical fiber length (Kelly et al. 1969, Anshid et al. 2008, Bos 2004, Roger et al. 1999).

Figure 6.8 demonstrates a comparison of the variation in experimental and theoretical modulus of elasticity (*ME*) of random oriented short fiber composites with weight fraction of fibers. It was observed that a very reasonable correlation exists between theoretical and experimental values in models, such as modified Bowyer-Bader for $L>L_c$, Kelly-Tyson, Hirsch, Cox-Krenchel and Halpin-Tsai. In the case of the Cox-Krenchel and Hirsch's models, it was found that the *ME* increased regularly with increases in the weight fraction of fibers. *ME* values obtained from the Cox-Krenchel model was lower than the experimental and Hirsch's model values. The modeling results underestimated the experimental data. Beg (2007) reported the same remark of the underestimated results using Cox-Krenchel. A good agreement was observed between the values obtained from Hirsch's model and the experimental values. Here the parameter *x*, which determines the stress transfer between the fiber and matrix, was introduced, and thus an agreement was observed between the theoretical and experimental values.
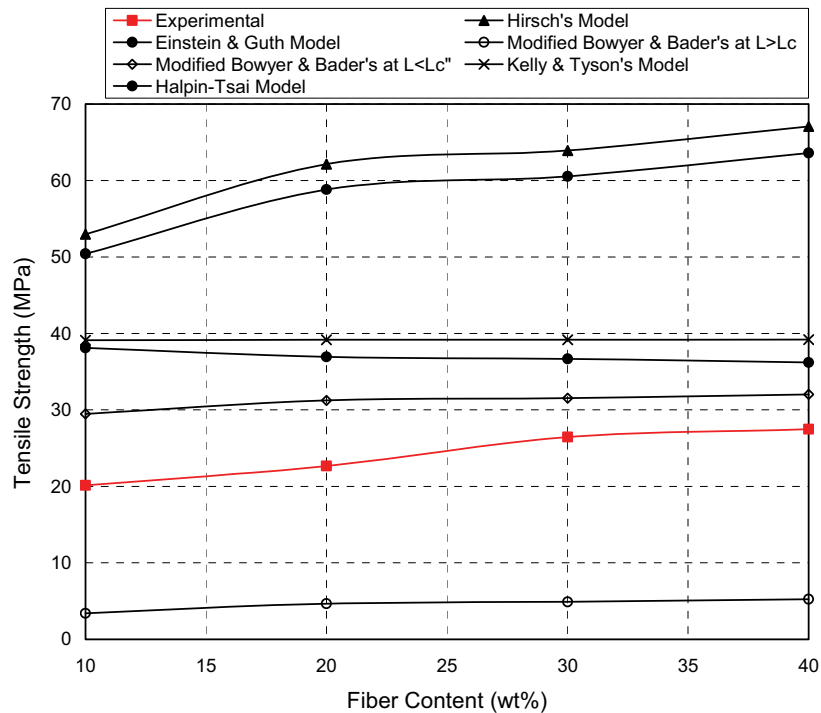
Figure 6.7 Variation of experimental and theoretical TS values as a function of weight fraction of fibers
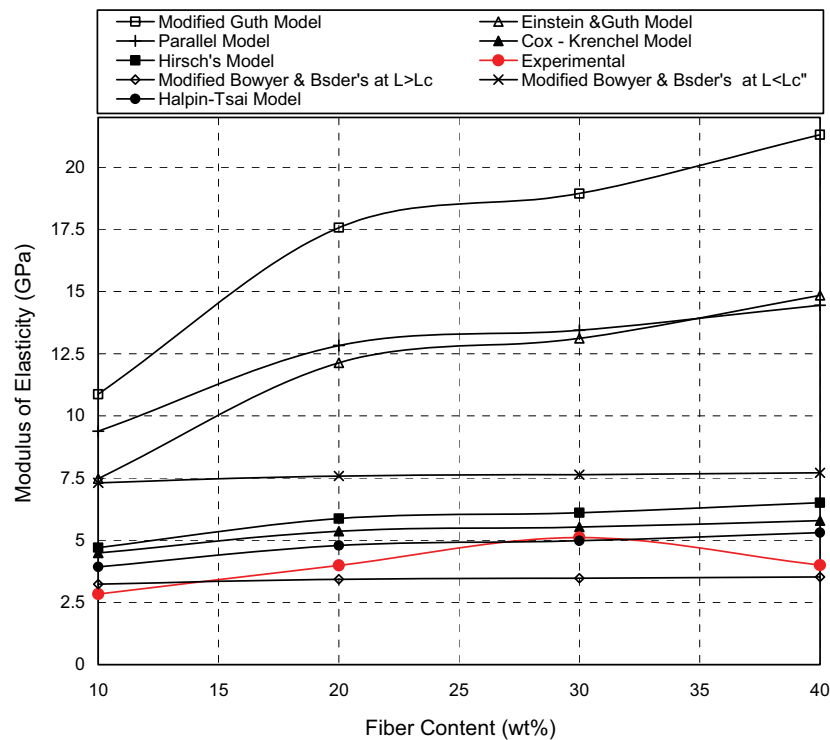
Figure 6.8 Variation of experimental and theoretical modulus of elasticity values as a function of weight fraction of fibers

6.2.4 Flexural Properties for Kenaf Fiber Composites

- **Effects of Alkali treatment**

Results in Figures 6.9 and 6.10 show the effects of fiber loading, alkali fiber treatment and post curing addition to fabricate specimens. Both flexural strength and modulus were found to increase significantly as the fiber weight fraction increased until 20wt%. At a low fiber weight fraction, the fiber ends act as stress concentrations and causes the bound between the fiber and matrix to break under low level of loading. At a higher weight fraction, the matrix is sufficiently restrained and the stress is more evenly distributed. Meanwhile, the increment of flexural strength was still beyond the virgin unsaturated polyester resin. Generally the treated short fiber composites with post curing gave higher flexural modulus values compared to the untreated and treated fibers. It is evident that the adhesion between the fiber and matrix improved with alkali treatment. For untreated fiber, the maximum flexural strength was at 10wt%, while with treated fiber the trend of the increasing of strength increased with increase of the fiber content until 20wt%. The same trend was observed for treated fiber with post curing. By increasing the weight fraction of the fiber more by than 20wt%, the flexural strength

and modulus decreased; this is possibly due to fiber-to-fiber interaction, void content and dispersion problems (Arib et al. 2006). As discussed earlier, the maximum value of the flexural modulus was at 20wt% and it was about 4.3 GPa, for treated and treated with post curing composites. The increase in percentages was 17% and 29% respectively compared to pure unsaturated polyester, respectively as Figure 6.10 shows.
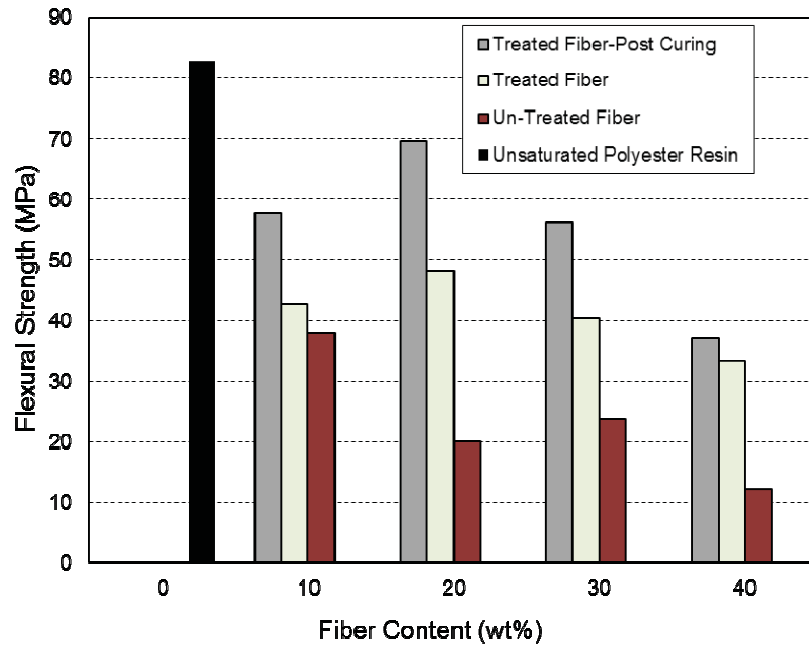
Figure 6.9 Flexural strength of kenaf / unsaturated polyester composites
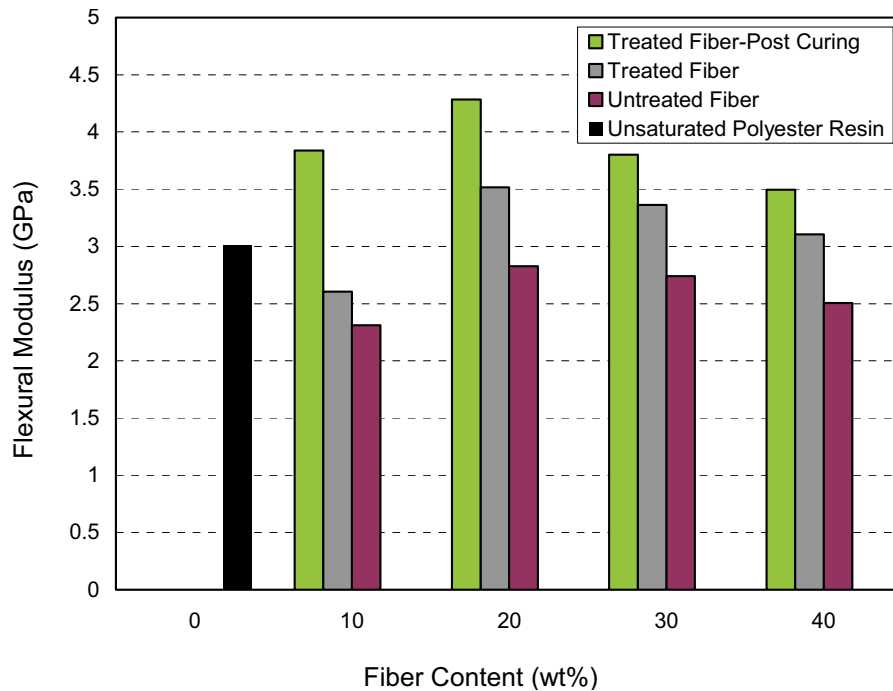
Figure 6.10 Flexural modulus of kenaf / unsaturated polyester composites

- **Effects of Fiber Length Parameter**

The flexural strength and flexural modulus of the kenaf composites with various lengths of 1-6mm and 10-30mm and fiber weight percentage of 10wt% to 40wt% with increment percentage of 10wt% are shown in Figures 6.11 and 6.12 respectively. The results show that the flexural strength decreased with increase fiber length. It was observed that the maximum flexural strength was around 69.62MPa for fiber size of 1-6mm composites; this maximum value was produced by 20wt% weight fraction of fiber, while the flexural strength for fiber length of 10-30 mm was 47.57 MPa. Compared to unsaturated polyester resin, the decreasing percentages were 19% and 74% for fiber lengths of 1-6mm and 10-30mm respectively. As the fiber content increased to 40wt%, for both lengths, the fibers were not well bonded by matrix and thus poor matrix adhesion occurred. Figure 6.12 exhibits the effect of kenaf fiber content on flexural modulus of the composites. In both lengths, reinforced polyester composites showed a significant improvement in flexural modulus compared with the polyester resin. These reveal that the incorporation of both different lengths of fiber into matrix is quite effective for reinforcing the matrix system. It is understandable that the flexural modulus increased with increase the fiber length and the increasing percentage was 3% at 20wt% compared with fiber length of 1-6mm. In comparison with pure unsaturated polyester resin the flexural modulus increased by 29% and 33%, for fiber lengths of 1-6mm and 10-30mm, respectively.
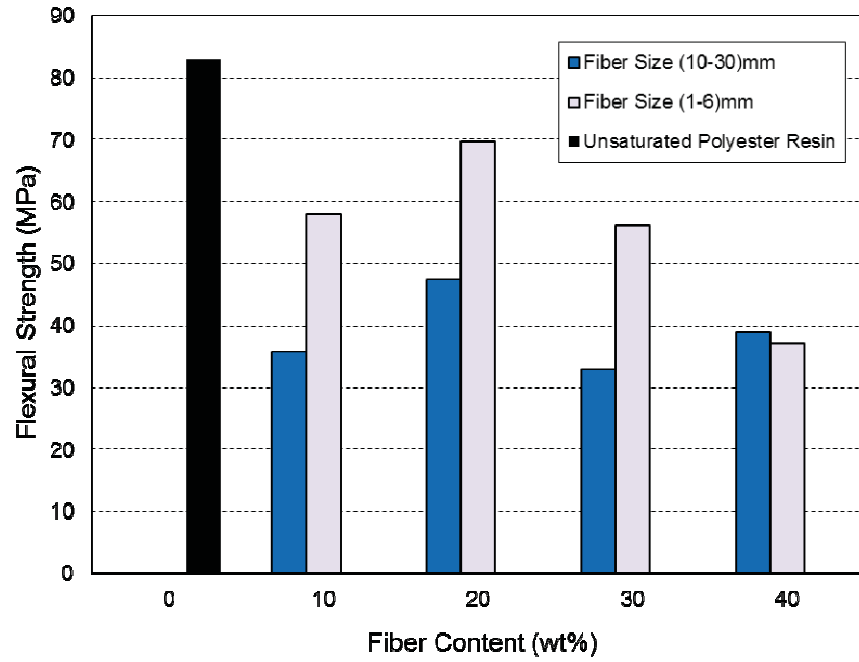
Figure 6.11 Flexural strength of polyester-kenaf consisting of various fiber lengths
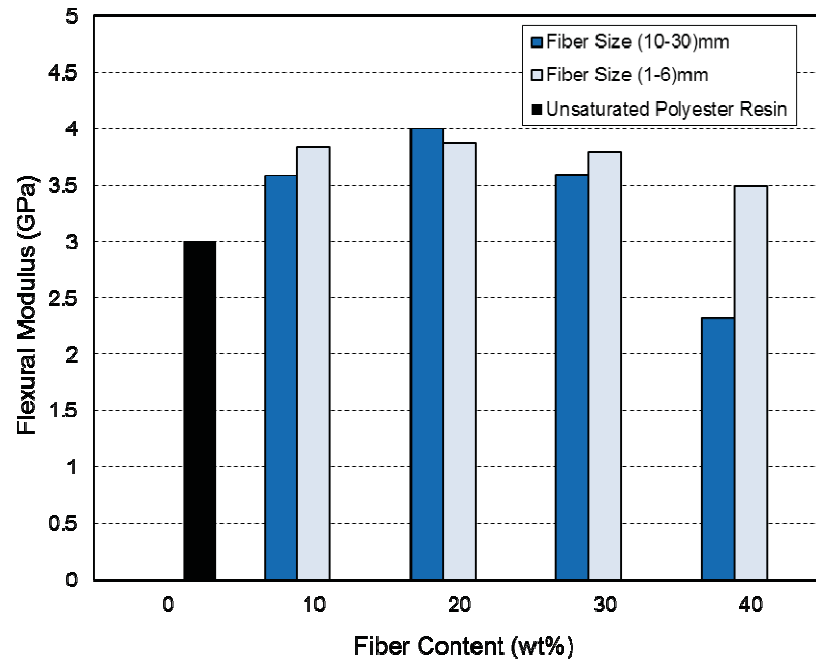
Figure 6.12 Flexural modulus of polyester-kenaf composites consisting of various fiber lengths

6.2.5 Impact Properties of Kenaf composites

- **Effect of Styrene Concentration**

Results of charpy impact test for composites at different weight fractions of untreated kenaf fiber size 1-6mm for different styrene concentrations are represented in Figure 6.13. It can be seen that the composites have the same trend for various styrene concentrations. It is observed that the optimum toughness is at 20wt% fiber weight fraction for both composites. The composite containing 40%ST generally did better than the 50%ST which indicates that the brittleness of material increased with increase of styrene concentrations. The impact strength was 10.63kJ/m^2 at 20wt% of 40%ST, while 50%ST of the same weight percentage was 7.47kJ/m^2. The increasing percentage was about 30%.
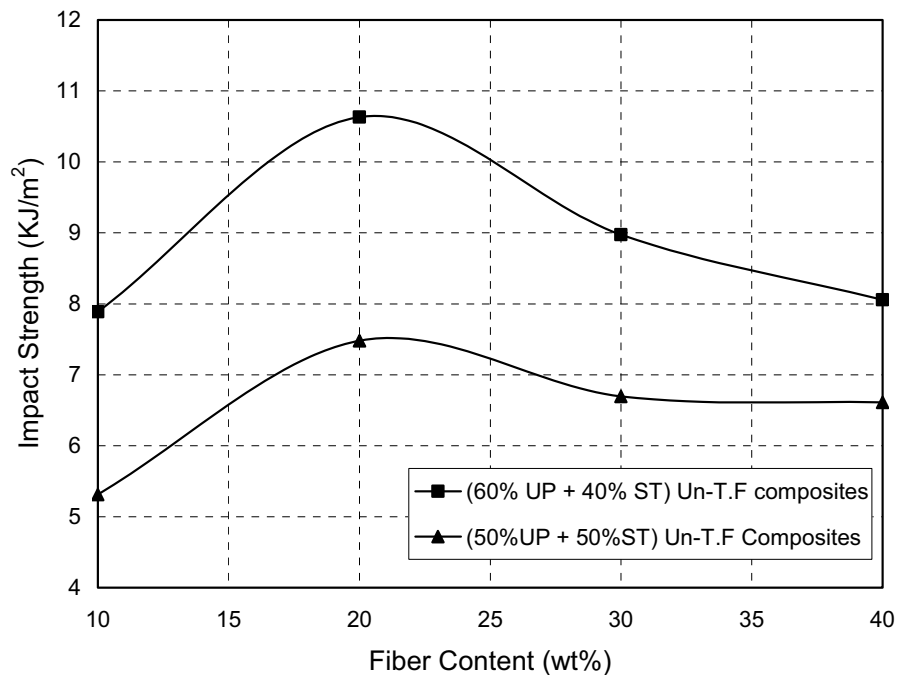
Figure 6.13 Comparison of different styrene concentrations composites at different weight fractions of untreated fibers size 1-6mm

- **Effect of Alkali Treatment and Post Curing**

Results in Figure 6.14 recommend the toughness of untreated short fiber composites is higher compared to those treated with post curing; the reason for that is the adhesion between the fiber and matrix improved by alkali treated. In the case of a strong fiber-

matrix interface, impact strength of composites decreased as a consequence of reduced fiber pullout due to the fact that the pullout mechanism absorbed a great amount of energy as friction work during impact. The fiber pullout was the active fracture mechanism in the fiber of 1-6mm size. Thus, treating the fiber with alkali led to a large decrease in impact strength of composites (Sharifah et al. 2004 a, b).

For untreated fiber the optimum impact strength was at 20wt% fiber, while with treated fiber the trend of the increasing of toughness increased with increase of fiber content until 20%wt after that decreased at 30%wt and continue increases with increase fiber content, and reached to the optimum strength value at 40%wt fiber weight fraction. Impact strength decreased when post curing was added to the fabricated specimens. In addition, the results have different trends for treated composites with post curing. The strength decreased with increase fiber content and the optimum toughness at the 40%wt fiber weight fraction; even with this increase, the optimum strength did not reach to the optimum value compared with treated and untreated fibers. The reason is the amount of fiber pullout decreased after the post curing process. In this case, there was a chance to increase the fiber volume fraction with treated composites via the post curing process.
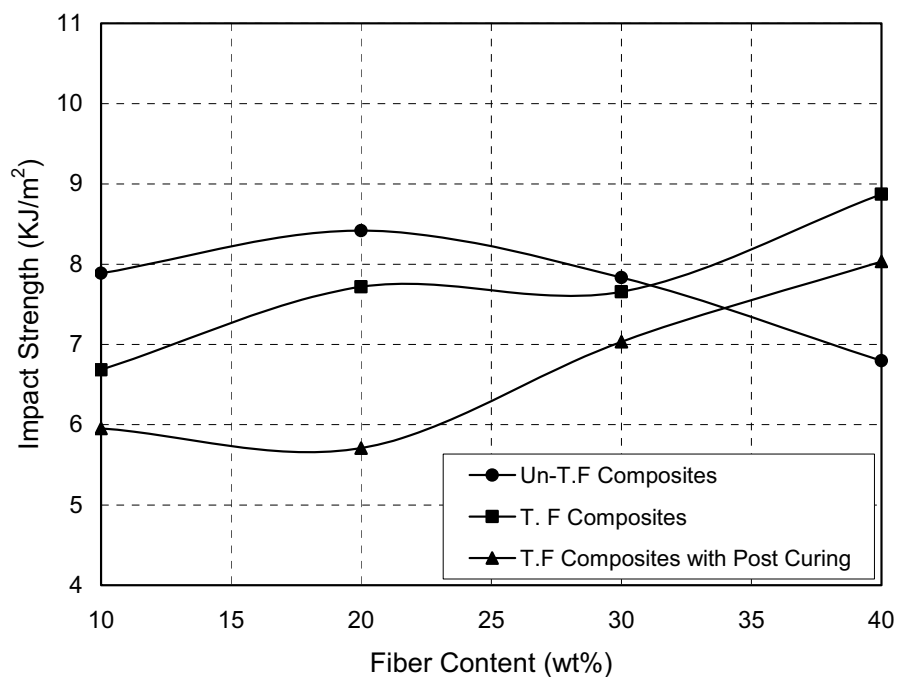
Figure 6.14 Comparison of treated and untreated fibers size 1-6mm composites for 40%ST

- **Effect of Fiber Length**

The impact strength of the composites reinforced with kenaf bast fiber with post curing depended on the amount and the length of fiber as shown in Figure 6.15. The results clarifies that the optimal values to obtain the highest impact strength were at 30%wt and 40%wt for 10-30mm and 1-6mm respectively. On the other hand, the optimum impact strength for untreated fiber composites was at 20%wt for both different lengths of fiber as Figure 6.16 illustrates. After these optimum values, the composites showed a steep decline beyond their optimal values. This was due to a higher fiber content which led to a higher fiber-to-fiber contact which affected the load transferred by the matrix to the fibers nearest the surface and continued from fiber to fiber via the matrix and interface (Beckerman 2007). When the interface was weak, effective load distribution was not achieved and the mechanical properties of the composites were impaired. Based on the results, impact strength increased with increase fiber length for a certain weight fraction of fiber as summarized in Figure 6.17 compared with unsaturated polyester and raw fiber.
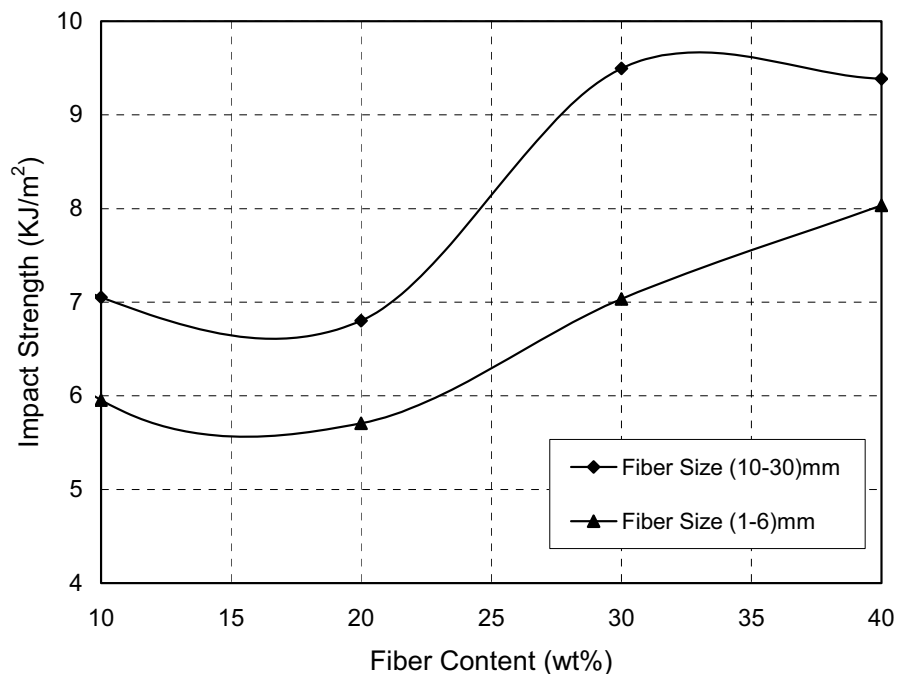
Figure 6.15 Comparison of treated fiber composites at different fiber lengths
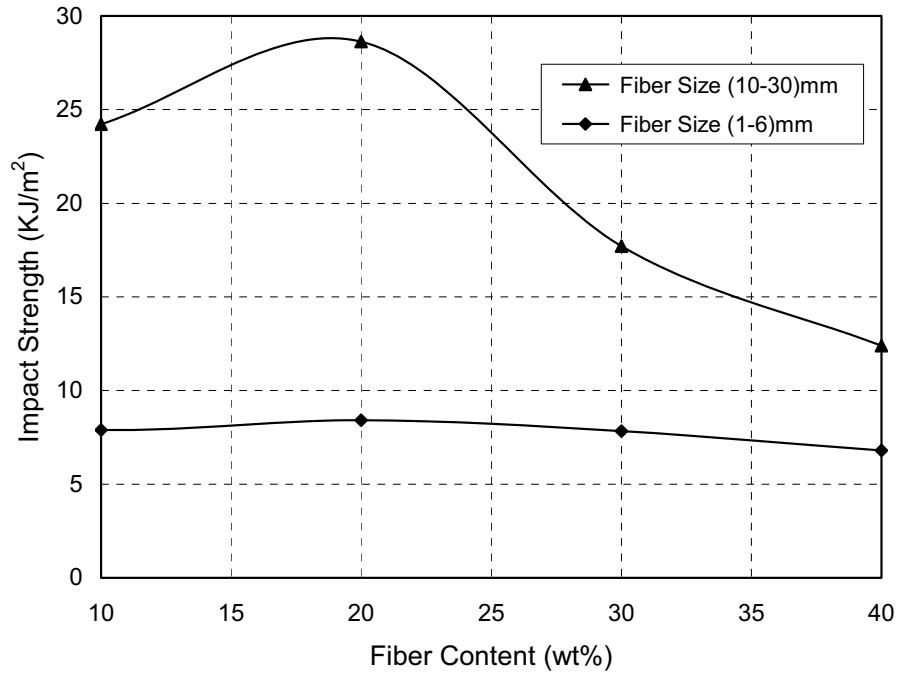
Figure 6.16 Comparison of untreated fiber composites at different fiber lengths
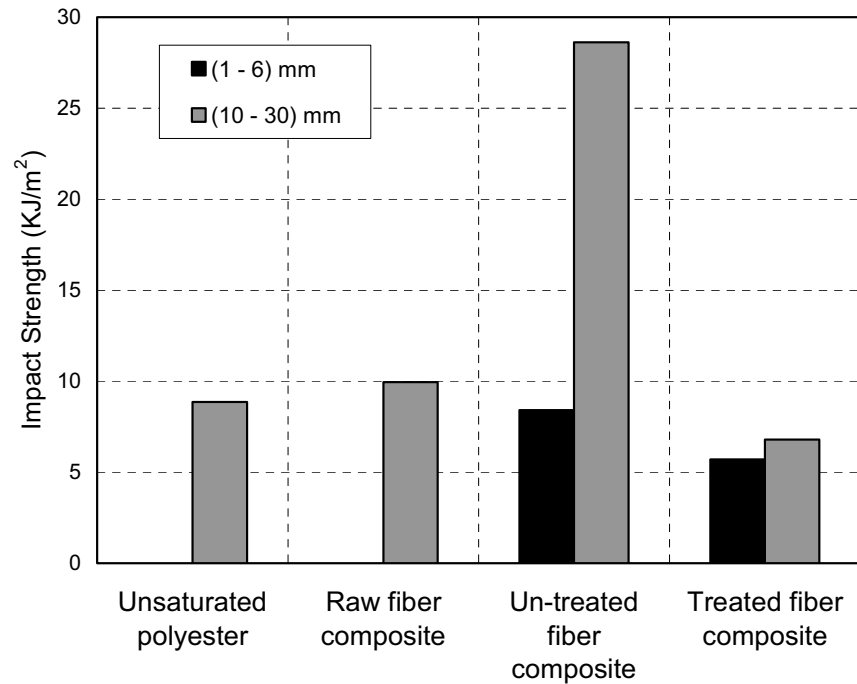
Figure 6.17 Comparison of raw, untreated and treated fiber composites at different fiber lengths (20wt %)

6.3 Hybrid Kenaf/Recycled Jute Fiber Composites

6.3.1 Tensile Properties

The tensile properties of the composites were strongly influenced by the fiber length. The effect of the fiber ends played an important role in the fracture of the short fiber

composites. To accomplish the maximum level of stress in the fiber, the fiber length L_f had to be at least equal to the critical fiber length L_c, the minimum length of fiber required for the stress to reach the fracture stress of fiber (Sreenivasan et al. 2010). Matthews et al. (2005) explicated about a schematic representation of the situation, when the composites possessing fibers had a length below L_c above L_c and at L_c, under tensile loading. Therefore, it is very important to optimise the fiber length for a particular matrix-fiber system, so the optimum value of properties can be obtained. The influence of recycled jute fiber length on the tensile properties of short kenaf/recycled jute unsaturated composites are shown in Figures 6.18 and 6.19. The tensile strength and modulus of elasticity increased with increase in the fiber length to 30mm. From Figure 6.18, it can be easily seen that the 75% of recycled jute length 30mm provided better improvement in the modules; the maximum improvement was about 17.8% compared to modulus of kenaf unsaturated composites, while the maximum improvement for strength was about 29%. The elongation value was not found to have any considerable variation with recycled jute fiber length as shown in Figure 6.20.
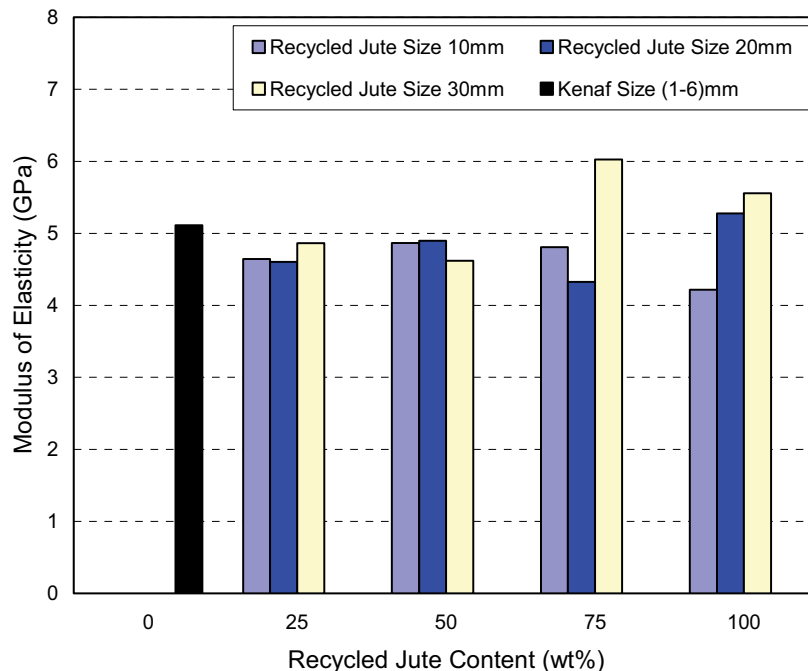
Figure 6.18 Modulus of elasticity of kenaf composites and kenaf/recycled jute composites consisting of various lengths of recycled jute fibers
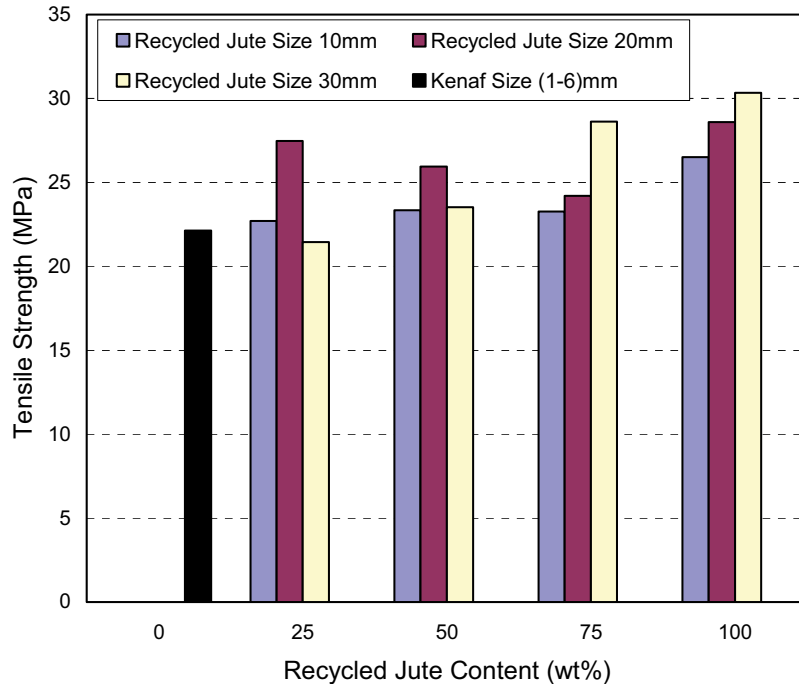
Figure 6.19 Tensile strengths of kenaf composites and kenaf/recycled jute composites at various lengths of recycled jute fiber [constant fiber weight percent 30%]
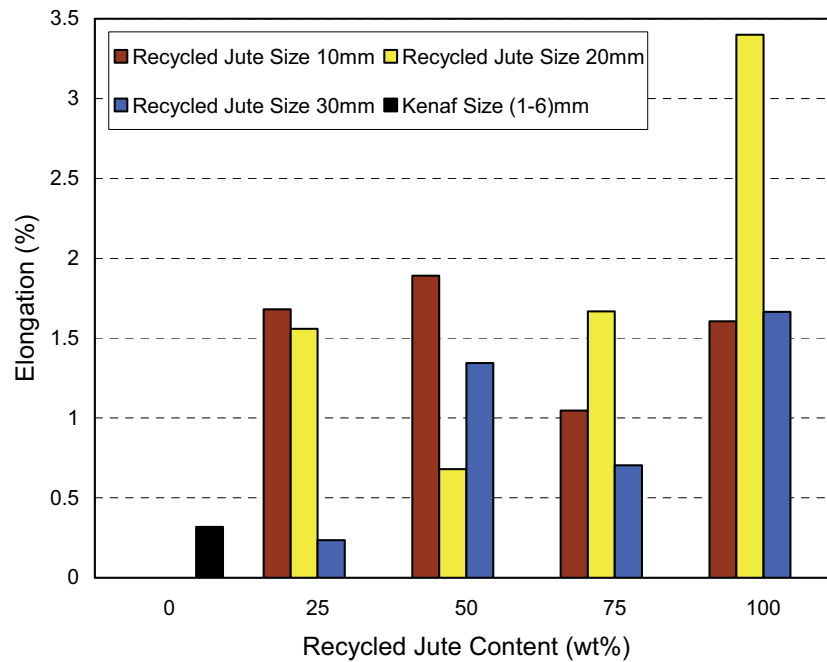
Figure 6.20 Tensile elongations of kenaf composites and kenaf/recycled jute composites at various lengths of recycled jute fiber [constant fiber weight percent 30%]

6.3.2 Flexural Behaviour

Results in Figures 6.21 and 6.22 exhibit the effects of recycled jute fiber of various lengths, adding to specimens fabricated at different percentages to a 20% fiber weight fraction of kenaf/recycled jute composites. Both flexural strength and modulus were found to decrease significantly as the percentage of recycled jute fiber of various jute lengths was increased. This is due to poor matrix adhesion occurring, which means the jute fiber length increase was not well bonded by the matrix. The longer fibers with poor adhesion to the unsaturated polyester matrix created stress concentration zones, and this is suggested as a reason for the decrease of the flexural properties of the hybrid composites made with kenaf /recycled jute of various lengths. At a specific jute length and weight percent, for example 75% jute fiber, 30mm length was the maximum value of flexural strength.

Figure 6.23 summarizes the variations of flexural strength and modulus with recycled jute fiber length of recycled jute unsaturated polyester composites. The flexural properties show an increasing trend with the increase of fiber length. Critical length of the fiber in the composites could be calculated from Equation 6.23 (Kelly et al. 1965).

$$L_c = \frac{D \sigma_f}{2 \tau_m} \tag{6.23}$$

where L_c is the critical length, D is the fiber diameter, σ_f is the fiber fracture stress, and τ_m is the interface shear strength. The critical length of the recycled jute fiber was 3.733mm (Shamsun et al 2011). The fiber's critical length is the minimum length necessary for shear stress transfer through the fiber-matrix interface to generate a tensile stress high enough to fracture the fiber. As a consequence of effective reinforcement, recycled jute fiber length should be larger than the critical length. This is the reason why the flexural properties showed a high value at 30mm (Cao et al. 2006). The fiber below the value of critical length was possibly pulled out and not broken out in the flexural test (Shibata et al. 2006).
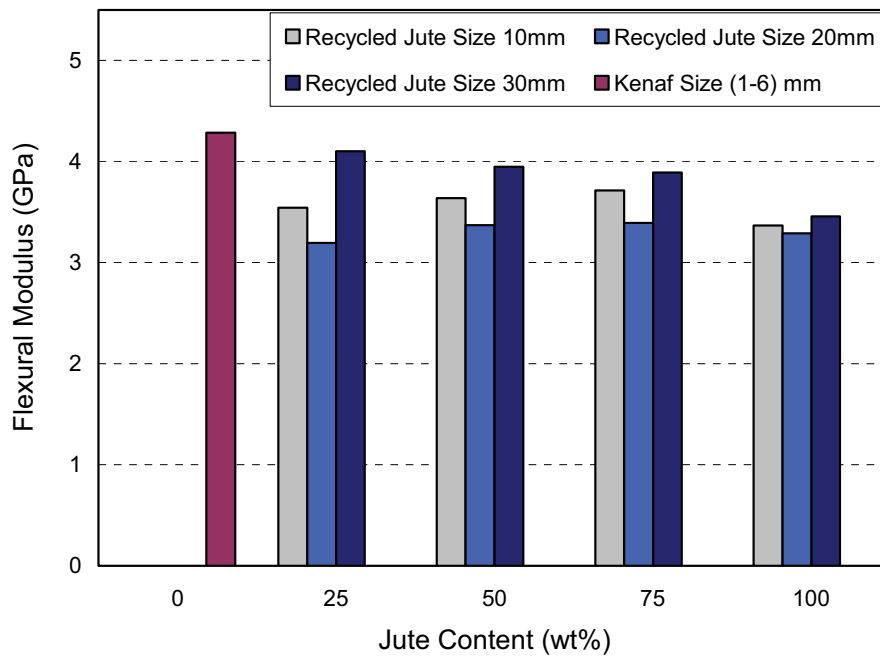
Figure 6.21 Flexural modulus curves of kenaf composites and kenaf/recycled jute composites at various lengths of recycled jute fiber [constant fiber weight percent 20%]
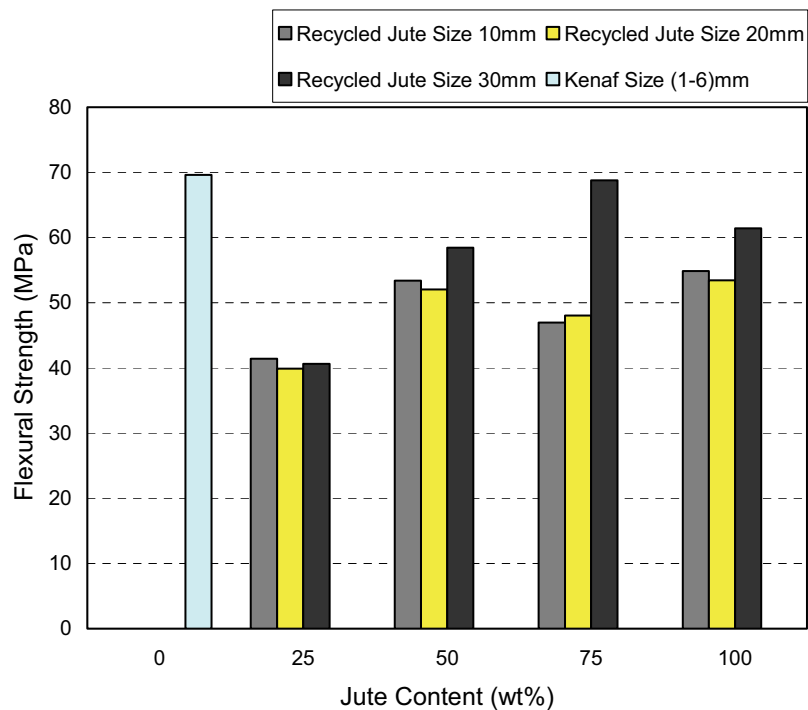
Figure 6.22 Flexural strength curves of kenaf composites and kenaf/recycled jute composites at various lengths of recycled jute fiber [constant fiber weight percent 20%]
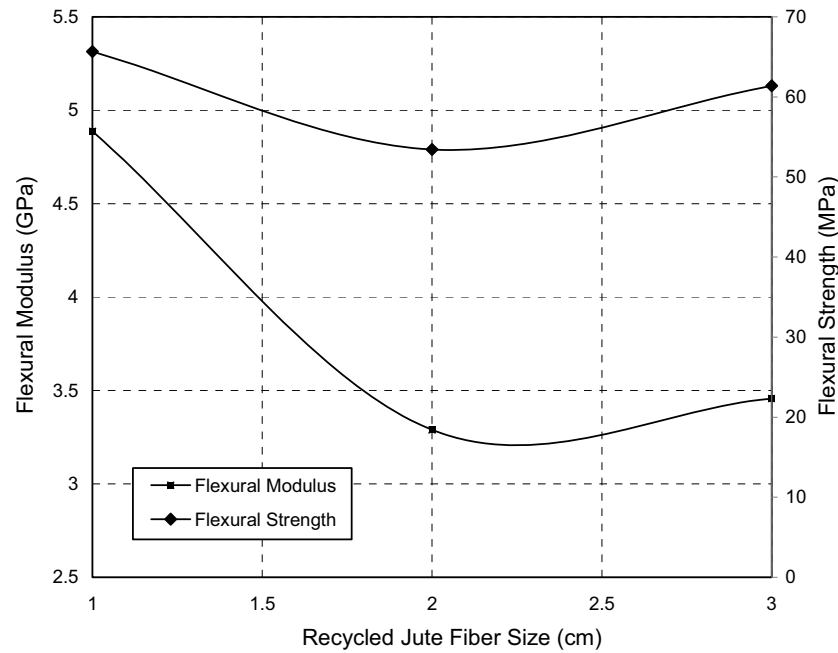
Figure 6.23 Flexural modulus curves of jute composites at various lengths of recycled jute fiber [constant fiber weight percent 20%]

6.3.3 Impact Properties

Figure 6.24 shows the variation of impact strength with recycled jute fiber weight percent for kenaf/recycled jute unsaturated polyester composites at varying jute lengths. In these composites the total weight fraction of fiber was 20wt%. 0 wt% along the x-axis of Figure 6.24 means there was no added jute fiber and it was 20wt% kenaf fiber, while 100wt% was 20wt% of jute fiber. The impact strength of the composites was found to increase with increase fiber length. Long fibers have a large absorption capacity, and distribution of impact energy occurs at a high speed (Sreenivasan et al. 2010). The increased impact resistance can be explained by the formation of a tortuous fracture path which retards crack propagation. Furthermore, increased polymer-fiber interaction decreases interfacial tension and reduces chances of crack initiation at the interface. By means of increasing interfacial interaction there could also be more efficient energy transfer to fibers which would help dissipate this energy through fiber breakage (Shenoy et al. 2007). Therefore, impact strength of hybrid composites increases with increase fiber length. However, after an optimum length of fiber which is 10mm, a large proportion of fiber will be pulled out of the matrix due to fiber entanglements compared to shorter lengths where fiber pull-out is the active fracture mechanism, thus leading to a small decrease in impact strength as observed by Arib et

al. (2006). It is observed that the maximum impact strength was $10.897 KJ/m^2$ at 50% weight fraction of recycled jute with fiber length of 10mm. In addition, there was insignificant improvement in the impact strength at 30 mm recycled jute fiber length for all formulations.
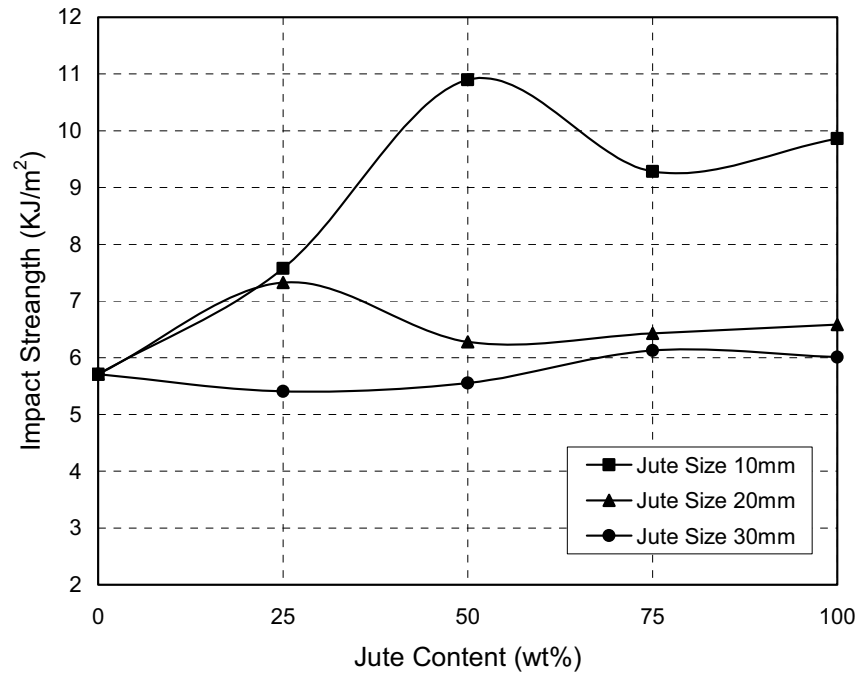
Figure 6.24 Impact strength curves of jute composites at various lengths of recycled jute fiber [constant fiber weight percent 20%]

6.4 Water Absorption Behavior and its Effect on the Mechanical Properties of Kenaf Unsaturated Polyester Composites

6.4.1 Absorption Behavior

The percentage of water absorption in the composites depended on two parameters, fiber content and environment temperatures. The results show that water absorption increased with increments of fiber content and surrounding temperature as shown in Figures 6.25 and 6.26. It can be seen that the composites absorbed water very rapidly at the initial stage, and later at 335hours and 671hours at 50°C and 25°C, respectively. A saturation level was attained without any further increase in water absorption.
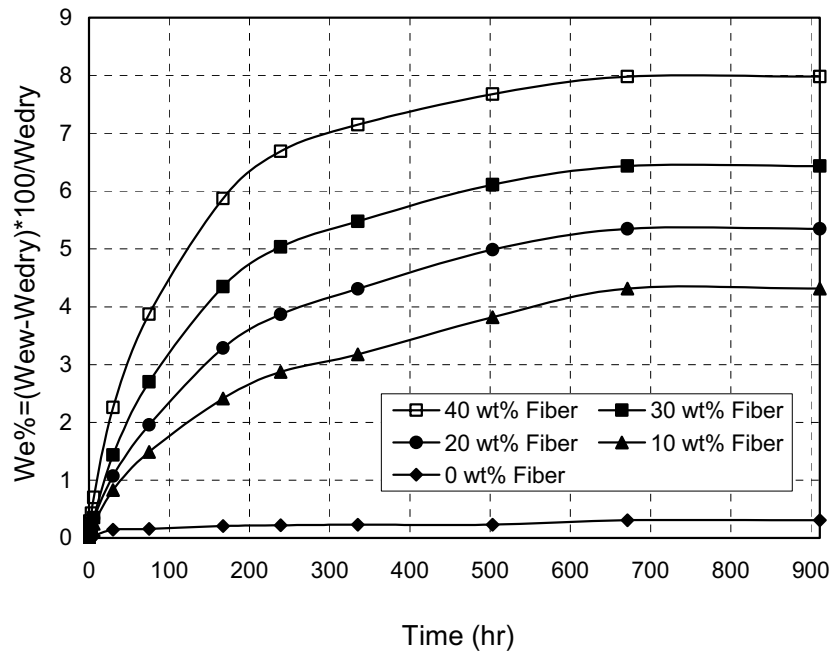
Figure 6.25 Water absorption of kenaf/unsaturated polyester composites at temperature of 25ºC
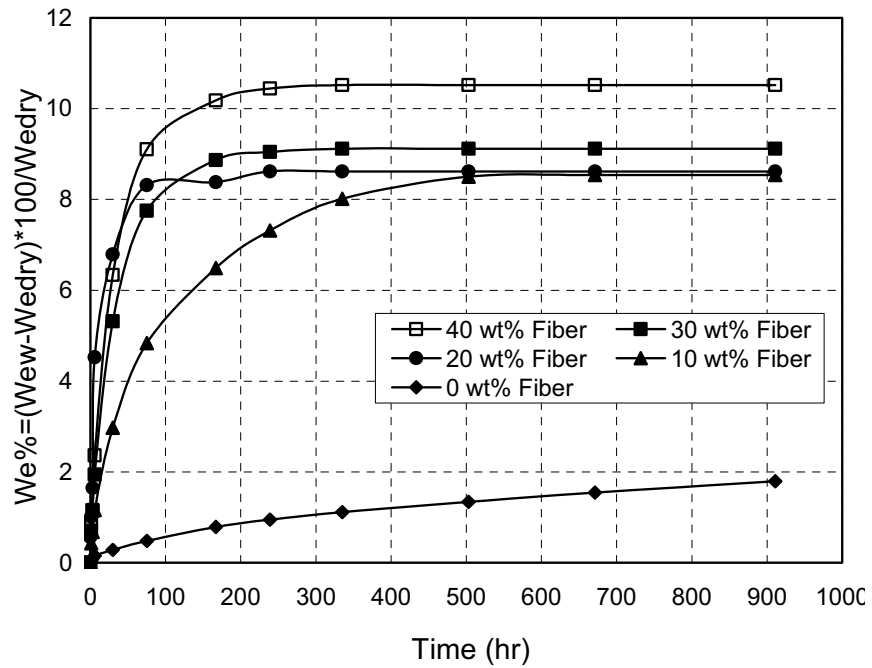
Figure 6.26 Water absorption of kenaf/unsaturated polyester composites at temperature of 50ºC

139

6.4.2 Mechanism of Water Transport

One of the most important parameter effects on the mechanical properties and dimensional stability of the composites is the poor resistances of the fibers to water absorption (Espert et al. 2004).

There are three major mechanisms of moisture absorption in natural fiber composites first, diffusion of water molecules inside the microgaps between polymer chains; second the capillary transport of water molecules into the gaps and flaws at the interface between fibers and the polymer due to the incomplete wettability; and the third mechanism is the transport of water molecules by micro cracks in the matrix, formed during the compounding process (Dhakal et al. 2007, Espert et al. 2004,Ahmad et al. 2010).

Among of these, there are three known cases of diffusion behavior (Ghasemi et al. 2009, Sheldon et al. 2005, Kushwaha et al. 2010) which are: Case 1 or Fickian diffusion, in which the rate of diffusion is much less than that of the polymer segment mobility. The equilibrium inside the polymer is rapidly reached and it is maintained with independence of time. Case 2 is relaxation control, in which penetrant mobility is much greater than other relaxation processes. This diffusion is characterized by the development of a boundary between the swollen outer part and the inner glassy core of the polymer. The boundary advances at a constant velocity and the core diminishes in size until an equilibrium penetrant concentration is reached in the whole polymer. Case 3 is when anomalous diffusion occurs where the penetrant mobility and the polymer segment relaxation are comparable. It is, an intermediate behavior between Cases 1 and 2 of diffusion. These three cases of diffusion can be distinguished theoretically by the shape of the sorption curve represented by:

$$\frac{M_t}{M_\infty} = kt^n \tag{6.24}$$

and

$$\log(\frac{M_t}{M_\infty}) = \log(k) + n\log(t) \tag{6.25}$$

where M_t, M_∞, k, and n are the water absorption at time t, the water absorption at the saturation point, and constants, respectively. The value of n is different for each case as follows: Case 1: $n = 0.5$, Case 2: $n > 0.5$, and Case 3: $0.5 < n < 1$. The coefficients (n and k) are calculated from the slope and intercept of log plot of M_t/M_∞ versus time which can be drawn from the experimental data. Figure 6.27 is an example of the fitting of the experimental data for 20wt% at 25°C and 50°C environmental temperatures. Table 6.1 presents the values of k and n resulting from the fitting of formulations at different temperatures.

Table 6.1 Moisture absorption constant for all formulations

Fiber wt%	25°C		50°C	
	n	*k*	*n*	*k*
0	0.4032	1.1128	0.5111	1.5073
10	0.6256	1.6823	0.4986	1.2605
20	0.6395	1.6818	0.4967	1.1053
30	0.685	1.7543	0.4783	1.0482
40	0.5838	1.486	0.4976	1.0829

The moisture uptake results in Table 6.1 show the values of slope for both various temperatures are close to $n = 0.5$. Therefore, it can be concluded that the water and moisture absorption of all formulations approach the Fickian diffusion behavior. The diffusion coefficient D is the most important parameter of Fick's model, which shows the ability of the water molecules to penetrate inside the composite. The diffusion coefficient can be calculated using the following equation (Thwe et al. 2002 and Sreenivasan et al. 2010).

$$D = \pi \left(\frac{mh}{4M_\infty} \right)^2 \tag{6.26}$$

where m is the initial slope of a plot of M_t versus $t^{0.5}$, and h is the thickness of the composite specimens. Figure 6.28 shows the calculated values of D at different weight fractions of fiber and environmental temperatures. Figures 6.29 and 6.30 show the diffusion curve fitting of composite for diffusion coefficients. The results show the water diffusion coefficients increased with the increment of fiber content for fixed

environment conditions, and increased with temperature increase. This was due to increment in water uptake for higher temperatures.
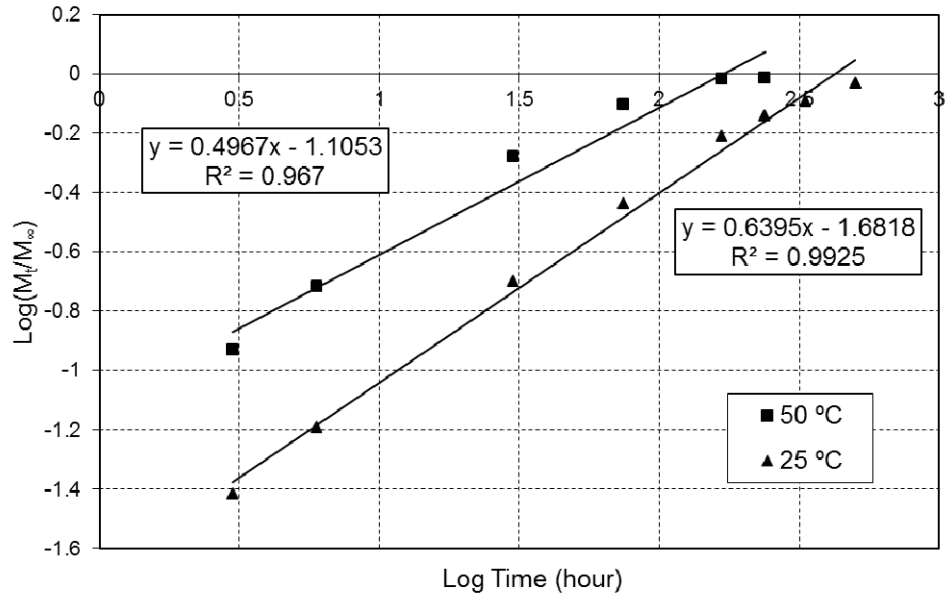
Figure 6.27 Diffusion curve fitting plots for 20wt% fiber composites for various temperatures to determine constants *n* and *k*
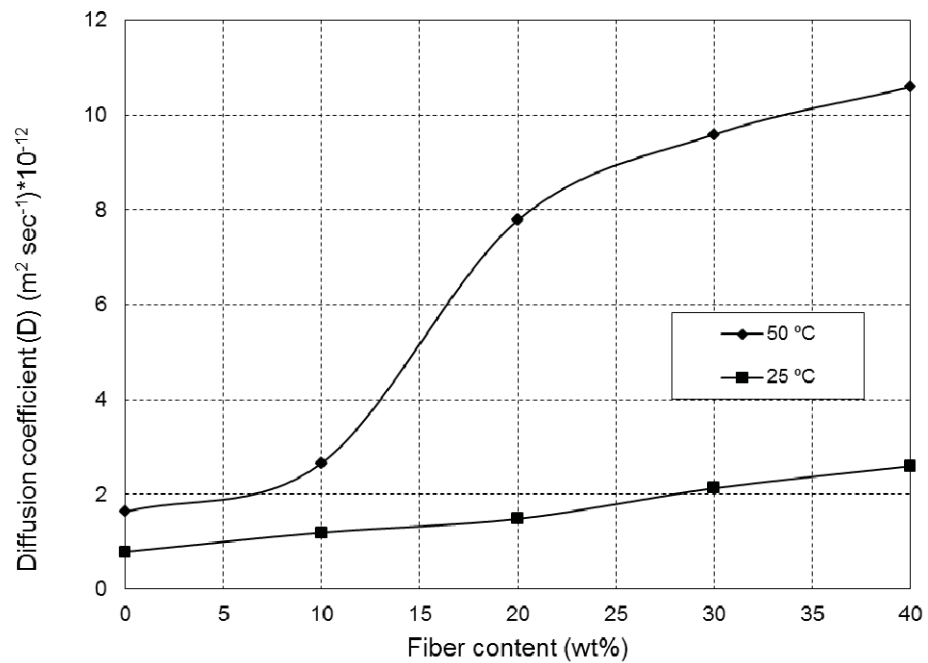
Figure 6.28 Diffusion coefficients for composites at various temperatures
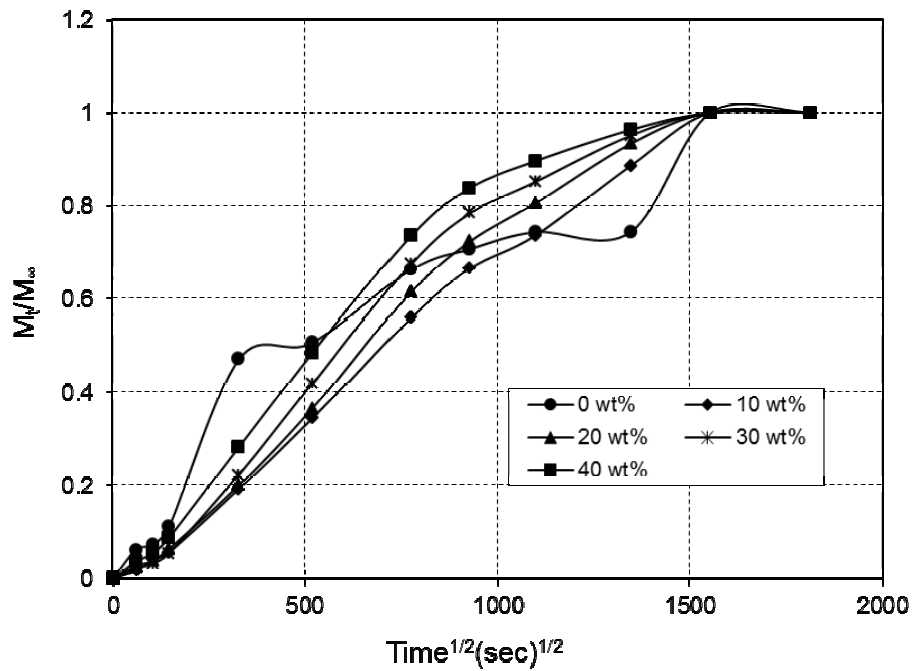
Figure 6.29 Diffusion curve fitting plots for composite diffusion coefficient at 25°C
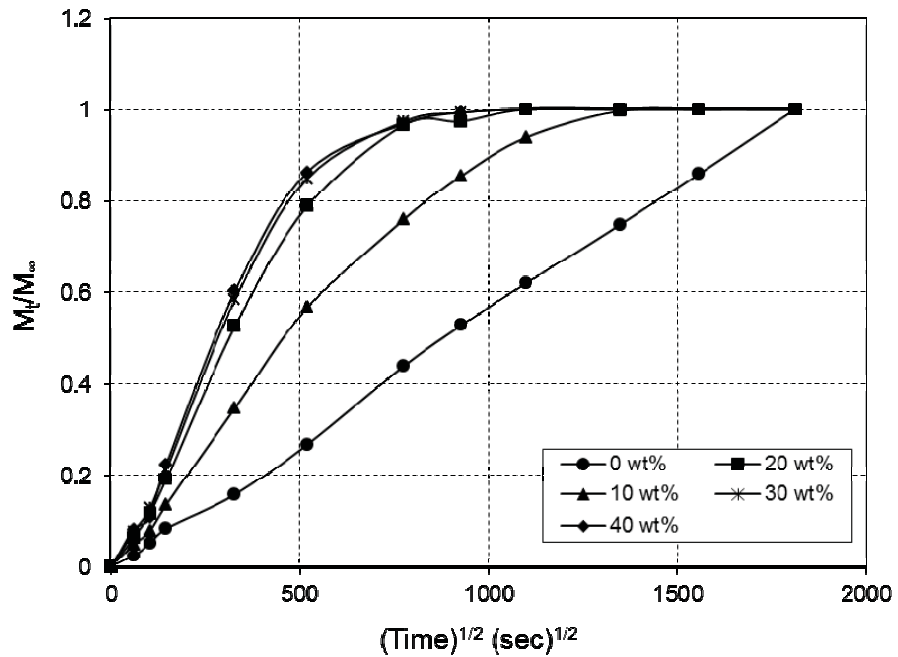
Figure 6.30 Diffusion curve fitting plots for composite diffusion coefficient at 50 °C

6.4.3 Effects of Recycled Jute Fiber

Figure 6.31 is an example of correlating experimental data for 20wt% hybrid composites at jute size 10mm at 25°C environmental temperature. Table 6.2 presents the values of k and n resulting from the fitting of all formulations, the values of slope for

both various recycled jute lengths were close to $n= 0.5$. Therefore, it can be concluded that water and moisture absorption of all formulations approach Fickian diffusion behavior. Results of the nonlinear curve fitting are presented in Table 6.2. Good relationships were found, as indicated by R^2 values.
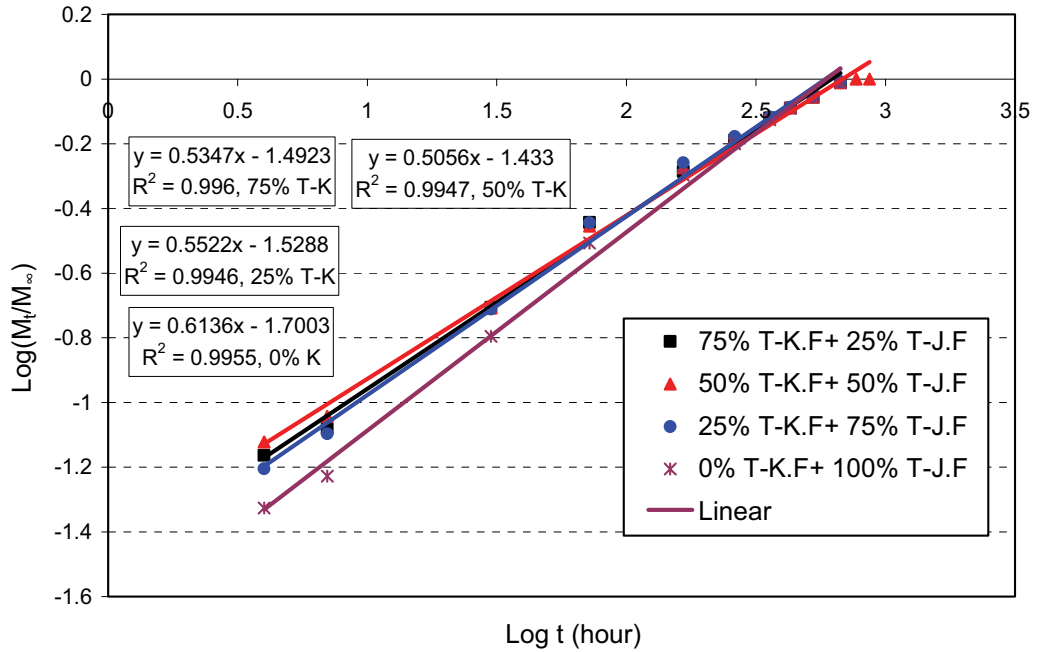
Figure 6.31 Diffusion curve fitting plots for 20wt% fiber composites for various temperatures to determine constants *n* and *k* for jute size 10mm

Table 6.3 shows calculated values of *D* at different percentages of treated recycled jute fiber and maximum water absorption.

Table 6.2 Moisture absorption constant

Composite code	Water absorption		
	Slope (n)	Intercept (k)	R^2
20WK	0.6395	1.6818	0.9925
20W(75K-25J10mm)	0.5347	1.4923	0.996
20W(50K-50J10mm)	0.5056	1.433	0.9947
20W(25K-75J10mm)	0.5522	1.5288	0.9946
20WJ10mm	0.6136	1.7003	0.9955
20W(75K-25J20mm)	0.5483	1.5128	0.9942
20W(50K-50J20mm)	0.5971	1.6443	0.9943
20W(25K-75J20mm)	0.596	1.6309	0.9922
20WJ20mm	0.6369	1.7496	0.9928
20W(75K-25J30mm)	0.5478	1.5026	0.9918
20W(50K-50J30mm)	0.5673	1.5594	0.994
20W(25K-75J30mm)	0.5906	1.619	0.9933
20WJ30mm	0.6399	1.7692	0.9963

Table 6.3 Maximum water absorption and water diffusion coefficients for all formulations

Composite code	Maximum water absorption (%)	Water diffusion coefficient (D) ($\times 10^{-12}$ m^{2}s^{-1})
20WK	5.346	1.485
20W(75K-25J10mm)	4.656	0.890
20W(50K-50J10mm)	4.528	0.919
20W(25K-75J10mm)	4.530	0.948
20WJ10mm	4.140	1.095
20W(75K-25J20mm)	5.168	1.616
20W(50K-50J20mm)	4.528	0.928
20W(25K-75J20mm)	4.670	0.855
20WJ20mm	4.098	1.1216
20W(75K-25J30mm)	4.917	0.789
20W(50K-50J30mm)	4.963	1.728
20W(25K-75J30mm)	4.647	0.874
20WJ30mm	3.900	1.199

Figure 6.32 shows the diffusion curve fitting for composite for diffusion coefficients. Results show that the water diffusion for various recycled jute fiber lengths was almost the same; this is evident that diffusion coefficients increase with increase fiber content for fixed environment conditions; length parameter does not affect diffusion coefficients and water absorption.
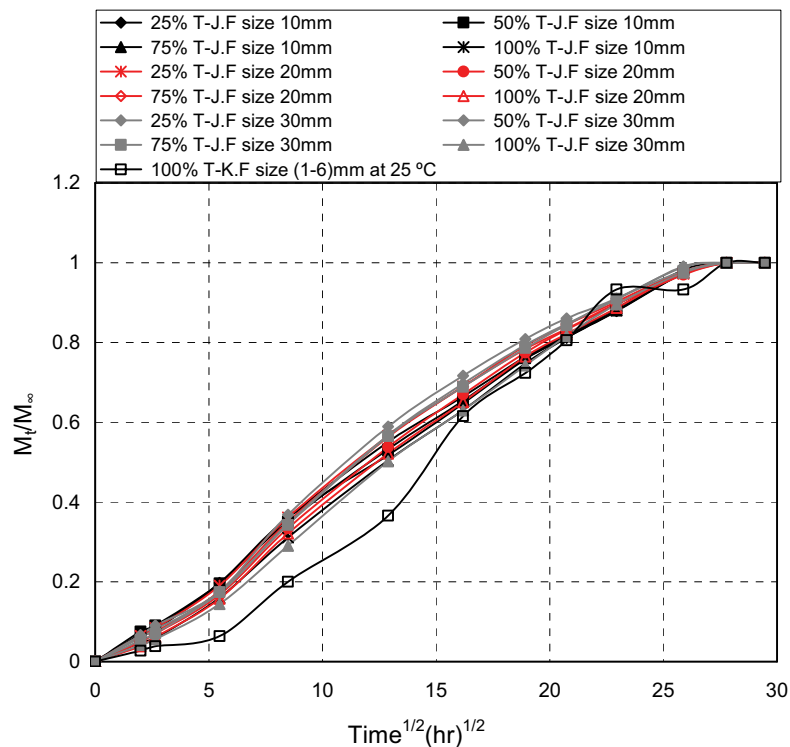
Figure 6.32 Water uptake ratios *(Mt/M∞)* of versus *(t$^{0.5}$)* for all formulations

- **Modeling Thickness Swelling Behaviour**

Five composite formulations were produced as indicated in Table 6.4. A compression moulding process was used for the fabrication process. A composite code such as 20W(75K-25J10mm) means the percentage of fiber was 20wt%; this percentage included 75% of kenaf fiber and 25% recycled jute fiber of length 10mm, and so on. Certain composites specimens were then post cured in an oven for 5 hours at 60ºC.

Shi et al. (2006) developed a model to quantify swelling rate behaviour in composite materials; in this model, a swelling rate parameter K_{SR} was determined through a nonlinear regression curve fitted to the experimental data. The swelling model can be expressed as follows:

$$TS(t) = \left[\frac{T_\infty}{T_o + (T_\infty - T_o)e^{-K_{SR}t}} - 1 \right] *100 \tag{6.28}$$

where T_∞ and T_o are the equilibrium and initial specimen thickness respectively. K_{SR} is a constant called the intrinsic relative swelling rate and $TS(t)$ is thickness swelling at time t. Sum of squares as determined using Equation 6.29 was used to compare how well the model fitted the experimental data.

$$SS = \sum_{i=1}^{n} \left(y_i - \hat{y} \right)^2 \tag{6.29}$$

where SS is the sum squares, y_i is the observed value, $\hat{y}$ is the predicted value and n is the number of observations. The lower SS means a better fit between the model and the experimental data. The results of the swelling rate parameter K_{SR} of composites are summarized in Table 6.4. The minimum K_{SR} was calculated for composites made of kenaf/recycled jute of various lengths. It is important to note that in the swelling model, K_{SR} was obtained considering the whole thickness process until it was equilibrated. The value of K_{SR} was dependent not only on the initial rate of swelling but also on the equilibrium thickness swelling of composites (Espert et al. 2004). There was less time required to reach the equilibrium thickness for kenaf composites. This can explain the very high K_{SR} value determined in this type of composites.

Table 6.4 Parameters of thickness swelling of 20wt% of kenaf and kenaf/recycled jute composites

Composite code	T_o	T_∞	TS(t) %	K_{SR} x 10^{-3} (h^{-1})	SS x 10^{-3}
20WK at 25 ^{o}C	3.7816	3.9833	5.3327	6.839	5.95
20W(75K-25J10mm)	3.9833	4.0633	2.007	7.104	0.506
20W(50K-50J10mm)	3.9266	4.0433	2.971	5.133	2.2
20W(25K-75J10mm)	3.92	4.025	2.678	5.044	0.34
20WJ10mm	3.95	4.053	2.616	4.033	1.35
20W(75K-25J20mm)	3.918	4.020	2.594	7.968	0.73
20W(50K-50J20mm)	3.986	4.080	2.341	5.883	0.502
20W(25K-75J20mm)	3.706	3.861	4.181	5.966	0.65
20WJ20mm	3.94	4.086	3.722	7.851	3.48
20W(75K-25J30mm)	3.628	3.776	4.088	6.605	0.71
20W(50K-50J30mm)	3.656	3.781	3.418	6.219	0.53
20W(25K-75J30mm)	3.561	3.700	3.883	5.587	0.348
20WJ30mm	3.815	3.971	4.106	5.056	1.18

- **Orthotropic Swelling**

Figure 6.33 exhibits the orthotropic swelling curves of the treated kenaf composites. It can be seen that the highest swelling took place in the thickness of the sample, followed by the width and length. It can be noted that the model had a good agreement fit between the experimental data and prediction data from Equation 6.28. Long-term water absorption isotherms of all case formulations are presented. The thickness swelling curve for kenaf composites and kenaf/recycled jute composites are illustrated in Figure 6.34, where the percentage of thickness swelling is plotted against time for all samples. As it is clearly seen, thickness swelling for kenaf composites increases with immersion time, reaching a certain value beyond which such swelling is not observed. The results clarified that the thickness swelling decreases by adding treated recycled jute of various lengths. Different thickness swelling among all manufactured composites can be attributed to changes in physical and chemical properties of recycled jute, like hemicellulose which is the most important parameter in moisture absorption as it reduces with heat and chemical treated (Najafi et al. 2011). Results show that the lowest thickness swelling composite at recycled jute of 10mm length which means that thickness swelling depends on fiber length for the same weight fraction of fiber composites.
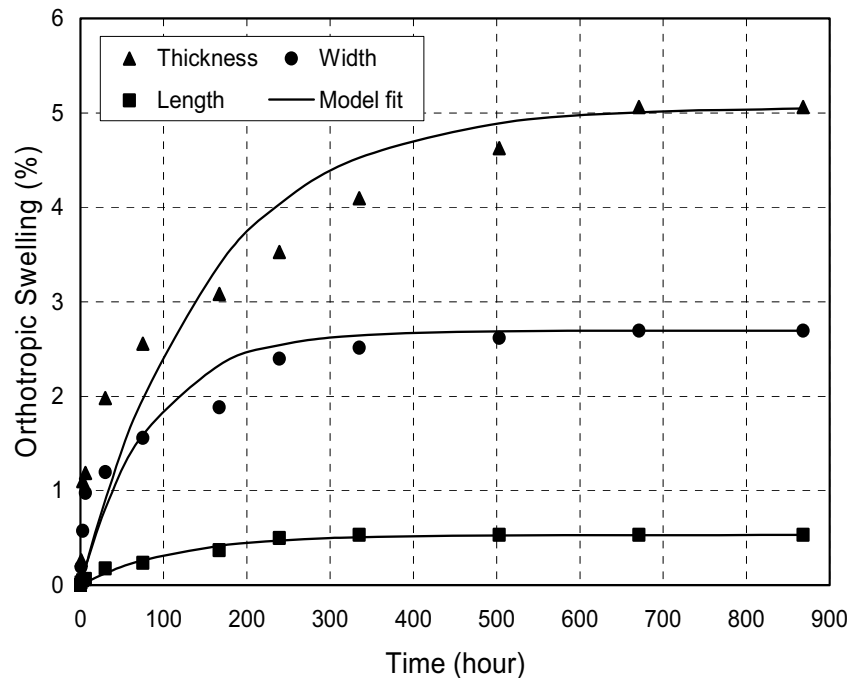
Figure 6.33 Orthotropic swelling behaviors of 20wt% kenaf/unsaturated polyester composites
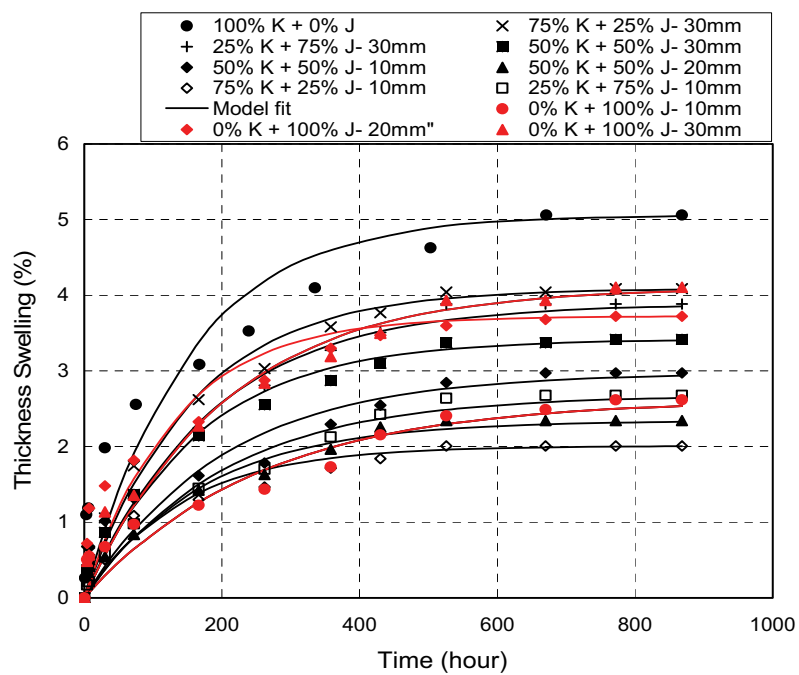
Figure 6.34 Thickness swelling model fit for kenaf and hybrid fiber /unsaturated polyester composites at 20wt%

6.4.4 Morphology

- **Treated Kenaf Composites**

Figure 6.35 shows the SEM micrograph of the bending fractured surface of kenaf fiber composite for 20wt% fiber weight fraction at various temperatures. In this case, fiber fracture and pull out were noticed and the sudden failure of the bending specimen caused the fiber to split, resulting in fine fibrils being exposed. It could be observed that in all the cases the fibers were still embedded in the resin together with some cavities left by pulled-out fibers. Fiber debonding was observed in Figure 6.35b. In addition, it could be seen there was a fiber misalignment and entanglement. Fiber alignment factors play a crucial role in the overall properties of composites. The random orientation of fibers produces lower mechanical properties compared to long undirectionally orientated fibers. This fiber entanglement can create resin rich areas, which can contribute to the formation of voids and porosity (Dhakal et al. 2007). At high environmental temperatures, a debonding developed between the fiber and matrix, a majority of fibers failed to pull out as shown in Figure 6.35b. It is interesting to note that there was a resin particle on the surface of fiber at 25$^{\text{o}}$C as shown in Figure 6.36a. The reason is due to microcracks developed at the interface between the fiber and the matrix. As the cracks developed, material was lost, most likely in the form of resin particles.

a

b

Figure 6.35 The SEM micrograph of bending fractured surface of the composites:
a) 25ºC at 37 days, b) 50ºC at 37 days

150
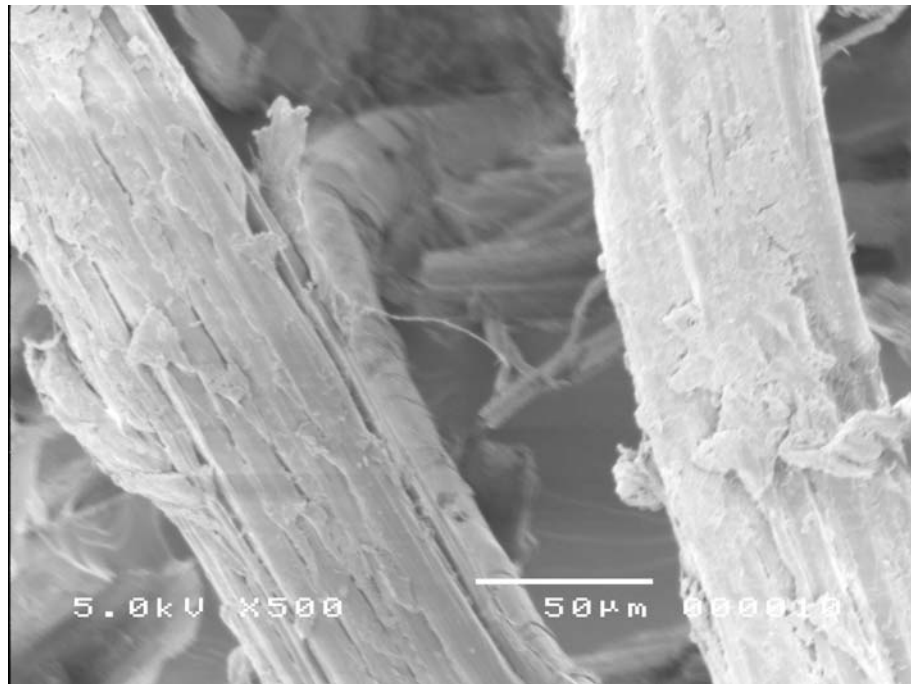
a
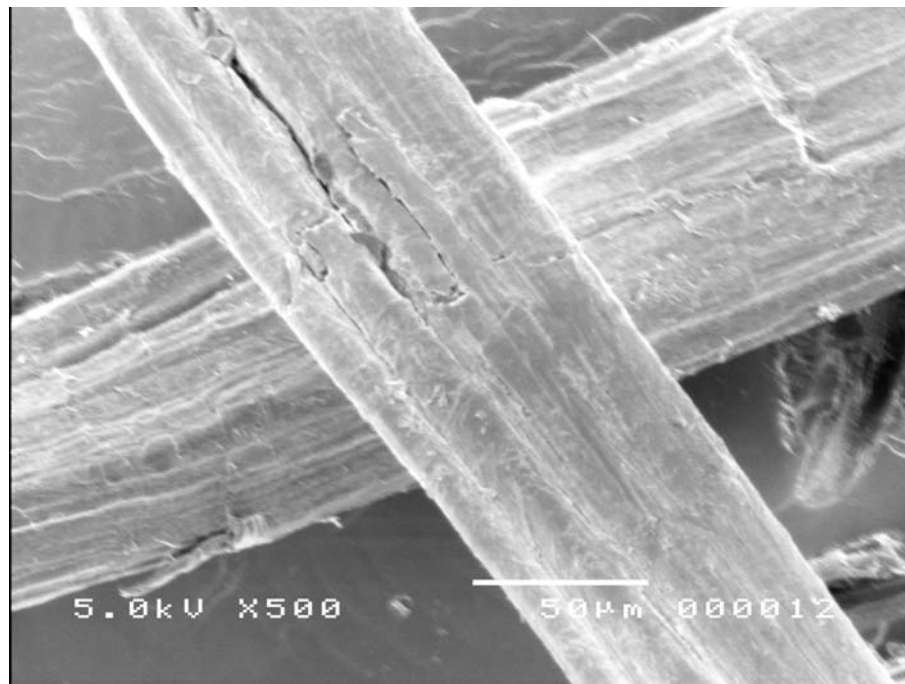
b

Figure 6.36 The SEM micrograph of fiber surface: a) 25 ^{o}C at 37 days, b) 50°C at 37 days

- **Hybrid composites**

The SEM micrograph showed the bending fractured surface of hybrid composite containing 20wt% fiber, 25wt% kenaf plus 75wt% jute fibers. In this case, fiber fracture

and pulled out are noticed and the sudden failure of the bending specimen is caused the fiber to split, resulting in fine fibrils being exposed. It could be observed that in all cases the fibers were still embedded in the resin together with some cavities left by pulled-out fibers. Fiber cracking was observed in Figure 6.37b. Morphological results evidently demonstrate that when the polymer resin matrix is reinforced at different fiber dimensions, morphological changes take place depending upon the interfacial interaction between the varying dimensions of fiber and the resin matrix. In addition, Figure 6.37 observes the poor interaction between different the fiber lengths and matrix. It is also evident from the figure that the kenaf and recycled jute fibers were easily pulled out from the matrix during flexural failure. The image analysis also shows the formation of voids due to the fiber pull-out. Further, due to the absence of the fiber-matrix interaction, the fibers tend to agglomerate into bundles and become unevenly distributed throughout the matrix
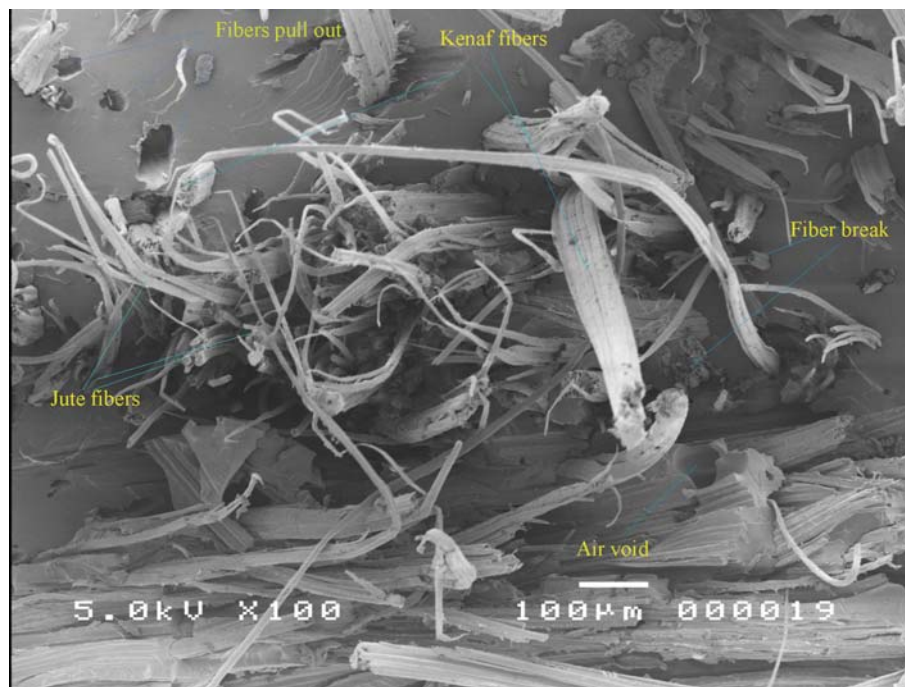
a
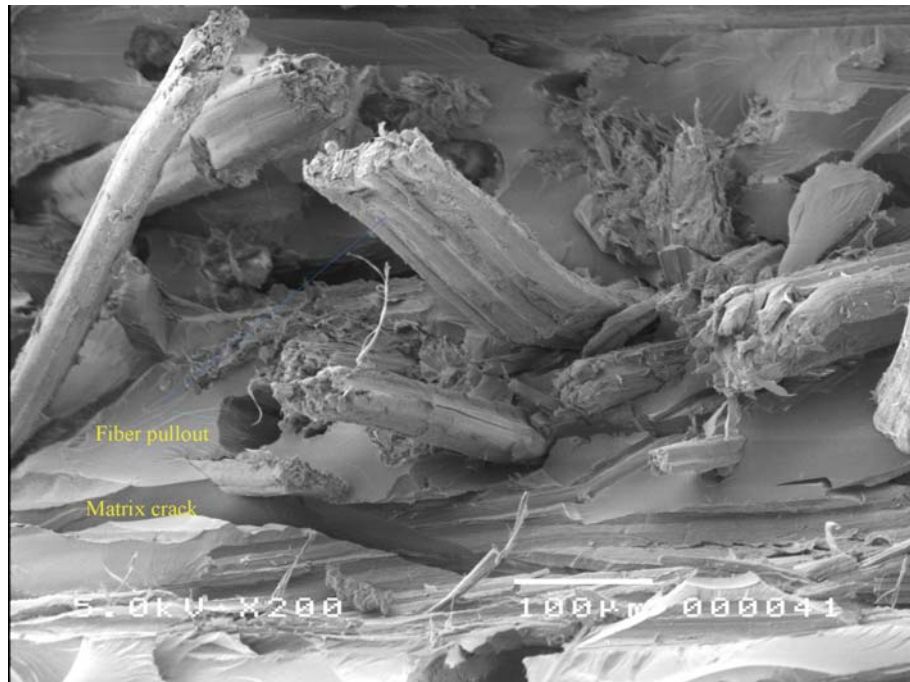
b
Figure 6.37 The SEM Micrograph of bending fractured surface of dry composites containing 20wt% fiber, 25wt% kenaf plus 75wt% jute fibers

6.4.5 Effects of Moisture Absorption on the Flexural Properties

- **Kenaf Fiber Composites**

Flexural strength and modulus of versus fiber weight fraction results are shown in Figures 6.38 and 6.39 under different conditions respectively. Both flexural strength and modulus for dry fiber were found to increase significantly as the fiber weight fraction increased until 20wt%. The maximum flexural strength and modulus dry composites were 69.6MPa and 4.28GPa respectively. After this increment, the flexural strength and modulus dropped dramatically as the fiber weight fraction increased. The flexural properties of the composites decreased drastically on exposure to water immersion, with increase in fiber content and environmental temperatures. The flexural strength at 20wt% was 25.17MPa and 16.44MPa at 25°C and 50°C respectively as Figure 6.38 clarifies. The same trend appeared for the flexural modulus, with 1.67GPa and 1.18GPa at 25°C and 50°C respectively. The reason for the decreases in flexural properties after water immersion is the formation of hydrogen bonding between the water molecules and cellulose fiber. In the presence of a high-OH group percentage, natural fibers tended to show low moisture resistance (Arib et al. 2006 and Acha et al. 2005). This led to

dimensional and color variations of composites products and poor interfacial bonding between the fiber and matrix, causing a decrease in the flexural properties.
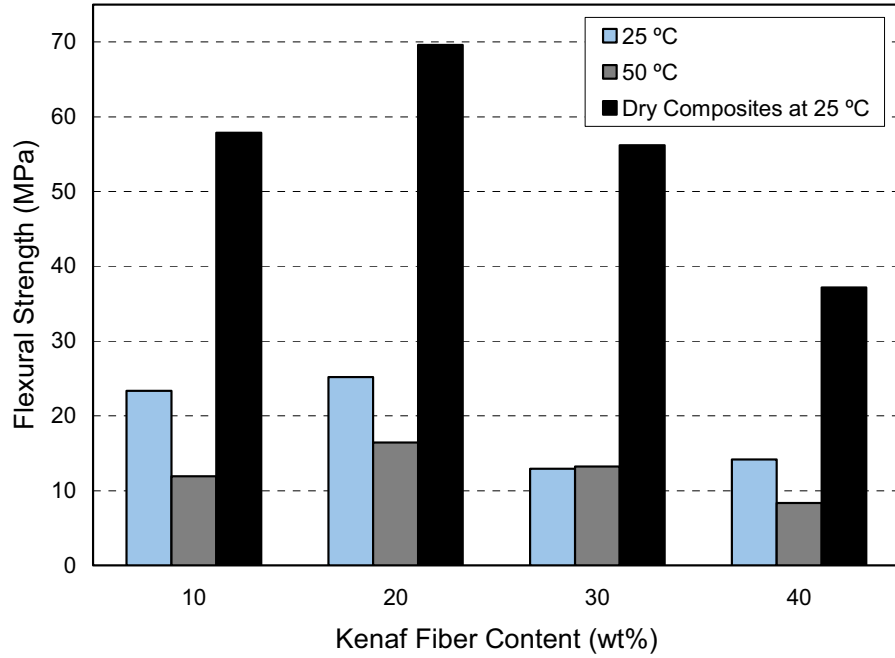
Figure 6.38 Effects of moisture uptake on the flexural strength
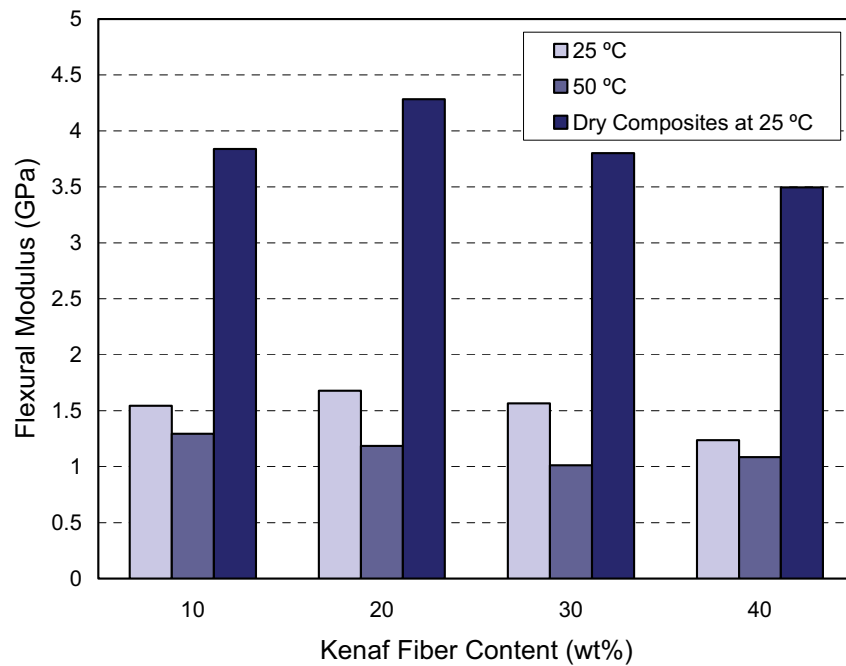
Figure 6.39 Effects of moisture uptake on the flexural modulus

154

- **Kenaf/recycled Jute Composites**

The results of flexural strength and modulus at diverse weight fraction of recycled jute fiber are shown in Figures 6.40 and 6.41 at different conditions. Alternatively, incorporated recycled jute fiber in composites decreases water uptake and enhances dimensions stability, the reason for that was the percentage of holocellulose for the jute is about 87.6 (Jahan et al, 2007), which is greater than holocellulose of kenaf bast fiber which is about 62% and this is leads to improvement in flexural properties of hybrid composites. Same trend appeared for flexural modulus, with 1.67GPa. Figure 6.40 clarified that 75wt% of the recycled jute length 30mm provided better improvement in the flexural strength, the maximum improvement was about 47.45% compared to modulus of kenaf unsaturated composites. While, the maximum improvement for flexural modulus was about 25.94% as an observed in Figure 6.41 after adding 25wt% of recycled jute size 10mm.
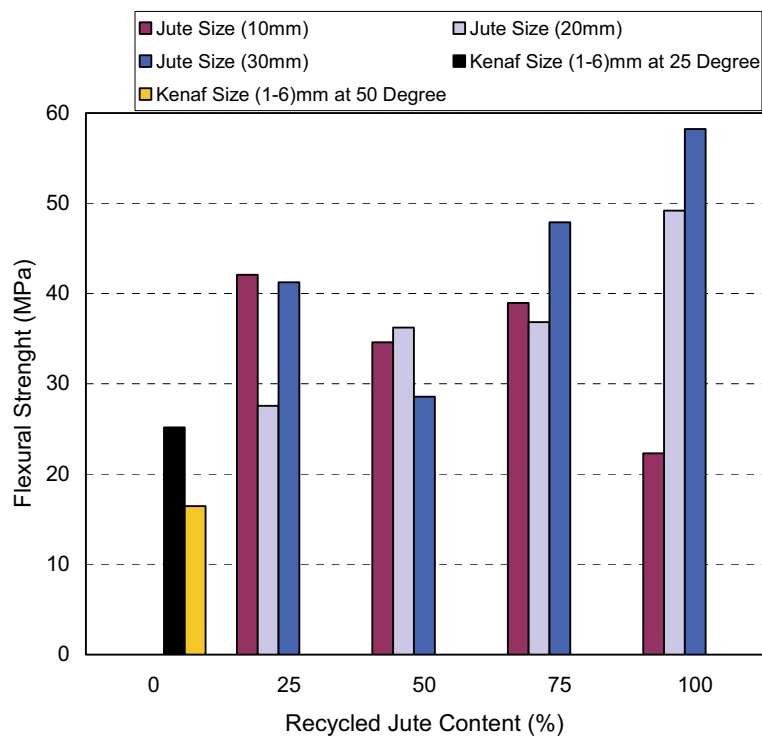
Figure 6.40 Comparison of flexural strength kenaf composites and hybrid composites
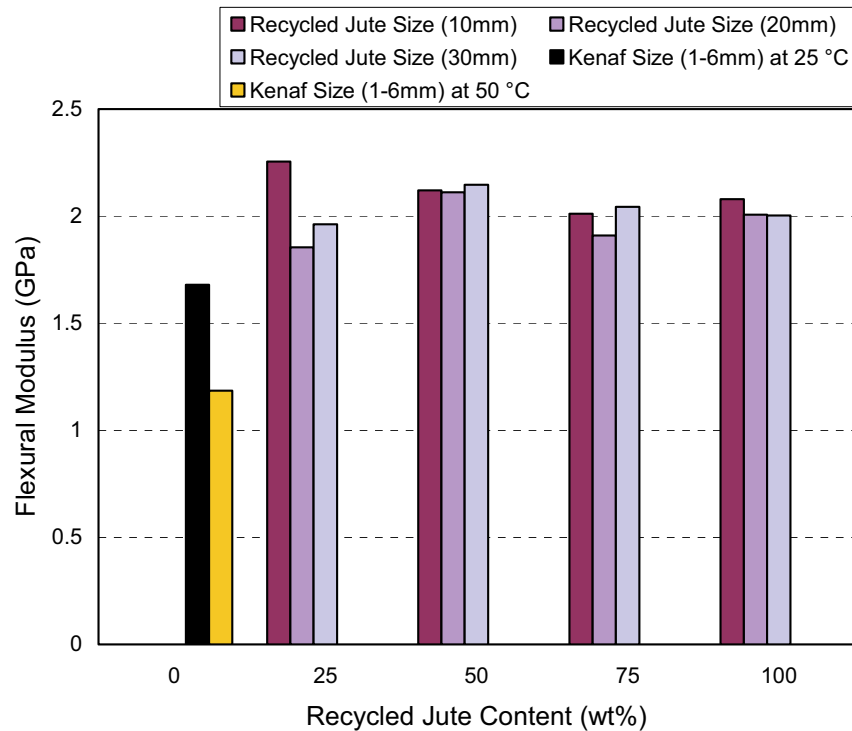
Figure 6.41 Comparison of flexural modulus of kenaf composites and hybrid composites

6.4.6 Effects of Moisture Content on Tensile Properties of Composites

- **Effect of Fiber Loading**

The effects of moisture absorption on tensile properties of KFUPC such as, modulus of elasticity (*ME*) and tensile strength (*TS*) are shown in Figures 6.42 and 6.43 respectively. Obviously it can clarified that the *ME* and *TS* of KFUPC dramatically dropped compared to dry samples. The highest water absorption was in the specimen containing 40wt% of kenaf fiber. Water absorption of composites is relatively high due to the hygroscopic nature of fiber. As fiber content is increased, water absorption was expected to be increased (France et al. 983 and LeVan et al. 1990). The moisture uptake, due to the immersion process, changes the structure and properties of fibers, matrix and the interface between them (Rashdi et al. 2010). The *ME* increased as fiber loading was increased for all KFUPC dry samples as Figure 6.42 demonstrates, while *ME* dropped compared to dry sample due to moisture uptake as represented in Figure 6.43. High fiber content in the specimen leads to more water penetration into the interface through the micro cracks induced by swelling of fibers creating swelling stresses which leads to composites failure (Rashdi et al. 2010). Tensile properties of

KFUPC specimens were found to decrease with increase in percentage moisture uptake mainly due to degradation of composites (Rashdi et al. 2009).
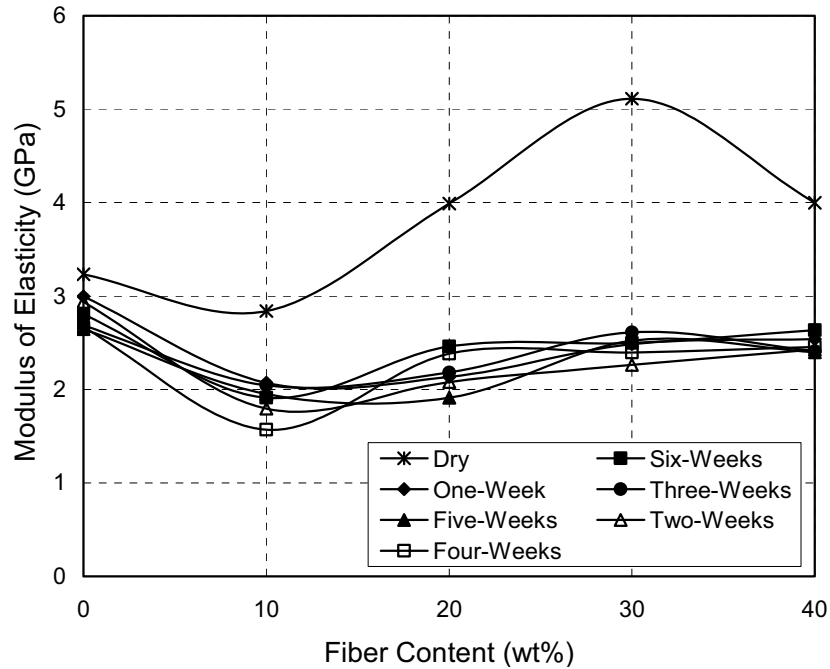
Figure 6.42 Modulus of Elasticity at versus immersion time
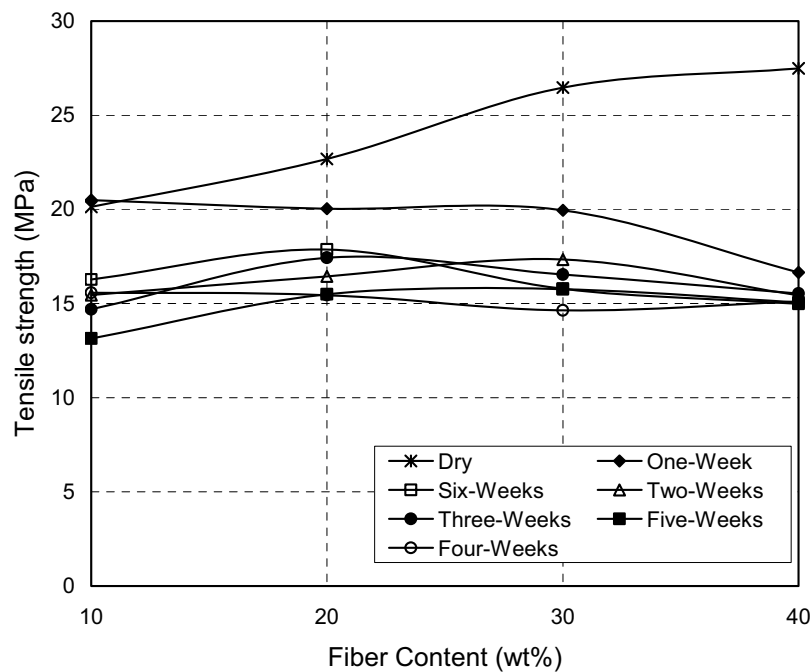
Figure 6.43 Tensile strength at versus immersion time

- **Effect of Immersion Time**

There was insignificant effect of water absorption on *TS* for *UP* samples. *TS* increased after water immersion in the first three weeks, in week four *TS* decreased, then for weeks five and six *TS* increased again. This increase in *TS* for the *UP* sample implies that further crosslinking or other mechanisms are taking place enhancing the material strength (Dhakal et al. 2007). It can be clearly seen that *TS* decreased for all weight fractions as the duration of immersion increased; all weight fractions followed the same trend. It is worth noticing that after exposure to water for over one week 168hours the *TS* started to increase slightly; this is due to the plasticizing effect (Beg 2007). *TS* decreased as fiber weight percentage increased because a high content of fiber absorbed more water. During the first week of immersion in water, mechanical properties for composites dropped dramatically as Figures 6.42 and 6.43 show. The reduction in the *ME* and *TS* is attributed to the changes occurring in the kenaf fiber, and the interface between matrix and fiber, as there in no reduction effect on the *UP* after aging. Swelling of natural fiber as a result of prolonged immersion to water led to the reduction in *ME* of fibers and also resulted in the development of shear stress at the interface that caused debonding of fibers from matrix (Rashdi et al. 2010). The percentage valuesreduction in *TS* and *ME* of *UP* and KFUPC are given in Table 6.5.

Table 6.5 Percentage retention in tensile properties at week six

Kenaf wt%	Tensile Strength (MPa)			Young's Modulus (GPa)		
	Dry Sample	Wet Sample	Reduction Value (%)	Dry Sample	Wet Sample	Reduction Value (%)
0	39.021	39.254	1.413	3.231	2.807	13.101
10	20.132	16.278	19.141	2.838	1.911	32.663
20	22.681	17.867	21.221	3.991	2.461	38.323
30	24.025	15.782	34.31	5.112	2.498	51.129
40	25.7595	14.991	41.803	3.998	2.634	51.81

Zero-stress aging is defined as the reduction of *TS* and *ME* when no stress is applied during the time of exposure to a given environment (Barbero et al. 2002 and Kalaprasad et al.1997).

$$E(t) = E_o \left(1 + \alpha\, t_a\right)^{-\beta} \qquad\qquad (6.30)$$

$$\sigma(t) = \sigma_o \left(1 + \alpha\, t_a\right)^{-\beta} \qquad\qquad (6.31)$$

where E_o and σ_o are modulus and strength respectively, at time zero, at the environment of exposure, α and β are the empirical constants adjusted to fit the experimental data. Figures 6.44 and 6.45 give a comparison of the variation in experimental and theoretical of tensile properties values of immersion time for 42days. The results show that in all cases the experimental value has a good fit with the theoretical value. Table 6.6 displays the values of empirical constant for a good fit.

Table 6.6 Zero-stress aging parameters after 42days immersion in water

		Kenaf 0 wt%	Kenaf 10 wt%	Kenaf 20 wt%	Kenaf 30 wt%	Kenaf 40 wt%
Modulus (GPa)	α (1/sec)	0.1536	598.93	1E+20	1E+20	1E+20
	β	0.099116	0.0408	0.0127	0.015133	0.009755
Strength (MPa)	α(1/sec)	0.004	0.0926	0.7091	0.2159	408.739
	β	0.2329	0.21706	0.1022	0.2219	0.0564
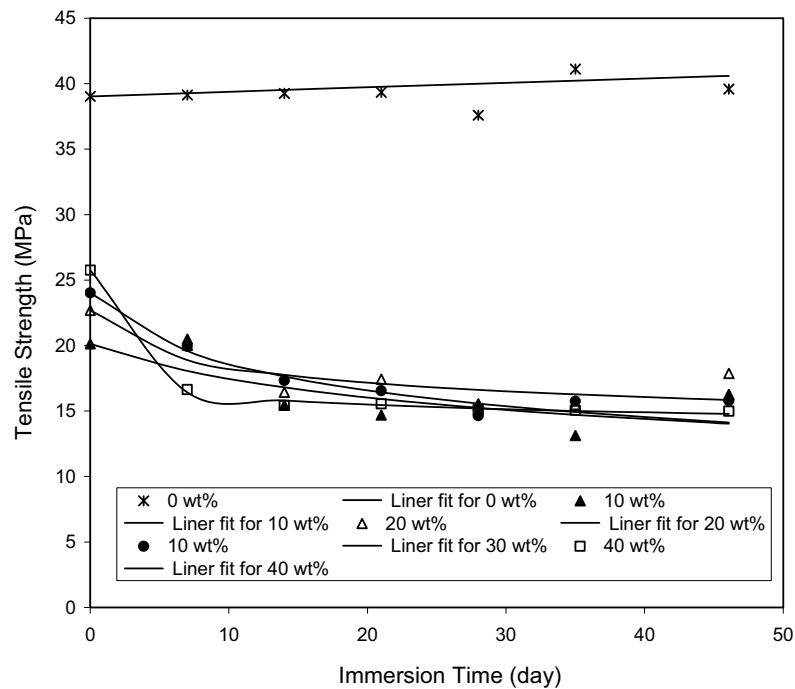
Figure 6.44 Variation of experimental and theoretical tensile strengths
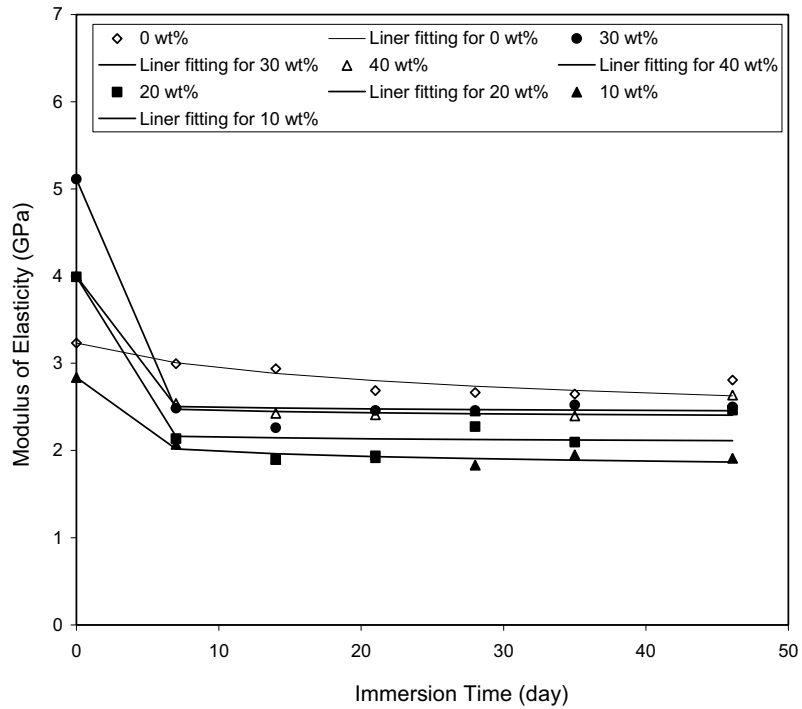
Figure 6.45 Variation of experimental and theoretical Young's modulus

6.5 Thermal and Dynamic Mechanical Properties of Kenaf Composites

6.5.1 Dynamic Mechanical Properties

The dynamic mechanical results expressed as storage modulus E', loss modulus E'' and loss tangent *tanδ* as a function of temperature and resin compositions are revealed in Figures 6.46 and 6.47a, b and c, respectively. The E' of (60%UP+40%ST) resin was about 2.313GPa which was higher than the E' of (50%UP+50%ST) resin which was about 2.279GPa as listed in Table 6.7. These results indicate that increase in styrene concentration affected the stiffness of materials. From the DMA curves, E' values fell steeply around the glass transition temperature T_g of the resins. Storage modulus values of unsaturated polyester based composites were higher than that of the unfilled *UP* resin, which indicates that stress transferred from the resin to the fiber (Hedenberget et al.1995). The E′ of both resin based composites decreased with increase fiber loading for certain values of fiber, then increased with increase fiber loading. The maximum value was at 30wt% of fiber content; after this value, the E′ decreased. This trend was observed that the composite with 30wt%fiber content was a stiffer material than the UP resin (Huda et al. 2007) as represented in Figures 6.46a, 6.47a and Table 6.7. At higher

temperatures water molecules adhering onto the fiber evaporated, making the fiber stiffer (Pothan et al. 2003).

The higher E' value of 60KFUPC than the E' value of 50KFUPC was due to greater interfacial adhesion and bond strength between the resin and fiber. This is in accordance with the explanation by Sharifah et al. (2004) and Vilay et al. (2008). Incorporation of treated fibers impartsed stiffness to the (60%UP+40%ST) and (50%UP+50%ST) resins. The E' initially had insignificant change at low temperatures. As the temperature increased, there was a sharp drop in the temperature region between 60ºC and 100ºC, which suggests that a glass transition occurred at this temperature range. The drop in the E' corresponded to the onset of segmental mobility of the polymer network, where the chains of the amorphous polymer began to coordinate large-scale motions, which indicates that the amorphous regions began to melt. After the glass transition, the rubbery modulus plateau was reached, where the polymer behaved like rubber. For the UP resin, the plateau region continued until the sample began to degrade because the crosslinks prevented the chains from slipping past one another. Obviously, with increase in fiber loading, the E' at the plateau region increased; thus, the crosslinking density increased (Zhan et al. 2010 and Pracella et al. 2010).

Table 6.7 Dynamic mechanical results for kenaf unsaturated polyester composites at different styrene concentrations

Specimens	E' (GPa)	E'' (GPa)	Tan δ	T_g (ºC)
(60%UP+40%ST)	2.313	0.2541	0.8612	70
10wt% 60KFUPC	2.090	0.1879	0.5054	90
20wt% 60KFUPC	2.772	0.3043	0.4095	80
30wt% 60KFUPC	2.925	0.2822	0.3182	86.8
40wt% 60KFUPC	1.685	0.1737	0.295	89.8
(50%UP+50%ST)	2.279	0.2349	0.9193	80
10wt% 50KFUPC	2.088	0.189	0.4912	90
20wt% 50KFUPC	2.495	0.2399	0.4511	86.65
30wt% 50KFUPC	2.663	0.2911	0.36	89
40wt% 50KFUPC	2.631	0.3016	0.3569	90

E'' is a measure of the energy dissipated or lost as heat per cycle of sinusoidal deformation. It is in fact the viscous response of the material. The loss factors are most sensitive to the molecular motions (Pothan et al. 2003). Figures 6.46b and 6.47b explain the variation of E'' with the temperature of composites with different values of fiber loading. It can be seen from Figure 6.46b that the E'' peak values at 20wt% of fiber for

60KFUPC, the peak values decreased with increase fiber content. At the same time the peak values of E'' increased with increase fiber content as shown in Figure 6.47b for 50KFUPC. The maximum heat dissipation occurred at the temperature where E'' was maximum, indicating the T_g of the system (Wunderlich 1990) as shown in Table 6.7. The glass transition was assigned to the energy dissipation possibilities across the free amorphous phase (Wunderlich 1990), and the lower T_g values would observe an easier mobility of the free amorphous phase in the composites. The T_g of all the composites shifted to a higher temperature when the treated kenaf fiber was presented in the *UP*. This trend is associated with the decreased mobility of the resin chains, due to the presence of the fibers. Due to the trend, the stress field surrounding the particles induced the shift in T_g (Huda et al. 2007). For the 60KFUPC all the values of T_g is close to each other even with increasing fiber load. *Tan δ* is a damping term that can be related to the impact resistance of a material (Pothan et al. 2003). In view of the fact that the damping peak occurred in the region of the glass transition which was the material change from a rigid to a more elastic state. It is simultaneous with the movement of small groups and chains of molecules within the polymer structure. In two dissimilar composites 60KFUPC and 50KFUPC, damping was affected through the incorporation of fibers. This was mainly to shear stress concentration at the fiber ends in association with the additional viscoelastic energy dissipation in the resin material (Pothan et al. 2003, Sharifah et al. 2004, Vilay et al. 2008, Zhan et al. 2010 and Wunderlich 1990). Figures 6.46c and 6.47c express that the height of the *tanδ* peak of the *UP* resin based composites containing 40wt% for both 60KFUPC and 50KFUPC were lower than that of the 10,20,30 wt% of fiber content and much lower than that of neat *UP* resin. One possible explanation is that there was no restriction to the chain motion in the case of neat *UP* resin, while the presence of the cellulose fibers hindered the chain mobility, resulting in the reduction of sharpness and height of the *tan δ* peak (Liu et al. 1997). Figures 6.46c and 6.47c observe the improvement in interfacial bonding in composites occurs as reflected by the lowering in *tanδ* values. The higher the damping at the interfaces, the poorer the interface adhesion.

a

b

c
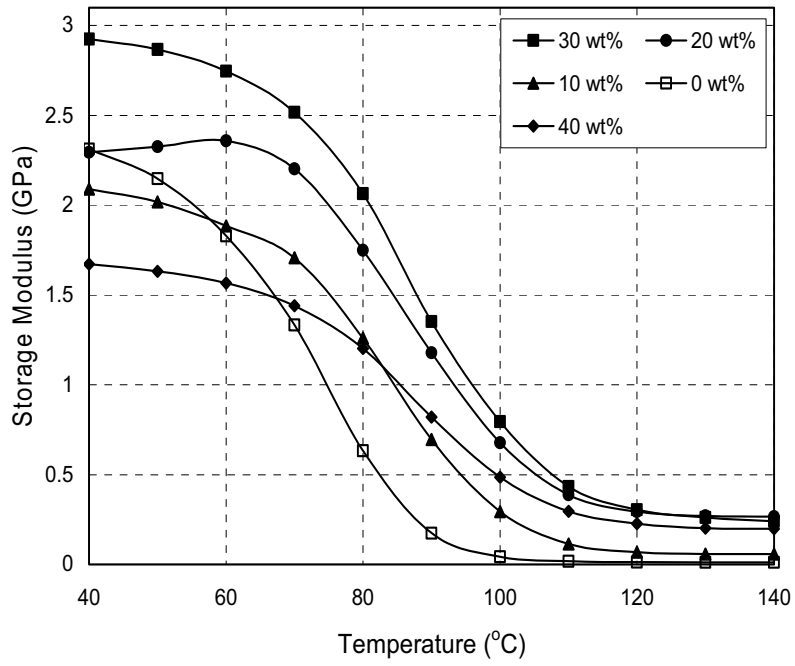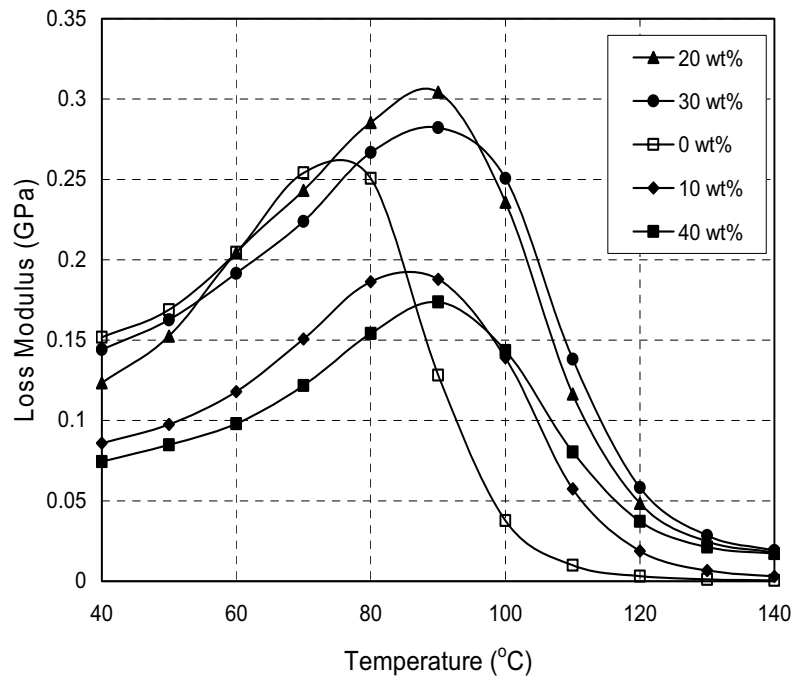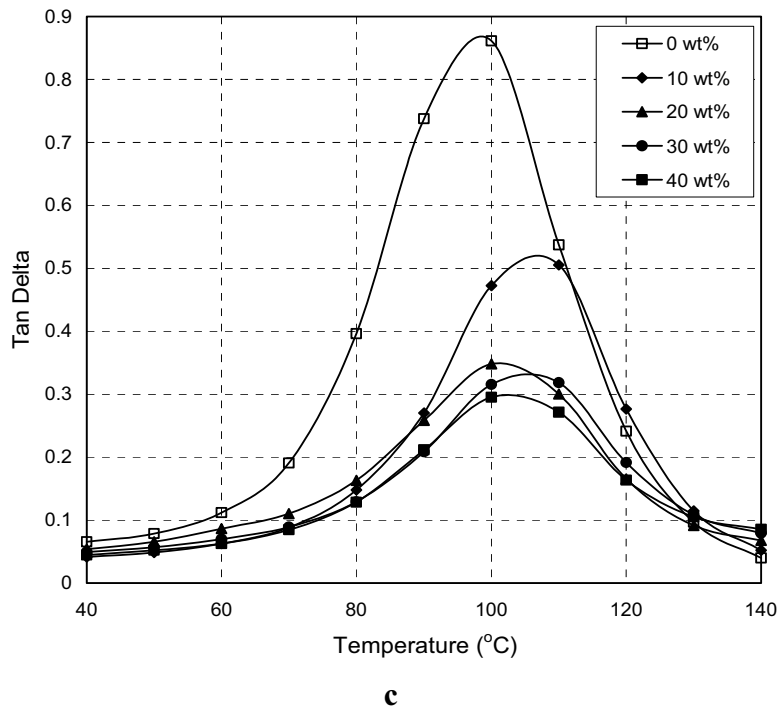
**Figure 6.46 Effects of fiber loading on dynamic data for (60%UP+40%ST) resin:
a) storage modulus vs. temperature, b) loss modulus vs. temperature
c) *tanδ* vs. temperature**

a
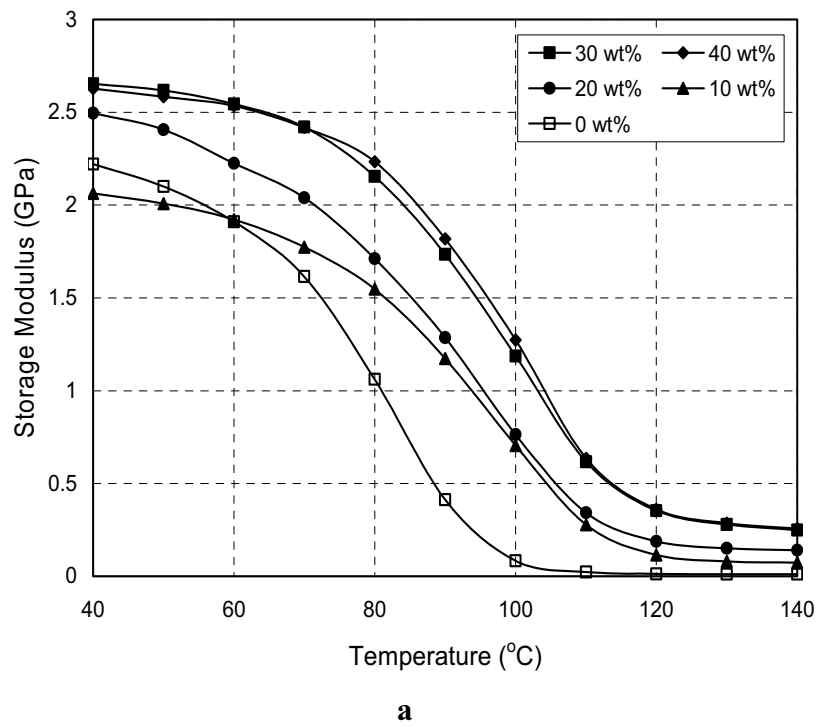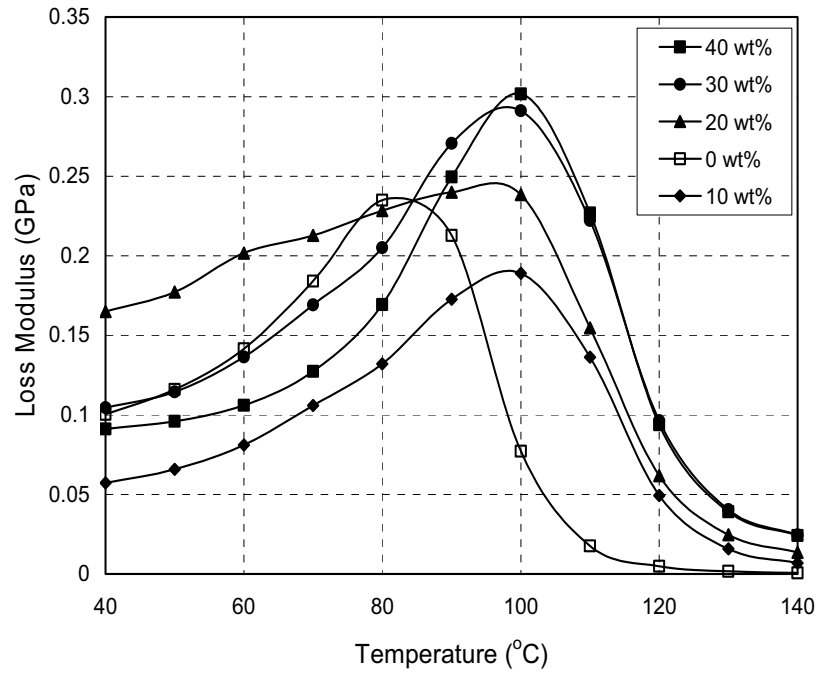
b
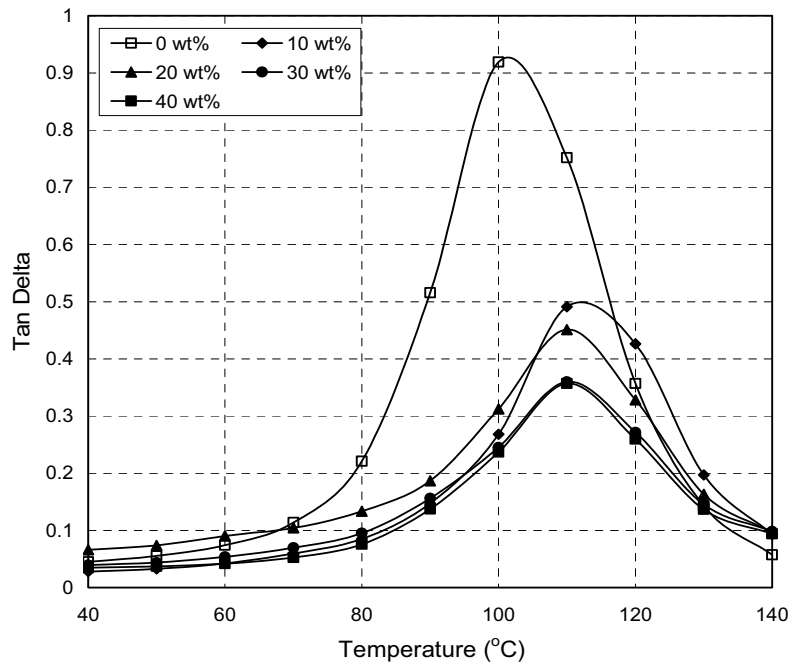
c

**Figure 6.47 Effects of fiber loading on dynamic data for (50%UP+50%ST) resin:
a) storage modulus vs. temperature, b) loss modulus vs. temperature,
c) tan delta vs. temperature**

- **Effects of Recycled Jute Fiber**

The temperature curves of the storage modulus, loss modulus, and loss factor for neat kenaf, kenaf/recycled jute unsaturated polyester composites at 20wt% fiber content are presented in Figure 6.48a, b, and c, respectively. The results show that the (50%K+50%RJ) and (25%K+75%RJ) composites have a higher storage modulus than neat kenaf fiber composites, neat recycled jute composites and other different recycled jute 30mm length. The storage modulus improved significantly with the addition of recycled jute to KFUPC. A much enhanced storage modulus of the composites was obtained for the (50%K+50%RJ) composites compared with the neat recycled jute composites which suggests that the adhesion between the matrix and recycled jute size 30mm was due to the critical fiber length of recycled jute which affected the mechanical and dynamic properties for natural fiber composites as indicated in Figure 6.48a. The loss modulus curves are accessible in Figure 6.48b. The glass transition temperatures T_g, which were derived from the loss modulus curves are included in Table 6.8. Based on the results, the values of T_g were the same which means that the recycled jute did not affected the stability of composites, the same as results reported by Sharifah et al. (2004). Figure 6.48c shows the effect of recycled jute on *tanδ* of the composites. Cellulose incorporation reduced the *tanδ* peak height by restricting the movement of the polymer molecules. Elevation of T_g was taken as a measure of the interfacial interaction (Pracella et al. 2010). The width of the *tanδ* peak also became broader than that of the neat kenaf composites. This behavior suggests that there are molecular relaxations in the composites that are not present in the pure matrix. Hence, the width of the *tanδ* peak is indicative of the increased volume of the interface (Pathan et al. 2003). The slight reduction in *tanδ* for the reacted-fiber composites means that the mobility of *UP* molecules was restricted due to the stronger interfacial interaction between kenaf/recycled fibers and *UP* matrix than that for neat kenaf composite.
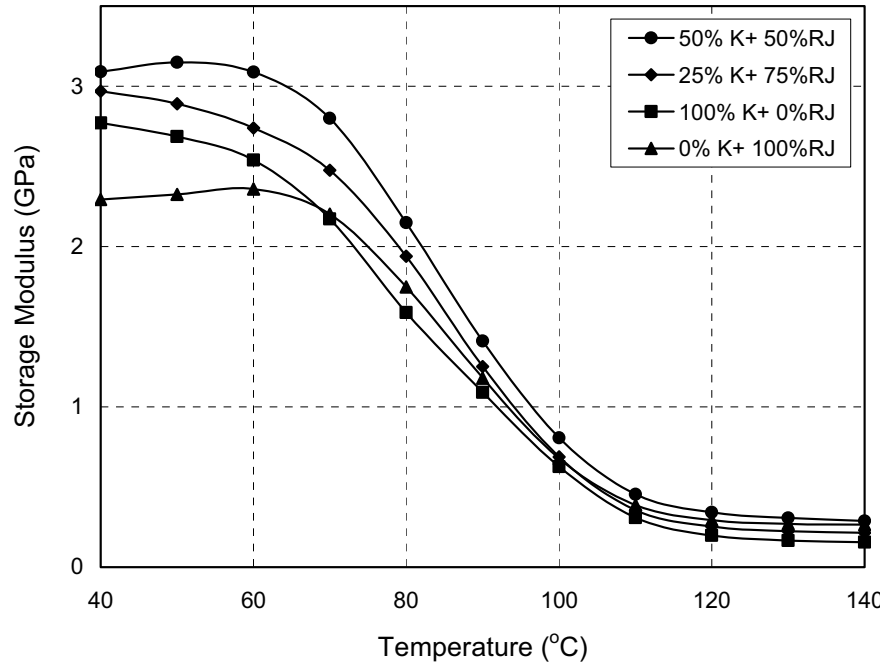
a
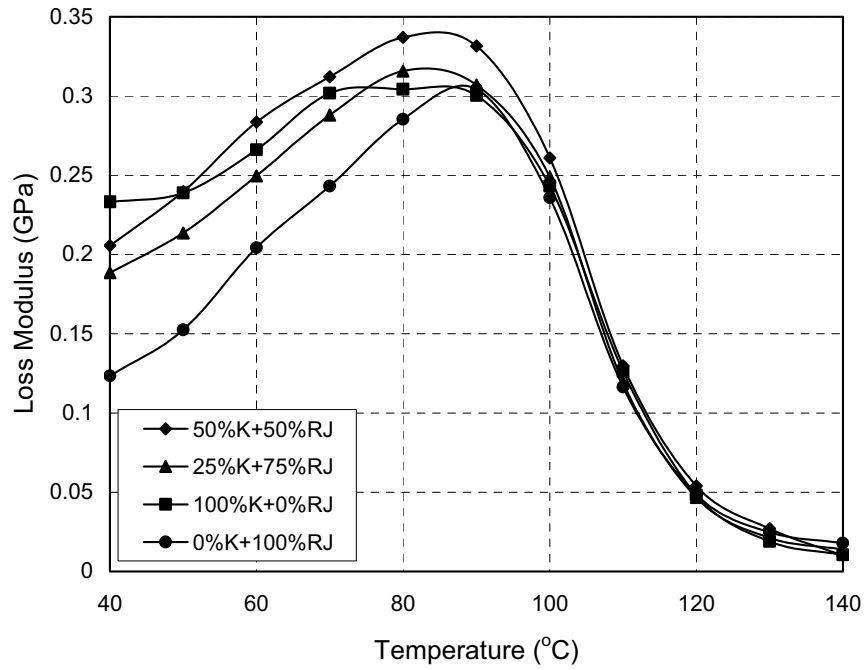
b
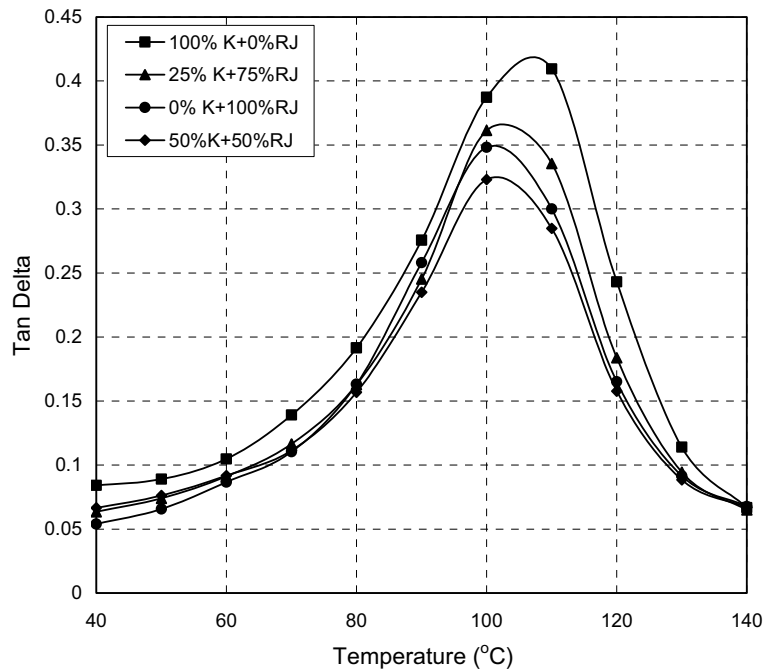
(c)

Figure 6.48 Effects of recycled jute on dynamic data for (60%UP+40%ST) resin: a) storage modulus vs. temperature, b) loss modulus vs. temperature, c) *tanδ* vs. temperature

Table 6.8 Summary of dynamic mechanical results for hybrid composites of various recycled jute weight fractions

20wt% Fiber composites	Storage modulus (GPa)	Loss modulus (GPa)	Tan δ	Glass transition temperature (ºC)
100%K+0%RJ30mm	2.772	0.364	0.409	90
50%K+50%RJ30mm	3.149	0.337	0.323	90
25%K+75%RJ30mm	2.969	0.315	0.361	90
0%K+100%RJ30mm	2.359	0.304	0.348	90

6.5.2. Thermal Properties

Instruments such as the Thermo Gravimetric Analysis TGA were used to determine thermal stability, melting points, heats of reaction, and moisture content. The TGA data for the various 60KFUPC kenaf loading is demonstrated in Figure 6.49. Totally, the curves of Figure 6.49 confirm that the thermal degradation began to occur only after the materials had absorbed certain amounts of heat energy. In all TGA curves of (60%UP+40%ST) resin, two stages of weight loss were observed and the first was in the range of 40 to 240ºC involving the loss of about 4.5% of the total mass. This can be attributed to the elimination of water adsorbed by the hydrophilic polymer, the second

with fragmentation of the polymer (Cerit et al. 2011). The thermograms show that the second degradation temperature of the (60%UP + 40%ST) resin was about 380ºC.

TGA was performed on the 60KFUPC degraded in three stages. The first stage at from 40 to 140ºC was due to the release of absorbed moisture in the fibers. In the second stage, the temperature range of the decomposition from 190 to 380ºC was related to the degradation of cellulose substances such as hemicelluloses and celluloses. The third stage at from 380 to 400ºC of the decomposition was due to the degradation of non-cellulosic materials in the fibers (Lee et al. 2009). Figure 6.49 confirms that the decomposition temperatures for the composite depended on the weight fraction of kenaf fiber. Generally, most of the cellulose fiber decomposed at a temperature of the range between 320-380ºC, the thermal stability of the composites materials increased with fiber content. This finding seems to be in agreement with Huda et al. (2007) and Tajeddin et al. (2009). A sudden drop in the mass of the sample indicated the thermal degradation of the materials, as illustrate in Figure 6.50. The thermal stability decreased with increase styrene content. Further, the first stage of weight loss started at range 40-60ºC and the second stage started at 90-340ºC.
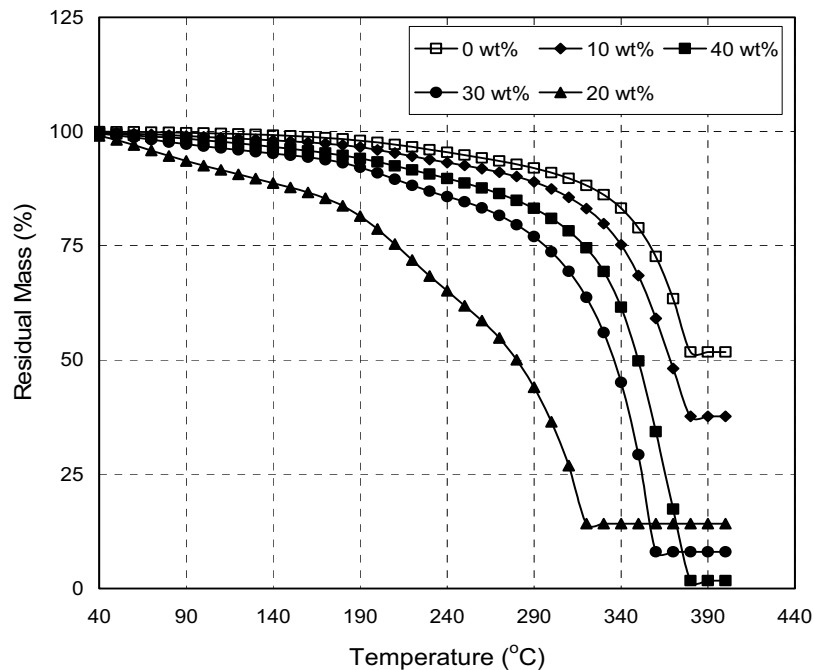
Figure 6.49 TGA curves of 60KFUPC at different treated kenaf fiber contents
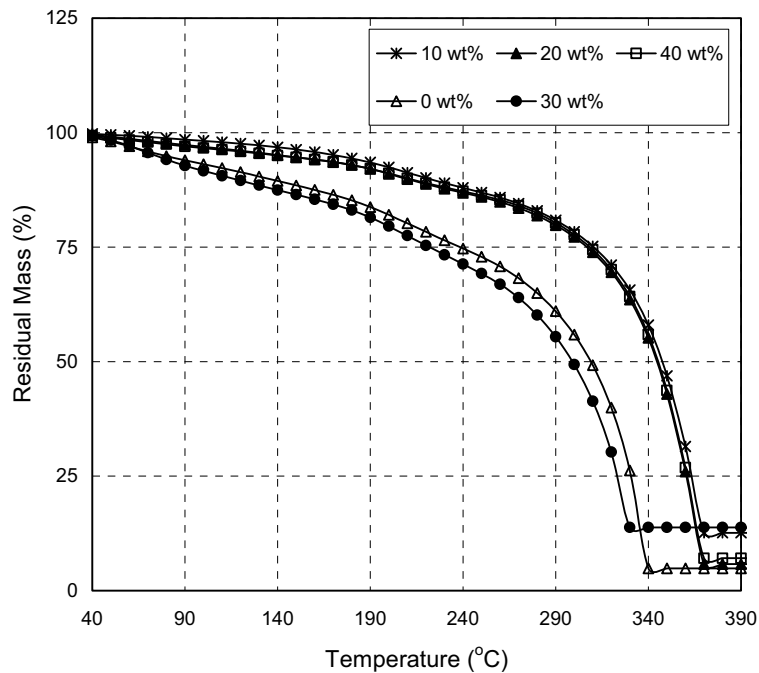
Figure 6.50 TGA curves of 50KFUPC with different treated kenaf fiber contents

- **Effects of Recycled Jute Fiber**

The thermal stability curves of hybrid composites as compared to pure unsaturated polyester and pure kenaf composites are shown in Figure 6.51. The initial weight loss observed between 40-140°C and between 140-190°C appears to be due to the loss of absorbed water on the surface of kenaf and hybrid fibers respectively; the same temperature for hybrid composites was absorbed for pure matrix (Al-Sagheer et al. 2010). A hybrid composite shows slower weight loss in the region between 190 to 290°C due to the decomposition of low molecular weight species. Thermal decomposition was more marked in the region between 90-240°C and from 240-340°C for both neat kenaf composite and for hybrid composite, relating to the complex dehydration of the saccharide rings, depolymerization, and decomposition of the acetylated and deacetylated units of the polymer (Peniche-Covas et al. 1993). From TGA curves, it was observed that pure kenaf and hybrid composites showed two-step degradation. Hybridization incorporation of recycled jute network and its interaction with the polymer increased the thermal resistance of the hybrids and consequently the thermal decomposition temperature. Hybridization of recycled jute with kenaf fibers resulted in considerable increase in the thermal stability of the hybrid composites which

is possibly due to the higher thermal stability of recycled jute fiber than kenaf fiber (Jawaid et al. 2012).
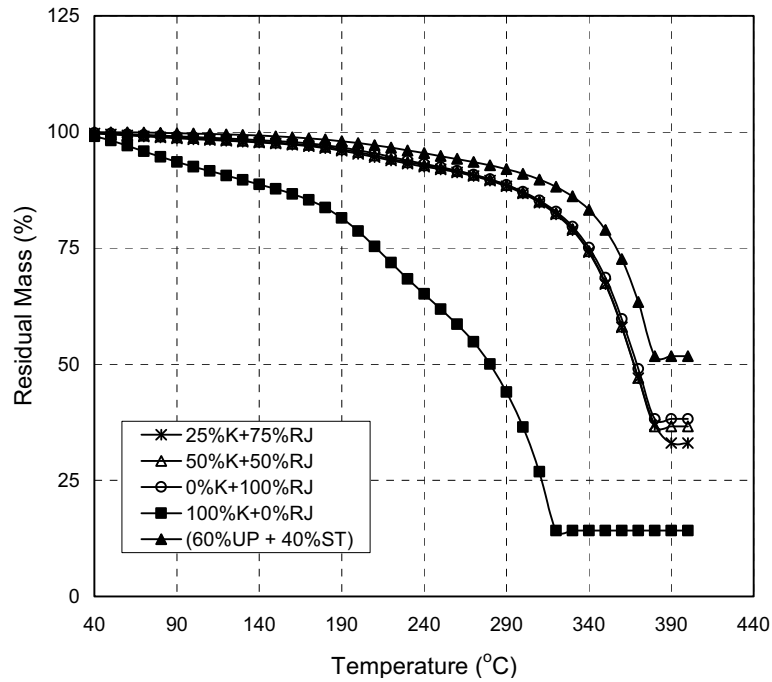
Figure 6.51 TGA curves of unsaturated polyester resin and hybrid composites at different treated recycled jute fiber contents

6.6 Viscoelastic Properties of Kenaf Reinforced Unsaturated Polyester Composites

6.6.1 Superposition Principle

Primarily the superposition principle was used to predict the viscoelastic material response a very large time scale. To reduce the time scale, the test temperature was raised. One can observe that a horizontal shift of a creep curve obtained at one temperature resulted in an accurate superposition of a creep curve considered at another temperature, which offered an extension of the curve measured at the second temperature. Mathematically this idea may be expressed as (Hadid et al. 2004)

$$\varepsilon(T_1, t) = \varepsilon\left(T_2 \frac{t}{a_T}\right) \tag{6.32}$$

where T_1, T_2 are the test temperatures; a_T is the temperature shift factor.

6.6.2 Time-Temperature Superposition Principle (TTSP)

The effect of time and temperature on a composites material can be determined using the time-temperature superposition principle, the basis of which is the equivalency of time and temperature. According to this principle, the effect of a constant temperature change on all time-dependent response functions, such as compliance and modulus, was equivalent to a uniform shift in the logarithmic time scale (Feng 2011). The William-Landel-Ferry (WLF) equation was employed for the calculation of shift factors, since the reference temperature lies within T_g and $T_g + 100^oC$ (Ferry 1980). If the reference temperature did not lie in this range, then the Arrhenius equation should be used (Ferry 1980). Nielsen et al. (1994) provided a modified WLF equation (Equation 6.33) to determine the shift factors when a temperature other than T_g is selected as the reference temperature.

$$Log\left(a_T\right)=\frac{-c_1\left(T-T_{ref}\right)}{c_2+\left(T-T_{ref}\right)} \tag{6.33}$$

where a_T is the horizontal shift factor for the corresponding elevated temperature, T (°C); T_{ref} is the reference temperature (°C); c_1 and c_2 are the empirical constants determined from Equations 6.34 and 6.35.

$$c_1=\frac{c_{1g}\,c_{2g}}{c_{2g}+T_{ref}-T_g} \tag{6.34}$$

$$c_2=c_{2g}+T_{ref}-T_g \tag{6.35}$$

where c_{1g} and c_{2g} are the empirical constants ($c_{1g}=17.44$ and $c_{2g}=51.6$ °C), T_g is the glass transition temperature (°C). By substituting the T_g (°C) of kenaf composites, the values of c_1 and c_2 were calculated.

6.6.3 Creep Modeling

According to Betten (2002 & 2005), the primary or transient creep is characterized by a monotonic decrease in the rate of creep and creep strain which can be described by the simple formula.

$$\varepsilon_c=a\sigma^n\,t^b \tag{6.36}$$

where a, n, and b are constants dependent on the temperature. ε is the creep strain and σ is the applied stress. Equation 6.36 was applied to the experimental creep data at room temperature.

6.6.4 Results and Discussion

- **Effect of Fiber Content**

Figures 6.52 and 6.53 show the short creep-strain and creep-compliance curves of composites made with different weight fractions of kenaf fiber. The highest creep properties are exhibited for the composites prepared from 10wt% kenaf fiber. The creep strain and creep compliance decreased as the kenaf fiber content increased. This behavior was expected from the increased rigidity of the composites (Nunez et al. 2004). From Figure 6.52, there was a clear trend that the increase of kenaf loading rate led to better creep resistance of the composites, as per the results found by Yanjun (2009). The deformation was noticeably less in the case of 40wt% composites and it was reduced when kenaf concentration was increased from 10 to 40 wt%.

There are three roles of the additives on creep resistance of the composites which can be proposed to explain the experimental observations. The first is the volume effect, where the additives reduced the relative volume of viscoelastic polymer matrix, which was prone to creep (Yanjun 2009). The second is the bridging effect, where the additives sustained part of the stress by connecting to each other. The third is the blocking effect, where the additives interacted with the molecular chains of polymer matrix and blocked them from moving under stress. Also, the high percentage of kenaf fiber distributed in the unsaturated polyester matrix made part of them connected to each other, so that the stress tended to be sustained by the high stiff additive network, which gave the matrix its stiffness (less creep) as summarised in Figures 6.54 and 6.55, which is in good agreement with previous findings (Nunez et al. 2004, Acha et al., 2007, Cyras et al., 2002, Perez et al. 2008).
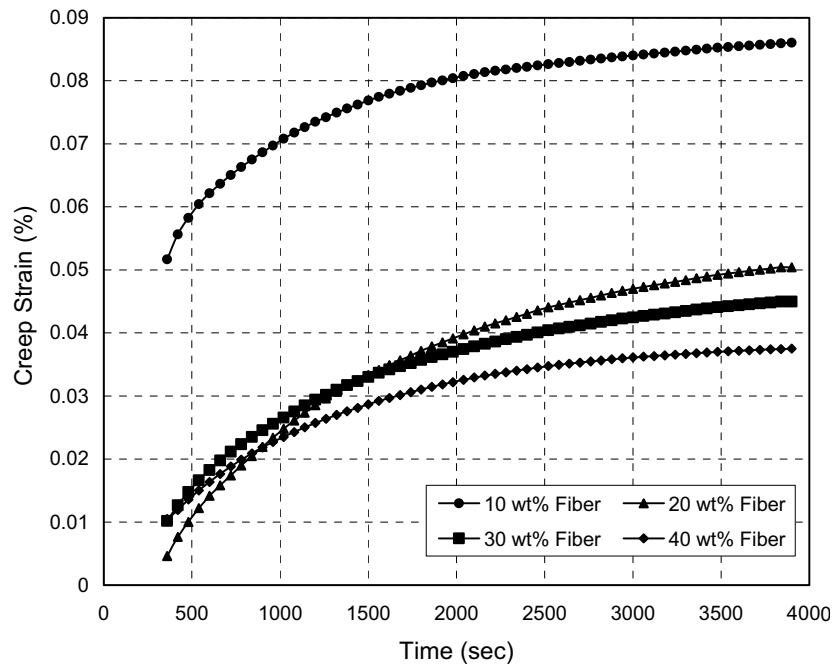
Figure 6.52 Creep strains of composites containing different weight fractions of the kenaf fiber

- **Effect of Temperature**

The representative experimental curves of creep strain and creep compliance vs. creep time of the different weight fractions of kenaf fiber based composites, tested at two different temperatures 30ºC and 50ºC, are presented in Figures 6.56 and 6.57 respectively. The creep strain and creep compliance were often larger at higher test temperature. It is well documented that this viscoelastic response depends on the material structure, which is strongly dependent on the testing temperature (Boyer 1973, Khanna et al. 1985, Read et al. 1997). Furthermore, the instantaneous deformation as well as the total deformation exhibited almost an exponential variation with the temperature.
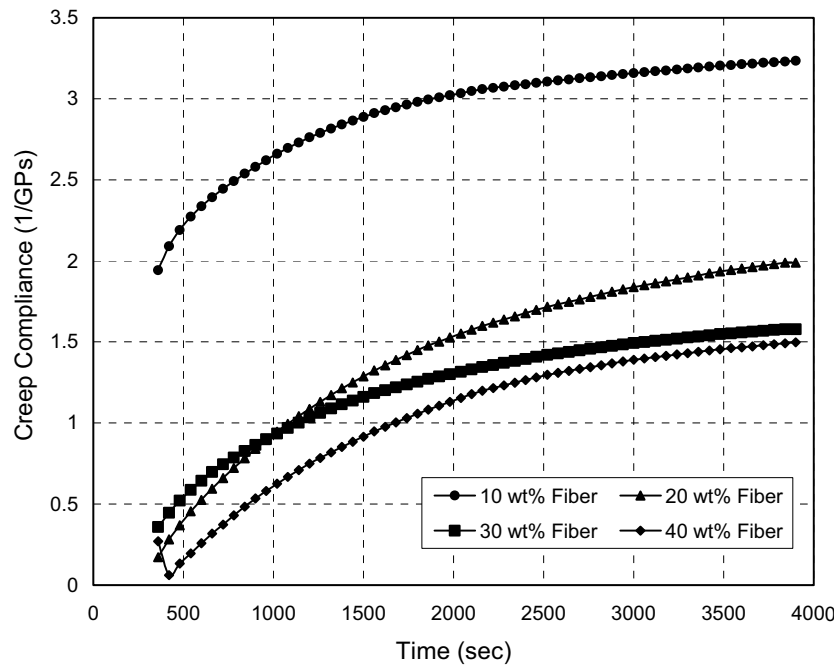
Figure 6.53 Creep compliances of composites containing different weight fractions of the kenaf fiber
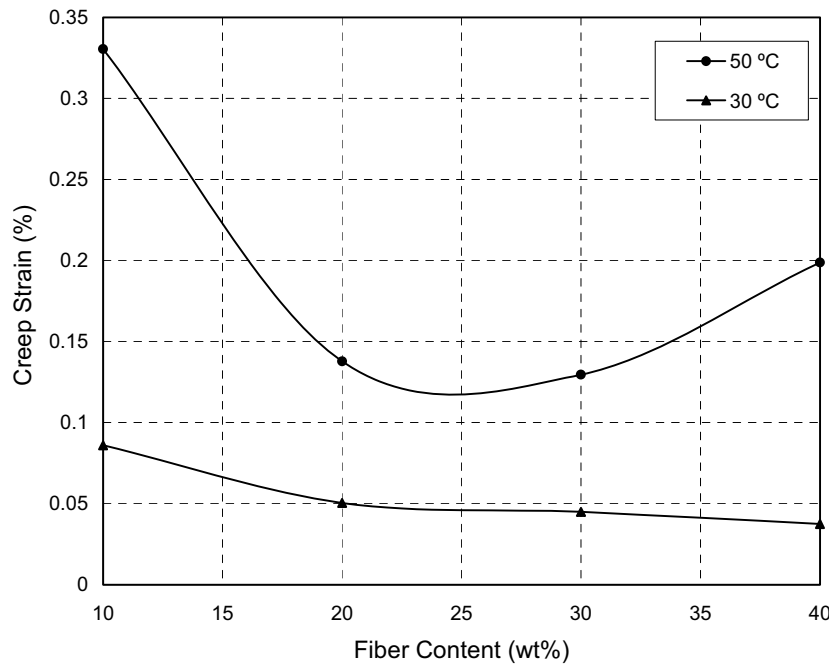
Figure 6.54 Summary of creep strain test for composites containing different weight fractions of fiber for two different temperatures at 60 minutes.
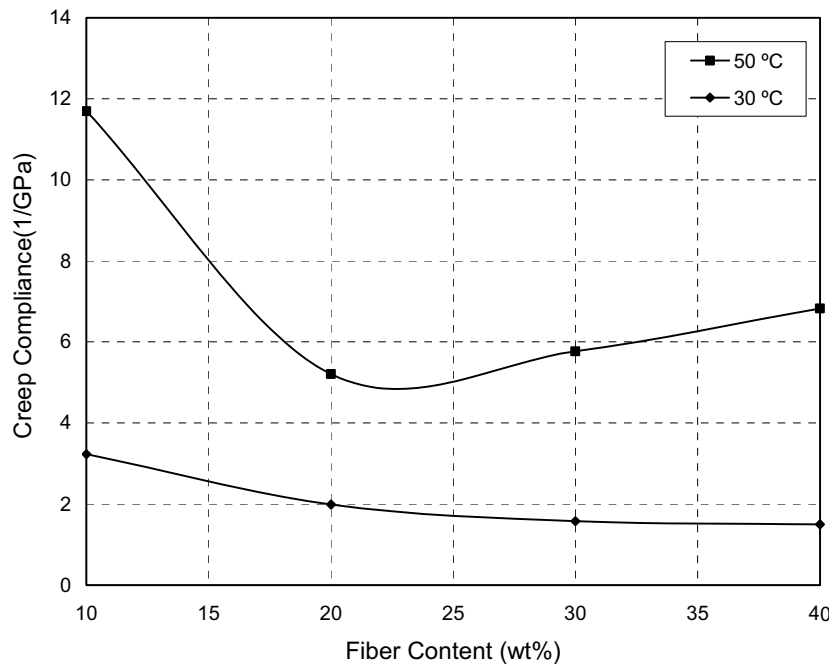
Figure 6.55 Summary of creep compliance test for composites containing different weight fractions of fiber for two different temperatures at 60 minutes.
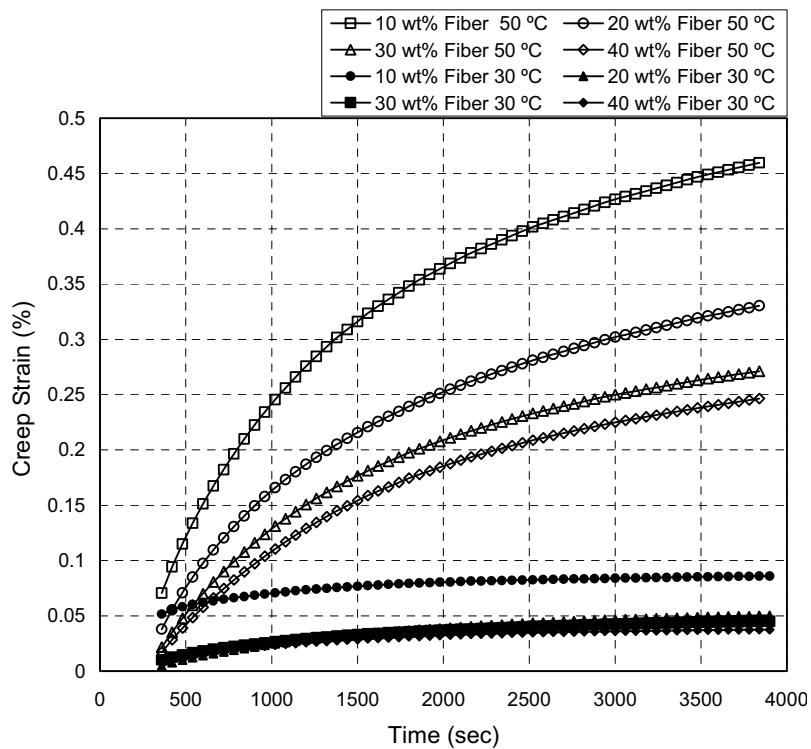
Figure 6.56 Creep strains of composites containing different weight fractions of kenaf fiber and different temperatures

176
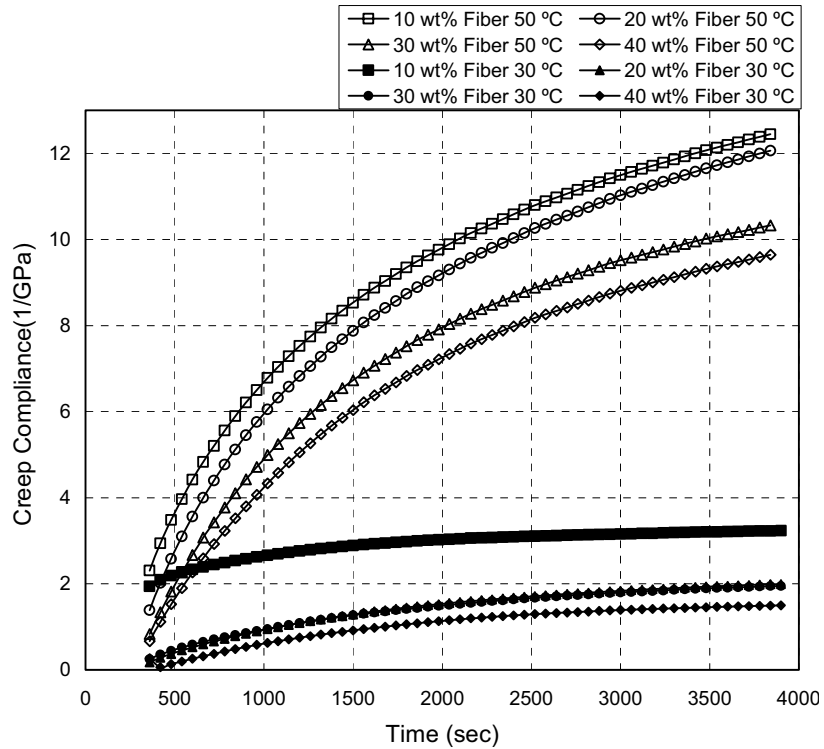
Figure 6.57 Creep compliances of composites containing different weight fractions of kenaf fiber and different temperatures

- **Effect of Styrene Concentration**

The creep strain and creep compliance behaviour of kenaf composites at two different styrene concentrations as a function of time at 50ºC testing temperature are shown in Figures 6.58 and 6.59, respectively at different weight fractions of fiber. The highest strain and compliance was for 10wt% fiber reinforced (60%UP+40%ST) unsaturated polyester composites. When the styrene was increased to 50%, Figures 6.58 and 6.59 suggest enhanced polymer mobility. The composite stiffness at 50%ST differed from those at 40%ST; it increased with decreasing density and viscosity of the polymer which affected the influence of adhesion and density of the composites. In fact, increased styrene concentration influenced the wettability between the fiber and matrix (Acha et al. 2007 and Kim et al. 2008). In order to show the effect of styrene concentration on the deformation of composites containing different weight fractions of fiber at two different temperatures, Figures 6.60a and b, Figures 6.61a and b summarize the creep strain and creep compliance. Both deformation and compliance were noticeably less in the case of (60%UP+40%ST) composites and they reduced when weight fractions of kenaf fiber increased from 10 to 40wt% at 30ºC. However, the

(50%UP+50%ST) composites had the same trend for increasing fiber content from 10 to 30wt% at 50ºC.
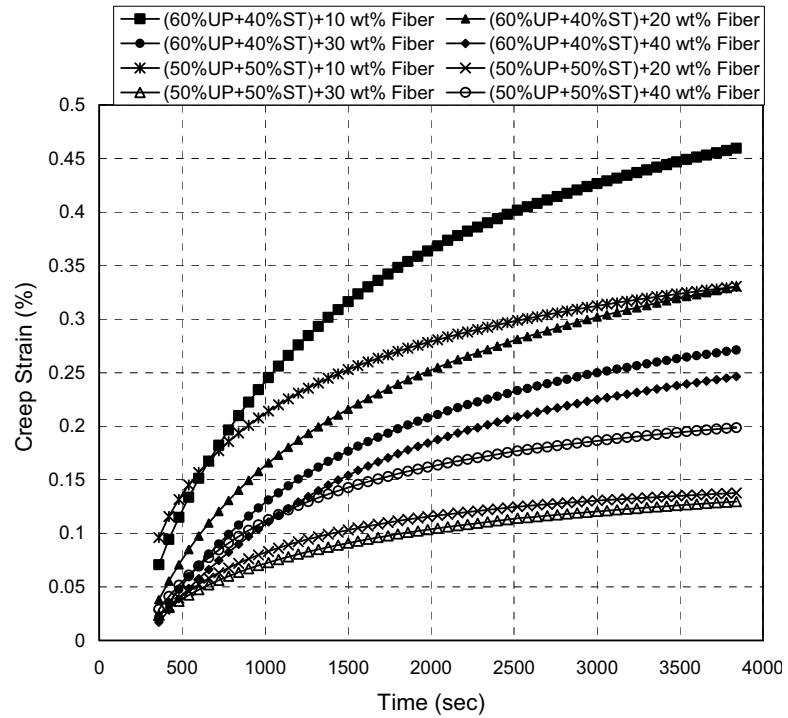
Figure 6.58 Creep strains of composites containing different weight fractions of kenaf fiber and various styrene concentrations at 50ºC
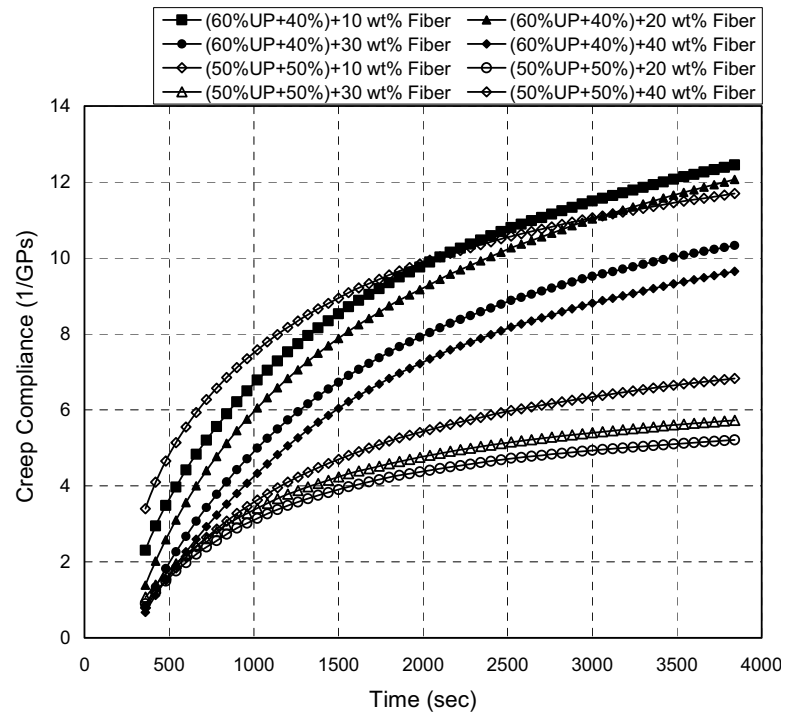
Figure 6.59 Creep compliances of composites containing different weight fractions of kenaf fiber and various styrene concentrations at 50ºC
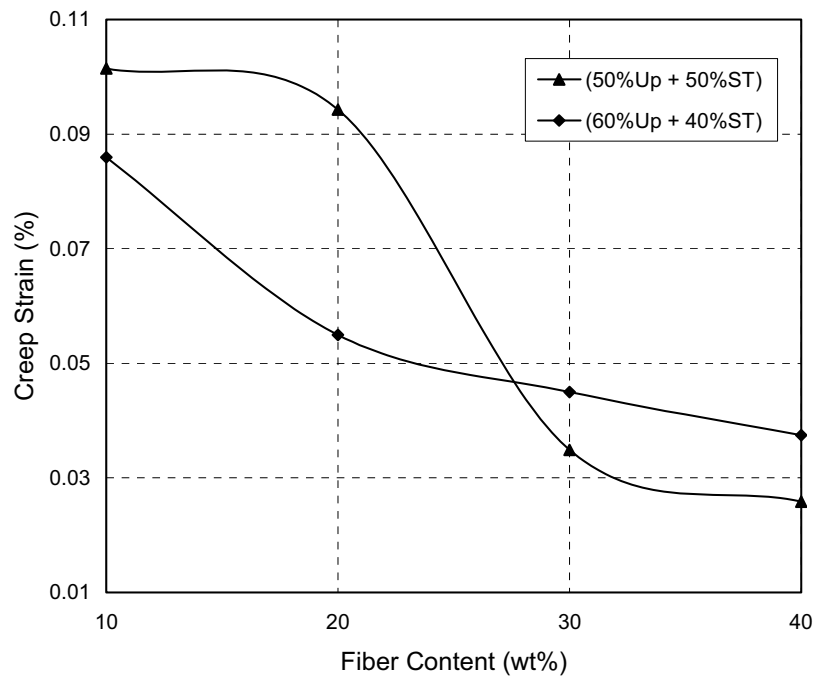
a
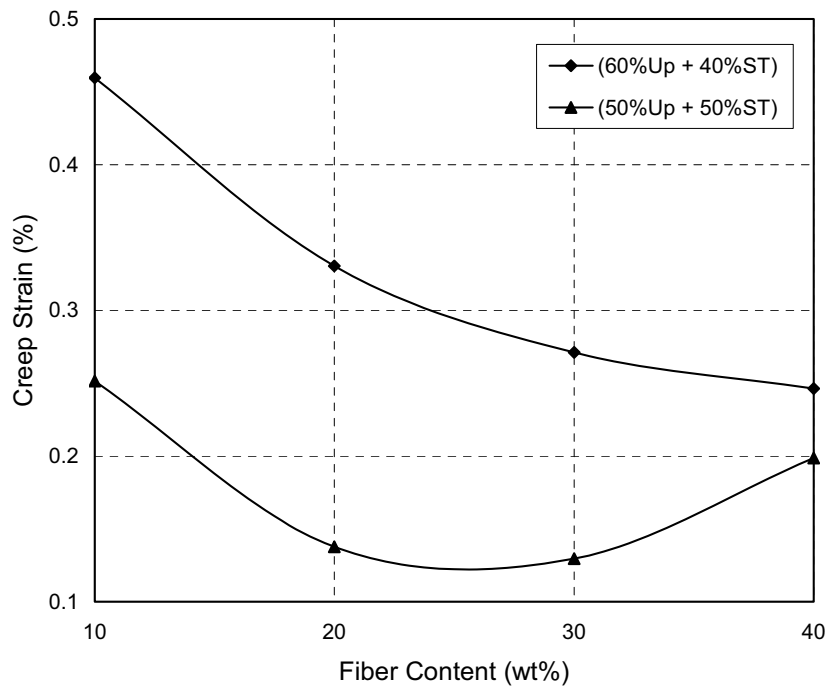
b

Figure 6.60 Creep strains of composites as a function of weight fraction of kenaf fiber and various styrene concentrations: a) at 30ºC, b) at 50ºC

179
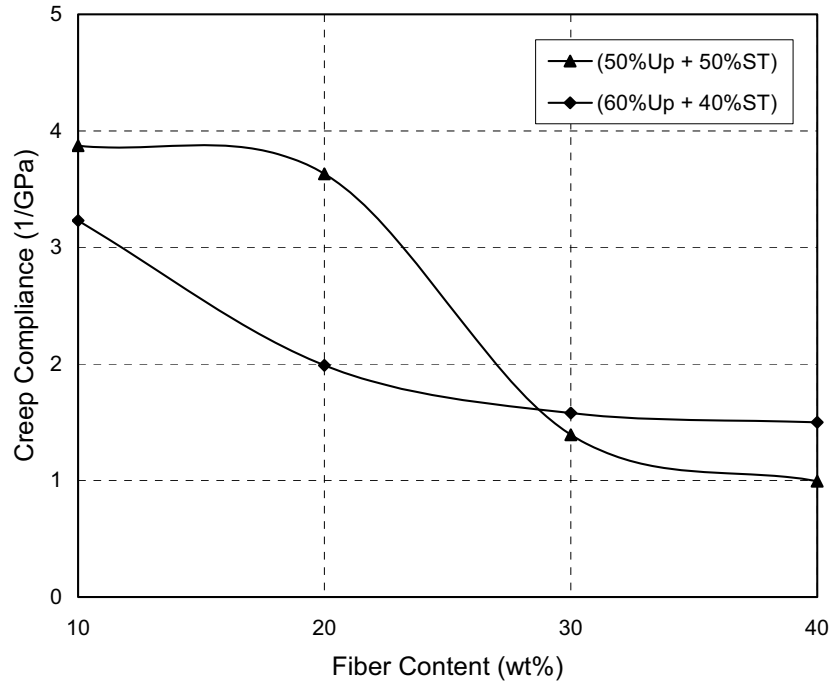
a
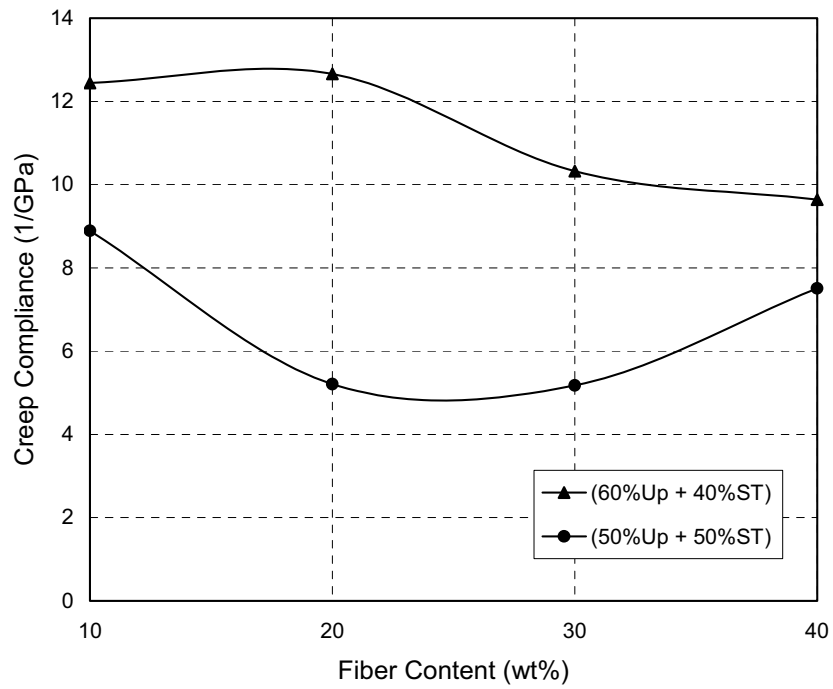
b

Figure 6.61 Creep compliances of composites as a function of weight fraction of kenaf fiber and various styrene concentrations: a) at 30ºC, b) at 50ºC

- **Creep Modeling and Master Curves**

The creep strains measured at two different temperatures were superposed rearranging the time scale using the time-temperature superposition principle. The horizontal shift factors and empirical constants for kenaf composites containing different styrene concentrations at 30ºC as a reference temperature are given in Table 6.9 and the master curves obtained are shown in Figure 6.62. The shift factor values depended on the value of glass temperatures T_g of fiber composites as used in Equation 6.33. The T_g in Table 6.9 was obtained from the previous study (see section 6.5.1 Table 6.7) measured by DMA. The creep strain curves at 50ºC for different weight fractions of fiber and various styrene concentrations were shifted to the right using the shift factors, while the creep strain curves at reference temperature 30ºC were not shifted as shown in Figure 6.62. The resulting master curve for 40 wt% composites is represented in Figure 6.63. The master curve predicted the creep response up to 5.5 days.
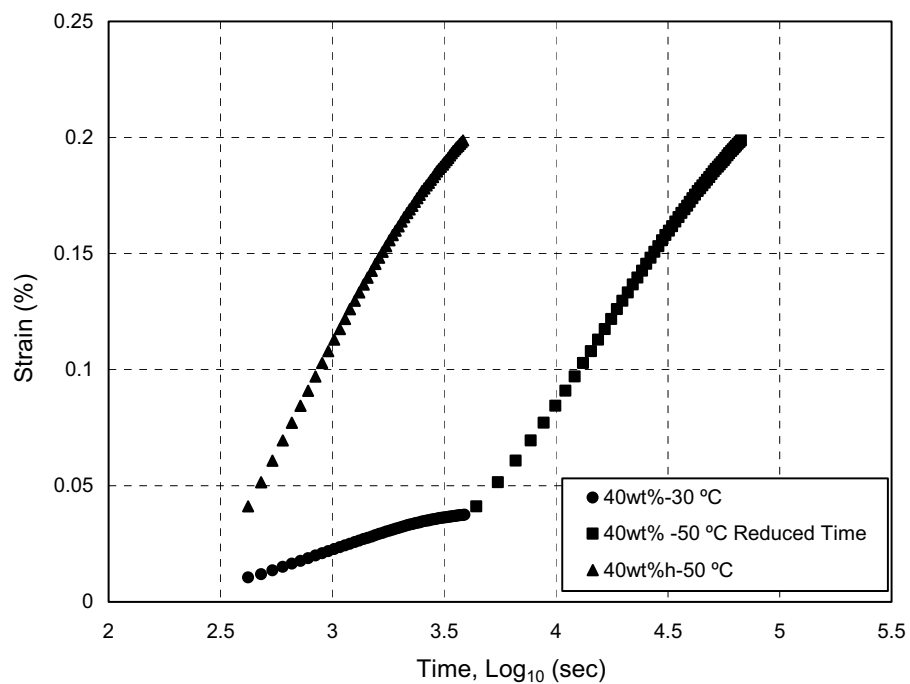
Figure 6.62 Sample of shifting creep strain curves for (50%UP+50%ST) composites at 30 ºC as a reference temperature

181

Table 6.9 Horizontal shift factor and empirical constants for different styrene concentrations at 30ºC as a reference temperature

Composites	Wt (%)	T_g (ºC)	a_T	c_1	c_2
60%UP + 40%ST	10	90	0.047702	8.4	107.1341
	20	88	0.159602	6.4	140.61
	30	86.8	0.28927	5.2	173.058
	40	89.8	0.054447	8.2	109.7444
50%UP + 50%ST	10	90	0.047702	8.4	107.1341
	20	86.65	0.309322	5.05	178.1988
	30	89	0.090129	7.4	121.6086
	40	90	0.047702	8.4	107.1341
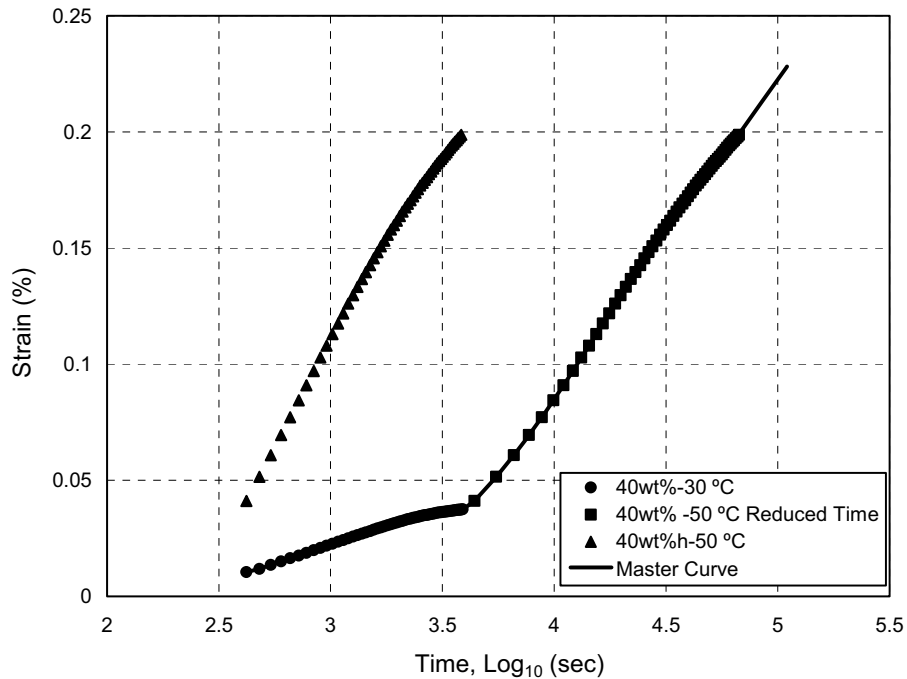
Figure 6.63 Sample of shifting creep strain curves for (50%UP+50%ST) composites at 30ºC as a reference temperature and the master curve

The short term creep curve 60 minutes was modeled with the primary creep strain model (Equation 6.36). The resulting curves were then plotted together with the experimental 60 minutes creep strain curve explained previously. This is presented in Figure 6.64. A good agreement can be observed between the experimental creep curve and the extrapolated curves. This clearly indicates that the power-law model is a very good method for predicting creep behavior. An excellent agreement was found in the

literature for kenaf polyethylene composites (Tajvidi et al. 2005). It was indicated earlier that the power-law model proved very satisfactory in predicting the long-term creep strain behavior for kenaf unsaturated polyester composites. These indications were represented in Figure 6.65. However, the results of this study must be used with caution because creep behavior is a complex phenomenon that is dependent on a variety of parameters, such as stress level, temperature, and environmental conditions (Tamrakar et al. 2011). The power-law constants were altered numerically to minimize the sum of square error between the experimental data and the theoretical data. Table 6.10 summarizes the values of the empirical constant that depended on the temperature. It is observed that the value of the constant for short-term is smaller than for the long-term, which is in agreement with the results found by Dastoorian et al. (2010).
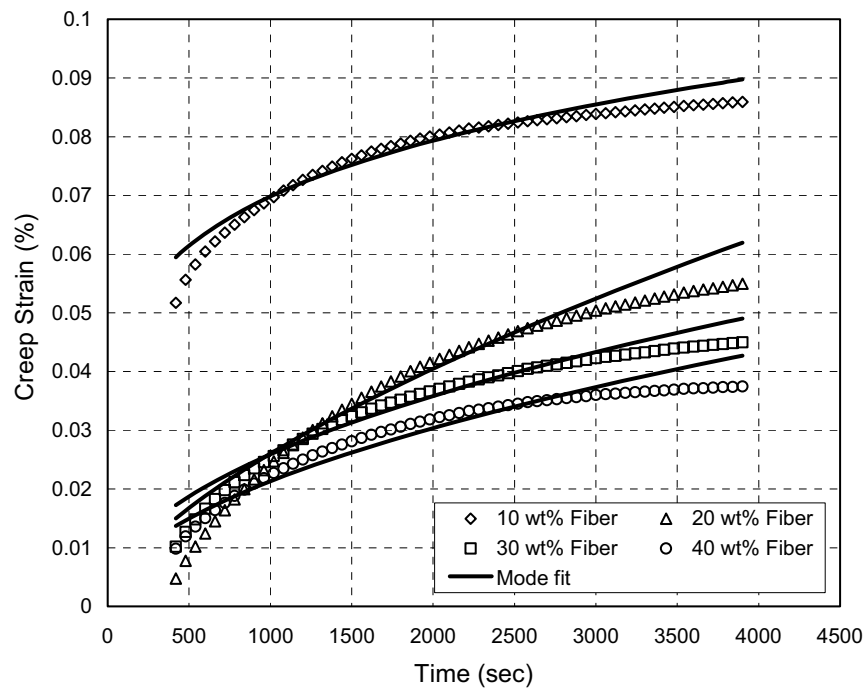
Figure 6.64 Power-law-extrapolated creep and actual creep data of (60%UP+40%ST) composites containing different weight fractions of fiber
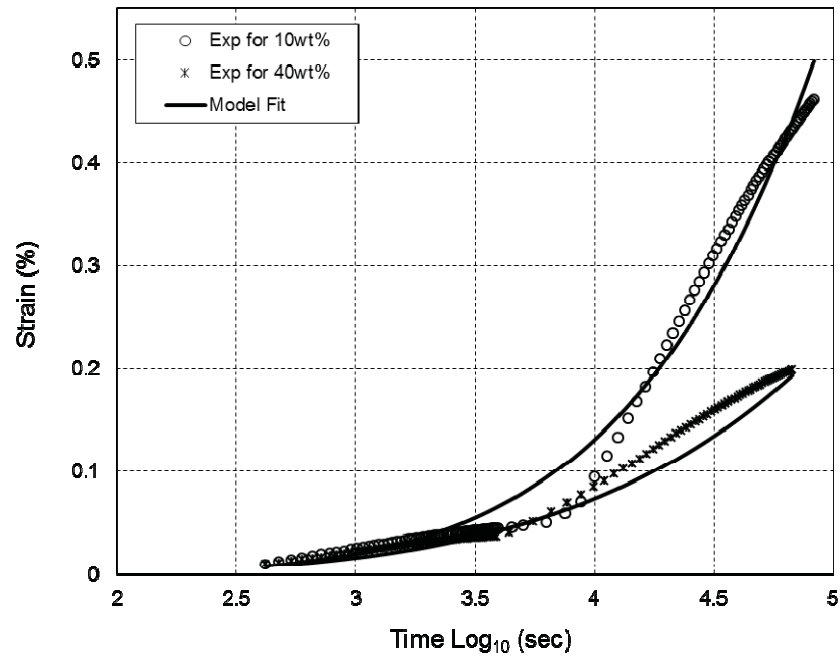
Figure 6.65 Comparison between the master and the creep model for (60%UP+40%ST) composites for smallest and highest weight fractions of fiber

Table 6.10 Empirical constants of short and long-term at reference temperature 30ºC

Composites	Fiber content (wt%)	*a*	*n*	*b*
(60%UP+40%ST) Short-term	10	0.00272124	0.7111111	0.46885485
	20	0.00114	0.92133	0.63774
	30	0.008797	-0.57404	0.184643
	40	0.000741	0.123428	0.511111
(60%UP+40%ST) Long-term	10	0.016448562	4.954841343	6.453679496
	20	0.02008908	3.61202651	4.73528604
	30	0.084395808	2.154040218	2.422163224
	40	2.2772508	7.5872506	5.1135641
(50%UP+50%ST) Short-term	10	0.01485117	-0.14887923	0.20995045
	20	0.00725	-0.371	0.25294
	30	0.002151	-0.36872	0.284814
	40	0.001721	0.102332	0.355864
50%UP+50%ST) Long-term	10	0.04756033	2.92282781	3.95039187
	20	0.077342805	2.268415028	2.697723082
	30	0.37956856	2.754791171	1.086070887
	40	1.0167283	7.1862192	5.2927619

6.7 Summary

Several major conclusions were drawn from the test results. The tensile and flexural properties of randomly oriented short kenaf composites were found to be dependent on the fiber treatment, fiber length and fiber weight fraction. Alkali treatment increased the impurities of fiber surface and increased the interface between the fiber and matrix, and also decreased the fiber pullout which enhanced tensile and flexural properties. Besides that, the post curing process increased the tensile and flexural properties for treated fiber composite. At fiber length of 1-6mm the maximum tensile strength and modulus of short kenaf composites were around 24.8MPa at 10wt% and 3.98GPa at 30wt% respectively, while they were 33.2MPa at 40wt%, 4.98GPa at 30wt% respectively, for fiber length 10-30mm.

Impact strength of kenaf unsaturated polyester composites increased with decreasing of styrene concentration for a certain value of MEKP. The increasing percentage was about 30% for styrene concentration ratio 40%ST compared to 50%ST. At 20wt% fiber weight fraction the impact strength was 8.035kJ/m^2 for 1-6 mm size untreated kenaf fiber composites and it was higher than the treated fiber composite. The increasing percentage was about 9% due to a great amount of fiber pullout in untreated fiber composites as SEM shows. Post curing decreased the impact strength for treated fiber composite. The decreasing percentage was about 10% for 40wt%. The untreated kenaf fiber length of 10–30mm gave the highest impact strength for 20wt% fiber weight fraction. The impact strength of 10–30mm kenaf fiber length increased 60% compared to 1–6mm. Different length had different optimum volume fractions of fiber.

The present study clarifies that the kenaf/recycled jute unsaturated polyester composites at various length loading were found to be dependent on the fiber length. A critical fiber length and maximum recycled jute fiber percent of 30mm and 75% respectively provided better improvement in the modulus of elasticity and tensile strength. However, the elongation value was not found to have any considerable variation with the recycled jute fiber length. The flexural properties of the hybrid composites decreased with increase of recycled jute fiber. The lower values of flexural properties may be attributed to fiber-to-fiber interaction, voids and dispersion problems. The flexural strength for recycled jute unsaturated polyester composites increased with increase of recycled jute

fiber; in fact, there was insignificant change in flexural properties for different lengths 10 and 20mm. The maximum value of impact energy was 10.897 KJ/m^2 at 50% weight fraction of recycled jute with fiber length 10 mm; the maximum improvement was about 47% compared to kenaf unsaturated composites. SEM analysis showed that the interaction between the hybrid fibers and unsaturated polyester matrix was poor such that fiber debonding, fiber pull-out, matrix fracture and fibers fracture occurred in short kenaf/recycled jute unsaturated polyester composites under bending loading.

Water absorption and environmental factors affected the tensile properties of KFUPC for different fiber contents, immersion times, and fabric pre-drying. Weight percentage of fiber content played a role in the rate of moisture uptake and overall uptake at saturated points of KFUPC. Increasing the weight percentage of fiber loading led to the increase in the *TS* and *EM* of composites for dry specimens, whereas increasing the weight percentage of fiber load led to a decrease in tensile properties of composites for immersion specimen due to degradation of composites. Water uptake behaviour was radically altered at increased weight fraction of kenaf fiber, exposure to moisture resulted in significant drops in tensile properties for composites due to degradation of fiber-matrix interface. At the same, time the results indicate that prolonged aging in water increased *TS* of *UP* resin. In conclusion, KFUPC could be developed to provide greatest tensile properties in certain parameters. However, a best ratio of fiber-matrix is required to achieve the superlative properties and results.

Effects of water absorption on flexural properties of kenaf composites and hybrid composites were studied. Results showed that moisture uptake decreased with the addition of recycled jute fiber *RJ* at different lengths. Results indicated that generally kenaf/recycled jute composites had considerably lower water absorption and thickness swelling as compared with original kenaf composites which were attributed to change in physical and chemical properties of composites. Water absorption patterns of these composites were found to follow Fickian behavior. Values obtained for diffusion coefficients were in agreement with range of values reported, in the order of 10^{-12} m^2/sec. Flexural properties of composites decreased drastically on exposure to moisture results due to the presence of voids (porosity) and degradation of fiber-matrix interface was suggested to have a strong influence on flexural properties of composites. The SEM analysis observed the poor interaction between different fiber lengths and matrix.

Further, when the polymer resin matrix was reinforced with the different fiber dimensions, morphological changes took place depending upon the interfacial interaction between the varying dimensions of fiber and the resin matrix.

A comparison between experimental results and the prediction from theory of the tensile properties was presented. Some of the models present a reasonable agreement with experimental tensile properties, while other models do not show a good correlation with experimental results of randomly oriented composites. The experimental modulus of elasticity for kenaf length of 1-6 mm composites was compared with the theoretical predictions and found to be in good agreement with Hirsch's model while the results obtained from Cox–Krenchel underestimated the experimental data.

Dynamic mechanical properties and thermal stability of the *UP* resin and short kenaf fiber reinforced composite observed unsaturated polyester composites were dependent on the styrene concentration. Moreover, dynamic mechanical properties and thermal stability were significantly affected via weight fraction of the fiber. The DMA results revealed that the incorporation of the fibers gave rise to a considerable increase of the E' (stiffness), T_g and a decrease in *tanδ* values. The maximum improvement in properties was observed for composites with 30wt% fiber loading. At the maximum possible fiber loading in this study i.e. 30wt% loading, the loss modulus peak broadened emphasizing the improved fiber/matrix adhesion. T_g temperature shifted positively with the addition of fiber which indicates that increasing fiber content slightly increases the glass transition temperature. Furthermore, thermal behaviors of the neat resins for various styrene concentrations were comparable, indicated on the two-stage weight loss mechanism, and three–stage weight loss mechanism for both 60KFUPC and 50KFUPC.

The storage modulus of kenaf composites is comparable with hybrid composites and it is clear from results that hybrid composites with (50%K+50%RJ) showed the highest storage modulus, neat RJ composite value lay between pure kenaf composites and hybrid composites of various weight fractions of RJ 30 mm length. Hybrid composites showed lower value of loss modulus compared to pure kenaf composites. The shifts in T_g of the polymer matrix with the addition of fiber as reinforcing phase indicates that fiber plays an important role above T_g. The *UP* resin had the highest *Tanδ* value indicating that there is a large degree of mobility, thus good damping behaviour.

Thermal analysis study indicated that thermal stability of pure kenaf composites increased with the addition of recycled jute fibers. Finally, it can be concluded that hybridizing of kenaf fiber and recycled jute fibers resulted in better dynamic mechanical and thermal properties.

The effects of temperature, kenaf content, as well as various styrene concentrations on the creep behavior of kenaf unsaturated polyester composites were studied. It was shown that the relative creep of the composites increased with an increase in temperature. This was explained by the mobility of the amorphous bulk and tie molecules of the kenaf composites. The composites stiffness at (50%UP + 50%ST) composites was better than (60%UP+40%ST) composites. This behavior was related to fiber surface and the efficiency of the adhesion mechanism between kenaf fibers and (50%UP+50%ST) matrix. The creep compliance decreased as the kenaf fiber content increased, as expected from the increased rigidity of the composites. Creep data were superimposed with a single horizontal shift to obtain a master curve covering a higher range of time. Shift factors conformed to a William-Landel-Ferry (WLF) equation. It appears that the master curve may have the potential to extend test data by many years. However, more long term creep data is needed in order to further validate the applicability of TTSP to this material. The power-law model was fitted to the 60-minutes creep data. The result was then extrapolated to 5.5 days; the creep strain of power-law model can be successfully used to predict the long-term creep behavior of natural fiber/thermoset composites.

CHAPTER SEVEN

CONCLUSIONS AND RECOMMENDATIONS

7.1 General

This thesis investigated the performance of kenaf fiber unsaturated polyester composites. Different parameters which affect the mechanical, thermal, and dynamic properties were studied. Most of the investigations included experiments and analytical modelling if the problem was tractable. From all these investigations, it can be seen that there are several common conclusions besides those remarks at the end of each chapter for the kenaf fiber and its composites.

7.2 Curing Behaviour and Mechanical Properties of Unsaturated Polyester Resin

The physical parameters of unsaturated polyester resin such as viscosity and density decreased with the increase of environmental temperature and styrene (*ST*) concentration. The *ST* concentration controls the reactivity of the unsaturated polyester and also the crosslinking density of the final network. The gelation point was found to correspond with the onset of the polymerization as expected for network formation via chain-growth polymerization. The gel time was found to be inversely related to the concentration of MEKP, NNDMA, fiber weight fraction and moisture content. The exotherm data obtained from curing under adiabatic conditions were consistent with these conclusions. The concentrations of *ST*, MEKP and NNDMA affected the mechanical and dynamic properties of the *UP* resin. The thermal stability of the *UP* resin reflected the extension of phase segregation.

7.3 Physical and Tensile Properties of the Kenaf Bast Fiber

Natural fibers exhibit superior advantages over the synthetic fibers especially in cost, environmental aspects and high specific modulus compared to synthetic fibers. The physical and mechanical properties of the kenaf fiber were observed. The results found good agreement within the range in the literature. However, the drawbacks of natural fibers include low shear interface strength, water absorption, biodegradation and photodegradation, limiting the potential of natural fiber composites in structural use. The drawbacks can be partially overcome by introducing chemical treatment.

7.4 Mechanical Properties of Composites

The mechanical properties of fiber reinforced composites are dependent upon the stability of the interfacial region. Thus, the characterization of the interface is of great importance. Alkali treatment increased the impurities of fiber surface and increased the interface between fiber and matrix, and also decreased the fiber pullout which enhanced tensile and flexural properties. Different parameters affected the mechanical properties of natural fiber composites in this investigation, namely curing process, MEKP and ST concentrations, fiber weight fraction, fiber length and fiber treatment. SEM analysis showed that the interaction between the hybrid fibers and unsaturated polyester matrix was poor such that fiber debonding, fiber pull-out, matrix fracture and fibers fracture occurred. The experimental data of tensile results for kenaf composites was compared with several theoretical predictions and found to be in good agreement with some of these models.

7.5 Effects of Water Absorption on Mechanical Properties of Composites

The results of this part discussed the water absorption characteristics and environmental affects on tensile and flexural properties of fiber composites at different fiber contents, immersion times, and fabric pre-drying. Fiber weight fraction and temperature surrounding played a role in the rate of moisture uptake and overall uptake at saturated points of KFUPC. The tensile, flexural and impact properties of natural fiber composites were found to be dependent on the fiber length and fiber weight fraction. Water

absorption patterns of these composites were found to follow Fickian behavior. Values obtained for diffusion coefficients were in agreement with the range of values reported in the literature.

7.6 Dynamic and Thermal Properties of Composites

Dynamic mechanical properties and thermal stability of short kenaf fiber reinforced unsaturated polyester composites were considerably dependent on fiber weight fraction. The results exposed that incorporation of the fibers gave rise to a considerable increase of the E', T_g and a decrease in the $tan\delta$ values. The loss modulus peak got broadened emphasizing the improved fiber/matrix adhesion. The T_g temperature shifted positively. Furthermore, thermal behavior of the kenaf composites was comparable, indicated on the three–step weight loss mechanism. Recycled jute improved the dynamic properties of the kenaf/recycled jute composites. The results of dynamic mechanical testing for the net kenaf fiber composites and the kenaf/recycled jute composites clarified that the hybrid composites had a higher storage modulus, which corresponded to a higher tensile modulus.

7.7 Viscoelastic Properties of Composites

Three important parameters affected the creep behavior of kenaf unsaturated polyester composites, which were fiber loading, temperature, and styrene concentrations. The creep data were superimposed with a single horizontal shifting to obtain a master curve covering a higher range of time. Shift factors conformed to a William-Landel-Ferry (WLF) equation. It appears that the master curve may have the potential to extend test data by many years. The creep strain of power-law model can be successfully used to predict the long-term creep behavior of natural fiber/thermoset composites.

7.8 Recommendations for Future Studies

Recommendations for future studies are made upon the conclusion of this research.

- A study on performance of natural fiber reinforced polymer composites under various weather conditions is required.
- Study the effects of composites fabrication of kenaf polymer composites.
- Different types of hybrid fiber in reinforced polymeric composites are required to find out the optimum performance of natural fiber reinforced polymer for different applications.
- Study the behaviour of long kenaf fiber as a woven composite at different angles reinforced polymer composites.
- Study the effects of water absorption for both kenaf and hybrid composites for more than two different temperatures via various weight fractions of fiber.
- For numerical investigations, a more physics-based model Zero-stress aging is defined as the reduction of *TS* and *ME* when no stress is applied during the time of exposure to a given environment. Weight fraction of fiber and heating effects should be constructed.
- In case of engineering materials, the key issues are the long-term properties. But only the creep behaviour from short-term tests was studied in this work. In the future, it is recommended to investigate the long-term creep behaviour at different temperatures and different stresses to predict the horizontal and vertical shifting factors and two-dimensional minimization methods to obtain master curves covering a higher range of stress for kenaf unsaturated polyester composites.

References

1. Abdalla, A. Ab. Rashdi, Mohd Sapuan Salit, Khalina Abdan and Megat M.H.M.. (2010) Water absorption behaviour of kenaf reinforced unsaturated polyester composites and its influence on their mechanical properties. Pertanika . Science. & Technology. 18 (2): 433 – 440.

2. Ahmad, S. H., Bonnia, N., Zainol, I., Mamun, A. A. and Bledzki, A. K. (2010) Polyester-kenaf composites: effects of alkali fiber treatment and toughening of matrix using liquid natural rubber, Composite Materials. 45(2): 203 – 217.

3. Andjelkovic, D. D., Culkin, D. A., and Loza, R.(2009) Unsaturated polyester resins derived from renewable resources. COMPOSITES & POLTCON, American Composites Manufactures Association, January 15-17.

4. Andersons, J., Sparnins, E. and Joffe, R. (2006) Stiffness and strength of flax fiber/polymer matrix composites. Polymer Composites, 27(2):221-229

5. Acha, B.A., Marcovich, N.E., Reboredo, M.M. (2005) Physical and mechanical characterization of jute fabric composites. Applied Polymer Science, 98:639-650.

6. Acha, B. A., Reboredo, M. M. and Marcovich, N. E. (2007) Creep and dynamic mechanical behavior of PP-jute composites: Effect of the interfacial adhesion. Composites Part A: Applied Science and Manufacturing, 38(6): 1507-1516.

7. Anshid, A., Haneef, A., Panampilly Bindu, Indose Aravind and Sabu Thomas (2008) Studies on tensile and flexural properties of short banana/glass hybrid fiber reinforced polystyrene composites. Journal of Composite Materials,42(15).

8. Aguilar-Veaga M. and Cruz-Ramos C. A. (1995), Properties of henequen cellulosic fibers. Applied. Polymer Science, 56: 1245.

9. Alger, M.S.M. (1996) Polymer Science Dictionary. 2nd: Chapman and Hall.

10. Al-Sagheer F. and Muslim S. (2010) Thermal and mechanical properties of chitosan/sio2 hybrid composites. Journal of Nanmaterials, ID 490679, 7 pages. Research Article

11. Alireza A. (2004) Development of high quality printing paper using kenaf (hibiscus cannabinus) fibers. PhD thesis, University Putra Malaysia

12. Amar K. Mohantt , Misra M., Lawrence T. Drzal. (2005) Natural fibers, biopolymers, and biocomposites , Book.

13. Anand, R., Sanadi, Daniel F. Caulfield, Rodney E. Jacobson, and Roger M. Rowell. (1995) Renewable agricultural fibers as reinforcing fillers in plastics: mechanical properties of kenaf –polypropylene composites, Reprinted from I&EC RESEARCH, 34.

14. Anuar, H. and Zuraida, A. (2011) Thermal properties of injection moulded polylactic acid-kenaf fiber bicomposites. Malaysian Polymer.6 (1):51-57.

15. Anshid, A., Haneef, A., Panampilly Bindu, Indose Aravind and Sabu Thomas (2008) Studies on tensile and flexural properties of short banana/glass hybrid fiber reinforced polystyrene composites. Journal of Composite Materials,42(15).

16. Arib, R.M.N., Sapuan, S.M., Ahmad, M.M.H.M., Paridah M.T.and Khairul Zaman, H.M.D. (2006) Mechanical properties of pineapple leaf fiber reinforced polypropylene composites. Material and Design, 27: 391-396.

17. ASTM D2734 – 94(2003) Standard test methods for void content of reinforced plastics.

18. Åström, B.T. (1997) Manufacturing of polymer composites. Chapman & hall, London.

19. Atta, A., Elnagdy S., Abdel-Raouf S., Elsaeed S. M. and Abdel-Azim A. (2005) Compressive properties and curing behaviour of unsaturated polyester resins in the presence of vinyl ester resins derived from recycled poly (ethylene terephthalate). Polymer Research Journal,12: 373-38.

20. Aziz, S. H., Ansell, M. P. (2004) The effect of alkalization and fiber alignment on the mechanical and thermal properties of kenaf and hemp bast fiber composites: part 1- polyester resin matrix. Composites Science and Technology, (63).

21. Azura, N. M. (2007) Synthesis, characterization and properties of the new unsaturated polyester resins for composite application, Thesis of Master of Science.

22. Banik, K., Abraham, T. N., Karger-Kocsis, J. (2007) Flexural creep Behavior of unidirectional and cross-ply all-poly (propylene) (PURE (R)) composites. Macromolecular Materials and Engineering, 292: 1280-1288.

23. Banik, K., Karger-Kocsis, J., Abraham, T. (2008) Flexural creep of all-polypropylene composites: Model analysis. Polymer Engineering and Science, 48: 941-948.

24. Barbero, J.B. and Damiani, T.M. (2002) Phenomenological prediction of tensile strength of E-glass composites from available aging and stress corrosion data. MSC paper.doc.

25. Batra, S. K. (1983) Other long vegetable fibers: abaca, banana, sisal, henequen, flax, hemp, sunn and coir, in Handbook of Fiber Science and Technology, IV, M Lewin and E. M. Pearce, Eds., Marcel Dekker, New York: 727-807.

26. Barbalace, K. (1995-2011, 08 22). Chemical Database. Retrieved 05 20, 2011, from Methyl ethyl ketone peroxide,Environmental Chemistry.com: http://environmentalchemistry.com

27. Beckermann,G (2007) Performance of hemp-fiber reinforced polypropylene composite materials .A Thesis of PhD in Materials and Process Engineering. The University of WAIKATO.

28. Beg MDH (2007) The improvement of interfacial bonding, weathering and recycling of wood fiber reinforced polypropylene composite, PhD thesis, the University of WAIKATO, New Zealand.

29. Beheshty, M., Nasiri, H. and Vafayan, M. (2005) Gel time and exotherm behaviors studies of an unsaturated polyester resin initiated and promoted with dual systems. Iranian Polymer Journal, 14: 990-999.

30. Bel-Berger, P., Hoven, T.V., Ramaswamy, G. N, Kimmel, L., and Boylson, E. (1999) Textile technology, cotton/kenaf fabrics: a viable natural fabric. The Journal of Cotton Science, (3).

31. Beijing, B. S. (2003) Improvement of kenaf yarn for apparel applications. Thesis for the Degree of Master of Science. School of the Human Ecology, University of Chemical Technology, Louisiana State University.

32. Bert, N. (2002) Kenaf fibers presentation of the 5th Annual Conference of The America Kenaf Society. Nov. 7-9, Memphis, TN.

33. Bledzki, A. K. and Gassan J. (1999) Composites reinforced with cellulose based fibers. Progress Polymer Science,24(221).

34. Betten, J. (2002) Creep Mechanics; Springer: New York

35. Betten, J., (2005) Creep Mechanics: 2nd Ed., Springer

36. Bonnia, N.N., Ahmad, SH., Zainol, I., Mamun, A.A., Beg, M.D.H. and Bledzki A.K. (2010) Mechanical properties and environmental stress cracking resistance of rubber toughened polyester/kenaf composite. eXPRESS Polymer Letters, 4, (2):55–61

37. Bos, H.L., Van Den Oever, M.J.A., O.C.J.J. (2002) Tensile and compressive properties of flax fibers for natural fiber reinforced composites. Materials Science, 37: 1683-1692.

38. Bos, H. (2004) The potential of flax fibers as reinforcement for composite materials, PhD thesis, Technische Universiteit Eindhoven, Netherland, ISBN 90-386-3005-0

39. Bowen, C.R., Dent, A.C., Stevens, R., Cain, M. and Stewart, M. (2005) Determination of critical and minimum volume fraction for composite sensors

and actuators, in 4March, Conference on Multi-Material Micro Manufacture, Elsevier: Karslruhe, Germany.

40. Buzarovska A., Bogoeva G., Grozdanov A., Avella M., Gentile G.,and Errico M. (2008) Potential use of rice straw as filler in eco-composite materials. Australian Journal of Crop Science. (2): 37-42.

41. Boyer, R. F. (1973) Glass temperatures of polyethylene. Macromolecules, 6(2): 288-299.

42. Calamari, T. A., Tao, W. and Goynes, W. R. (1997) A Preliminary study of kenaf fiber bundles and their composite cells. Tappi Journal, 80 (8): 149-154.

43. Cao, Y., Goda, K., Chen, H. (2007) Research and development of green composites, Chinese Journal Of Materials Research, 21(2): 119 – 125.

44. Cao, Y., Shibata, S. and Fukumoto, I. (2006) Fabrication and flexural properties of bagasse fiber reinforced biodegradable composites, Macromolecular Science, Part B, 45(4): 463-474.

45. Cazaurang-Martinez M. N., Herrear-Franco P. J., Gonzalez-Chi P. I., and Aguilar-Vega M.,(1991), Physical and mechanical properties of henequen fibers Applied. Polymer Science, 43(749).

46. Cerit A, Ahmetli G and Kurbanli R. (2011) Effect of unsaturated keto-groups on physico-mechanical and thermal properties of modified polystyrene. Applied polymer Science, 121:1193-1202.

47. Chen L., Columbus E. P., Pote J. W., Fuller M. J., and Black J. G., (1995), Kenaf Bast and Core Fiber Separation. Kenaf Association, Irving, TX: 15-19.

48. Chen H.-L., and Porter R. S., (1994), Composites of polythylene and kenaf, a natural cellulose fiber. Applied. Polymer. Science, 54:1781.

49. Chin L.S. (2008) Characterization of natural fiber polymer composites for structural application. MSc Thesis. University Technology Malaysia (UTM). Faculty of Civil Engineering. Malaysia.

50. Clemons, G. Sanadi A. R (2007) Reinforced Plastics Composites, 26(15):1587

51. Clemons C. M. (2002) Wood plastic composites in The United States. J. Forest Products 52(6):10-18.

52. Cook J. G., (1960), Handbook of textile fiber. Merrow publishing, Watford, UK.

53. Cook W. (1990) Composites and polymers. Polycot Polyester Products Applications Manual, 7th Edition, CCP.

54. Coppens d'Eeckenbrugge, G. and Leal, F. (2003) Morphology, anatomy and taxonomy. In: Bartholomew, DP, Paull, RE and Rohrbach, KG (eds) The Pineapple: Botany, Production and Uses. CABI Publishing, Oxon, UK:13-32.

55. Cox, H. L., Brit, J. (1952) The Elasticity and strength of paper and other fibrous materials. Applied. Physics, 3: 72-79.

56. Cyras, V. P., Martucci, J. F., Iannace, S. and Vazquez, A. (2002) Influence of the fiber content and the processing conditions on the flexural creep behavior of sisal-PCL-starch composites. Thermoplastic Composite Materials, 15(3): 253-265.

57. Dastoorian, F., Tajvidi, M. and Ebrahimi, G. (2010) Evaluation of time dependent behavior of a wood flour/high density polyethylene composites. Reinforced Plastic and Composites, 29 (1/2010): 132-143.

58. De Albuquerque, A.C., Joseph, K., Hecker de Carvalho, L., and d'Almeida, J.R.M. (2000) Effect of wettability and ageing conditions on the physical and mechanical properties of uniaxially oriented jute-roving-reinforced polyester composites. Composites Science and Technology, 60(6): 833-844.

59. Dhakal, H.N., Zhang, Z.Y. and Richardson, M.O.W. (2007) Effect of water absorption on the mechanical properties of hemp fiber reinforced unsaturated polyester composites. Composites Science and Technology, 6(19): 1674-1683

60. DMA 2980, (2002) Manual.

61. Du, Y., Zhang, J. and Xue, Y. A. (2008) Temperature-duration effects on tensile properties of kenaf bast fiber bundles (statistical table). Journal of Forest Product.

62. Espert, A., Vilaplana, F. and Karlsson, S. (2004) Comparison of water absorption in natural cellulosic fibers from wood and one year crops in polypropylene composites and its influence on their mechanical. Composites Part: A, 35:1267-1276.

63. Evans, W.J., Isaac, D.H., Suddell, B.C. and Crosky, A. (2002). Natural fibres and their composites: A global perspective. In the Proceedings of the 23rd Risoe International Symposium on Materials Science. Sustainable Natural and Polymeric Composites. Eds. Lilholt H. et al. Risoe National Laboratory, Roskilde, Denmark. 1-14.

64. France, P.W., Duncan, D.J., Smith, D.J. and Beales, K.J. (1983). Strength and fatigue of mulit-composites optical glass fibers. Materials Science,.18: 785-792.

65. Feng, C.C. (2011) Creep behaviour of wood-plastic composites. PhD Thesis, University of British Columbia, Vancouver.

66. Ferry, J. D. (1980). Viscoelastic properties of polymers, 3rd Edition, Wiley, New York.

67. Fukuda, H. and Takao, Y. (2000), Thermoelastic properties of discontinuous fiber composites. Comprehensive Composite Material, 1(13): 377-401.

68. Gamstedt, E. K. and Almgren, K. M. (2007) Natural fiber composites -with special emphasis on effects of the interface between cellulosic fibers and polymers. Proceedings of the 28th Ris∅ International Symposium on Materials Science.

69. Gharles, L., Harbans, L, and Venita, K. (2002) Kenaf production: fiber, feed and seed, trends in new crops and new uses. ASHS Press, Alexandria, VA.

70. Ghosh, P., Bose, N.R., Mitra B.C. and Das S. (1997) Dynamic mechanical analysis of frp composites based on different fiber reinforcements and epoxy resin as the matrix material. Applied. Polymer Science,64: 2467.

71. Ghasemi, I. and Kord, B. (2009) Long-term water absorption behaviour of polypropylene/wood flour/organoclay hybrid nanocomposite. Iranian Polymer Journal, 18(9): 683-691.

72. George, J., Weyenberg V., Ivens, I.J. and Verpoest, I. (1999) mechanical properties of flax fiber reinforced epoxy composite. Leuven, Belgium 2nd International Wood and Natural Fiber Composites Symposium June 28-29, Kassel, Germany.

73. George, J., Janardhan, J., Anand, J. S., Bhagwan, S. S. and Thomas, S. (1996) Melt rheological behaviour of short pineapple fiber reinforced low density Polethylene Composites. Polymer, 37: 5421-5431.

74. George, J., Sreekala, M. and Thomas, S. (1998) Stress relaxation behavior of short pineapple fibre reinforced polyethylene composites. Reinforced Plastics Composites, 17: 651–72.

75. Gere, J. M. (2004) Mechanics of material, 6th Edition, Thomson, Brooks/Cole.

76. Goertzen, W. E. and Kessler, M. R. (2007) Dynamic mechanical analysis of carbon/epoxy composites for structural pipeline repair. Composites: Part B (38):1-9.

77. Greco, A., Musardo C.and Maffezzoli, A. (2007) Flexural creep behaviour of PP matrix woven composite. Composites Science and Technology, 67: 1148–1158.

78. Hadid, M., Rechak, S. and Tati A. (2004) Long-term bending creep behavior prediction of injection molded composites using stress-time correspondence principle. Materials Science and Engineering, 385: 54-58.

79. Harun, J., Paridah Md, T., Abd. S. NorAini and Khalina Abdan, (2009) Kenaf-its establishment and journey towards energizing the wood-based and bicomposites industry in Malaysia, international conference on prospect of jute and kenaf as natural fibers, Dhakar-Bangladesh.

80. Hayaty, M., Beheshty, M. and Shrinkage H. (2004) Cure characterization and processing of unsaturated polyester resin containing PVAc low-profile additive. Iranian Polymer Journal, 1:389-396.

81. Hedenberg, P and Gatenhol, P. (1995) Conversion of plastic/cellulose waste into composites. I. Model of the interphase. Apply Polymer Science,56:641-651.

82. Hohane G.W.H., Hemminger W.F., Flammersheim H.-J. (2003) Differential Scanning Calorimetry. Book, Second Edition, Springer-Verlag Berlin Heidelberg New York.

83. Houshyar, S. and Shanks, R. A. (2004) Tensile properties and creep response of polypropylene fibre composites with variation of fibre diameter. Polymer International, 53: 1752–1759.

84. Houshyar, S., Shanks, R. A. and Hodzic, A. (2005) Tensile creep behaviour of polypropylene fibre reinforced polypropylene composites. Polymer Testing, 24: 257–264.

85. Houshyar, S. and Shanks, R. A. (2007) Mechanical and thermal properties of toughened polypropylene composites. Applied Polymer Science, 105: 390–397.

86. Huda MS, Drzal LT, Mohanty AK and Misra M. (2007) The effect of silane treated-and untreated-talc on the mechanical and physico-mechanical properties of poly(lactic acid)/newspaper fibers/talc hybrid composites. Composites:Part B, Vol.38, pp.367-379.

87. http://files.hanser.de/hanser/docs
88. http://www.cvl.gunma-ct.ac.jp/~aoi/aoihtml/kena_6.html
89. http://www.chinaconsultinginc.com/paperpulp.htm
90. http://www.tapplastics.com/shop/product.
91. http://www.bolton.ac.uk/CODATE/SPGuidetoComposites.pdf
92. http://www.kenaffiber.com/
93. http://www.3dchem.com

94. Idicula, M., Boudenne, A., Uma Devi, L., Ibos, L.,Candau, Y. and Thomas S. (2006) Thermophysical properties of natural fiber reinforced polyester composites, Composites Sciences and Technology,66(15).

95. Ichhaporia, P. K. (2008), Composites from natural fibers, PhD thesis North Carolina State University, USA.

96. Iijima T., Tochimoto T., and Tomoi M., (1991). Modification of epoxy resin with poly (Aryl Ether Ketone). Applied. Polymer. Science, 43: 1685.

97. Imai, T. (1967) Infrared study of the cure of unsaturated polyester. Applied Polymer Science, 11:1055-1063.

98. Izer, A., Barany, T. (2010) Effect of consolidation on the flexural creep behaviour of all-polypropylene composite. eXPRESS Polymer Letters,4(4): 210–216

99. Jawaid, M., Abdul Khalil, H. P. S. and Alattas, O. S. (2012). Woven hybrid bicomposites: dynamic mechanical and thermal properties. Composites: Part A, 43: 288-293.

100. Jeefferie, A. R., Nurul Fariha, O., Mohd Warikh, A. R., Yuhazri, M. Y., Haeryip Sihombing and Ramli, J. (2011). Preliminary study on the physical and mechanical properties of tapioca starch / sugarcane fiber cellulose composite. Engineering and Applied Sciences, 6(4): 7-15.

101. John, M. J. and Anandjiwal, R. D. (2008) Recent developments in chemical modification and characterization of natural fiber-reinforced composites, Polymer Composites, 29(2): 187-207

102. John Wiley & Sons, Encyclopedia of Textiles, Fibers, and Nonwoven Fabrics (M. Grayson, Ed.). New York, 1984, p.175.

103. John, M. J., Anandjiwala, R. D. and Thomas, S.(2008) Characterization of interface in composites using micro-mechanical techniques, chapter 20, Handbook of Vinyl Polmera.

104. Joseph, P.V., Rabello, M.S., Mattoso, L.H.C., Joseph, K., and Thomas, S. (2002) Environmental effects on the degradation behaviour of sisal fiber reinforced polypropylene composites. Composites Science and Technology, 62(10-11): 1357-1372.

105. Joung, M., Park J.-N. .K. and Koicichi, G. (2000) Composites, 60): 439-450.

106. Kalaprasad, G., Joseph, K., Thomas, S. and Pavithran, C. (1997) Theoretical modelling of tensile properties of short sisal fibre-reinforced low-density polyethylene composites. Materials Science, 32: 4261- 4267.

107. Kaldor, A. F. 1989. Preparation of kenaf barks and core fibers for pulping. Ankal ethod. Tappi Journal, 72 (9): 137-140.

108. Kano, T. (1997), Development and prospect of kenaf board. Kenaf society of kochi and economic reports of ehime. Nov.10, 25(44). Japanese.

109. Kathiresen, H. (2004) Lignocelluloses based hybrid laminate composite: physical, mechanical and flammability properties of oil palm fiber /glass fiber reinforced epoxy resin. Thesis of Master of Science

110. Kelly, A. and Tyson, W.R. (1965) Tensile properties of fiber-reinforced metals: copper/tungsten and copper/molybdenum. Journal of the Mechanics and Physics of Solids, 13: 329-350.

111. Kelly, A. and Tyson, W.R. (1969) Journal of Mechanics and Physics of Solids, 13: 329-336

112. Kerns, KR, Collins, JL and Kim, H. 1936. Developmental studies of the pineapple Ananas comosus (L.) Merr. The New Phytologist, 35: 305-317.

113. Kenaf Eco Fibers Italy S.p.A. (1999), http://www.kenaf-fiber.com/en/cenni-storici.asp.

114. KENAF ECO FIBRES ITALIA S.p.A., N. f. a. k. f. t. i., acoustic insulation, green building and automotive industry. (2005), http://www.kenaf-fibre.com/en/infotec-abella10.asp.

115. Khanna, Y. P., Turi, E. A., Taylor, T. J., Vickroy, V. V. and Abbott, R. F (1985) Dynamic mechanical relaxations in polyethylene. Macromolecules, 18(6): 1302-1309.

116. Kim, K. J., Yu, W-R. and Harrison, P.(2008) Optimum consolidation of self-reinforced polypropylene composite and its time-dependent deformation behavior. Composites Part A: Applied Science and Manufacturing, 39:1597–1605.

117. Kuan, H. T., Cantwell, W. and Dd Akil, H. (2009) The mechanical properties of hybrid composites based on self-reinforced polypropylene, Malaysian Polymer, 4(2): 71-80.

118. Kuang, W. and Richardson, A. A. (2007) New amine promoter for low temperature cure of MEKP initiator unsaturated polyester resin systems. Composites Research Journal, 1(4).

119. Kuang, W. (2006) A new amine promoter for low-temperature cure of MEKP initiated unsaturated polyester resin systems. COMPOSITES Convention and Trade Show American Composites Manufacturers Association, St. Louis, MO USA, October 18-20.

120. Kushwaha, P.K. and Kumar, R. (2010) Studies on water absorption of bamboo-polyester composites: effect of silane treatment of mercerized bamboo". Polymer-Plastics Technology and Engineering, 49: 45-52.

121. Lee, S. M. (1991) International Encyclopedia of Composites,Vol. 4, VCH, New York, P: 9.

122. Lee, B.H., Kim, H.J., and Yu, W.R. (2009) Fabrication of long and discontinuous natural fiber reinforced polypropylene bicomposites and their mechanical properties, Fibers and Polymers, 10(1): 83-90.

123. Lee, B.H., Kim, H.S., Lee, S., Kim, H.J. and Dorgan, J.R. (2009) Bio-composites of kenaf fibers in polylactide: role of improved interfacial adhesion in the carding process. Composites Science and Technology, 69: 2573-2579.

124. Lee, Y.J., Lee, H.K., Shim, M. and Kim, S.W. (2000) Thermal decomposition characteristics of epoxy network chemically toughened with liquid rubber using dynamic TG analysis. Industrial and Engineering Chemistry, 6: 250-255.

125. LeVan, S.L. and Winandy, J.E. (1990) Effects of fire retardant treatment on wood strength: A Review. Wood and Fiber Science, 22(1):113-131.

126. Li, D. (2002), Kenaf production, Research and Development in China. International Kenaf Symposium. T. N. USA.

127. Lilholt, H. and Lawther, J.M. (2000) Natural organic fibers, in comprehensive composite materials, T.-W. Chou, Editor. Elsevier Science: Oxford: 303-325.

128. Lin, P., Lin, L., Wu, J. and Lin, N. (2004) Breeding of FuHong4, A Kenaf Variety with High- Yielding and Resistance. Plant Fiber and Products 26(1):1-4.

129. Liu, Y. (2005) Thesis of MSc, Diallel and stability analysis of kenaf (hibiscus cannabinus l.) in South Africa. Faculty of Natural and Agricultural Sciences, University of the Free State, Bloemfontein South Africa.

130. Liu, X., Dever, M., Fair, N. and Benson, R.S. (1997) Thermal and mechanical properties of poly(lactic acid) and poly(ethylene/butylene succinate) blends. Environ Polym Degrad, 5: 225-36.

131. Louis, R. and Ross, P. J. (2007). Effects of Methyl Ethyl Ketone Peroxide on the Performance of Cast Polymers. Composites Research Journal, 1 (4):14-23

132. Lu, J.Z., Wu, Q. and McNabb, H.S. (2000) Chemical coupling in wood fiber and polymer composites: a review of coupling agents and treatments. Wood and Fiber Science, 32(1): 88-104.

133. Lu, M.G., Shim, M.J., and Kim, S.W. (1997) Dynamic DSC analysis for the polymerization of an unsaturated polyester/styrene system. Applied Chemistry, 1: 357-360

134. Lukasz, L. and Jörg, D. (2006) Differential scanning calorimetry. 20th November Winter Semester 07.

135. Luo, S. and Netravali, A. N. (1999). Mechanical and thermal properties of environment-friendly ''green'' composites made from pineapple leaf fibers and poly(hydroxybutyrate-co-valerate) resin. Polymer Composites, 20: 367–378.

136. Madson, B. O. and Liholit, H. (2003). Physical and mechanical properties of unidirectional plant fiber composites—an evaluation of the influence of porosity. Composite Science and Technology, 63: 1265–1272.

137. Matthews, F.L. and Rawlings, R.D. (2005) Composites materials, engineering and science. 1st ed. Cambridge: Woodhead Publishing Ltd, 169(73): 310-11.

138. Maldas, D. and Kokta, B.V. (1994) Role of Coupling Agents on the Performance of Woodflour-Filled Polypropylene Composites. International Journal of Polymeric Materials, 27: 77-88.

139. Mallick, P. K. (1993) Fiber-reinforced composite materials, manufacturing, and design. Arcel Decker, Inc., New York:

140. Menard, H.P. (2008), Dynamic mechanical analysis. Second Edition. Book, CRC Press. Taylor and Francis Group.

141. Mingchao, W., Zuoguang, Z. and Zhijie, S. (2009) The hybrid model and mechanical properties of hybrid composites reinforced with different diameter fibers. Journal of Reinforced Plastics and Composites, 28(257).

142. Mirbagheri, J., Tajvidi, M., Hermanson, J. C. and GHASEMI, I. (2007), Tensile properties of wood flour/kenaf fiber polypropylene hybrid composites. Applied Polymer Science, 105(5): 3054-3059.

143. Mokhtar, M., Rahmat, A. and Hassan, A. (2007) Characterization and treatments of pineapple leaf fibre thermoplastic composite for construction application, RMC, Malaysia

144. Mohanty, A., Misra, M. and Drzal L. (2005) Natural fibers, biopolymers, and biocomposites, CRC Press, New York

145. Mohanty, A.K., Misra, M., and Drzal, L.T. (2002) Sustainable biocomposites from renewable resources: opportunities and challenges in the green materials world. J Polymers and the Environment, 10: 19-26

146. Mohanty, A., Misra, M. and Hinrichsen, G. (2000) Biofibers, biodegradable polymers and biocomposites. An overview, Macromol. Mater, Eng., 1: 276-277.

147. Moreau, J. P., Bel-Berger, P. and Tao, W. (1995) Mechanical Processing of kenaf for nonwovens. Tappi Journal, 78 (2): 96-105.

148. Mukherjea, R. N., Pal, S.K., Sanyal, S. K. and Phani K. K. (1984) Role of interface in fiber reinforced polymer composites with special reference to natural fibers. Polymer. Material, 1(69).

149. Najafi, S., Sharifnia, H. and Tajvidi, M. (2008) Effect of water absorption on creep behavior of wood plastic composites, Journal of Composite Material, 42(10): 933 – 1002.

150. Najafi, A. and Khademi-Eslam H. (2011) Lignocellulosic filler/recycled HDPE composites: effect of filler type on physical and flexural properties. BioResources, 6(3): 2411-2424.

151. Nickel, J. and Riedel, U. (2003), Acticities in biocomposites, J Materials Today: 44-48.

152. Nielsen, L.F. and Landel, R.F. (1994) Mechanical properties of polymers and composites. New York, NY: Marcel Dekker, Inc.

153. Nishino, T., Hirao, K., Kotera, M., Nakamae, K. and Inagaki H. (2003) Kenaf reinforced biodegradable composite. Composites Science and Technology, 63: 1281-1286.

154. Noorunnisa Khanam, P., Reddy, M. M., Raghu, K., John, K., and Naidu, S. V. (2007) Tensile, flexural and compressive properties of sisal/silk hybrid composites. Reinforced Plastics and Composites, (26): 1065.

155. Nunez, A. J., Marcovich, N. E. and Aranguren, M. I. (2004) Analysis of the creep behavior of polypropylene-woodflour composites. Polymer Engineering and Science, 44(8): 1594-1603.

156. Ochi, S. (2008) Mechanical properties of kenaf fibers and kenaf/PLA composites, Mechanics of Materials, 40: 446–452.

157. Ochi S. (2010) Tensile properties of kenaf fiber bundle. SRX Materials Science, Vol.2010, ID. 152526.

158. Onal, L. and Karaduman, Y. (2009) Mechanical characterization of carpet west natural fiber-reinforced polymer composites. Composites Materials, 43(16): 1751-1768.

159. Painchaud, Y., Poulin, M., Morin, M. and Guy, M. (2006) Fiber bragg grating based dispersion compensator slope-matched for LEAF fiber. Fiber Optics Components.

160. Paridah, M. T., NorHafizah Abd. Wahab, and Jalaluddin H. (2007) Properties of kenaf board bonded with formaldehyde-based adhesives 2007 D5 IUFRO Forest Products and Environment: A Productive Symbiosis Taipei, Taiwan, 29 October to 2 November.

161. Pathan, L.A., Oommn, Z. and Thomas, S. (2003) Dynamic mechanical analysis of banana fiber reinforced polyester composites. Composites Science Technology, 63: 283-293.

162. Pavithran, C., Mukherjee, P.S., Brahmakumar, M. and Damodaran, A.D. (1987) Impact properties of natural fiber composites. Materials Science Letters, 6: 882-884.

163. Peniche-Covas, C., Arg¨uelles-Monal, W. and Rom´an J. S. (1993) A kinetic study of the thermal degradation of chitosan and a mercaptan derivative of chitosan. Polymer Degradation and Stability, 39(1): 21–28.

164. Peijs, T. (2002) Novel concepts for obtaining sustainable composites based on synthetic polymers. In the Proceedings of the 23rd Risoe International Symposium on Materials Science. Sustainable Natural and Polymeric Composites. Eds. Lilholt H. et al. Risoe National Laboratory, Roskilde, Denmark. 61-75.

165. Penczek, Piotr, Czub, and Pielichowski (2005) Unsaturated polyester resins. Chemistry and Technology, Advance Polymer. Science, 184: 1-95.

166. Perez, C.J., Alvarez, V.A. and Vazquez, A. (2008) Creep behaviour of layered silicate/starch–polycaprolactone blends nanocomposites. Materials Science and Engineering A, 480: 259–265.

167. Placket D., (2002), The natural fiber polymer composites industry in europe- technology and markets. In 7th Toronto Conference on "Progress in Woodfiber-Plastic Composites". Toronto, Canada.

168. Polymers (From Various Sources, Including the Canadian CBD 158/159, Text, ect).

169. Pothan, L.A., Oommen, Z. and Thomas, S. (2003) Dynamic mechanical analysis of banana fiber reinforced polyester composites. Composites Science and Technology, 63: 283-293.

170. Pracella, M., Minhaz-UI Haque, Md. and Alvarez, V. (2010). Functionalizatio, compatibilization and properties of polyolefin composites with natural fibers. Polymers, 2: 554-574.

171. Prasad, S. V., Pavithran, C. and Rohatgi, P. K. (1983) Alkali Treatment of Coir Fibers for Coir-Polyester Composites, Material Science, 18: 1443.

172. Pritchard, G. (1980) Developments in reinforced plastics. Applied Science, London:32

173. Öztürk, S. (2010) Effect of fiber loading on the Mechanical Properties of Kenaf and Fiberfrax fiber reinforced Phenol – Formaldehyde Composite, Journal of Composite Materials, 0(00): 1-24.

174. Rahmat, A. R. and Day, R. J. (2003) Curing characteristics of unsaturated polyester/ aramid reinforced composites. Technology, University Technology Malaysia: 83-96.

175. Rashdi, A.A.A,, Sapuan, S.M,, Ahmad M.M.H.M. and Khalina, A. (2009) Water absorption and tensile properties of soil buried kenaf fiber reinforced unsaturated polyester composites (KFRUPC), Journal of Food, Agriculture & Environment,7 (3&4): 909 – 911.

176. Rashdi, A.A.A., Sapuan, S.M., Ahmad, M.M.H.M. and Khalina, A. (2010) Combined effects of water absorption due to water immersion, soil buried and natural weather on mechanical properties of kenaf fiber unsaturated polyester

composites (KFUPC). International Journal of Mechanical and Materials Engineering (IJMME), 5(1): 11-17.

177. Ray, D., Sarka,r B. K., Rana, A. K. and Bose, N. R. (2001) The mechanical properties of vinylester resin matrix composites reinforced with alkali treated jute fibers, Composites Part A, 32:119.

178. Ray, D. Sarkar, B.K., Das, S. and Rana A. K. (2002), Dynamic mechanical and thermal analysis of vinylester resin matrix composites reinforced with alkali treated jute fibers. Composites Science Technology, 2: 911.

179. Read, B. E. and Tomlins, P. E. (1997) Creep and physical aging of injection molded fiber reinforced polypropylene. Polymer Engineering and Science, 37(9): 1572-1581.

180. Reinhart, T.J. and. Clements, L.L (1987) Introduction to composites, Volume 1 Engineered Materials Handbook: Composites, ASM International (Metals Park OH).

181. Riande, E., Galleja, R. D., Prolongo, M. G., Masegosa, R. M. and Salom, C. (2000) Polymer viscoelasticity stress and strain in practice. Marcel Dekker A.G, Switzerland.

182. Roger, M., Rowell, Anand Sanadi, Rod Jacobson (1999) Caulfield's test using canola oil as in: Kenaf Properties, Processing and Products; Mississippi State University, Ag & Bio Engineering: 381-392. ISBN 0-9670559-0-3. Chapter 32n.

183. Roger, M. R., Anand, R. S. and Daniel, F. C. (1997) Utilization of natural fibers in plastic composites: problems and opportunities. Report.

184. Rong, M.J., Zhang M.Q., Liu, Y., Yang, G.C., Zeng, H.M. (2001) The effect of fibre treatment on the mechanical properties of unidirectional sisal-reinforced epoxy composites. Composites Science and Technology, 61:1337-1447.

185. Rout, J., Mishra, M., Tripathy, S. S., Nayak, S. K. and Mohanty, A. K. (2001) The influence of fiber surface modification on the mechanical properties of coir-polyester composites, Polymer Composites, 22:468.

186. Ross, L. R., Petersen, J. A. and Lakatos, C. W. (2007) Effects of Methyl Ethyl Ketone Peroxide on the performance of cast polymers. Composites Research, 1(4): 14 – 23.

187. Rowell, R. M., Han, J. S. and Rowell, J. S. (2000) Characterization and factors. effecting fiber properties, in natural polymers and agrofibers composites, E. L.A.a.M.: Sao Carlos, Brazil:115-134

188. Rowell, R. M. and Han, J.S. (1999) Changes in kenaf properties and chemistry as a function of growing time. in: kenaf properties, Processing and Products. Mississippi State University. Mississippi State, MS: 32-57.

189. Rowell, R.M. (1997) Chemical modification of agro-resources for property enhancement, in paper and composites from agro-based resources. CRC Press: 351-375.

190. Sabbagh, A. E.L., Steuernagel, L. and Ziegmann, G. (2009) Processing and modeling of the mechanical behavior of natural fiber thermoplastic composite: flax/polypropylene. Polymer Composites, 30(4): 510-519.

191. Saha, A.K., Das S., Bhatta, D. and Mitra, B.C. (1999) Study of Jute Fiber Reinforced Polyester Composites by Dynamic Mechanical Analysis. Applied. Polymer. Science, 71: 1505.

192. Sanadi, A.R., Young, R.A., Clemons, C.M. and Rowell, R.M. (1994) Recycled newspaper fibers as reinforcing fillers in thermoplastics: Part 1 – Analysis of tensile and impact properties in polypropylene. Journal of Reinforced Plastics and Composites, 13: 54-67.

193. Sanadi, A. R., Hunt, J.F., Caulfield, D.F., Kovacsvolgyi, G. and Destree, B. (2002) High fiber-low matrix composites: kenaf fiber/polypropylene, Sixth International Conference on Wood Fiber-Plastic Composites, Forest Research Society, May 15-16, Madison, Wisconsin Madison, WI: 121-124.

194. Sanchez, E.M.S., Zavaglia, C.A.C. and Felisberti, M.I. (2000) Unsaturated polyester resins: influence of the styrene concentration on the miscibility and mechanical properties. Polymer, 41: 765–769.

195. Sarkar, B. K., Roy R. and Ray, D. (1997) Emerging dominance of composites as a structural material. Inst. Eng. India, 78(31).

196. Sartorius User's Manual, (2008). Density Determination Kit, 98647-002-37.0000.

197. Shamsun Nahar, Khan, R. A., Dey, K., Sarker, B., Das, A. K. and Ghosha, S. (2011) Comparative studies of mechanical and interfacial properties between jute and bamboo fiber-reinforced polypropylene-based composites. Thermoplastic Composite Materials, DOI: 10.1177/0892705711404725.

198. Shi, S. Q. and Gardner, D. J. (2006) Effect of density and polymer content on the hygroscopic thickness swelling rate of compression molded wood fiber/polymer composites. Wood Fiber Science. 38: 520-526.

199. Sheldon, Q.S. and Douglas, J.G. (2005) Hygroscopic thickness swelling rate of compression molded wood fiberboard and wood fiber/polymer composites. Composites: Part A, 37:1276-1285.

200. Sharifah, H. A. and Martin, P. A. (2004, a) The effect of alkalization and fiber alignment on the mechanical and thermal properties of kenaf and hemp bast fiber composites: part 1- polyester resin matrix. Composites Science and Technology, 63.

201. Shrifah, H. A. and Martin, P. A. (2004, b) The effect of alkalization and fiber alignment on the mechanical and thermal properties of kenaf and hemp bast fiber composites: part 1- cashew nut shell liquid matrix. Composites Science and Technology, 63.

202. Shukla, S., Shukla, A.K., Singh, P.K., Singhla, R. and Nagpal, A.K. (2006) Effects of concentration of Methyl Ethyl Ketone Peroxide on gelation characteristics and shrinkage of solventless polyester varnish. Oleo Science, 55(6):299-303.

203. Sinha, R. (2000) Outlines of polymer technology. Prentice-Hall by India Private Ltd, New Delhi.10001.

204. Sharifah, H.A. and Martin, P. A. (2004) The effect of alkalization and fiber alignment on the mechanical and thermal properties of kenaf and hemp bast fiber composites: Part 1-polyester resin matrix. Composites Science Technology, 64:1219-30.

205. Satish, K.G., Siddeswarappa, B. and Mohamed, K. (2010) Characterization of in-plane mechanical properties of laminated hybrid composites. Minerals & Materials Characterization & Engineering, 9(2): 105-114.

206. Satyanarayana, K. G., Pai, B. C., Sukumaran, K., and Pillai, S. G. K. (1990) Fabrication and Properties of Lignocellulosic Fiber-Incorporated Polyester Composites. Handbook of Ceramics and Composites, Cheremisinoff, N. P., (1), Marcel Dekker, New York, P: 341, Chap. 12.

207. Shenoy, M. A. and Melo, D. J. D. (2007) Evaluation of mechanical properties of unsaturated polyester-guar gum/hydoxypropyl guar gum composites. eXPRESS Polymer Letters, 1: 622-628.

208. Shibata, S., Yong, C. and Fukumoto, I. (2005) Press Forming of Short Natural Fiber-Reinforced Biodegradable Resin: Effects of Fiber Volume and Length on Flexural Properties. Polymer Testing, 24(8): 1005-1011.

209. Shibata S, I. Fukumoto I. (2006) Effects of Bamboo and Kenaf Fibers on the Mechanical Properties of Lightweight Porous Composites. Global Plastic Environment Conference GPEC, Orland, Florida, USA.

210. Shibata, S., Yong, C. and Fukumoto, I. (2006), Fabrication of Composites Made from Kenaf Fiber and Biodegradable Resin by a Hot Press and the Flexural Properties. Journal Transaction of the Japan Society of Mechanical Engineers, 72: 676-681.

211. Shibata, S. Fukumoto, I. and Cao, Y. (2006) Effects of fiber compression and length distribution on the flexural properties of short kenaf fiber- reinforced biodegradable composites. Polymer Composites, 27(2):170 -176,

212. Singha, A. S. and Thakur, V. K. (2008) Saccaharum Cilliare Fiber Reinforced Polymer Composites. E-Journal of Chemistry, 5:782-791.

213. Sinha, R. (2000) Outlines of Polymer Technology. Prentice-Hall by India Private Ltd. New Delhi-10001.

214. Sjöström, E. (1981) Wood polysaccharides. Wood Chemistry, Fundamentals and Applications, Academic Press, New York, NY, Chapter 3, 51.

215. SP Guide to Composites www.spsystems.com

216. Skrifvars, M. (2000) Synthetic modification and characterisation of unsaturated polyesters. Academic Dissertation, University of Helsinki, August 11.

217. Sombastsompop, N. and Chaochanchikul, K. (2004) Effect of moisture content on mechanical properties, thermal and structural stability and extruded texture of poly (vinyl chloride)/wood sawdust composites. Polymer, 53:1210-8.

218. Sreenivasan, V. S., Ravindran, D., Manikandan, V. and Narayanasamy, R. (2010) Mechanical properties of randomly oriented short sansevieria cylindrica fiber/polyester composites. Materials and Design, 11(42).

219. Strong, A.B. (1989) Fundamentals of composites manufacturing: materials, methods, and applications. Society of Manufacturing Engineers, Dearborn, MI.

220. Taj, S., Munawar, M.and Khan, S. (2007) Natural Fiber Reinforced Polymer Composites. Proc.Pakistan Acad.Sci,44 (2):129-144.

221. Tajeddin, B. Abdul Rahman, R., Abdulah, L. C., Ibrahim, N. A. and Yusof ,Y. A. (2009) Thermal properties of low density polyethylene-filled kenaf cellulose composites. European Journal of Scientific Research, 32(2):223-230.

222. Tajvidi, M., Falk, R. H. and Hermanson, J. C. (2005) Time-temperature superposition principle applied to a kenaf-fiber/high-density polyethylene composites. Applied Polymer Science, 97, 1995-2004.

223. Tajividi, M., Flak, R. H. and Hermanson, J. C. (2006) Effects of natural fibers on thermal and mechanical properties of natural fiber polypropylene composites studied by dynamic mechanical analysis. Applied Polymer Science, 101:4341-4349.

224. Tamrakar, S., Lopez-Anido, R. A, Kiziltas, A. and Gardner, D. J. (2011) Time and temperature dependent response of a wood–polypropylene composite. Composites: Part A, 42: 834–842.

225. Takahashi, S. (1964) Journal of Japan. Soc. Colour Material, 37(155).

226. Tao, W., Moreau, J. P. and Calamari, T. A. (1994) Properties of nonwoven mats from kenaf fiber. Tappi Journal, 78(8): 165-169.

227. Tao, W., Calamari, T.A., Shis, F. F. and Cao, C. (1997) Characterization of kenaf fiber bundles and their nonwoven mats. Tappi Journal. 80(12):162-166.

228. Termonia, Y. (1990) Tensile strength of discontinuous fiber-reinforced Composites. Material Science, 25:4644-4650.

229. Thiruchitrambalam, M., Alavudeen, A., Athijayamani, A., Venkateshwaran N. and Elaya Perumal A. (2009) Improving mechanical properties of banana/kenaf polyester hybrid composites using sodium laulryl sulfate treatment. Materials Physics and Mechanics, 8:165-173.

230. Thomason, J. L., Vlug, M. A. (1996) Influence of fiber length and concentration on the properties of glass fibre-reinforced polypropylene: Tensile and flexural modulus. Composites: Part A, 27(A):477-484.

231. Thwe, M. M. and Liao, K. (2002) Effects of environmental aging on the mechanical properties of bamboo-glass fiber reinforced polymer matrix hybrid composites. Composites: Part A, 33:43-52.

232. Tucker, III C. L. and Liang, E. (1999) Stiffness predictions for unidirectional short fiber composites: review an evaluation. Composites Science and Technology. (59): 655-671.

233. Vilay, V., Mariatti, M., Taib, R.M. and Todo, M. (2008) Effect of fiber surface treatment and fiber loading on the properties of Bagasse fiber-reinforced unsaturated polyester composites. Composites Science and Technology, 68:631-638.

234. Waigaonkar, S., Babu, B. J C. and Rajput, A. (2011) Curing studies of unsaturated polyester resin used in FRP Products. Indian Journal of Engineering and Materials Sciences, 18:31-39.

235. Walker, J.C.F. (1993) Basic Wood chemistry and cell wall ultrastructure, in primary wood processing. Chapman and Hall: London:43-67.

236. Wallenberger, F. T. and Weston, N. (2004) Natural fibers, plastics and composites natural. Materials Source Book from C.H.I.P.S. Texas.

237. Walker, J. C. (1993) Timber preservation in primary wood processing. Chapman and Hall: London. P: 285-289.

238. Wambua, P., Ivens, J. and Veroest, I. (2003) Natural fibers: can they replace glass in fiber reinforced plastics. Composites Science and Technology, 63(9): 1259-1264.

239. Webber III C. L., Bledose V. K., and Bledsoe R. E. (2002) Kenaf harvesting and processing, Trends in New Crops and New Uses, Janick J. and Whipkey A., Eds., ASHS Press, Alexandria.

240. Wielage, B., Lampke, T., Marx, G., Nestler, K. and Starke, D. (1999) Thermogravimetric and differential scanning calorimetric analysis of natural fibers and polypropylene. Thwemochim. Acta, 337(169).

241. Wunderlich, B. (1990) Thermal analysis. San Diego: Academic Press.

242. Xiaolin, Xu. (2008) Cellulose fiber reinforced Nylon 6 or Nylon 66 composites. A Thesis of PhD. Georgia Institute of Technology.

243. Xue, Y., Du, Y., Elder, S., Sham, D., Horstemeyer, M. and Zhang, J. (2007) Statistcal tensile properties of kenaf fiber and its composites. Proceeding of 9th International Conference on Wood and Biofiber Plastic Composite, Madison, USA.

244. Xue, Y., Du, Y., Elder S., Wang, K. and Zhang, J. (2009) Composites: Part B, 40:189.

245. Xu, Y., Kawata, S., Hosoi, K., Kawai, T., and Kuroda, S. (2009) Thermomechanical properties of the silanized-kenaf/polystyrene composites. eXPRESS Polymer Letters, 3(10): 657-664.

246. Yanjun, X. (2009) Creep behavior of natural fiber reinforced polymer composites. PhD Thesis, Louisiana State University,

247. Yildiz, S., Gezer, E. D., and Yildiz, U. C. (2006) Mechanical and chemical behavior of spruce wood modified by heat. Building and environment, 41(12): 1762-1766.

248. Zgoul, M. H., Habali, S. M. (2008) An investigation into plastic pipes as hot water transporters in domestic and industrial applications. Jordan Journal of Mechanical and Industrial Engineering, 2:191-200.

249. Zhan, M. and Wool, R. P. (2010) Biobased composites resins design for electronic materials. Applied Polymer Science, 118:3274-3283.

LIST OF PUBLICATIONS

Journal papers:

1. **E. Osman**, A. Vakhguelt, I. Sbarski; S. Mutasher, (2011) Mechanical Properties of Kenaf -Unsaturated Polyester Composites: Effect of Fiber Treatment and Fiber Length, Journal of Advanced Materials Research. Vols. 311-313, pp 260-271.

2. **Ekhlas A. Osman**, Anatoli Vakhguelt, Igor Sbarski; Saad A. Mutasher, (2012), The Effect of Styrene Concentration Ratio on the Unsaturated Polyester Properties. Malaysian Polymer Journal. Vol. 7 No. 2, pp 46 - 55.

3. **Ekhlas A. Osman**, Anatoli Vakhguelt, Igor Sbarski; Saad A. Mutasher, (2012). Kenaf /Recycled Jute Natural Fibers Unsaturated Polyester Composites: Water Absorption /Dimensional Stability and Mechanical Properties. International Journal of Computational Materials Science and Engineering, vol.1, No.1, DOI: 10.1142/S2047684112500108.

4. **Ekhlas A. Osman**, Anatoli Vakhguelt, Igor Sbarski; Saad A. Mutasher, (2012). Effect of Water Absorption on Tensile Properties of Kenaf fiber Unsaturated Polyester Composite, Accepted, Suranaree Journal of Science and Technology.
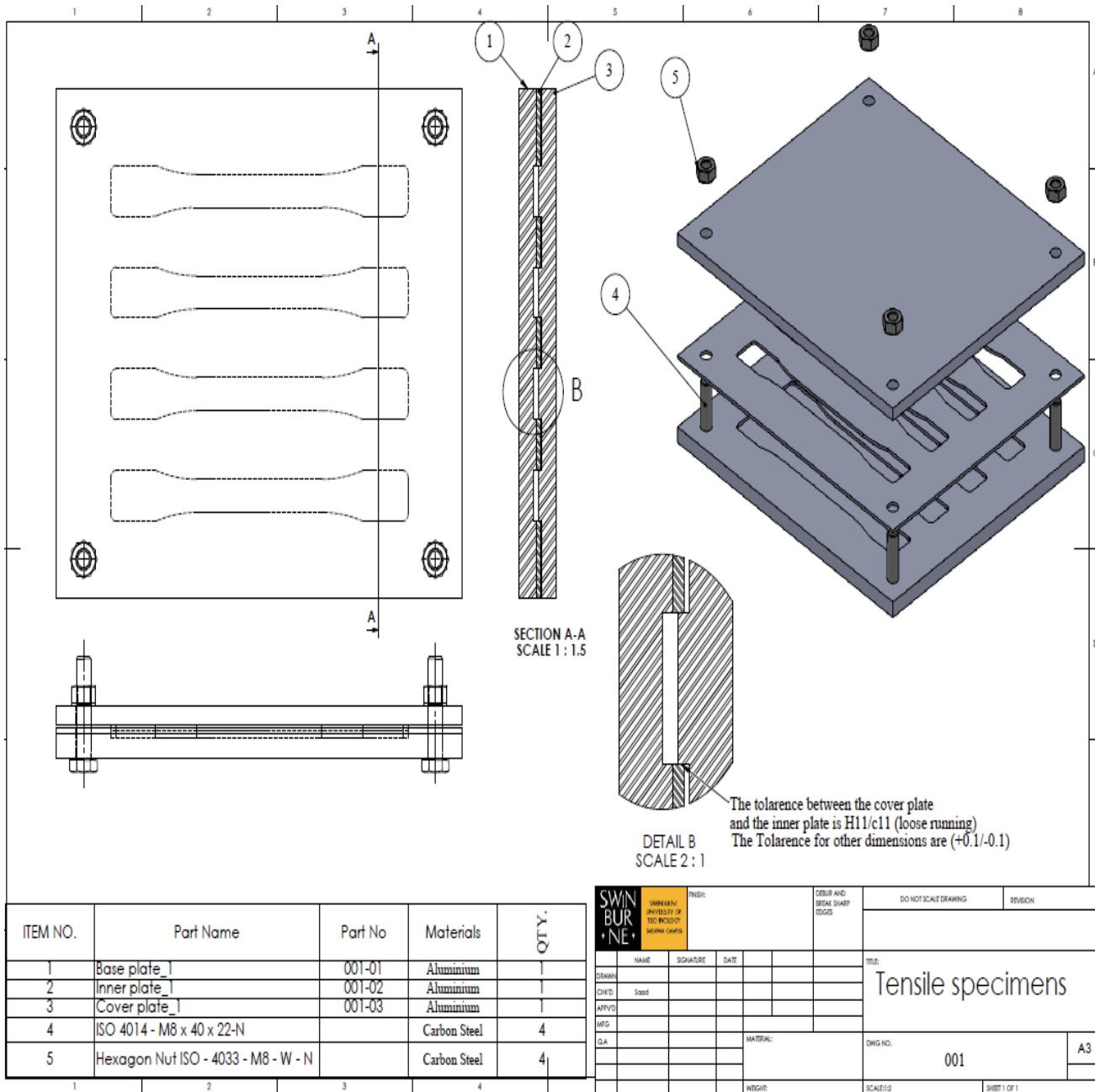
Conference papers:

1. **Ekhlas A. Osman**, Anatoli Vakhguelt, Igor Sbarski; Saad A. Mutasher, (2009) Kenaf Fiber Polymer Composite, A Review. In proceedings of the International Conference on Kenaf and Allied Fibers (ICKAF09) University Putra Malaysia, December 01-03, Malaysia.

2. **Ekhlas A. Osman**, Anatoli Vakhguelt, Igor Sbarski; Saad A. Mutasher, (2010) Fiber Preparation and Unsaturated Polyester Rheological Properties of Kenaf Natural Fiber Composite. In proceedings of 7th International Materials Technology Conference and Exhibition (INNOVATION FOR SUSTAINABILITY) (IMTCE2010) 13th-16th June Kuching, Sarawak, Malaysia.

3. **Ekhlas A. Osman**, Anatoli Vakhguelt, Igor Sbarski; Saad A. Mutasher (2011), The Impact Properties of Kenaf Fiber Unsaturated Polyester Composites, in proceedings of ASEAN Australian Engineering Congress AAEC2011, 25 – 27 July, Kuching, Sarawak, Malaysia.

4. **Ekhlas A. Osman**, Anatoli Vakhguelt, Igor Sbarski; Saad A. Mutasher (2011), Water Absorption Behavior And Its Effect on the Mechanical Properties of Kenaf Natural Fiber Unsaturated Polyester Composites, in proceedings of 18th International Conference on Composite Materials (ICCM18), Jeju, Korea August 21-26.

5. **Ekhlas A. Osman**, Anatoli Vakhguelt, Igor Sbarski; Saad A. Mutasher, (2012), Mechanical Properties of Hybrid Kenaf/ Recycled Jute fibers Composites, in proceedings of Brunei International Conference in Engineering and Technology (BICET) 25 -26 January, Bandar Seri Begawan, Brunei.

6. **Ekhlas A. Osman,** Anatoli Vakhguelt, Igor Sbarski; Saad A. Mutasher, (2012), Thermal and Dynamic Mechanical Properties of Kenaf Unsaturated Polyester composites: Using DMA and TGA Tests, in proceedings of Kazakhstan International World Congress on Engineering & Technology, Almaty, Kazakhstan, 1-3 June 2012
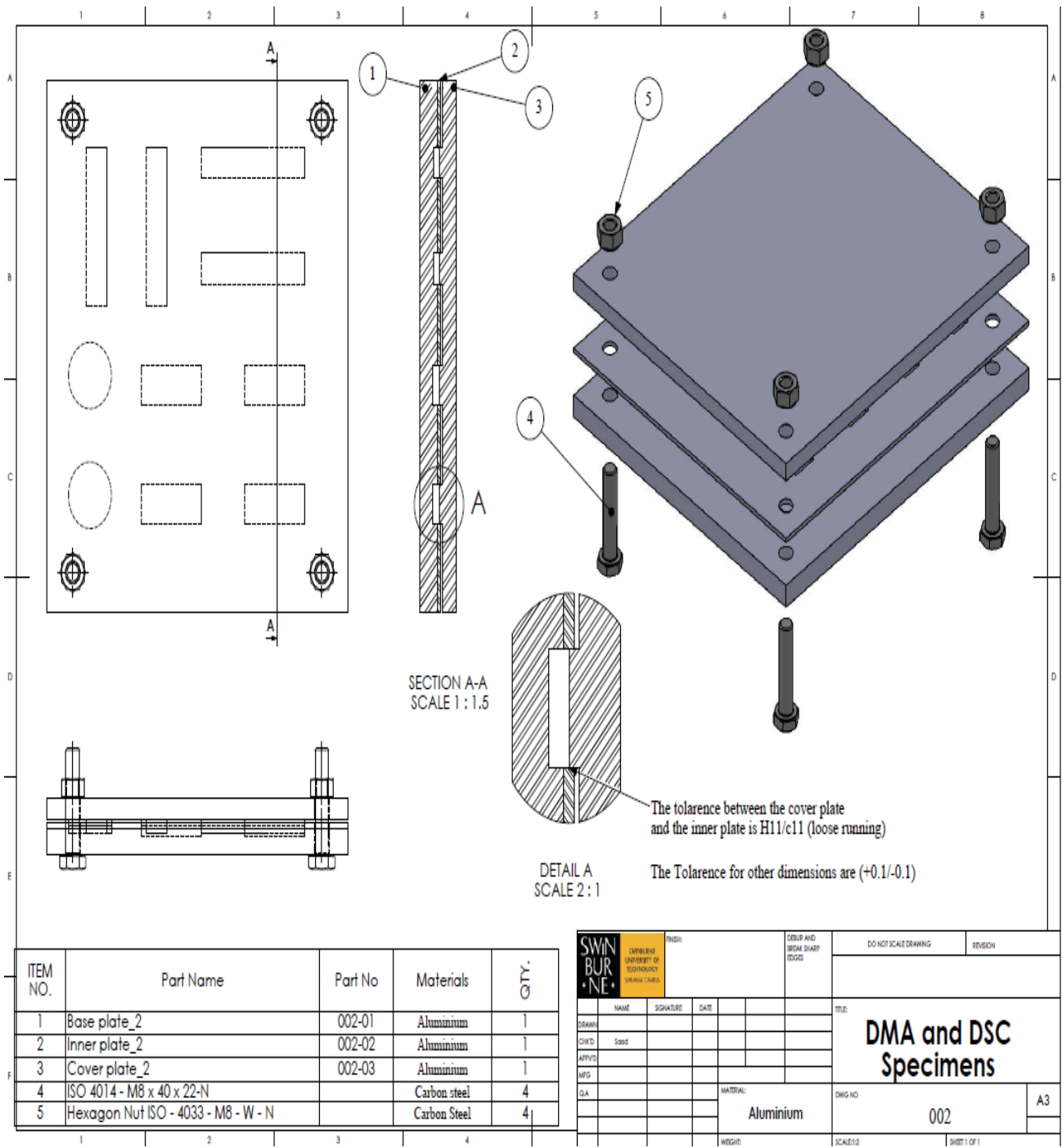
APPENDICES

## Appendixes A

- Design the mold for tensile specimens

ITEM NO.	Part Name	Part No	Materials	QTY.
1	Base plate_1	001-01	Aluminium	1
2	Inner plate_1	001-02	Aluminium	1
3	Cover plate_1	001-03	Aluminium	1
4	ISO 4014 - M8 x 40 x 22-N		Carbon Steel	4
5	Hexagon Nut ISO - 4033 - M8 - W - N		Carbon Steel	4

SECTION A-A
SCALE 1 : 1.5

The tolarence between the cover plate
and the inner plate is H11/c11 (loose running)
The Tolarence for other dimensions are (+0.1/-0.1)

DETAIL B
SCALE 2 : 1

Tensile specimens

DWG NO. 001   A3

- Design the mold for DMA specimens

SECTION A-A
SCALE 1 : 1.5

DETAIL A
SCALE 2 : 1

The tolarence between the cover plate
and the inner plate is H11/c11 (loose running)

The Tolarence for other dimensions are (+0.1/-0.1)

ITEM NO.	Part Name	Part No	Materials	QTY.
1	Base plate_2	002-01	Aluminium	1
2	Inner plate_2	002-02	Aluminium	1
3	Cover plate_2	002-03	Aluminium	1
4	ISO 4014 - M8 x 40 x 22-N		Carbon steel	4
5	Hexagon Nut ISO - 4033 - M8 - W - N		Carbon Steel	4

TITLE:
DMA and DSC Specimens

MATERIAL: Aluminium

DWG NO 002
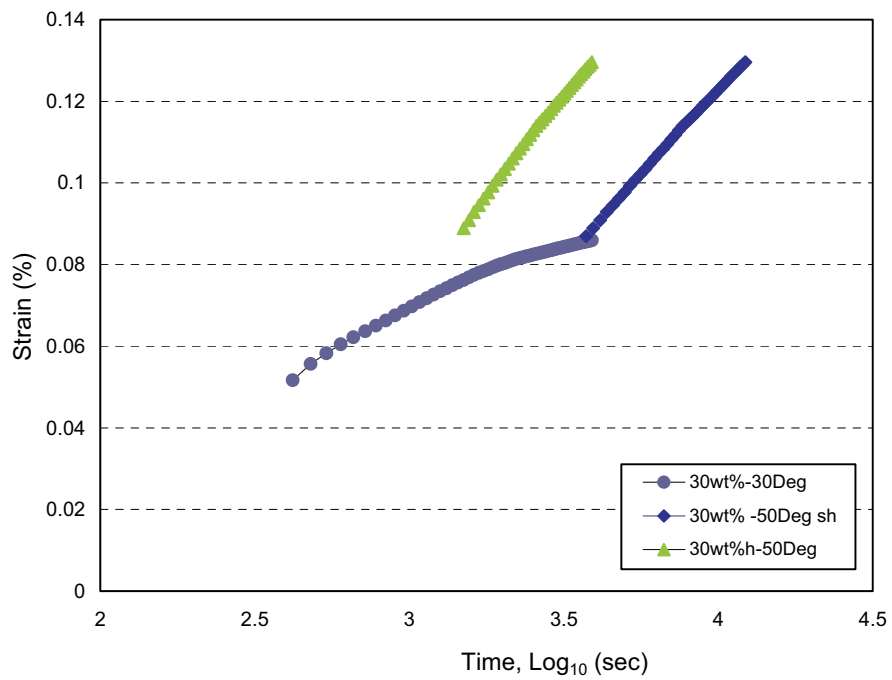
A3

SCALE:1:2   SHEET 1 OF 1

Appendixes B

- Sample of shifting creep strain curves for (50%UP+50%ST) composites with 30°C as a reference temperature.
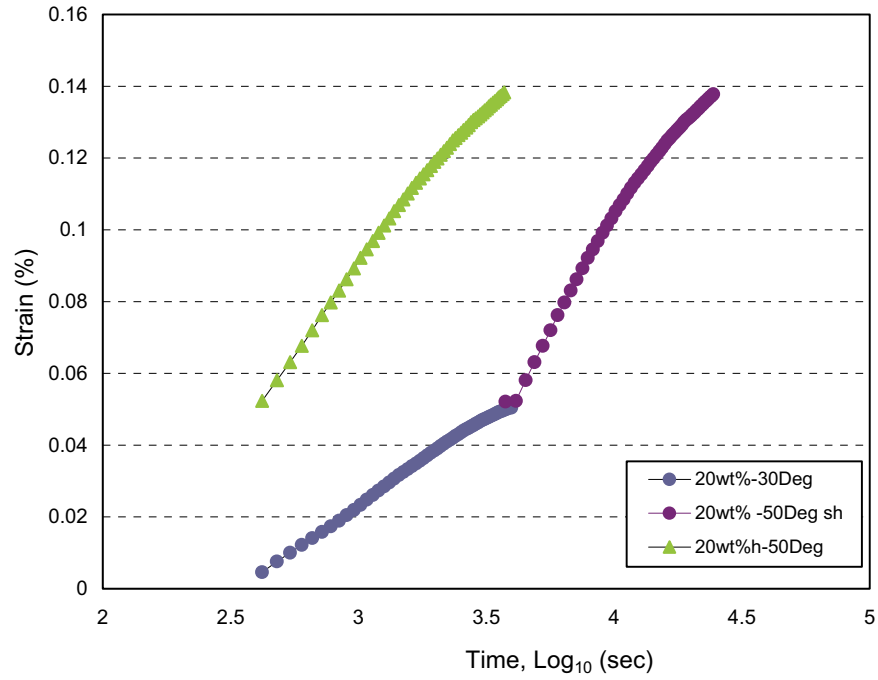

Shifting creep strain curves for (60%UP+40%ST) composites with 30°C as a reference temperature for 20wt% fiber content.
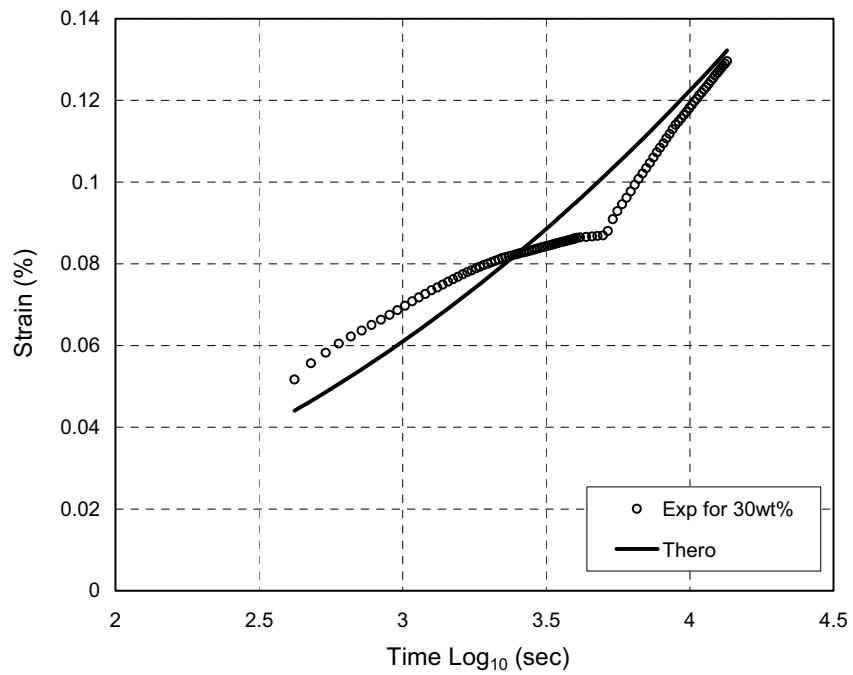

Shifting creep strain curves for (60%UP+40%ST) composites with 30°C as a reference temperature for 30wt% fiber content.

- Sample of Comparison between the master and the creep model for (60%UP+40%ST) composites for smallest and highest weight fraction of fiber
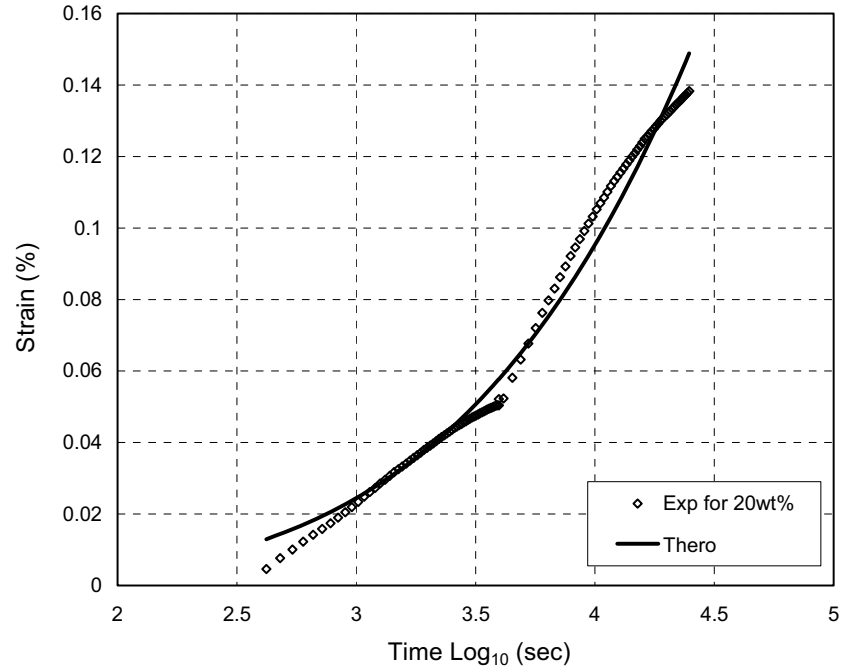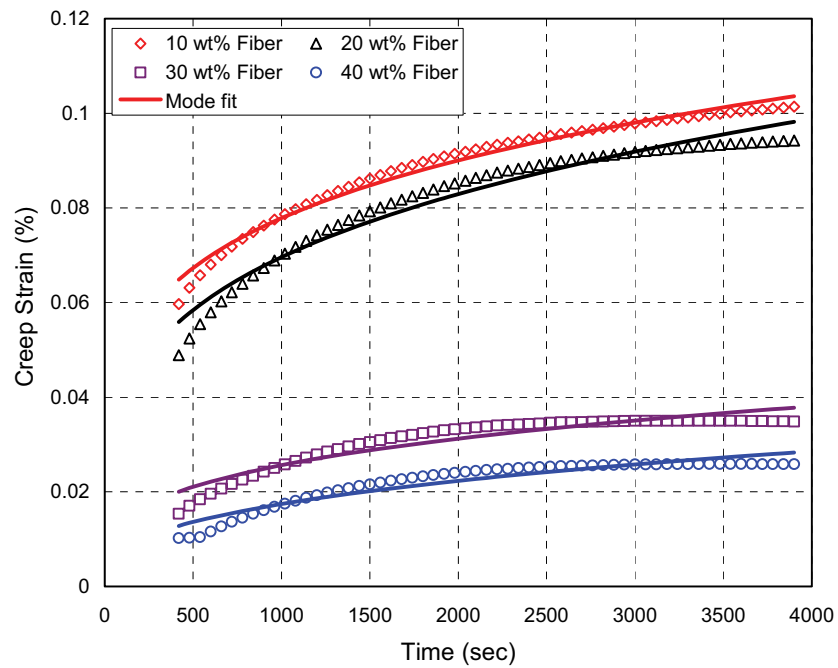

Comparison between the master and the creep model for (60%UP+40%ST) composites at 20wt% weight fraction of fiber
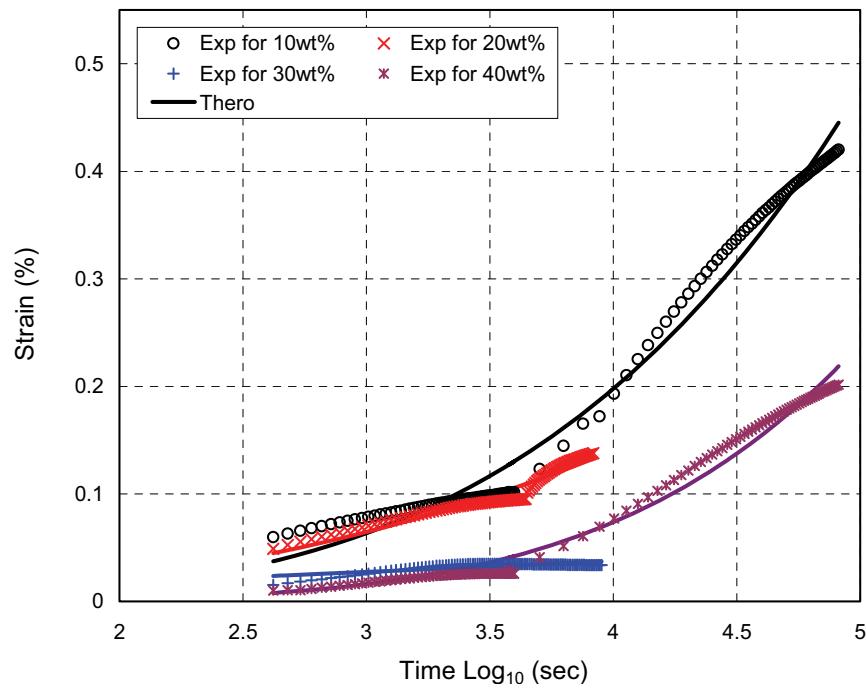

Comparison between the master and the creep model for (60%UP+40%ST) composites at 30wt% weight fraction of fiber

- Power-law-extrapolated creep and actual creep data of (50%UP+50%ST) composites containing different weight fraction of fiber

Power-law-extrapolated creep and actual creep data of (50%UP+50%ST) composites

- Sample of Comparison between the master and the creep model for (50%UP+50%ST) composites at four different weight fraction of fiber

Comparison between the master and the creep model for (60%UP+40%ST) composites

218